**The Pursuit of Unshocking Hsp90 Inhibitors: Development of Gedunin and
Cruentaren A as Chemical Leads**

By

Gary E. L. Brandt

Submitted to the graduate degree program in Medicinal Chemistry and the graduate faculty of
The University of Kansas in partial fulfillment of the requirements for the degree of Doctor of
Philosophy

Committee:

_____
Brian S. J. Blagg, Ph.D
Committee Chair

_____
Apurba Dutta, Ph.D

_____
Ryan A. Altman, Ph.D

_____
Michael Rubin, Ph.D

_____
Jeffrey P. Krise, Ph.D

Date defended: September 30th, 2011

The Dissertation Committee for Gary E. L. Brandt certifies that this is the approved version of the following dissertation:

The Pursuit of Unshocking Hsp90 Inhibitors: Development of Gedunin and Cruentaren A as Chemical Leads

_____

Brian S. J. Blagg, Ph.D
Committee Chair

Date approved: _____

Abbreviations:

17-AAG = 17-allylamino-17-demethoxygeldanamycin
17-DMAG = 17-dimethylamino-17-demethoxygeldanamycin

A4 = C-terminal Hsp90 ligand developed by the Blagg Laboratory at KU
Abl = v-abl Abelson murine leukemia viral oncogene homologue-1
ACN = acetonitrile
AD-mix = Sharpless Asymmetric Dihydroxylation commercial reagent
ADP = adenosine diphosphate
Aha1 = activator of Hsp90 ATPase homologue-1
AKT = serine/threonine protein kinase
ATP = adenosine triphosphate
AUY922 = Novartis' Hsp90 inhibitor under partnership agreement with Vernalis

Bag-2 = Bcl-2-associated athanogene-2
Bcr = breakpoint cluster region
Bcr-Abl = Philadelphia chromosome, chromosomal abnormality associated with CML
BRAF = v-Raf murine sarcoma viral oncogene homolog B1
^{t}BuLi = *tert*-butyl lithium
^{t}BuOH = *tert*-butanol

CAB = chiral acyloxy borane
CAN = ceric ammonium nitrate
CARD = Caspase activation and recruitment domains
CBr_4 = tetrabromomethane (carbon tetrabromide)
CBS = Corey-Bakshi-Shibata catalyst
CD147 = cluster of differentiation 147 (basigin)
CDC37 = cell division cycle 37 (p50, Hsp90 kinase client co-chaperone)
CDK4 = cyclin-dependent kinase-4
CFTR = cystic fibrosis transmembrane conductance regulator
CHIP = carboxy terminus of Hsp70 interacting protein
CK2 = casein kinase-2
c-Met = MNNG HOS transforming gene
CML = chronic myelogenous leukemia
CNF2024 = Conforma Therapeutics' small molecule Hsp90 inhibitor
$(COBr)_2$ = oxalyl bromide
COMU = (1-cyano-2-ethoxy-2-oxoethylidenaminooxy)dimethylamino-morpholino-carbenium
        hexafluorophosphate

DCM = dichloromethane
DHN = 4-deshydroxy novobiocin
DHQ_2PHAL = cinchona alkaloid based chiral ligand applied in the Sharpless asymmetric
        dihydroxylation
DIPA = diisopropylamine
DIPEA = *N,N*-diisopropylethylamine

DMAP = 4-dimethylaminopyridine
DMF = dimethylformamide
DMP = dimethoxypropane
DNA = deoxyribonucleic acid

EEF1A1 = eukaryotic translation elongation factor 1 a 1
EGCG = epigallocatechin-3-gallate
EGFR = epidermal growth factor receptor
ERa = estrogen receptor alpha
erbB2 = human epidermal growth factor receptor-2 (HER-2 synonym)
ERK = extracellular signal-regulated kinase
ESI = electrospray ionization
Et_2O = diethyl ether
EtOAc = ethyl acetate

F_1F_o-ATP synthase = factor-1 factor-oligomycin ATP synthase
Fak = focal adhesion kinase
FAS = F_1F_o-ATP synthase
FK228 = natural product depsipeptide HDAC inhibitor developed by Gloucester Pharmaceuticals
FKBP52 = FK506 binding protein 52
FGFR = fibroblast growth factor receptor

GCUNC45 = protein unc-45 homolog A
GDA = geldanamycin
GHKL = Family of ATPAses consisting of DNA <u>G</u>yrase, <u>H</u>sp90, Histidine <u>K</u>inase, and Mut <u>L</u>
Grp = glucose regulated protein (endoplasmic reticulum Hsp90 isoform)
GSK3 = glycogen synthase kinase 3

H_2O = water
HBV = hepatitis B virus
HCl = hydrochloric acid
HDAC = histone deacetylase
HER-2 = human epidermal growth factor receptor-2 (erbB2 synonym)
Hex = hexanes, mixture of isomers
Hif -1a = hypoxia inducible factor-1a
HOP = Hsp70/Hsp90 organizing protein
HPLC = high performance liquid chromatography
HRMS = high resolution mass spectrometry
Hsc70 = heat shock cognate isoform of Hsp70
HSF1 = heat shock factor 1 (Hsp transcription factor)
Hsp = heat shock protein
HspBP1 = Hsp70-binding protein-1
HtpG = bacterial Hsp90 homologue
HTS = highthroughput screen

ICE = interleukin-1b-converting enzyme

IDH1 = isocitrate dehydrogenase 1
IKK = IkB kinase
IPAF = ICE protease activating factor (NLRC4 synonym)
Ipc = isopinocampheyl

KO^{t}Bu = potassium *tert*-butoxide

LAB = lithium amidotrihydroborate
lacZ = operon that encodes b-galactosidase enzyme
LAH = lithium aluminum hydride
LAQ-824 = non-hydroxamide containing HDAC inhibitor developed by Novartis
LDA = lithium diisopropylamide

MAPK = mitogen activated protein kinase
MCF-7 = Michigan Cancer Foundation – 7 (breast cancer cell line)
Mek = MAPK/ERK kinase
MeOH = methanol
Mik1 = mitosis inhibitor protein kinase-1
MMP = matrix metalloproteinase
MNNG HOS = osteosarcoma cell line
MnO_2 = manganese dioxide
MOM = methoxymethyl
MOMCl = chloromethyl methyl ether
MS-275 = benzamide containing HDAC inhibitor developed by Syndax
MTS/PMS = (3-(4,5-dimethylthiazol-2-yl)-5-(3-carboxymethoxyphenyl)-2-(4-sulfophenyl)-2H-
        tetrazolium/phenazine methosulfate
Myt1 = myelin transcription factor-1

$NaBH_4$ = sodium borohydride
NAH = sodium hydride
NB = novobiocin
NCI-60 = National Cancer Institute 60 cell line screen
nF-κB = nuclear factor kappa-light-chain-enhancer of activated B cells
NIH = National Institues of Health
NIH 3T3 = NIH 3-day transfer, inoculum 3 x 10^5 fibroblast cell line derived from mouse embryo
NIK = nF-kB inducing kinase
NLR = nucleotide-binding domain, leucine rich containing protein 4
NLRC4 = NLR family CARD domain-containing protein 4
NMO = *N*-methylmorpholine-*N*-oxide
NMR = nuclear magnetic resonance
NOD = nucleotide-binding oligomerization domain protein
NSP = nonstructural polyprotein

OsO_4 = osmium tetroxide

p23 = chaperone associated protein 23 kDa

p53 = tumor protein 53
P2X = purinergic ligand gated ion channel
P2Y = purinergic G protein-coupled receptor
PCC = pyridinium chlorochromate
PDC = pyridinium dichromate
PFKFB3 = gene encoding for 6-phosphofructo-2-kinase/fructose-2,6-biphosphatase 3 enzyme
PMB = *para*-methoxybenzyl ether
PP30 = polyribosomal protein 30
PP5 = protein phosphatase-5
PPh$_3$ = triphenylphosphine
PPTS = pyridinium *para*-toluenesulfonate

SAR = structure-activity relationship
SDH = succinate dehydrogenase
SDS-PAGE = sodium dodecyl sulfate polyacrylamide gel electrophoresis
siRNA = small interfering RNA
SKBr3 = Sloan-Kettering breast cancer cell line
SNX-5422 = Serenex's lead small molecule Hsp90 inhibitor
Swe1 = *Sarcchomyces* Wee1 homologue

RAD = radicicol
RAF-1 = serine/threonine protein kinase
RCAM = ring-closing alkyne metathesis
RCM = ring-closing metathesis
Rip = ribosome inactivating protein
RNA = ribonucleic acid

TBAI = tetrabutylammonium iodide
TFA = trifluoroacetic acid
TFAA = trifluoroacetic anhydride
Tf$_2$O = trifluoromethanesulfonic anhydride
THF = tetrahydrofuran
THP = tetrahydropyran
TLC = thin layer chromatograhy
TMS = tetramethylsilane
TPAP = tetrapropylammonium perruthenate
TPR = tetratricopeptide repeat
TsOH = *para*-toluenesulfonic acid

UCP2 = mitochondrial uncoupling protein 2

v-src = viral-sarcoma oncogene tyrosine-protein kinase

Wee1 = nuclear serine/threonine protein kinase (from Scottish dialect word wee meaning small)

Abstract: The 90 kDa heat shock protein (Hsp90) is a molecular chaperone that is critical cellular survival and growth under both typical and stressful conditions. Hsp90 is responsible for the maturation and stability of more than 200 client proteins involved in a diverse assortment of cellular processes. Disruption of Hsp90's chaperoning activity causes client protein degradation and ultimately leads to cytostasis and/or apoptosis. While this phenomenon is observed in normal cells, the effects of Hsp90 inhibition are more pronounced in oncogenic cell lines as a result of higher expression levels and increased cellular dependence on Hsp90 activity. As such, targeting Hsp90 inhibition with small molecules has emerged as a powerful strategy for the development of anticancer chemotherapeutics.

Several small molecule Hsp90 inhibitors are currently under evaluation in FDA sanctioned clinical trials for the treatment of various cancers, however, some undesired side effects have been observed. All of the Hsp90 targeting small molecules involved in these trials are ATP competitive inhibitors that bind at the N-terminal ATP binding domain. Inhibitors of this class elicit non-specific client protein degradation and cause the induction of the heat shock response that results in an upregulation of Hsp90 and other Hsp expression levels following incubation within cells. As a result, untoward toxicological effects are observed and the determination of appropriate dosing schedules to mitigate the heat shock response is highly complicated. A new strategy for Hsp90 inhibition capable of targeting specific client proteins for therapeutic efficacy that avoids heat shock response induction is desired.

Presented herein are preliminary studies that investigate potential strategies to target the selective degradation of Hsp90 client proteins while avoiding the heat shock response. Specifically, small molecule natural products that elicit Hsp90 co-chaperone disruption are considered and the chemical and biological results are discussed. These studies provide the first

steps toward developing a second generation of Hsp90 inhibitors that circumvent the detrimental

effects observed for clinically evaluated inhibitors.

Acknowledgements

I was never informed that the successful completion of a Ph.D. in medicinal chemistry would necessitate so much failure. I have come to view failure almost with anticipation, because it makes success that much sweeter when it is finally obtained. I did not come to this realization by myself, however, and could never have undergone the transformation required in order to succeed in obtaining my Ph.D. without the support of several individuals.

I am forever indebted to my wife, Amy Brandt, and five children, Alexander, Keller, Rosaleigh, Michael-Finley, and Sawyer. Without this anchor to reality I would have never been capable of finishing my graduate schooling. These six very special people endured an exhausted, absent-minded, and stressed out husband/father with patience and love at a level I almost cannot understand. I am very excited to spend the rest of my life with them and so thankful that I have them.

A huge amount of gratitude is reserved for my Ph.D. advisor, Professor Dr. Brian S. J. Blagg. All of the usual thank you's here: letting me pursue what I was interested in, providing ample intellectual stimulation, and fostering scientific creativity. A special thank you must be said, however, for putting up with me throughout my five years as a graduate student. There are certain times, I am sure he is aware, that I cannot believe he did not do the easy thing and politely ask me to find another lab. For whatever reason, Dr. Blagg decided to mold this head-strong, arrogant, out-spoken, uncooperative, know-it-all graduate student into a more mature head-strong, somewhat less arrogant, out-spoken, sort of cooperative, know-it-all doctor of medicinal chemistry. I am confident in the continued success of his scientific studies and hope that I am able to live up to the Blagg Lab name.

I am grateful to my parents, Gary and Lynette Brandt, for never allowing me to settle

with simply "good enough" and always forcing me to live up to what they knew I was truly capable of. They provided ample support during my entire educational career and for that I thank them both dearly. I love them both very much and will always consider their involvement with my life as critical to my success.

I would like to thank my committee members Dr. Apurba Dutta, Dr. Ryan Altman, Dr. Michael Rubin, and Dr. Jeffrey Krise.

I dedicate this work to Lauren Leigh Brandt, RN (1980-2009). I miss you so much big sis, and

wish you could have witnessed my graduation.

Love,

little g

Table of Contents

List of Sections:

Chapter I
Structure, Function, Mechanism and Strategies for Inhibition of Hsp90

Chapter II

Chemical and Biological Investigation of Gedunin, a Novel Disruptor of the CDC37-Hsp90 Interaction

Chapter III

Total Synthesis of Cruentaren A, Selective F$_1$F$_o$ ATP Synthase Inhibitor Isolated from

Byssovorax cruenta

Chapter IV

A Conformation-Based Approach for the Design of Simplefied Natural Product Analogues

of Trienomycin A

List of Figures:

Chapter I

Structure, Function, Mechanism, and Strategies for Inhibition of Hsp90

Chapter II

Chemical and Biological Investigation of Gedunin, a Novel Disruptor of the CDC37-Hsp90

Interaction

Chapter III

Total Synthesis of Cruentaren A, Selective F1Fo ATP Synthase Inhibitor Isolated from

Byssovorax cruenta

Chapter IV

A Conformation-Based Approach for the Design of Simplefied Natural Product Analogues

of Trienomycin A

List of Schemes:

Chapter IV

A Conformation-Based Approach for the Design of Simplefied Natural Product Analogues

of Trienomycin A

List of Tables:

List of Charts:

Chapter II

Chemical and Biological Investigation of Gedunin, a Novel Disruptor of the CDC37-Hsp90

Interaction

Chapter I

Structure, Function, Mechanism and Strategies for Inhibition of Hsp90

I.1   Introduction to Hsp90 as a Therapeutic Target

According to a 2010 report from the World Health Organization, cancer will soon replace heart disease as the number one cause of death.[1] To combat this global problem, many cancers are now treated as chronic illnesses and managed by chemotherapy, requiring long-term care. In order to minimize deleterious side effects observed with traditional chemotherapies, new therapies that target cancer specific pathways are sought.

One such therapeutic approach employs targeted multi-kinase inhibitors. While some success has been achieved, resistance development and the emergence of detrimental side effects remain a serious concern.[2] For example, in a recent renal cell carcinoma clinical trial with the multi-kinase inhibitor sorafenib, nearly 30% of patients left the study due to negative side effects, including gastrointestinal and dermatological toxicities.[3] Furthermore, in a clinical trial for chronic myeloid leukemia, resistance to multi-kinase inhibitors developed rapidly in 26%, 73%, and 95% of patients with chronic, accelerated, or blast phase illness, respectively.[4] Clearly, diminishing side effects and overcoming resistance is central to the long-term success for chronic treatment strategies.

A therapeutic strategy that targets both cancer specific pathways and mechanisms of resistance could potentially eliminate side effects and be less prone to resistance development. The family of heat shock proteins (Hsps) represent a class of molecular targets around which such a strategy is being developed. Hsps function within cells as molecular chaperones and regulate/maintain proper protein function in normal cells. However, the chronic stress that results

from the cancer phenotype renders Hsps critical in oncogenic cells for survival, proliferation, and disease progression amid highly aberrant signaling pathways.[5]

Protein dysfunction is a common physiological phenomenon, even in healthy cells. The accumulation of dysfunctional proteins, however, can lead to various pathological states.[6-11] As a means to both promote cell survival and maintain genetic integrity, living cells have evolved mechanisms to refold or induce the degradation of misfolded proteins.[12-14] This process is enabled by molecular chaperones, such as the Hsps, that comprise the class of bio-machinery responsible for quality control over protein structure.[15-18]

One of the most studied molecular chaperones is the 90 kDa heat shock protein, Hsp90.[19-25] Potential clinical roles for Hsp90 inhibition are heavily pursued. Its therapeutic potential as a target for the development of cancer chemotherapeutics is particularly exciting.[26-30] Toward this objective, several small molecules have been identified as Hsp90 inhibitors such as geldanamycin (GDA), radicicol (RAD), and novobiocin (NB) (Figure 1.1).[31-33] Thus far, Hsp90 targeting ligands have been discovered that bind the N-terminal ATP binding pocket,[34-43] C-terminal nucleotide-binding domain,[44-47] or that target one of Hsp90's protein-protein interactions.[48-51] These mechanisms for target modulation provide various opportunities for the development of Hsp90 inhibitors with clinical applications toward multiple disease states.

Figure 1.1. Representative examples of natural product and synthetic inhibitors of the Hsp90 protein folding machinery.
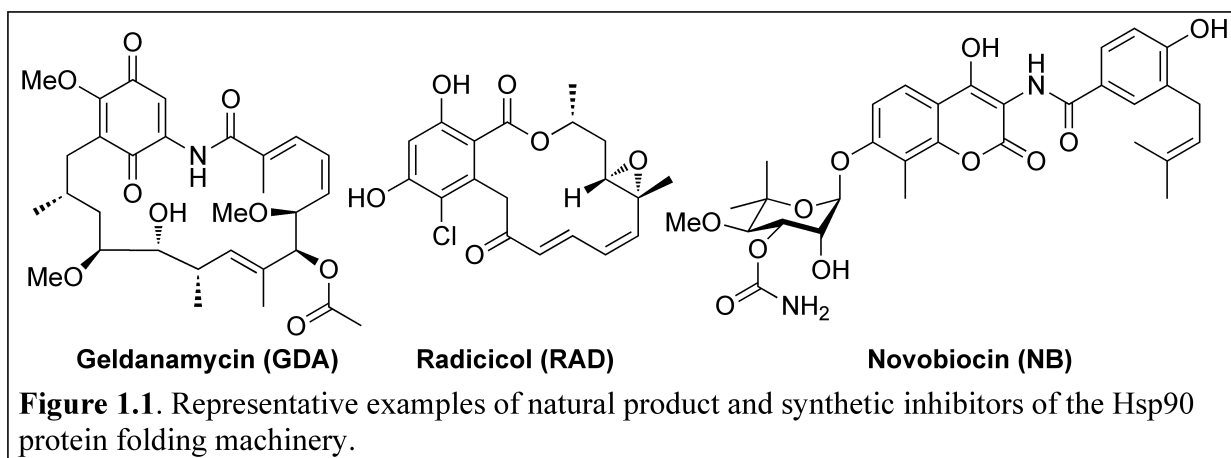
Currently, the primary focus of Hsp90 modulation is based on competitive displacement of ATP from the N-terminal nucleotide-binding domain. Molecules that manifest this mode of activity have progressed from pre-clinical studies into human clinical trials for cancer,[52-55] serving to validate Hsp90 as a target for cancer,[56] and opening the door for other therapeutic options including neurodegenerative disorders, cystic fibrosis, and pathological infection. After a discussion of the Hsp90 chaperoning process, these and other therapeutic areas will be discussed in more detail below.

I.2   Hsp90, Master Chaperone

Hsp90 is responsible for regulating cellular dysfunction by identifying denatured/misfolded proteins and stimulating either their rematuration or proteasomal degradation.   This master chaperone also facilitates the three-dimensional maturation and transport of more than 200 client proteins, i.e. proteins that require Hsp90 in either limited or extensive capacity for proper function (a complete listing of Hsp90 clients can be found at http://www.picard.ch/downloads/Hsp90interactors.pdf).[57] The total protein folding process requires involvement of several macromolecular interactors (co-chaperones and/or partner proteins) that comprise the dynamic Hsp90 protein folding machinery, or the super chaperone complex (Table 1.1).[15, 21, 58, 59] Through a series of conformational switching events that are dependent upon Hsp90's ATPase activity, the super chaperone complex enables both protein refolding and the conformational maturation of clients.[60-63]

Table 1.1. Examples of Hsp90 co-chaperones and partner proteins, interactive domain, and function.

Co-Chaperone/Partner Protein	Interactive Domain	Function
Hsp70	C-terminus via HOP	Facilitates protein client loading
HOP	C-terminal MEEVD domain	ATPase inhibitor, allows client loading
Aha1	Middle domain	ATPase activator, facilitates chaperoning
CDC37	N-terminal domain	ATPase inhibitor, required for protein kinase client loading
FKBP52	Binds both C- and N-termini	Facilitates steroid hormone receptor client folding, peptidyl prolyl isomerase
PP5	C-terminal MEEVD domain	Regulates Hsp90 activity, dephosphorylates other co-chaperones, negatively regulates HSF1
p23	N-teriminal domain	Facilitates ATPase activity
GCUNC45	Binds both C- and N-termini	Facilitates steroid hormone receptor client folding upstream of FKBP52, peptidyl prolyl isomerase
CK2	Highly charged region near N-terminus	Phosphorylates and activates CDC37 and Hsp90, phosphorylates and depresses FKBP52 activity

I.2.1   *Hsp90 Structure*

Hsp90 exists as a homodimer in solution and contains three distinct structural domains: the C-terminus, the middle domain, and the N-terminus (Figure 1.2). Each domain participates in the protein folding process.[64]

The Hsp90 C-Terminus

The Hsp90 C-terminus is important for stabilizing Hsp90's

Figure 1.2. Pictorial representation of the 3 Hsp90 structural domains.
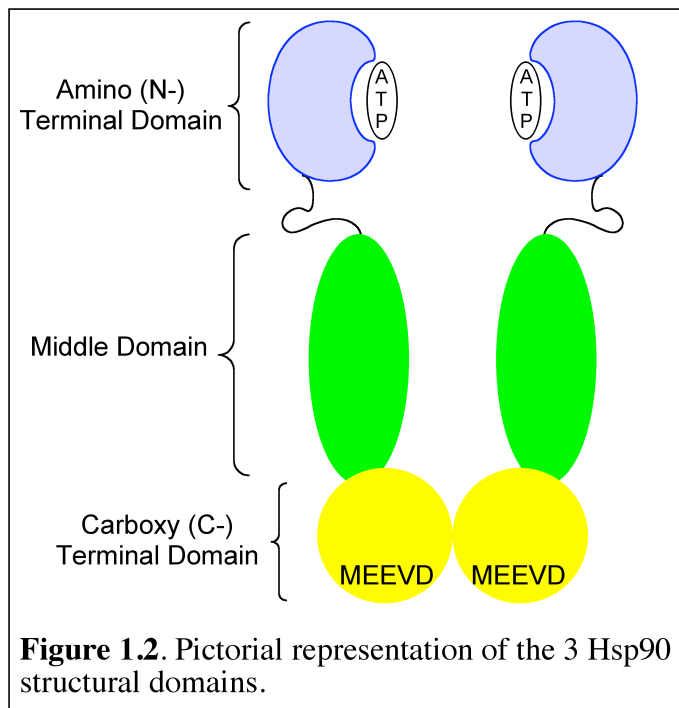
homodimeric nature and exhibits allosteric control over Hsp90's N-terminal domain.[23, 65] Intermonomeric interactions create a dimeric surface that consists of a stable four-helix bundle, of which two-helices are contributed from each monomer, and forms an aromatic rich dimerization interface.[19, 64] While this region does not house Hsp90's ATPase activity, it provides allosteric regulation of N-terminal ATPase activity.[66, 67] The C-terminal domain does, however, contain a non-hydrolyzing, nucleotide binding site responsible for exerting this allosteric control. When this site is occupied, ligands bound to the N-terminus, such as ADP or ATP-competitive inhibitors, are displaced through nucleotide switching.[46, 47, 68-72] The C-terminal nucleotide-binding site is targeted by C-terminal Hsp90 inhibitors such as NB and its analogues.[31, 47]

The dimeric interface of Hsp90 at the C-terminus is critical for super chaperone complex assembly. Several co-chaperone and immunophilin components of the complex (*e.g.* HOP [Hsp organizing protein] and FKBP52 [FK506 binding protein 52])[67, 73] associate with Hsp90 *via* the

5

C-terminus. Such members of the complex express tetratricopeptide repeats (TPR, a conserved 34 amino acid sequence) that recognize and bind to the C-terminal MEEVD domains of dimeric Hsp90. Transient MEEVD-TPR interactions between Hsp90 and various super chaperone components imparts essential mechanistic consequences throughout the protein folding process. For example, early stage HOP binding to the Hsp90 C-terminus facilitates client protein loading by halting N-terminal ATPase activity.[74, 75] HOP is later displaced by FKBP52 following steroid hormone receptor client loading and primes reinitiation of the N-terminal ATPase cycle.[76] A host of other co-chaperones, partner proteins, and immunophillins similarly participate at different stages of the protein folding process in a client protein dependent manner.[77] While few client protein-specific super chaperone complexes have been described, further investigation will enable the development of strategies for selective rather than global client degradation. This attribute will allow the design of "tunable" Hsp90 inhibitors for specific clinical applications.

The Hsp90 Middle Domain

The middle domain of Hsp90, appended to the N-terminal domain by a charged linker, is intimately involved with super chaperone complex function.[78] A majority of Hsp90-client protein interactions occur among middle domain amino acid residues.[79, 80]

The precise mechanism responsible for this domain's ability to stabilize client proteins is not well understood. In fact, only one crystal structure of Hsp90 bound to a client protein has been solved (Hsp90 bound to CDK4).[81] While this crystal structure provides insights into important intra-protein interactions required for client binding, a fluid description of the overall maturation process remains inaccessible. Other processes mediated by the middle domain include ATP binding and hydrolysis, due to interactions with the gamma-phosphate of ATP

bound to the N-terminus, and coordination of several partner proteins such as Aha1 (activator of Hsp90 ATPase homologue 1), appropriately named for its ATPase stimulating effects.[64, 80, 82]

The Hsp90 N-Terminus

The N-terminus of Hsp90 contains the catalytically active ATPase domain that is responsible for ATP hydrolysis. Hsp90 is dependent on ATP hydrolysis for proper function.[64] As a member of the GHKL family of ATPases, (Gyrase, Hsp90, Histidine Kinase, and MutL Kinase) Hsp90 exhibits a unique N-terminal nucleotide-binding pocket[83] reminiscent of other members of the GHKL family of proteins.[80]

The N-terminal ATP binding domain is distinct from the C-terminal nucleotide binding domain. The Bergerat fold containing ATPase domains of GHKL proteins like Hsp90 bind ATP in a unique, bent conformation.[83] ATP binding leads to formation of the "lid" segment of the Hsp90 molecular clamp by promoting an N-terminal dimerization event, thereby "locking" client proteins into the super chaperone complex.[84, 85] The N-terminus of Hsp90 also participates in protein-protein interactions critical for super chaperone complex formation (*e.g.* its interaction with the ATPase-inhibiting co-chaperone CDC37).[86]

I.2.2 *Hsp90 Protein Folding Mechanism*

Both intra- and intermolecular interactions between Hsp90's three domains and various co-chaperones/partner proteins operate in concert to organize the super chaperone complex into a protein folding machine that acts as a master regulator of protein conformation.[87] The mechanism by which the Hsp90 protein folding machinery manifests its protein folding abilities has been extensively reviewed (Figure 1.3).[15, 21, 23, 29, 59, 64, 86, 88] To highlight the diverse nature of components required for client proteins manifested by the super chaperone complex, the protein

folding mechanism for steroid hormone receptor and kinase clients will be considered. Specifically, the client loading process for these two families is distinct.

Nascent kinase polypeptides first associate with Hsp70, Hsp40, and CDC37 in the cytosol. HOP then bridges this heteroprotein complex by simultaneously binding to the Hsp70 and Hsp90 MEEVD domains at distinct TPR expressing regions. The association of HOP with Hsp90 facilitates kinase client transfer by prohibiting N-terminal dimerization and ATP hydrolysis. In contrast, steroid hormone receptor client loading to Hsp90 ensues without stabilization by CDC37. Following client loading, a similar process for both client protein classes involving multiple co-chaperones and immunophillins is initiated. HOP displacement by FKBP52 or other immunophillins allows ATP binding and subsequent N-terminal dimerization, wherein the client is effectively clamped within the super chaperone complex. This clamped conformation is further stabilized by recruitment of p23 to the N-terminus of Hsp90. Aha1 association with the middle domain sequentially induces ATP hydrolysis, proper client maturation, and finally client release (Figure 1.3).[80]
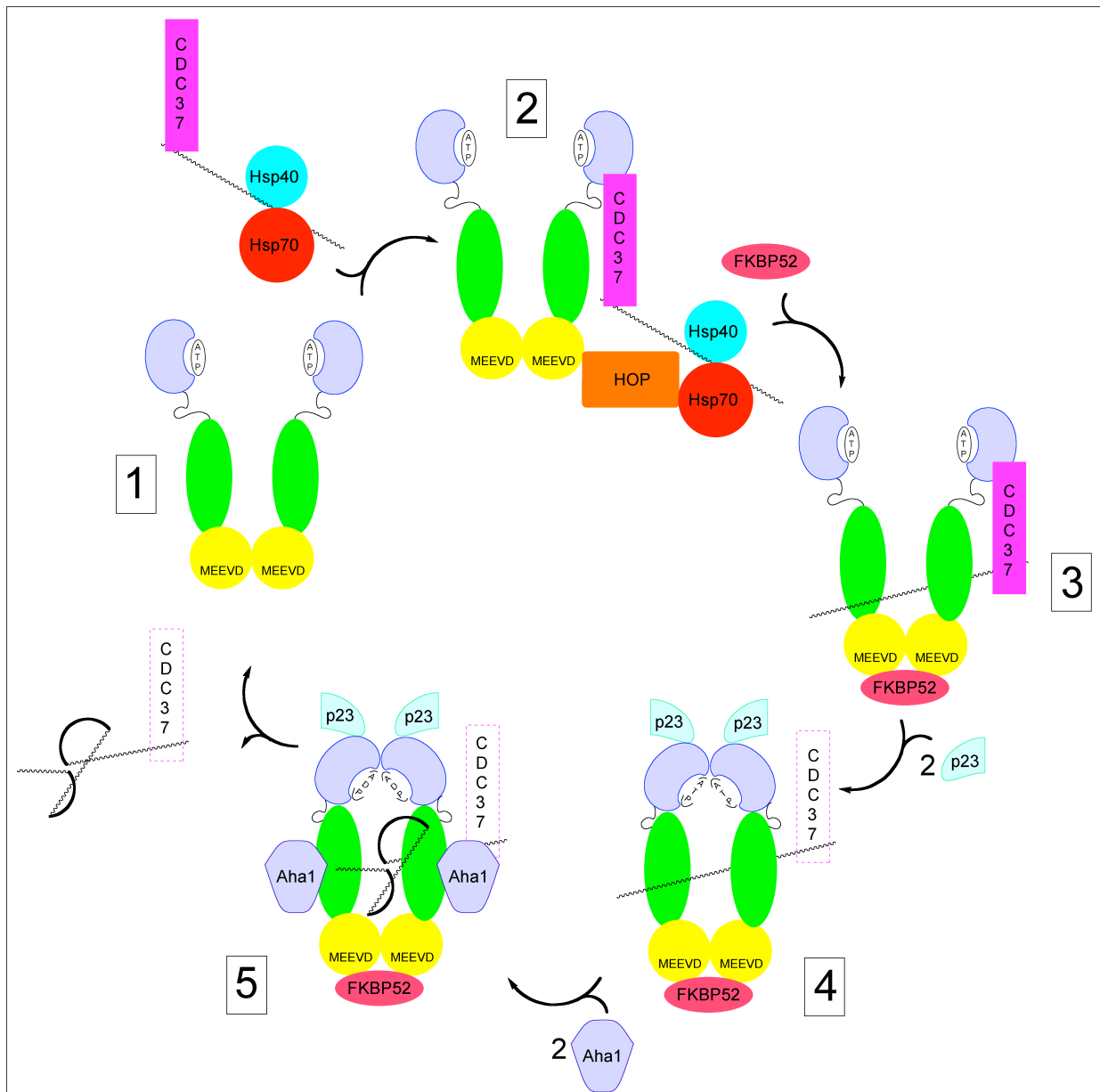
Figure 1.3. Hsp90 protein folding process for kinase clients. 1–2) After associating with Hsp70, Hsp40, and CDC37, the nascent polypeptide is recruited to Hsp90 by HOP and CDC37, both of which inhibit ATP hydrolysis. 2–3) The peptide is loaded onto Hsp90 and FKBP52 (or other immunophillin) displaces the HOP/Hsp70/Hsp40 complex. 3–4) p23 is recruited to the super chaperone complex and stabilizes Hsp90 N-terminal dimerization. 4–5) Aha1 binds the Hsp90 middle domain facilitating client structural maturation and ATP hydrolysis. 5–1) ATP hydrolysis to ADP destabilizes dimerization at the N-terminus. Hsp90 adopts an "open" conformation where mature client is released and ATP displaces ADP for propagation of the catalytic cycle.

9

I.3 Clinical Evaluation of Hsp90 Inhibitors

Several classes of Hsp90 inhibitors are under development for therapeutic applications. Currently, all clinically investigated compounds are anti-cancer agents.[25, 36, 89-91] This anti-cancer activity derives from multiple oncogenic proteins being Hsp90 clients. In fact, individual members of this large clientele subset are implicated in all six hallmarks of cancer as defined by Weinberg and Hanahan (Table 1.2).[27-29, 92] Consequently, therapeutic inhibition of Hsp90 results in the simultaneous disruption of all six hallmarks of cancer through modulation of a single target. As opposed to traditional cancer chemotherapy that utilizes a drug cocktail to affect multiple cancer pathways, the same effect can be accomplished by administration of a single Hsp90 inhibitor.

Justification for Hsp90 as a target for the development of cancer chemotherapeutics has been extensively reviewed.[17, 22, 30, 32, 35, 52, 54, 56, 89, 93, 94] Hsp90 has been implicated in oncogenic transformation, by stabilizing otherwise highly unstable oncoproteins/mutated clients and

Table 1.2. Select Hsp90 client proteins associated with the six hallmarks of cancer as defined by Weinberg and Hanahan.

Client Protein	Stage of Cancer Development
RAF-1, AKT, HER-2, Mek, Bcr-Abl, EGFR, FGFR	1. Self-sufficiency in growth signals
Wee 1, Myt1, CDK4	2. Insensitivity to anti-growth signals
Rip, AKT, mutant p53, survivin	3. Evasion of apoptosis
Telomerase	4. Unlimited replicative potential
Fak, AKT, Hif-1a	5. Sustained angiogenesis
c-Met, MMP	6. Metastasis and tissue invasion

promoting oncogenic progression. Furthermore, oncogene addiction and cancer related environmental stress renders these oncoproteins more dependent on Hsp90 function than the native forms found in normal cells. In fact, Hsp90 comprises 4–6% of total protein in cancer cells, four times higher than levels found in normal cells. Due to increased activity, Hsp90 is found highly associated with the super chaperone complex in cancer cells. Within the complex, Hsp90 displays higher affinity for both ATP and competitive inhibitors than the homodimeric form. These attributes result in a high differential selectivity, which has been observed for Hsp90 inhibitors in transformed versus non-transformed cells. The cumulative effect of these attributes has poised Hsp90 as an attractive, highly sought chemotherapeutic target.

I.3.1 *Initial Natural Product Based Clinical Candidates*

Clinically evaluated Hsp90 inhibitors, all of which target the N-terminal ATP binding domain,[95] demonstrate efficacious disease treatment, however, therapeutic limitations have manifested. Hepatotoxicity and the development of multidrug resistance *via* the overexpression of Pgp efflux pumps were the first limitations observed in clinical trials for the ansamycin-based inhibitors, 17-AAG and 17-DMAG (Figure 1.4).[37] This observed toxicity arises from reactive structural motifs present in these inhibitors, rather than as a consequence of Hsp90 inhibition. As semi-synthetic derivatives of GDA, both 17-AAG and 17-DMAG contain a redox active benzoquinone capable of contributing to off target effects.

I.3.2 *Second Generation Synthetic Clinical Candidates*

The structural drawbacks associated with GDA-based inhibitors spurred the design of several synthetic Hsp90 inhibitors currently undergoing clinical evaluation. Examples include the purine containing CNF2024 developed by Biogen Idec., the benzamide containing SNX-5422 developed by Serenex, and the resorcinylic based AUY922 developed by Novartis (Figure

Figure 1.4. Examples of Hsp90 N-terminal inhibitors in clinical trials.
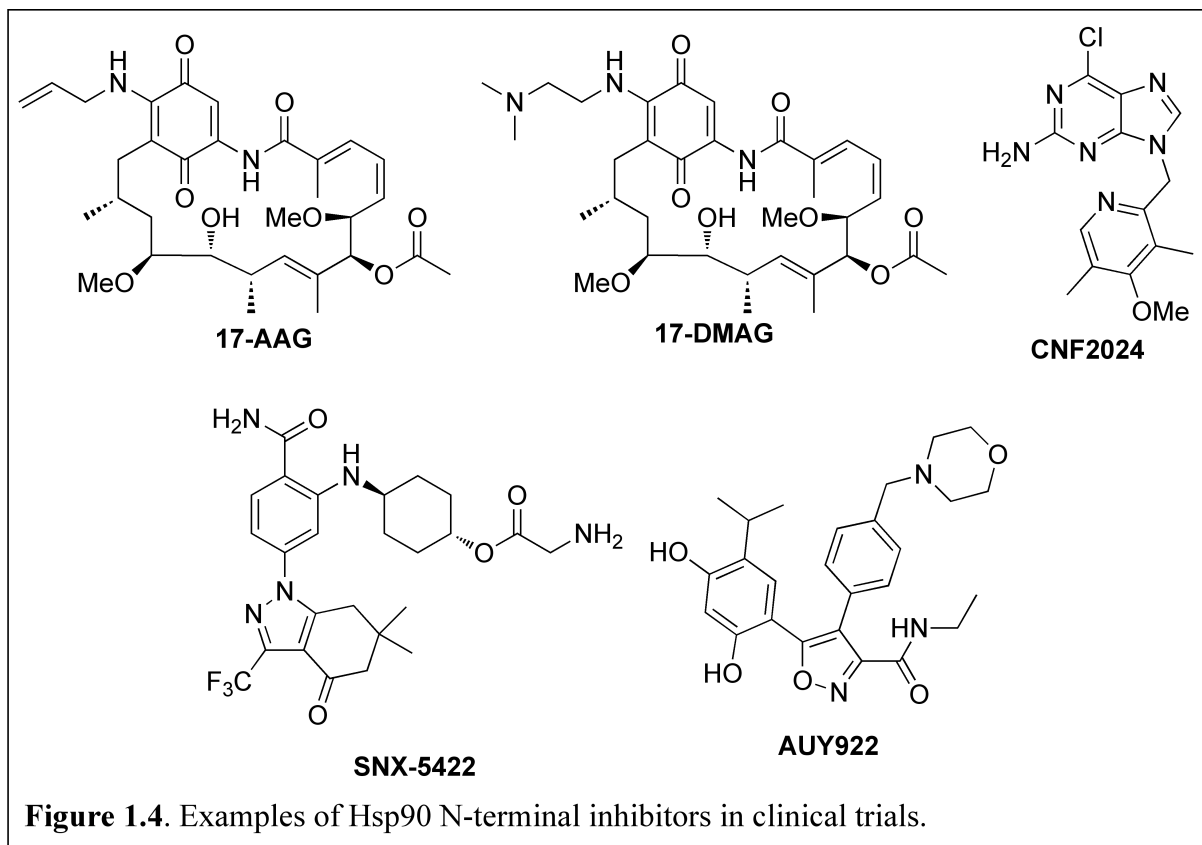
1.4).[90, 95] These compounds avoid some of the toxicological issues associated with the GDA-derived inhibitors, a compromising hallmark of N-terminal Hsp90 inhibition remains, induction of the heat shock response.

I.4 Induction of the Heat Shock Response

All Hsp90 modulators that bind to the N-terminal ATP binding site induce the over-expression of Hsps including Hsp27, Hsp40, Hsp70, and Hsp90.[96] This phenomenon, known as the heat shock response, also occurs in the presence of cellular stressors such as extreme temperatures, oxidative stress, and nutrient deprivation.[97] The transcription factor responsible for Hsp induction is heat shock factor 1 (HSF1), which is normally bound to Hsp90 and is a component of the super chaperone complex.[98] N-Terminal inhibitors disassemble the Hsp90-HSF1 complex, stimulating HSF1 trimerization, hyperphosphorylation, and translocation to the nucleus.[99] Subsequently, trimeric HSF1 binds DNA at heat shock binding elements and initiates

Figure 1.5. Cellular stress and Hsp90 N-terminal inhibitors disassemble the Hsp90/HSF1 complex, which ultimately induces the overexpression of Hsps and, therefore, a prosurvival effect
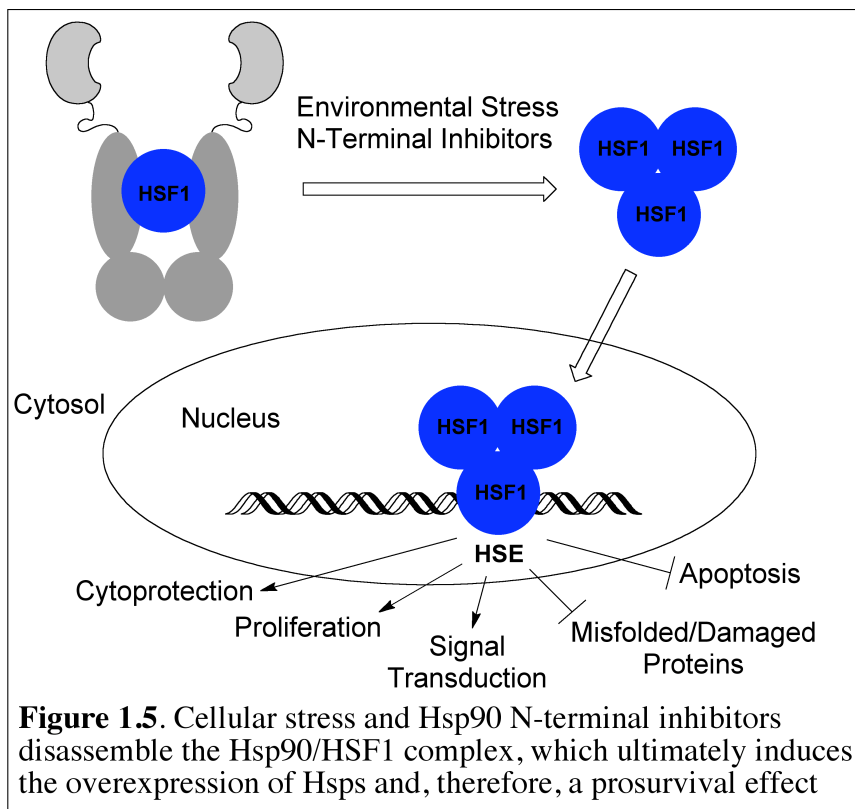
transcription of heat shock genes (Figure 1.5). Due to the anti-apoptotic and pro-survival effects manifested by Hsps, their overexpression in cancer may limit the potential of N-terminal inhibitors as anti-cancer agents by complicating dose schedules and potentially leading to resistance.[96, 100]

I.4.1 *Clinical Application of the Heat Shock Response*

Neurodegenerative Disorders

While the heat shock response may be detrimental to the treatment of cancer, its induction may prove beneficial for the treatment of neurodegenerative diseases. Several diseases associated with the central and peripheral nervous system result from the accumulation of misfolded proteins, and several agents that induce the heat shock response are now considered as potential therapeutic leads (Figure 1.6). The upregulation and overexpression of Hsps not only prevents protein aggregation, but also refolds denatured proteins and resolubilizes protein aggregates.[101, 102] Therefore, Hsp's

Figure 1.6. A4, induces heat shock response at concentrations as low as 1 nM, however, exhibits no anti-proliferative activity at 100 μM.
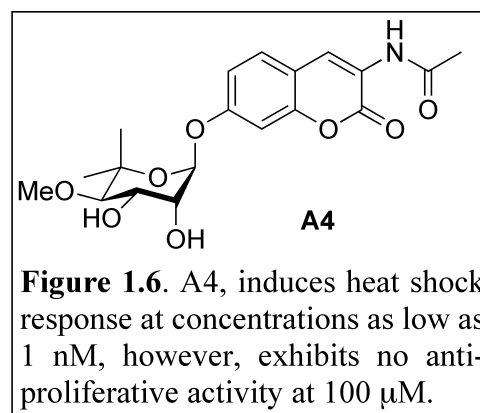
may exhibit promising activities for the treatment of Alzheimer's disease, Parkinson's disease, amyotrophic lateral sclerosis, multiple sclerosis, polyglutamine disease, spinal bulbar muscular atrophy, diabetic peripheral neuropathy, and Huntington's disease.[103]

Inflammation and the Immune Response

In contrast to both cancer and neurodegenerative disorders, it is not clear whether the heat shock response stimulated by N-terminal inhibitors is beneficial or detrimental to regulating the effects of inflammatory and immune responses from a therapeutic perspective. Several diseases including chronic and rheumatoid arthritis,[104] systemic lupus erythematosus,[105] atherosclerosis,[106] and diabetes[16] result from aberrant inflammatory processes and/or auto-immune responses that are regulated by Hsp90. Therefore, completely delineating Hsp90's role in these stimulatory processes could lead to additional therapeutic options for Hsp90 inhibitors.

The overexpression of Hsp70 and other Hsps due to the heat shock response has been shown to inhibit inflammatory processes.[107] Heat shock adversely affects the transcriptional activity of nF-κB, thereby inhibiting the pro-inflammatory responses. Similarly, Hsp90 function is required for the proper functioning of Monarch-1, a negative regulator of NIK, the nF-κB inducing kinase.[108] However, Hsp90 is also associated with several proteins necessary for pro-inflammatory signaling. For instance, Hsp90 is required for the stabilization of the IKK complex, a pro-inflammatory mediator.[109] Other examples include NOD1, NOD2, IPAF/NLRC4, and cryopyrin. Altogether, inhibition of Hsp90 appears to illicit a multifaceted approach toward the regulation of inflammation.[109]

I.5   Hsp90 Inhibition: Heat Shock and Alternate Therapeutic Applications

The collection of Hsp90 protein clients participate in numerous physiological processes and conduct a broad spectrum of functions. This diversity makes Hsp90 unique among other

chaperones and presents the opportunity for affecting a variety of signaling pathways through the modulation of a single target. Hsp90, therefore, offers the potential to affect several therapeutic areas including pathogenic infection, cystic fibrosis, and male contraception. Similar to cancer therapy, induction of the heat shock response would be contraindicated in these disease states, and therefore, the development of Hsp90 inhibitors that do not cause such a response are desired.

I.5.1   *Pathogenic Infection*

Molecular chaperones play a key role during the infection process of multiple invasive organisms including fungi, bacteria, and viruses. Upon entering a host cell, the pathogen is presented to a stressed environment and relies upon the expression of molecular chaperones for the maintenance of protein function.[110] Several species of pathogenic fungi, including *Candida albicans*, *Cryptococcus neoformans*, *Aspergillus spp.*, *Histoplasma capsulatum*, and *Paracoccidioides brasiliensis*, rely upon the expression of molecular chaperones for successful host infection and survival. The fungal Hsp90 homologe, Hsp82, is particularly essential. Unlike its mammalian counterpart, Hsp82 is not intimately involved with *de novo* protein folding. Rather, it is commonly associated with unstable proteins such as Wee1, Mik1, and Swe1. The level of Hsp82 overexpression in mouse fungal infection is directly proportional to increased virulence. Hsp82 is also extensively expressed on the cell surface of several fungal species, and acts as an immune response signal to the host.

Targeting Hsps for the treatment of fungal infection is a valid approach. Several known Hsp90 inhibitors (GDA, RAD, NB, and cisplatin) manifest antifungal activity in whole cell assays. Targeting cytosolic or membrane bound Hsps with selective small molecule inhibitors or anti-body fragments respectively are potential approaches for antifungal therapy and overcoming drug resistance.[111-116]

Similar to pathogenic fungal species, several pathogenic bacterial and protozoan species rely upon molecular chaperones for successful invasion and virulence. Bacterial and protozoan species express both cytosolic and membrane bound Hsps. In bacterial species, the homologue of Hsp90 is HtpG.[117] Strategies for targeting bacterial and protozoan infections such as *Escherichia coli* or *Leishmania*, respectively, would largely be the same as those that target fungal infections and would include selective pathogen Hsp inhibition and pathogen membrane bound recognizing antibodies.[118-121]

Similarly, viral infection also requires molecular chaperones. However, in contrast to fungal, bacterial, and protozoan infection, several viruses (e.g. Denge virus, Hepatitis B, Hepatitis C, the influenza virus and the vesicular stomatitis virus) are capable of hijacking the host cell's protein folding machinery for the maturation of viral encoded proteins associated with virus entry and multiplication. For example, host Hsp90 is required for the maturation of hepatitis B (HBV) reverse transcriptase, hepatitis C NSP2/3 protein, and RNA-dependent RNA polymerase of Influenza A. In addition, certain client proteins, such as AKT, are implicated in viral infection. In some cases, the virus incorporates host chaperones within its capsid prior to leaving the host cell, and are therefore immediately available upon subsequent cellular infection. Less commonly, viral genomes can encode for chaperone-like molecules.[76, 110, 122-124]

Treatment of cells with Hsp90 inhibitors is efficacious in models of viral infection. Also of significance, targeting host Hsp90 in viral infected cells may prove an important strategy for circumventing resistance. Most viral DNA does not encode for molecular chaperones. Therefore, viral mutation would not lead to a mechanism for acquired resistance to Hsp90 inhibition.

I.5.2   *Cystic Fibrosis*

Cystic fibrosis is a disease characterized by protein dysfunction. Generally, the cystic fibrosis transmembrane conductance regulator (CFTR) suffers a mutation, most commonly ΔF508, which prevents proper folding and trafficking to the cell membrane. Wild type CFTR undergoes an extensive, complicated, and inefficient biological synthesis and requires several chaperones, including the Hsc70/Hsp70-Hdj-1/2 cohort, calnexin, CHIP, Hsp90, Bag-2, and HspBP1. Only about 25 to 60% of wt-CFTR synthesized ever completely matures depending on the cell line. The biogenesis of mutated CFTR is even more inefficient. Hsp90 chaperoning is involved in promoting the degradation of mutant CFTR by the proteasome. Both Hsp90 inhibitors and siRNA knockdown of Aha1, an activator of Hsp90 ATPase activity, have been demonstrated to revert levels of mutant CFTR degradation by the proteasome to levels similar to that of wild type CFTR, suggesting that association of the Hsp90 heteroprotein complex with mutant CFTR may play a role in facilitating the aberrant protein function underlying cystic fibrosis. This has therapeutic effects since mutant CFTR retains its intended activity, and, therefore the disassociation of CFTR from the Hsp90 protein folding machinery manifests efficacious activity.[19, 125-127]

I.5.3   *Male Contraception*

Several Hsp90 inhibitors show male contraceptive activity, including celastrol, gedunin, and gamendazole. Mechanistic investigations of gamendazole have provided evidence that suggest Hsp90 inhibition in concert with inhibition of EEF1A1 are responsible for the observed contraceptive effects.[33]

Sertoli cells are responsible for spermatogenesis. Both Hsp90 and EEF1A1 demonstrated affinity for binding gamendazole in affinity chromatography experiments suggesting that these

proteins represent cellular targets for this small molecule. Both of these protein targets are known to promote the integrity of AKT1, which is important for maintaining Sertoli cell-spermatid junctions. The modest inhibitory activity of both Hsp90 and EEF1A1 simultaneously may be responsible for gamendazole's selective effect on Sertoli cells. Several other effects resulting from gamendazole administration to Sertoli cells were also observed, including nF-κB down regulation and the disruption of actin bundles.[33]

I.6   Emerging Strategies for Hsp90 Inhibition

Growing interest in the field of Hsp90 modulation is now focused on the development of strategies for chaperone inhibition through mechanisms that do not induce the heat shock response. Such strategies may not only provide an effective means for targeting Hsp90 in cancer, but also for safely attenuating the effects incurred in other diseases. The most extensively studied strategy for affecting super chaperone activity without concomitant induction of the heat shock response involves molecules that bind the Hsp90 C-terminal domain. Recent progress in this field is highlighted below, followed by a discussion of newly emerging strategies.

I.6.1   *C-Terminal Inhibition*

The nucleotide binding site located at the Hsp90 C-terminus provides allosteric regulation of N-terminal ATPase activity.[23, 65] Thus, targeting the C-terminal binding domain presents a novel molecular strategy toward controlling Hsp90 chaperone activity. As a strategy for cancer chemotherapy, C-terminal inhibition possesses a major advantage over N-terminal inhibition. Unlike N-terminal inhibitors, C-terminal Hsp90 inhibitors do not elicit the heat shock response.[45-47, 128] Several C-terminal targeting small molecules of a diverse structural nature have been identified. Examples include epigallocatechin-3-gallate (EGCG), the main antioxidant component of green tea;[129] cis-platin, a clinically applied anticancer agent that causes DNA

crosslinking and induces apoptosis;[130, 131] molybdate, an oxyanion mimic of phosphate;[70] and taxol, a microtubule stabilizing, clinically applied anticancer agent.[131, 132] NB and the related coumarin compounds, however, are the only C-terminal inhibitors undergoing development as potential therapeutic agents at present.

The coumarin antibiotics, NB, chlorobiocin, and coumarmycin A1, represent the originally identified Hsp90 inhibitors that target the C-terminus.[46, 47] Among these, NB is the most extensively investigated for pre-clinical development as an anticancer lead compound.

NB was formerly investigated for clinical application in Europe as an antimicrobial drug with potent affinity for the ATP-binding domain of DNA gyrase B.[133] This DNA gyrase B inhibitory activity spurned researchers to evaluate NB affinity for the ATP-binding domain of Hsp90. As members of the GHKL protein family, both DNA gyrase B and Hsp90 induce a unique, bent conformation of ATP upon ligand binding due to complimentary binding site topology.

Marcu *et al*. hypothesized that the coumarin antimicrobial agents would display affinity for Hsp90 due to structural similarities between the ATP-binding sites of the DNA gyrase B and Hsp90. This hypothesis was confirmed through affinity chromatography by observing Hsp90 retention on sepharose beads containing immobilized NB. Interestingly, neither solubilized GDA nor RAD effectively eluted Hsp90 from the NB containing sepharose beads. These seminal studies were the first to identify an alternate Hsp90 inhibitor binding mode distinct from the well known N-terminal ATP binding domain.[46, 47]

Hsp90 inhibition by NB was confirmed by evaluating the effects on client and non-client proteins. This method of evaluating a compounds ability to cause Hsp90 inhibition is a common primary screen used to validate the molecular target. In the presence of an inhibitor, Hsp90

clients are degraded in a dose-dependent manner while non-clients, such as actin, demonstrate consistent levels. SKBr3 breast cancer cells and v-src-transformed NIH 3T3 fibroblasts were treated with varying NB concentrations and depletion of RAF-1, erbB2, mutant p53, and v-src client proteins was observed between 300 μM and 800 μM, but the non-client protein scinderin, an actin associating protein, was unaffected. Intriguingly, levels of Grp78, a chaperone related to Hsp70 that is overexpressed during the heat shock response, remained unaffected. This latter result was in contrast to GDA and RAD, which commonly induce the expression of Grp78, and thus provided the first indication that Hsp90 inhibition by NB did not induce a heat shock response.[46, 47] Since it was observed that GDA and RAD did not compete for NB binding, it was proposed that NB might interact with Hsp90 *via* a novel mechanism.

Prior to the studies by Marcu *et al.* described above, Csermly *et al.* proposed the expression of multiple nucleotide binding domains on the Hsp90 protein surface,[23] and consequently, this potential was investigated. Additional affinity chromatography experiments employing truncated Hsp90 fragments were conducted to identify regions of preferential NB binding. While fragments corresponding to the N-terminal and middle domains of Hsp90 were not retained by NB-bound sepharose beads, the C-terminal fragment was retained. C-terminal fragments were then exposed to NB-bound sepharose beads and Hsp90 amino acid residues 657 through 677 were identified as critical to NB binding. This observation confirmed the earlier hypothesis that suggested the existence of a C-terminal nucleotide binding domain proximal to the dimer interface.[46, 47]

Other phenotypic effects derived from NB inhibition of Hsp90 have been investigated. Proteolytic fingerprinting, through Hsp90 trypsinolysis and fragment characterization, indicated the presence of a distinct conformational effect in NB-bound Hsp90 when compared to GDA-

bound Hsp90 under the same conditions. The influence of NB on components of the super chaperone complex has also been investigated. Co-immunoprecipitation experiments revealed that NB reduced the amount of co-adsorbed super chaperone components Hsc70, p23, HOP, PP5, and FKBP52[68] but had no effect on the interaction between CDC37 and Hsp90.[134]

Despite a lack of potency, the unique biological consequences of NB administration encouraged its consideration as an attractive lead for the development of C-terminal Hsp90 inhibitors.[44, 45, 135] No definitive structural information of the C-terminal binding domain exists, nevertheless, significant structure-

Figure 1.7. The transformation of NB, a DNA gyrase B inhibitor (DNA gyrase IC50 of 1 μM, Hsp90 IC50 of ~700 μM), into lead compound **DHN2** (DNA gyrase IC50 of >500 μM, Hsp90 IC50 of 1 μM) for the development of novel C-terminal inhibitors. Dashed boxes highlight regions where removal of functionality lead to increased potency.

activity relationships for NB have been formulated. Burlison *et al.* demonstrated that few chemical changes were required for conversion of this antimicrobial agent into a selective and potent Hsp90 inhibitor with anticancer activity.[128] This transformation was accomplished by removal of the 4-hydroxy group on the coumarin scaffold and carbamate moiety of the noviose sugar and resulted in the discovery of DHN2 (Figure 1.7).

Significant optimization of the lead compound DHN2 has since ensued. Several highly potent Hsp90 inhibitors have been discovered and a detailed analysis of structure-activity relationships for these coumarin containing compounds has been collected (Figure 1.8).

Figure 1.8. SAR developments garnered from coumarin substituent effects investigated by Donnely *et al*. Methoxy substituent at R^1 increases activity, bulky alkoxy substituents tolerated at R^2, substitution at R^3 decreases Hsp90 inhibitory activity, most active side chain is indole at R^4.
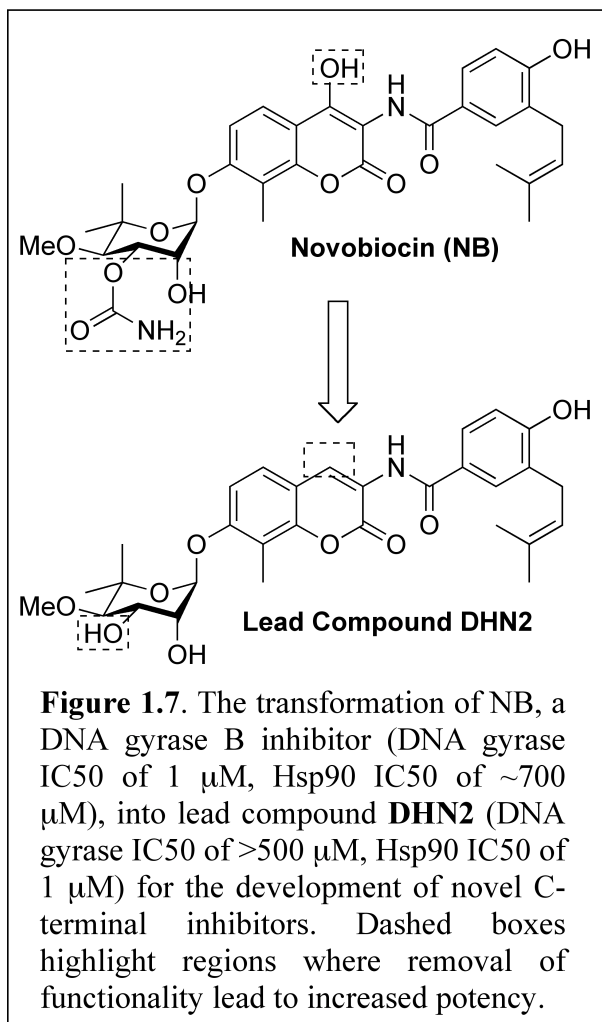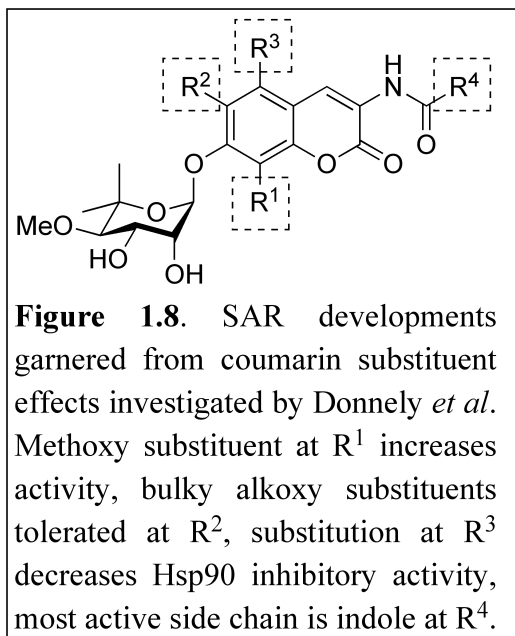
Limitations of C-Terminal Inhibition

The C-terminal Hsp90 inhibitors have been successful in circumventing a major drawback derived from N-terminal inhibition. These inhibitors manifest potent cytotoxic effects similar to the N-terminal counterparts while simultaneously avoiding induction of the heat shock response. This is a significant achievement, however, both strategies of Hsp90 inhibition cause non-specific client protein degradation, and the clinical implications of this effect are still unknown. As Hsp90 is ubiquitously expressed, targeting specific client proteins for degradation may lead to better clinical outcomes. It remains unknown whether N- or C-terminal inhibitors are capable of eliciting this type of specificity. Alternate strategies of Hsp90 inhibition that avoid induction of the heat shock response should be pursued where selective client protein degradation is possible. These strategies will be discussed below with a particular emphasis on the selective disruption of Hsp90-co-chaperone interactions

I.6.2 *Disruption of Hsp90's interaction with client proteins.*

Most strategies for Hsp90 inhibition elicit an unbiased degradation of client proteins. The multipronged biological consequences of these strategies are desirable for aggressive treatment of a subset of cancers that display multilateral cell signaling cascade deregulation. However, the effects of global Hsp90 client degradation over an extended time course are unknown. The potential toxic effects of long-term Hsp90 inhibitor administration may thwart their indication for chronic cancer management or other disease states.

The aberrant expression or deregulation of a single biological pathway is implicated in some cancers and various other disease states. Targeting specific, rather than global, Hsp90 client degradation in such disease states may prove to be a more efficacious treatment strategy. Such an inhibitor would avoid potential toxicities due to global client degradation and allow the application of selective Hsp90 inhibition for chronic therapy. Targeting selective Hsp90 client protein degradation is under investigated, however, success in this realm has been achieved. The nine amino acid polypeptide, shepherdin, displays anticancer activity by selectively disrupting the survivin client protein association with Hsp90.[136, 137]

Survivin, a cancer promoting Hsp90 client protein, has emerged as a validated target for cancer chemotherapy.[138] As a member of the "Inhibitors of Apoptosis" protein family, survivin manifests anti-apoptotic/cancer promoting effects through caspase inhibition.[139] While survivin is highly expressed in most tumors, terminally differentiated cell lines are devoid of survivin expression.[140] Selective disruption of the Hsp90-survivin interaction has been achieved. Plescia, *et al.* designed the polypeptide shepherdin by first determing survivin amino acid residues critical to the interaction with Hsp90. The researchers observed pronounced survivin-Hsp90 disruption for mutations of survivin residues 79 – 87. Following incubation of this amino acid sequence (KHSSGCAFL, shepherdin) client selective degradation of survivn was observed. This effect is cancer cell specific, as normal cell lines were unaffected by shepherdin administration. However, pan client protein degradation was observed at increased shepherdin concentrations. The survivin binding domain of Hsp90 is proximal to the N-terminal ATP binding pocket. The observation of pan client degradation may result from ATP displacement by shepherdin at increased concentrations. Interestingly, shepherdin treatment does not lead to induction of a heat

Figure 1.9. Examples of HDAC inhibitors that manifest Hsp90-dependent client protein degradation.
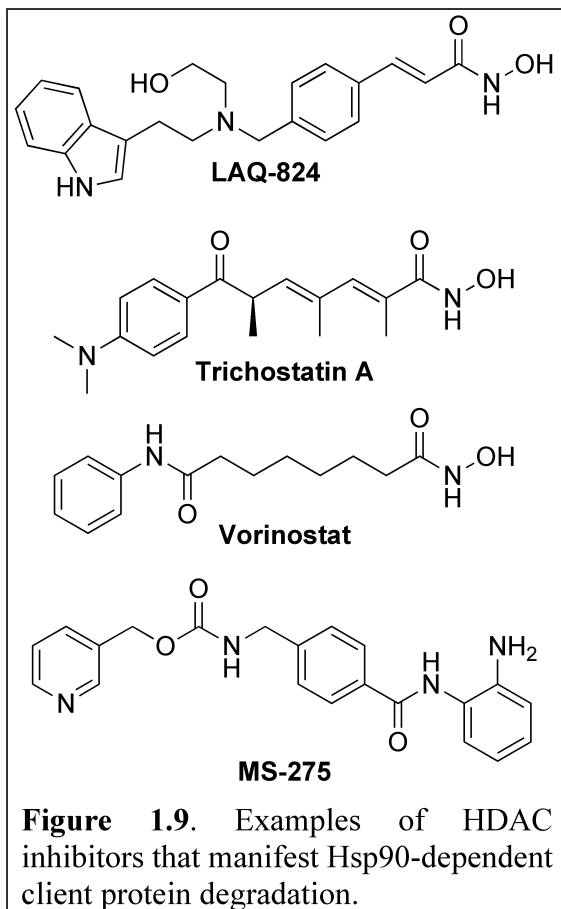
shock response.[141] The design of shepherdin represents an important discovery toward targeting selective client protein degradation.

I.6.3 *Hsp90 Hyperacetylation by HDAC Inhibition*

Histone deacetylase (HDAC) inhibition represents a target for cancer chemotherapy with multiple anticancer effects. In adition to catalyzing lysine deacetylation on histones, HDACs also deacetylate lysines on Hsp90 and other proteins.[142, 143] Specifically, HDAC6 has been shown to deacetylate Hsp90, and a role for HDAC1 in this process has also been proposed.[144] Inhibitors of HDAC6 present a novel opportunity for indirect Hsp90 inhibition that avoids induction of the heat shock response. Prior studies have demonstrated that the super chaperone complex is inactivated by Hsp90 hyperacetylation during HDAC knockdown.[145] siRNA induced HDAC6 specific or global HDAC knockdown as well as treatment with HDAC6 specific or pan-HDAC inhibitors effectively dissolves Hsp90/client protein association. Several selective and pan-HDAC inhibitors have been investigated for their effects on Hsp90, including trichostatin A,[146] LAQ-824,[147] vorinostat,[148] and MS-275 (Figure 1.9),[149] all of which led to degradation of Hsp90-dependent client proteins and manifestation of anti-proliferative effects. Specific inhibition of HDAC6 using siRNA has manifested induction of the heat shock response,

however, the non-specific HDAC inhibitors FK228 and vorinostat lead to hyperacetylation of both Hsp90 and Hsp70, and demonstrate no heat shock response.[148]

I.6.4 *Targeting Co-chaperone-Hsp90 interactions.*

Hsp90 is the central component of a large cohort of proteins that comprise the super chaperone complex.[150] Each protein-protein interaction presents the opportunity for disruption of the protein folding process, and therefore, a potential therapeutic target. In addition, the requirement for different super chaperone components of specific client proteins may allow for selective client targeting. To date, three such approaches are being investigated and include the interaction between Hsp90 and the partner protein HOP, co-chaperone CDC37, and co-chaperone F_1F_o-ATP synthase. The latter two approaches are central to the focus of this dissertation.

Disruption of the HOP/Hsp90 interaction.

HOP is essential for facilitating client protein loading to Hsp90, and is therefore an essential component of the protein folding process.[75] Small molecule disruptors of this protein-protein interaction are
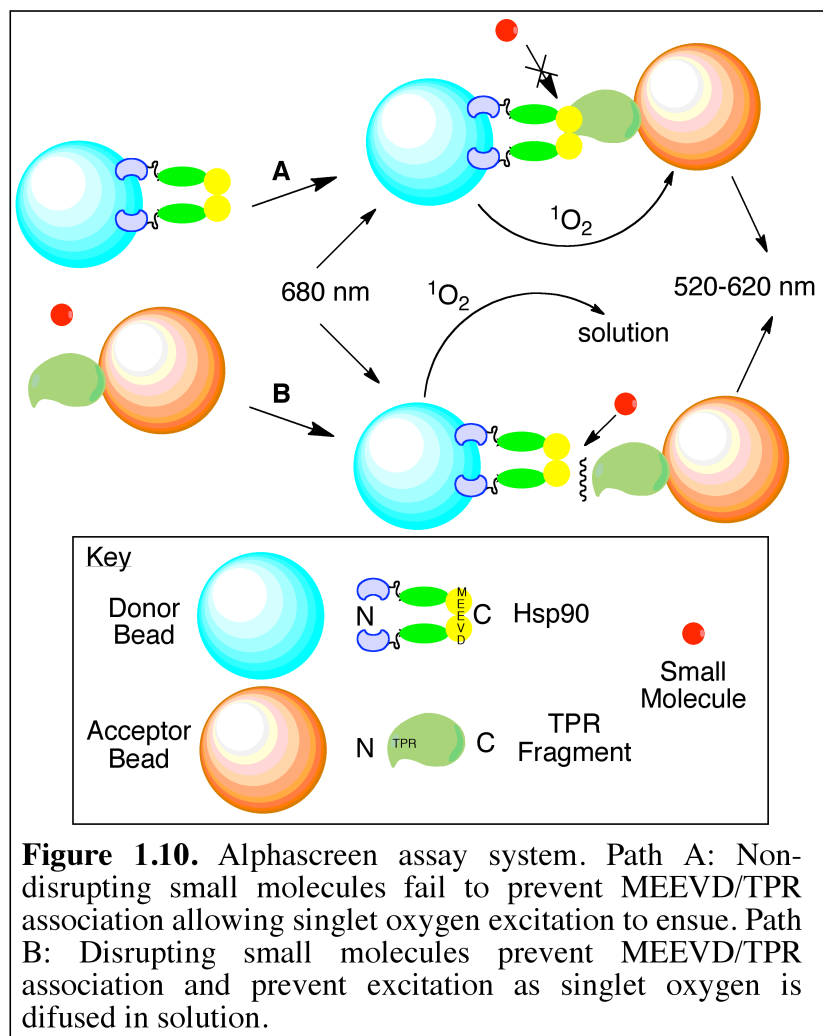
Figure 1.10. Alphascreen assay system. Path A: Non-disrupting small molecules fail to prevent MEEVD/TPR association allowing singlet oxygen excitation to ensue. Path B: Disrupting small molecules prevent MEEVD/TPR association and prevent excitation as singlet oxygen is difused in solution.

capable of preventing Hsp90 client proteins from receiving chaperone activity. No natural product inhibitors have been described that manifest this

Figure 1.11. Compounds identified through AlphaScreen HTS to inhibit Hsp90/Hop interaction by binding to the TPR domain of HOP
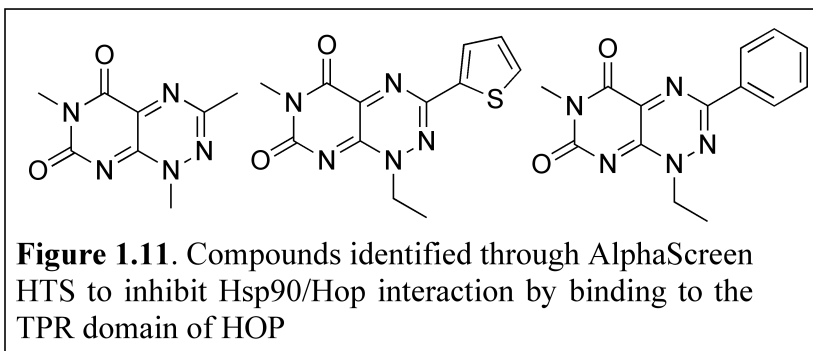
biological activity. However, Yi and Regan have reported the identification of a class of synthetic small molecules capable of disrupting this interaction by binding to the TPR domain of HOP.[49, 50] The researchers developed an AlphaScreen-based high-throughput assay capable of identifying this desired phenotype (Figure 1.10). Succinctly, Hsp90 is N-terminally linked to a donor bead while an N-terminal TPR expressing protein fragment is C-terminally linked with an acceptor bead. The TPR domain is free to interact with the MEEVD domain of Hsp90. Excitation of the donor bead at 680 nm leads to the production of singlet oxygen, which is capable of traveling the 200 nm distance between the donor and acceptor. If the MEEVD and TPR domains are interacting, the acceptor bead undergoes chemiluminescence at 520 nm to 620 nm. In the presence of a HOP/Hsp90 disruptor, the MEEVD and TPR domains are kept separate, and no chemiluminescence is observed. Several small molecules were identified during initial screening with this assay (Figure 1.11). Although optimization of the hit compounds has not been reported, the results appear encouraging. Of note, these small molecule disrupters do not appear to manifest the heat shock response, suggesting that disruption of the HOP/Hsp90 complex could eventually lead to efficacious alternatives to N-terminal inhibition.

Disruption of the Hsp90/CDC37 interaction.

CDC37 is required for the maturation of Hsp90-dependent protein kinases, and is critical for the stabilization of several otherwise unstable oncoprotein kinases, e.g. BRAF and EGFRvIII,

in cancer cells.[151-154] CDC37 overexpression has been linked to oncogenic transformation, and interruption of its interaction with Hsp90 has been explored as a therapeutic target.[155-157] siRNA experiments have been conducted that demonstrate CDC37 knockdown is associated with the depletion of several Hsp90 protein kinase clients including HER-2, RAF-1, CDK4, and AKT. Also of significance, siRNA-mediated knockdown of CDC37 does not induce the heat shock response, therefore providing a favorable mechanism for Hsp90 modulation.[158, 159]

Prior to the work described herein, the natural product celastrol was the only compound reported to disrupt Hsp90/CDC37 protein-protein interactions.[48] Celastrol (Figure 1.12) is a quinone methide triterpene isolated from

Figure 1.12. Celastrol, a known Hsp90 inhibitor that disrupts the Hsp90/CDC37 interaction, gedunin (this work), a potential disruptor.

Tripterygium wilfordii Hook F. (the Chinese Thunder of God vine).[160] It has been hypothesized that celastrol targets the Hsp90 N-terminus at the binding site of CDC37, effectively blocking the protein-protein interaction from occurring.[48] However, a recent report suggests that celastrol forms a Michael adduct with cysteine residues of CDC37, and therefore acts as an irreversible inhibitor.[161] Celastrol has also been reported to induce the heat shock response, in concert with its Hsp90/CDC37 disrupting activity.[162, 163] It appears as though celastrol may manifest anti-proliferative effects through several mechanisms, and therefore, further studies into the exact mechanism of celastrol's inhibitory effects on Hsp90 remain under investigation.

Identification and subsequent validation of celastrol as a small molecule disruptor of Hsp90/CDC37 interactions could lead to the elucidation of additional small molecules that exhibit similar activities. For instance, celastrol was recognized as a novel Hsp90 inhibitor from evaluation of its biological effects through the novel Connectivity Map technology.

The Connectivity Map technology represents a systematic tool for identifying connections between diseases, genetic perturbations, and drug action. This technology provides potential for the discovery of novel protein targets and lead compounds for the development of directed therapeutic strategies against various disease states. Briefly, a "connectivity map" is generated by evaluating the positive or negative expression levels of mRNA that result upon incubation of small molecules with cellular models of various diseases. It was hypothesized that similar profiles of mRNA expression levels after evaluation would be indicative of small molecules that manifest similar mechanisms of action or related protein dysfunctions. In a demonstration of connectivity mapping, Lamb *et al*. evaluated several small molecules and disease states and determined "connections" during their publication. Of significance, the natural products gedunin and celastrol were identified as inhibitors of the Hsp90 protein folding machinery through this technology.[164]

Gedunin (Figure 1.12), a tetranortriterpenoid from *Azadirachta indica* (Indian Neem Tree) was simultaneously identified with celastrol in the seminal studies of the Connectivity Map.[164, 165] Structural similarities between celastrol and gedunin, along with the similar applications in traditional medicinal of their respective sources,[166-168] indicate a potential common mechanism of action. Both the Thunder of God vine and the Neem Tree are used in traditional medicine practices to treat a variety of inflammatory and auto-immune diseases including cancer, and both natural products manifest anti-spermatogenic properties.[169, 170]

Figure 1.13. Structural diagram of membrane bound FAS. F_o domain is housed within the innermitochondrial membrande projecting the F_1 domain into the mitochondrial matrix. During ATP synthesis, H^+'s are shuttled from the innermitochondrial space into the matrix.
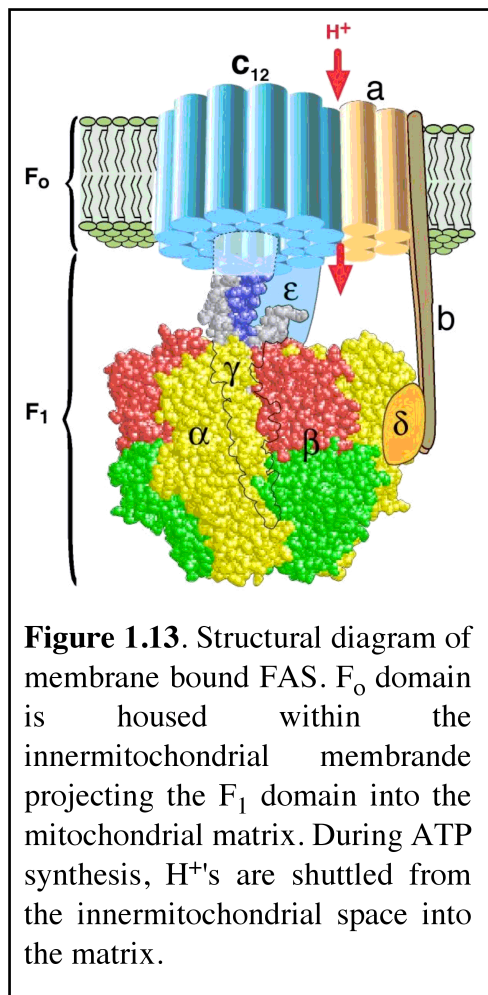
Through connectivity map screening, both celastrol and gedunin induced expression levels of varying mRNA molecules analogous to 17-AAG. Hsp90 inhibition was then validated through Western blot analyses to demonstrate the induced degradation of Hsp90-dependent client proteins. While celastrol has not undergone extensive investigation, a significant effort toward the application of gedunin as a lead compound for anticancer therapy is described in Chapter II. The synthesis of several semi-synthetic analogues and their biological activity will be described, as well as a detailed description of evidence suggesting that gedunin manifests Hsp90 inhibition by disruption of the Hsp90/CDC37 interaction.[171]

Disruption of the F_1F_o-ATP synthase/Hsp90 Interaction

F_1F_o-ATP synthase (FAS) is a highly conserved, multidomain containing macromolecular motor localized to the innermitochondrial membrane (Figure 1.13).[172] A majority of the ATP required for every cellular event is provided by FAS-catalyzed oxidative phosphorylation of ADP.[173] As such, proper FAS function is critical for maintaining homeostasis under normal conditions, while aberrant function is associated with several disease states (e.g. cancer, autoimmune disorders, or cardiac ischemia) and is a therapeutic target of interest.[174] A discussion of FAS as a target for cancer chemotherapy will be detailed in Chapter IV.

While FAS manifests dual catalytic propensity, capable of either ATP synthesis or hydrolysis, the membrane potential that exists as a result of the proton motive force between the perimembrane space and the mitochondrial matrix drives ATP synthesis under typical conditions.[175] The F_o domain of FAS contains the binding site of the natural product inhibitor oligomycin and is membrane bound, largely hydrophobic, and consists of three subunits, *a*, *b*, and *c* of respective stoichiometry 1:2:12. The F_o domain subunits combine to form the proton pore that rotates as individual protons are actively transported from the innermitochondrial space to the mitochondrial matrix. Rotation of the F_o domain results in likewise rotation of the stalk that bridges this domain to the F_1 domain wherein ATP synthesis occurrs. The F_1 domain is comprised of the α, β, γ, δ, ε subunitis of respective stoichiometry 3:3:1:1:1. The β and γ subunits form the central stalk that tethers the two domains and couples ATP synthesis to proton transport.[176]

Until very recently, the observation of ectopically expressed FAS was highly controversial. In early reports where FAS was discovered in extramitochondrial cellular locations (e.g. in the plasma membrane or endoplasmic reticulum) this observation was assumed to be the result of sample contamination.[177] Modern proteomic techniques for fractionating and analyzing specific cellular compartments has ruled this possibility out and not only confirmed the presence of ectopically expressed FAS, but delineated several possible biological roles for this expression.[177] One such role involves the discovery FAS is an Hsp90 co-chaperone and component of the super chaperone complex.

The co-chaperoning propensity of FAS was discovered by Papathanassiu *et al.* through several co-immunoprecipitation experiments. FAS was found to immunoprecipitate from cancer cell lysates with both Hsp90 and several Hsp90 client proteins.[178] This report was the first

indication of the chaperoning capability and association of FAS with Hsp90. Additional evidence for such an association has since been observed in both mammalian cell lines and yeast strains.[179]

Following the discovery of FAS involvement in the super chaperone complex, the researchers investigated the effects of three known FAS inhibitors (i.e. efrapaptin, oligomycin, and 7-chloro-4-nitrobenzo-2-oxa-1,3-diazole) on Hsp90 activity.[178, 180] Each FAS inhibitor adversely impacted the co-chaperoning activity of FAS, as no immunoprecipitation was observed between FAS and Hsp90 or client proteins in the presence of inhibitors. Typical antiproliferative activity after incubation of various inhibitor concentrations in breast and colon cancer cell lines, but three distinct features of indirect Hsp90 inhibition by FAS inhibitors were observed. 1) Effects of FAS inhibition on Hsp90 occurred independent of cellular ATP levels suggesting the FAS-Hsp90 relationship extended beyond the ability of FAS to supply ATP. At FAS inhibitor concentrations that caused protein degradation, ATP levels remained unchanged. Additionally, the Hsp90-FAS interaction remained unaffected in cancer cells treated with rotenone, a non-FAS targeting cellular ATP depleter. 2) Hsp70 and Hsp90 detection by western blot analysis demonstrated no induction of the heat shock response, as both proteins were degraded in a dose dependent manner, suggesting that FAS inhibition is not coupled to HSF1-Hsp90 association. 3) Selective client protein degradation was also observed. While FAS co-immunoprecipitated with Hsp90, ERα, and mutant p53 in several cancer cell lines, FAS inhibitors selectively prevented FAS immunoprecipitation with Hsp90, ERα, and mutant p53, but had no effect on the RAF-1 kinase client.

These initial discoveries indicate that targeting FAS for indirect Hsp90 inhibition is an attractive strategy for selective client protein degradation that avoids the heat shock response. Promising results were obtained from the investigation of efrapeptins, oligomycin, and 7-chloro-

4-nitrobenzo-2-oxa-1,3-diazole, however, all of these inhibitors display a high degree of cross-activity with other ATPases, such as the Vacuolar- and Na,K-ATPases.[180, 181] In fact, this is a common feature of most known FAS inhibitors. Cruentaren A is a cytotoxic polyketide macrocycle belonging to the benzolactone class of natural products that selectively targets FAS with no affinity for any other ATPase.[182-184] As a means to facilitate evaluation of indirect Hsp90 inhibition by a selective FAS inhibitor, the convergent total synthesis of cruentaren A is described in Chapter III.

I.7   Concluding Remarks

Hsp90 has emerged as a therapeutic target to treat a variety of disease states including cancer, neurodegenerative disorders, inflammation, pathogenic infection, cystic fibrosis, and may represent a novel based strategy to ameliorate male contraception. At present, clinical applications for Hsp90 modulation have focused primarily on the treatment of cancer, and all clinically administered agents are competitive inhibitors of the N-terminal ATP binding site. While efficacy is achieved, induction of the heat shock response occurs, leading to potential drawbacks for N-terminal inhibitory use. Results from ongoing clinical trials will be integral in determining whether induction of the heat shock response will produce clinical limitations for N-terminal Hsp90 inhibitors as anti-cancer agents.

Induction of a heat shock response is desirable in some therapeutic areas where a deficiency of Hsp chaperoning activity is observed.   Examples include various neurodegenerative disorders, aberrant inflammatory and immuno-response diseases, and cardio-protection. Non-toxic, N-terminal inhibitors could find application in these areas, however, none of these currently exist.

In contrast, a subset of disorders would benefit from the clinical development of Hsp90 inhibitors that do not induce the heat shock response. In particular, agents that cause the disruption of Hsp90/co-chaperone interactions may be of particular importance as these also demonstrate selective client protein degradation. In the case of CDC37-Hsp90 disruptors, selective degradation of kinase clients is observed. FAS inhibitors that disrupt the co-chaperone's association with Hsp90 also demonstrate selective client protein degradation, but further investigation is required to delineate what characteristic clients are affected.

The past fifteen years have witnessed an exponential growth in Hsp90 research. From defining Hsp90s role in numerous biological processes to validating Hsp90 as target for cancer chemotherapy, and at present, establishing Hsp90 as a potential target for other therapeutic areas.

I.8   References

1.   Accardi, R.; Adebamowo, C.; Anderson, B.; Autier, P.; Baan, R.; Barbacid, M.; Boffetta, P.; Boniol, M.; Boyle, P.; Brady, J.; Bredart, A.; Brennan, P.; Burrion, J.-B.; Caboux, E.; Cavalli, F.; Cho, Y.-e.; Clifford, G.; Cogliano, V.; Curado, M.-P.; Currow, D.; Dangou, J.-M.; Dinshaw, K.; Dolbeault, S.; Dore, J.-F.; Doroshenk, M.; Duell, E.; Farfan, M.; Farrington, J.; Feijo, R.; Ferlay, J.; Ferrari, P.; Franceschi, S.; hainaut, P.; Hasan, U.; Hashibe, M.; Heanue, M.; Heck, J.; Herceg, Z.; Herron, L.-M.; Hung, R. J.; Jenab, M.; Kasler, M.; Kerr, D.; Keita, N.; Kovar, H.; Vecchia, C. l.; Leon-Roux, M.; Levin, B.; Li, N.; Madi, H.; Maisonneuve, P.; McArdle, K.; McKay, J.; McVie, G.; Muwonge, R.; Nascimento, M.-C.; Ngoma, T.; Ohgaki, H.; Omi, S.; Pelucchi, C.; Ashton, L. P.; Plianbangchang, S.; Plummer, M.; Plymoth, A.; Qing, Q.; Ramadas, K.; Randi, G.; Razavi, D.; Rinaldi, S.; Ringborg, U.; Rizzo, S.; Rodger, A.; Roses, M.; Samiei, M.; Sankaranarayanan, R.; Sauvaget, C.; Scelo, G.; Schier, M. J.; Semiglazov, V.; Shin, H.-R.; Srivastava, S.; Steliarova-Foucher, E.; Straif, K.; Sylla, B.; Tavtigian, S.; Tommasino, M.;

Tuncer, M.; Karsa, L. v.; Weis, J.; Zeng, Y.-X.; Zhang, Y.; Zhao, P.; Zheng, T. *World Cancer Report 2008*; International Agency for Research on Cancer: Lyon Cedex, 2008.

2.   Padmanabhan, S.; Ravella, S.; Curiel, T.; Giles, F. Current status of therapy for chronic myeloid leukemia: a review of drug development. *Future Oncol.* **2008,** 4, 359-377.

3.   La Vine, D. B. T.; Coleman, T. A.; Davis, C. H.; Carbonell, C. E.; Davis, W. B. Frequent dose interruptions are required for patients receiving oral kinase inhibitor therapy for advanced renal cell carcinoma. *Am. J. Clin. Oncol.* **2010,** 33, 217-220.

4.   Lee, F.; Fandi, A.; Voi, M. Overcoming kinase resistance in chronic myeloid leukemia. *Int. J. Biochem. Cell Biol.* **2008,** 40, 334-343.

5.   Brandt, G. E. L.; Blagg, B. S. J. Alternate strategies of Hsp90 modulation for the treatment of cancer and other diseases. *Curr. Top. Med. Chem.* **2009,** 9, 1447-1461.

6.   Paul, S. Dysfunction of the ubiquitin-proteasome system in multiple disease conditions: therapeutic approaches. *Bioessays.* **2008,** 30, 1172-1184.

7.   Messaed, C.; Rouleau, G. A. Molecular mechanisms underlying polyalanine diseases. *Neurobiol. Dis.* **2009,** 34, 397-405.

8.   Thomas, S. R.; Witting, P. K.; Drummond, G. R. Redox control of endothelial function and dysfunction: molecular mechanisms and therapeutic opportunities. *Antioxid. Redox. Signal.* **2008,** 10, 1713-1753.

9.   Clavaguera, F.; Bolmont, T.; Crowther, R. A.; Abramowski, D.; Frank, S.; Probst, A.; Fraser, G.; Stalder, A. K.; Staufenbiel, M. B. M.; Jucker, M.; Goedert, M.; Tolnay, M. Transmission and spreading of tauopathy in transgenic mouse brain. *Nat. Cell Biol.* **2009,** 11, 909-914.

10.   Vardiman, J. W. Chronic myelogenous leukemia, BCR-ABL1+. *Am. J. Clin. Pathol.* **2009,** 132, 250-260.

11.   Jouret, F.; Devuyst, O. CFTR and defective endocytosis: new insights in the renal phenotype of cystic fibrosis. *Pflugers Arch.* **2009,** 457, 1227-1236.

12.   Naidoo, N. The endoplasmic reticulum stress response and aging. *Rev. Neurosci.* **2009,** 20, 23-37.

13.   Alcain, F. J.; Villalba, J. M. Sirtuin activators. *19* **2009,** 4, 403-414.

14.   Lehman, N. L. The ubiquitin proteasome system in neuropathology. *Acta Neuropathol.* **2009,** 118, 329-347.

15.   Wegele, H.; Muller, L.; Buchner, J. Hsp70 and Hsp90-a relay team for protein folding. *Rev. Physiol. Biochem. Pharmacol.* **2004,** 151, 1-44.

16.   Soti, C.; Nagy, E.; Giricz, Z.; Vigh, L.; Csermely, P.; Ferdinandy, P. Heat shock proteins as emerging therapeutic targets. *Br. J. Pharmacol.* **2005,** 146, 769-780.

17.   Soo, E. T. L.; Yip, G. W. C.; Lwin, Z. M.; Kumar, S. D.; Bay, B.-H. Heat shock proteins as novel therapeutic targets in cancer. *in vivo* **2008,** 22, 311-316.

18.   Caplan, A. J.; Mandal, A. K.; Theodoraki, M. A. Molecular chaperones and protein kinase quality control. *Trends Cell. Biol.* **2007,** 17, 87-92.

19.   Pearl, L. H.; Prodromou, C.; Workman, P. The Hsp90 molecular chaperone: an open and shut case for treatment. *Biochem. J.* **2008,** 410, 439-453.

20.   Neckers, L.; Tsutsumi, S.; Mollapour, M. Visualizing the twists and turns of a molecular chaperone. *Nat. Struct. Mol. Biol.* **2009,** 16, 235-236.

21.   Wandinger, S. K.; Richter, L.; Buchner, J. The Hsp90 chaperone machinery. *J. Biol. Chem.* **2008,** 283, 18473-18477.

22.   Whitesell, L.; Bagatell, R.; Falsey, R. The stress response: implications for the clinical development of Hsp90 inhibitors. *Curr. Cancer Drug Targets* **2003,** 3, 349-358.

23.   Csermely, P.; Schnaider, T.; Soti, C.; Prohaszka, Z.; Nardai, G. The 90-KDa molecular chaperone family: structure, function, and clinical applications. A comprehensive review. *Pharmacol. Ther.* **1998,** 79, 129-168.

24.   Maloney, A.; Clarke, P. A.; Workman, P. Genes and proteins governing the cellular sensitivity to Hsp90 inhibitors: a mechanistic perspective. *Curr. Cancer Drug Targets* **2003,** 3, 331-341.

25.   Solit, D. B.; Chiosis, G. Development and application of Hsp90 inhibitors. *Drug Discov. Today* **2008,** 13, 38-43.

26.   Stravopodis, D. J.; Margaritis, L. H.; Voutsinas, G. E. Drug-mediated targeted disruption of multiple protein activities through functional inhibition of the Hsp90 Chaperone Complex. *Curr. Med. Chem.* **2007,** 14, 3122-3138.

27.   Bishop, S. C.; Burlison, J. A.; Blagg, B. S. J. Hsp90: a novel target for the disruption of multiple signaling cascades. *Curr. Cancer Drug Targets* **2007,** 7, 369-388.

28.   Chaudhury, S.; Welch, T. R.; Blagg, B. S. J. Hsp90 as a target for drug development. *ChemMedChem* **2006,** 1, 1331-1340.

29.   Blagg, B. S. J.; Kerr, T. D. Hsp90 inhibitors: small molecules that transform the Hsp90 protein folding machinery into a catalyst for protein degradation. *Med. Res. Rev.* **2006,** 26, 310-338.

30.   Solit, D. B.; Rosen, N. Hsp90: a novel target for cancer therapy. *Curr. Top. Med. Chem.* **2006,** 6, 1205-1214.

31.   Donnelly, A.; Blagg, B. S. J. Novobiocin and additional inhibitors of the Hsp90 C-terminal nucleotide-binding pocket. *Curr. Med. Chem.* **2008,** 15, 2702-2717.

32.   Amolins, M. W.; Blagg, B. S. J. Natural product inhibitors of Hsp90: potential leads for drug discovery. *Mini Rev. Med. Chem* **2009,** 9, 140-152.

33.   Tash, J. S.; Chakrasali, R.; Jakkaraj, S. R.; Hughes, J.; Smith, S. K.; Hornbaker, K.; Heckert, L. L.; Ozturk, S. B.; Hadden, M. K.; Kinzy, T. G.; Blagg, B. S. J.; Georg, G. I. Gamendazole, an orally active indazole carboxylic acid male contraceptive agent, targets Hsp90AB1 (Hsp90BETA) and EEF1A1 (eEf1A), and stimulates Il1a transcription in rat sertoli cells. *Biol. Reprod.* **2008,** 78, 1139-1152.

34.   Hadden, M. K.; Lubbers, D. J.; Blagg, B. S. J. Geldanamycin, radicicol, and chimeric inhibitors of the Hsp90 N-terminal ATP binding site. *Curr. Top. Med. Chem.* **2006,** 6, 1173-1182.

35.   Workman, P. Overview: translating Hsp90 biology into Hsp90 drugs. *Curr. Cancer Drug Targets* **2003,** 3, 297-300.

36.   Chiosis, G.; Rodina, A.; Moulick, K. Emerging Hsp90 inhibitors: from discovery to clinic. *Anticancer Agents Med. Chem.* **2006,** 6, 1-8.

37.   Breinig, M.; Caldas-Lopes, E.; Goeppert, B.; Malz, M.; Rieker, R.; Bergmann, F.; Schirmacher, P.; Mayer, M.; Chiosis, G.; Kern, M. A. Targeting heat shock protein 90 with non-quinone inhibitors: a novel chemotherapeutic approach in human hepatocellular carcinoma. *Hepatology* **2009,** 50, 102-112.

38.   Li, X.; Shocron, E.; Song, A.; Patel, N.; Sun, C. L. Discovery of 5-substituted 2-amino-4-chloro-8-((4-methoxy-3,5-dimethylpyridin-2-yl)methyl)-7,8-dihydropteridin-6(5H)-ones   as potent and selective Hsp90- inhibitors. *Bioorg. Med. Chem. Lett.* **2009,** 19, 2860-2864.

39.   Hadden, M. K.; Blagg, B. S. J. Synthesis and evaluation of radamide analogues, a chimera of radicicol and geldanamycin. *J. Org. Chem.* **2009,** 74, 4697-4704.

40.   Duerfeldt, A. S.; Brandt, G. E. L.; Blagg, B. S. J. Design, synthesis, and biological evaluation of conformationally constrained cis-amide Hsp90 inhibitors. *Org. Lett.* **2009,** 11, 2353-2360.

41.   Wang, M.; Shen, G.; Blagg, B. S. J. Radanamycin, a macrocyclic chimera of radicicol and geldanamycin. *Bioorg. Med. Chem. Lett.* **2006,** 16, 2459-2462.

42.   Shen, G.; Blagg, B. S. J. Radester, a novel inhibitor of the Hsp90 protein folding machinery. *Org. Lett.* **2005,** 7, 2157-2160.

43.   Clevenger, R. C.; Blagg, B. S. J. Design, synthesis, and evaluation of a radicicol and geldanamycin chimera, radamide. *Org. Lett.* **2004,** 6, 4459-4462.

44.   Shen, G.; Yu, X. M.; Blagg, B. S. Syntheses of photolabile novobiocin analogues. *Bioorg. Med. Chem. Lett.* **2004,** 14, 5903-5906.

45.   Yu, X. M.; Shen, G.; Neckers, L.; Blake, H.; Holzbeierlein, J.; Cronk, B.; Blagg, B. S. J. Hsp90 inhibitors identified from a library of novobiocin analogues. *J. Am. Chem. Soc.* **2005,** 127, 12778-12779.

46.   Marcu, M. G.; Schulte, T. W.; Neckers, L. Novobiocin and related coumarins and depletion of heat shock protein 90-dependent signaling proteins. *J. Natl. Cancer Inst.* **2000,** 92, 242-248.

47.   Marcu, M. G.; Chadli, A.; Bouhouche, I.; Catelli, M.; Neckers, L. M. The heat shock protein 90 antagonist novobiocin interacts with a previously unrecognized ATP-binding domain in the carboxyl terminus of the chaperone. *J. Biol. Chem.* **2000,** 275, 37181-37186.

48.   Zhang, T.; Hamza, A.; Cao, X.; Wang, B.; Yu, S.; Zhan, C.-G.; Sun, D. A novel Hsp90 inhibitor to disrupt Hsp90/Cdc37 complex against pancreatic cancer cells. *Mol. Cancer Ther.* **2008,** 7, 162-170.

49.   Yi, F.; Regan, L. A novel class of small molecule inhibitors of Hsp90. *ACS Chem. Biol.* **2008,** 3, 645-654.

50.   Yi, F.; Zhu, P.; Southall, N.; Inglese, J.; Austin, C. P.; Zheng, W.; Regan, L. An Alphascreen-based high-throughput screen to identify inhibitors of Hsp90-cochaperone interaction. *J. Biomol. Screen.* **2009,** 14, 273-281.

51.   Cortajarena, A. L.; Yi, F.; Regan, L. Designed TPR modules as novel anticancer agents. *ACS Chem. Biol.* **2008,** 3, 161-166.

52.   Usmani, S. Z.; Bona, R.; Li, Z. 17 AAG for Hsp90 inhibition in cancer--from bench to bedside. *Curr. Mol. Med.* **2009,** 9, 654-664.

53.   Tofilon, P. J.; Camphausen, K. Molecular Targets for Tumor Radiosensitization. *Chem. Rev.* **2009,** 109, 2974-2988.

54.   Banerji, U. Heat shock protein 90 as a drug target: some like it hot. *Clin. Cancer Res.* **2009,** 15, 9-14.

55.   Solit, D. B.; Osman, I.; Polsky, D.; Panageas, K. S.; Daud, A.; Goydos, J. S.; Teitcher, J.; Wolchok, J. D.; Germino, F. J.; Krown, S. E.; Coit, D.; Rosen, N.; Chapman, P. B. Phase II trial of 17-allylamino-17demethoxygeldanamycin in patients with metastatic melanoma. *Clin. Cancer Res.* **2008,** 14, 8302-8307.

56.   Neckers, L. Using natural product inhibitors to validate Hsp90 as a molecular target in cancer. *Curr. Top. Med. Chem.* **2006,** 6, 1163-1171.

57.   Pratt, W. B.; Morishima, Y.; Osawa, Y. The Hsp90 chaperone machinery regulates signaling by modulating ligand binding clefts. *J. Biol. Chem.* **2008,** 283, 22885-22889.

58.   Voellmy, R.; Boellmann, F. Chaperone Regulation of the Heat Shock Protein Response. In *Molecular Aspects of the Stress Response: Chaperones, Membranes and Networks*, Csermely, P.; Vigh, L., Eds. Landes Bioscience and Springer Science+Business Media: New York, 2007; Vol. 594, pp 89-99.

59.   Zuehlke, A.; Johnson, J. L. Hsp90 and co-chaperones twist the functions of diverse client proteins. *Biopolymers* **2009,** 93, 211-217.

60.   Powers, M. V.; Workman, P. Targeting of multiple signalling pathways by heat shock protein 90 molecular chaperone inhibitors. *Endocr. Relat. Cancer* **2006,** 13, 125-135.

61.   Nadeau, K.; Das, A.; Walsh, C. T. Hsp90 chaperonins posses ATPase activity and bind heat shock transcription factors and peptidyl prolyl isomerases. *J. Biol. Chem.* **1993,** 268, 1479-1487.

62.   Obermann, W. M. J.; Sondermann, H.; Russo, A. A.; Pavletich, N. P.; Hartl, F. U. In vivo function of Hsp90 is dependent on ATP binding and ATP hydrolysis. *J. Cell Biol.* **1998,** 143, 901-910.

63.   Panaretou, B.; Prodromou, C.; Roe, S. M.; O'Brien, R.; Ladbury, J. E.; Piper, P. W.; Pearl, L. H. ATP binding and hydrolysis are essential to the function of the Hsp90 molecular chaperone in vivo. *EMBO J.* **1998,** 17, 4829-4836.

64.   Pearl, L. H.; Prodromou, C. Structure and mechanism of the Hsp90 molecular chaperone machinery. *Annu. Rev. Biochem.* **2006,** 75, 271-294.

65.   Prodromou, C.; Siligardi, G.; O'Brien, R.; Woolfson, D. N.; Regan, L.; Panaretou, B.; Ladbury, J. E.; Piper, P. W.; Pearl, L. H. Regulation of Hsp90 ATPase activity by tetracopeptide repeat (TPR)-domain co-chaperones. *EMBO J.* **1999,** 18, 754-762.

66.   Retzlaff, M.; Stahl, M.; Eberl, H. C.; Lagleder, S.; Beck, J.; Kessler, H.; Buchner, J. Hsp90 is regulated by a switch point in the C-terminal domain. *EMBO Rep.* **2009,** 10, 1147-1153.

67.   Onuoha, S. C.; Coulstock, E. T.; Grossmann, J. G.; Jackson, S. E. Structural studies on the co-chaperone Hop and its complexes with Hsp90. *J. Mol. Biol.* **2008,** 379, 732-744.

68.   Yun, B. G.; Huang, W.; Leach, N.; Hartson, S. D.; Matts, R. L. Novobiocin induces a distinct conformation of Hsp90 and alters Hsp90-cochaperone-client interations. *Biochemistry* **2004,** 43, 8217-8229.

69.   Hartson, S. D.; Thulasiraman, V.; Huang, W.; Whitesell, L.; Matts, R. L. Molybdate inhibitos Hsp90. induces structural changes in its C-terminal domain, and alters its interactions with substrates. *Biochemistry* **1999,** 38, 3837-3849.

70.   Hartson, S. D.; Thulasiraman, V.; Huang, W.; Whitesell, L.; Matts, R. L. Molybdate inhibits Hsp90, induces structural changes in its C-terminal domain, and alters its interactions with substrates. *Biochemistry* **1999,** 38, 3837-3849.

71.   Garnier, C.; Lafitte, D.; Tsvetkov, P. O.; Barbier, P.; Leclerc-Devin, J.; Millot, J.-M.; Briand, C.; Makarov, A. A.; Catelli, M. G.; Peyrot, V. Binding of ATP to heat shock protein 90. *J. Biol. Chem.* **2002,** 277, 12208-12214.

72.   Soti, C.; Vermes, A.; Haystead, T. A. J.; Csermely, P. Comparative analysis of the ATP-binding sites of Hsp90 by nucleotide affinity cleavage: a distinct nucleotide specificity of the C-terminal ATP-binding site. *Eur. J. Biochem.* **2003,** 270, 2421-2428.

73. Chadli, A.; Bruinsma, E. S.; Stensgard, B.; Toft, D. Analysis of Hsp90 cochaperone interactions reveals a novel mechanism for TPR protein recognition. *Biochemistry* **2008,** 47, 2850-2857.

74. Odunuga, O. O.; Longshaw, V. M.; Blatch, G. L. Hop: more than and Hsp70/Hsp90 adaptor protein. *Bioessays.* **2004,** 26, 1058-1068.

75. Chen, S.; Smith, D. F. Hop as an adaptor in the heat shock protein 70 (Hsp70) and Hsp90 chaperone machinery. *J. Biol. Chem.* **1998,** 273, 35194-35200.

76. Reyes-del Valle, J.; Chavez-Salinas, S.; Medina, F.; del Angel, R. M. Heat shock protein 90 and heat shock protein 70 are components of dengue virus receptor complex in human cells. *J. Virol.* **2005,** 79, 4557-4567.

77. Caplan, A. J. What is a co-chaperone? *Cell Stress and Chaperones* **2003,** 8, 105-107.

78. Hainzl, O.; Lapina, M. C.; Buchner, J.; Richter, K. The charged linker region is an important regulator of hsp90 function. *J. Biol. Chem.* **2009,** 284, 22559-22567.

79. Hawle, P.; Siepmann, M.; Harst, A.; Siderius, M.; Reusch, H. P.; Obermann, W. M. The middle domain of Hsp90 acts as a discriminator between different types of client proteins. *Mol. Cell Biol.* **2006,** 26, 8385-8395.

80. Meyer, P.; Prodromou, C.; Hu, B.; Vaughan, C.; Roe, S. M.; Panaretou, B.; Piper, P. W.; Pearl, L. H. Structural and functional analysis of the middle sigment of Hsp90: implications for ATP hydrolysis and client protein and cochaperone interactions. *Mol. Cell.* **2003,** 11, 647-658.

81. Vaughan, C. K.; Gohlke, U.; Sobott, F.; Good, V. M.; Ali, M. M. U.; Prodromou, C.; Robinson, C. V.; Saibil, H. R.; Pearl, L. H. Structure of an Hsp90-Cdc37-Cdk4 complex. *Molecular Cell* **2006,** 23, 697-707.

82.   Lotz, G. P.; Lin, H.; Harst, A.; Obermann, W. M. J. Aha1 binds to the middle domain of Hsp90, contributes to client protein activation, and stimulates the ATPase activity of the molecular chaperone. *J. Biol. Chem.* **2003,** 278, 17228-17235.

83.   Dutta, R.; Inouye, M. GHKL, an emergent ATPase/kinase superfamily. *Trends Biochem. Sci.* **2000,** 25, 24-28.

84.   Stirling, P. C.; Bakhoum, S. F.; Feigl, A. B.; Leroux, M. R. Convergent evolution of clamp-like binding sites in diverse chaperones. *Nat. Struct. Mol. Biol.* **2006,** 13, 865-870.

85.   Prodromou, C.; Panaretou, B.; Chohan, S.; Siligardi, G.; O'Brien, R.; Ladbury, J. E.; Roe, S. M.; Piper, P. W.; Pearl, L. H. The ATPase cycle of Hsp90 drives a molecular 'clamp' via transient dimerization of the N-terminal domains. *EMBO J.* **2000,** 19, 4383-4392.

86.   Roe, S. M.; Ali, M. M.; Meyer, P.; Vaughan, C. K.; Panaretou, B.; Piper, P. W. The mechanism of Hsp90 regulation by the protein kinase-specific cochaperone p50cdc37. *Cell* **2004,** 11, 87-98.

87.   Cunningham, C. N.; Krukenberg, K. A.; Agard, D. A. Intra- and intermonomer interactions are required to synergistically facilitate ATP hydrolysis in Hsp90. *J. Biol. Chem.* **2008,** 283, 21170-21178.

88.   Hartson, S. D.; Irwin, A. D.; Shao, J.; Scroggins, B. T.; Volk, L.; Huang, W.; Matts, R. L. p50cdc37 is a nonexclusive Hsp90 cohort which participates intimately in Hsp90-mediated folding of immature kinase molecules. *Biochemistry* **2000,** 39, 7631-7644.

89.   Li, Y.; Zhang, T.; Schwartz, S. J.; Sun, D. New developments in Hsp90 inhibitors as anti-cancer therapeutics: mechanisms, clinical prespective and more potential. *Drug Resistance Updates* **2009,** 12, 17-27.

90.   Taldone, T.; Gozman, A.; Maharaj, R.; Chiosis, G. Targeting Hsp90: small-molecule inhibitors and their clinical development. *Curr. Opin. Pharmcol.* **2008,** 8, 370-374.

91.   Huang, K. H.; Veal, J. M.; Fadden, R. P.; Rice, J. W.; Eaves, J.; Strachan, J. P.; Barabasz, A. F.; Foley, B. E.; Barta, T. E.; Ma, W.; Silinski, M. A.; Hu, M.; Partridge, J. M.; Scott, A.; DuBois, L. G.; Freed, T.; Steed, P. M.; Ommen, A. J.; Smith, E. D.; Hughes, P. F.; Woodward, A. R.; Hanson, G. J.; McCall, W. S.; Markworth, C. J.; Hinkley, L.; Jenks, M.; Geng, L.; Lewis, M.; Otto, J.; Pronk, B.; Verleysen, K.; Hall, S. E. Discovery of novel 2-aminobenzamide inhibitors of heat shock protein 90 as potent, selective and orally active antitumor agents. *J. Med. Chem.* **2009,** 52, 4288-4305.

92.   Hanahan, D.; Weinberg, R. A. The hallmarks of cancer. *Cell* **2000,** 100, 57-70.

93.   Mahalingam, D.; Swords, R.; Carew, J. S.; Nawrocki, S. T.; Bhalla, K.; Giles, F. J. Targeting Hsp90 for cancer therapy. *Br. J. Cancer* **2009,** 100, 1523-1529.

94.   Koga, F.; Kihara, K.; Neckers, L. Inhibition of cancer invasion and metastasis by targeting the molecular chaperone heat-shock protein 90. *Anticancer Res.* **2009,** 29, 797-807.

95.   Chiosis, G.; Lopes, E. C.; Solit, D. Heat shock protein-90 inhibitors: a chronicle from geldanamycin to today's agents. *Curr. Opin Investig. Drugs* **2006,** 7, 534-541.

96.   Schmitt, E.; Gehrmann, M.; Brunet, M.; Multhoff, G.; Garrido, C. Intracellular and extracellular functions of heat shock proteins: repercussions in cancer therapy. *J. Leukoc. Bio.* **2007,** 81, 15-27.

97.   Pespeni, M.; Hodnett, M.; Pittet, J. F. In vivo stress preconditioning. *Methods* **2005,** 35, 158-164.

98.   Shamovsky, I.; Nudler, E. New insights into the mechanism of heat shock response activation. *Cell Mol. Life Sci.* **2008,** 65, 855-861.

99.   Guettouche, T.; Boellmann, F.; Lane, W. S.; Voellmy, R. Analysis of phosphorylation of human heat shock factor 1 in cells experiencing a stress. *BMC Biochem.* **2005,** 6.

100.   Bagatell, R.; Paine-Murrieta, G. D.; Taylor, C. W.; Pulcini, E. J.; Akinaga, S.; Benjamin, I. J.; Whitesell, L. Induction of a heat shock factor 1-dependent stress response alters the cytotoxic activity of Hsp90-binding agents. *Clin. Cancer Res.* **2000,** 6, 3312-3318.

101.   Lu, Y.; Ansar, S.; Michaelis, M. L.; Blagg, B. S. J. Neuroprotective activity and evaluation of Hsp90 inhibitors in an immortalized neuronal cell line. *Bioorg. Med. Chem.* **2009,** 17, 1709-1715.

102.   Ansar, S.; Burlison, J. A.; Hadden, M. K.; Yu, X. M.; Desino, K. E.; Bean, J.; Neckers, L.; Audus, K. L.; Michaelis, M. L.; Blagg, B. S. J. A non-toxic Hsp90 inhibitor protects neurons from Abeta-inducted toxicity. *Bioorg. Med. Chem. Lett.* **2007,** 17, 1984-1990.

103.   Peterson, L. B.; Blagg, B. S. J. To fold or not to fold: modulation and consequences of Hsp90 inhibition. *Future Medicinal Chemistry* **2009,** 1, 267-283.

104.   Rice, J. W.; Veal, J. M.; Fadden, R. P.; Barabasz, A. F.; Partridge, J. M.; Barta, T. E.; Dubois, L. G.; Huang, K. H.; Mabbett, S. R.; Silinski, M. A.; Steed, P. M.; Hall, S. E. Small molecule inhibitors of Hsp90 potently affect inflammatory disease pathways and exhibit activity in models of rheumatoid arthritis. *Arthritis Rheum.* **2008,** 58, 3765-3775.

105.   Stephanou, A.; Latchman, D. S.; Isenberg, D. A. The regulation of heat shock proteins and their role in systemic lupus erythematosus. *Semin. Arthritis Rheum.* **1998,** 28, 155-162.

106.   Chatterjee, A.; Black, S. M.; Catravas, J. D. Endothelial nitric oxide (NO) and its pathophysiologic regulation. *Vascul. Pharmacol.* **2008,** 49, 134-140.

107. Pittet, J.-F.; Lee, H.; Pespeni, M.; O'Mahony, A.; Roux, J.; Welch, W. J. Stress-induced inhibtion of the NF-kB signaling pathway results from the insolubilization of the IkB kinase complex following its dissociation from heat shock protein 90. *J. immunol.* **2005,** 174, 384-394.

108. Arthur, J. C.; Lich, J. D.; Aziz, R. K.; Kotb, M.; Ting, J. P. Heat shock protein 90 associates with monarch-1 and regulates its ability to promote degradation of NF-kappaB-inducing kinase. *J. Immunol.* **2007,** 179, 6291-6296.

109. Salminen, A.; Paimela, T.; Suuronen, T.; Kaarniranta, K. Innate immunity meets with cellular stress at the IKK complex: regulation of the IKK complex by Hsp70 and Hsp90. *Immunol. Lett.* **2008,** 117, 9-15.

110. Neckers, L.; Tatu, U. Molecular chaperones in pathogen virulence: emergin new targets for therapy. *Cell Host Microbe* **2008,** 4, 519-527.

111. Burnie, J. P.; Carter, T. L.; Hodgetts, S. J.; Matthews, R. C. Fungal heat-shock proteins in human disease. *FEMS Microbiol. Rev.* **2006,** 30, 53-88.

112. Matthews, R.; Burnie, J. The role of Hsp90 in fungal infection. *Immunol. Today* **1992,** 13, 345-348.

113. Cowen, L. E.; Steinback, W. J. Stress, drugs, and evolution: the role of cellular signaling in fungal drug resistance. *Eukaryot. Cell* **2008,** 7, 747-764.

114. Cowen, L. E.; Singh, S. D.; Kohler, J. R.; Collins, C.; Zaas, A. K.; Schell, W. A.; Aziz, H.; Mylonakis, E.; Perfect, J. R.; Whitesell, L.; Lindquist, S. Harnessing Hsp90 function as a powerful, broadly effective therapeutic strategy for fungal infectious disease. *PNAS* **2009,** 106, 2818-2823.

115. Semighini, C. P.; Heitman, J. Dynamic duo takes down fungal villains. *PNAS* **2009,** 106, 2971-2972.

116.   Matthews, R. C.; Burnie, J. P. Recombinant antibodies: a natural partner in combinatorial antifungal therapy. *Vaccine* **2004,** 22, 865-871.

117.   Lopatin, D. E.; Combs, A.; Sweier, D. G.; Fenno, J. C.; Dhamija, S. Characterization of heat-inducible expression and cloning of HtpG (Hsp90 homologue) of Porphyromonas gingivalis. *Infect. Immun.* **2000,** 68, 1980-1987.

118.   Acharya, P.; Kumar, R.; Tatu, U. Chaperoning a cellular upheaval in malaria: heat shock proteins in Plasmodium falciparum. *Mol. Biochem. Parasitol.* **2007,** 153, 85-94.

119.   Pavithra, S. R.; Kumar, R.; Tatu, U. Systems analysis of chaperone networks in the malarial parasite Plasmodium falciparum. *PLoS Comput. Biol.* **2007,** 3, 1701-1715.

120.   Lund, P. A. Microbial molecular chaperones. *Adv. Microb. Physiol.* **2001,** 44, 93-140.

121.   Arsene, F. The heat shock response of Escherichia coli. *Int. J. Food Microbiol.* **2000,** 55, 3-9.

122.   Ujino, S.; Yamaguchi, S.; Shimotohno, K.; Takaku, H. Heat-shock protein 90 is essential for stabilization of the hepatitis C virus nonstructural protein NS3. *J. Biol. Chem.* **2009,** 284, 6841-6846.

123.   Chase, G.; Deng, T.; Fodor, E.; Leung, B. W.; Mayer, D.; Schwemmle, M.; Brownlee, G. Hsp90 inhibitors reduce influenza virus replication in cell culture. *Virology* **2008,** 377, 431-439.

124.   Dutta, D.; Bagchi, P.; Chatterjee, A.; Nayak, M. K.; Mukherjee, A.; Chattopadhyay, S.; Nagashima, S.; Kobayashi, N.; Komoto, S.; Taniguchi, K.; Chawla-Sarkar, M. The molecular chaperone heat shock protein-90 positively regulates rotavirus infectionx. *Virology* **2009,** 391, 325-333.

125.   Amaral, M. D. Therapy through chaperones: Sense or antisense? Cystic fibrosis as a model disease. *J. Inherit. Metab. Dis.* **2006,** 29, 477-487.

126. Fuller, W.; Cuthbert, A. W. Post-translational disruption of the DF508 cystic fibrosis transmembrane conductance regulator (CFTR)-molecular chaperone complex with geldanamycin stabilizes DF508 CFTR in the rabbit reticulocyte lysate. *J. Biol. Chem.* **2000,** 275, 37462-37468.

127. Sun, F.; Mi, Z.; Condliffe, S. B.; Bertrand, C. A.; Gong, X.; Lu, X.; Zhang, R.; Latoche, J. D.; Pilewski, J. M.; Robbins, P. D.; Frizzell, R. A. Chaperone displacement from mutant cystic fibrosis transmembrande conductance regulator restores its function in human airway epithelia. *FASEB J.* **2008,** 22, 3255-3263.

128. Burlison, J. A.; Neckers, L.; Smith, A. B.; Maxwell, A.; Blagg, B. S. J. Novobiocin: redesigning a DNA gyrase inhibitor for selective inhibition of Hsp90. *J. Am. Chem. Soc.* **2006,** 128, 15529-15536.

129. Palermo, C. M.; Westlake, C. A.; Gasiewicz, T. A. Epigallocatechin gallate inhibits aryl hydrocarbon receptor gene transcription through an indirect mechanism involving binding to a 90 KDa heat shock protein. *Biochemistry* **2005,** 44, 5041-5052.

130. Itoh, H.; Ogura, M.; Komatsuda, A.; Wakui, H.; Miura, A. B.; Tashima, Y. A novel chaperone-activity-reducing mechanism of the 90-kDa molecular chaperone Hsp90. *Biochem. J.* **1999,** 343, 697-703.

131. Soti, C.; Raez, A.; Csermely, P. A nucleotide-dependent molecular switch controls ATP binding at the C-terminal domain of Hsp90. *J. Biol. Chem.* **2002,** 277, 7066-7075.

132. Byrd, C. A.; Bornmann, W.; Erdjument-Bromage, H.; Tempst, P.; Pavletich, N.; Rosen, N.; Nathan, C. F.; Ding, A. Heat shock protein 90 mediates macrophage activation by Taxol and bacterial lipopolysaccharide. *Proc. Natl. Acad. Sci.* **1999,** 96, 5645-5650.

133. Nichols, R. L.; Finland, M. Novobiocin; a limited bacteriologic and clinical study of its use in forty-five patients. *Antibiotic Med. Clin. Ther.* **1956,** 2, 241-257.

134.   Allan, R. K.; Mok, D.; Ward, B. K.; Ratajczak, T. Modulation of chaperone function and cochaperone interaction by novobiocin in C-terminal domain of Hsp90. *J. Biol. Chem.* **2006,** 281, 7161-7171.

135.   Bras, G. L.; Radanyi, C.; Peyrat, J. F.; Brion, J. D.; Alami, M.; Marsaud, V.; Stella, B.; Renoir, J. M. New novobiocin analogues as antiproliferative agents in breast cancer cells and potential inhibitors of heat shock protein 90. *J. Med. Chem.* **2007,** 50, 6189-6200.

136.   Plescia, J.; Whitney, S.; Fang, X.; Pennati, M.; Zaffaroni, N.; Daidone, M. G.; Meli, M.; Dohi, T.; Fortugno, P.; Nefedova, Y.; Gabrilovich, D. I.; Colombo, G.; Altieri, D. C. Rational design of shepherdin, a novel anticancer agent. *Cancer Cell* **2005,** 7, 457-468.

137.   Gyurkocza, B.; Plescia, J.; Raskett, C. M.; Garlick, D. S.; Lowry, P. A.; Carter, B. Z.; Andreeff, M.; Meli, M.; Colombo, G.; Altieri, D. C. Antileukemic activity of shepherdin and molecular diversity of Hsp90 inhibitors. *J. Natl. Cancer Inst.* **2006,** 98, 1068-1077.

138.   Grossman, D.; McNiff, J. M.; Li, F. Z.; Altieri, D. C. Expression and targeting of the apoptosis inhibitor, survivin, in human melanoma. *J. Invest. Dermatol.* **1999,** 113, 1076-1081.

139.   Kanwar, J. R.; Kamalapuram, S. K.; Kanwar, R. K. Targeting survivin in cancer: the cell-signalling perspective. *Drug Discov. Today* **2011,** 16, 485-494.

140.   Chiou, S. K.; Jones, M. K.; Tarnawski, A. S. Survivin - an anti-apoptosis protein: its biological roles and implications for cancer and beyond. *Med. Sci. Monit.* **2003,** 9, 125-129.

141.   Plescla, J.; Salz, W.; Xia, F.; Pennati, m.; Zaffaroni, N.; Daidone, M. G.; Meli, M.; Dohi, T.; Fortugno, P.; Nefedova, Y.; Gabrilovich, D. I.; Colombo, G.; Altieri, D. C. Rational design of Shepheridin, a novel anticancer agent. *Cancer Cell* **2005,** 7, 457-468.

142.   Scroggins, B. T.; Robzyk, K.; Wang, D.; Marcu, M. G.; Tsutsumi, S.; Beebe, K.; Cotter, R. J.; Felts, S.; Toft, D.; Karnitz, L.; Rosen, N.; Neckers, L. An acetylation site in the middle domain of Hsp90 regulates chaperone function. *Mol. Cell* **2007,** 25, 151-159.

143.   Thomas, S.; Munster, P. N. Histone deacetylase inhibitor induced modulation of anti-estrogen therapy. *Cancer Letter* **2009,** 280, 184-191.

144.   Kovacs, J. J.; Murphy, P. J.; Gaillard, S.; Zhao, X.; Wu, J. T.; Nicchitta, C. V.; Yoshida, M.; Toft, D. O.; Pratt, W. B.; Yao, T. P. HDAC6 regulates Hsp90 acetylation and chaperone-dependent activation of glucogorticoid receptor. *Mol. Cell* **2005,** 18, 601-607.

145.   Rao, R.; Fiskus, W.; Yang, Y.; Lee, P.; Joshi, R.; Fernandez, P.; Mandawat, A.; Atadja, P.; Bradner, J. E.; Bhalla, K. HDAC6 inhibition enhances 17-AAG--mediated abrogation of hsp90 chaperone function in human leukemia cells. *Blood* **2008,** 112, 1886-1893.

146.   Kekatpure, V. D.; Dannenberg, A. J.; Subbaramaiah, K. HDAC6 modulates Hsp90 chaperone activity and regulates activation of aryl hydrocarbon receptor signaling. *J. Biol. Chem.* **2009,** 284, 7436-7445.

147.   Fiskus, W.; Ren, Y.; Mohapatra, A.; Bali, P.; Mandawat, A.; Rao, R.; Herger, B.; Yang, Y.; Atadja, P.; Wu, J.; Bhalla, K. Hydroxamic acid analogue histone deacetylase inhibitors attenuate estrogen receptor-alpha levels and transcriptional activity: a result of hyperacetylation and inhibition of chaperone function of heat shock protein 90. *Clin. Cancer Res.* **2007,** 13, 4882-4890.

148.   Wang, Y.; Wang, S.-Y.; Zhang, X.-H.; Zhao, M.; Hou, C.-M.; Xu, Y.-J.; Du, Z.; Yu, X.-D. FK228 inhibits Hsp90 chaperone function in K562 cells via hyperacetylation of Hsp70. *Biochem. Biophys. Res. Commun.* **2007,** 356, 2007.

149.   Nguyen, A.; Su, L.; Campbell, B.; Poulin, N. M.; Nielsen, T. O. Synergism of heat shock protein 90 and histone deacetylase inhibitors in synovial sarcoma. *Sarcoma* **2009,** 2009, in press.

150.   Brandt, G. E. L.; Blagg, B. S. Alternate strategies of Hsp90 modulation for the treatment of cancer and other diseases. *Curr. Top. Med. Chem.* **2009,** 9, 1447-1461.

151.   Caplan, A. J.; Ayan, A. M.; Wilis, I. M. Multiple kinases and system robustness: a link between Cdc37 and genome integrity. *Cell Cycle* **2007,** 6, 3145-3147.

152.   Vaughn, C. K.; Mollapour, M.; Smith, J. R.; Truman, A.; Hu, B.; Good, V. M.; Panaretou, B.; Neckers, L.; Clarke, P. A.; Workman, P.; Piper, P. W.; Prodromou, C.; Pearl, L. H. Hsp90-dependent activation of protein kinases is regulated by chaperone-targeted dephosphorylation of Cdc37. *Mol. Cell* **2008,** 31, 886-895.

153.   Grammatikakis, N.; Lin, J. H.; Grammatikakis, A.; Tsichlis, P. N.; Cochran, B. H. p50cdc37 acting in concert with Hsp90 is required for Raf-1 function. *Mol. Cell. Bio.* **1999,** 19, 1661-1672.

154.   Karnitz, L. M.; Felts, S. J. Regulation of the kinome: when to hold 'em and when to fold 'em. *STKE* **2007,** pe22, 1-3.

155.   Pearl, L. H. Hsp90 and Cdc37 - a chaperone cancer conspiracy. *Curr. Opin. Genet. Dev.* **2005,** 15, 55-61.

156.   Gray, P. J. J.; Prince, T.; Cheng, J.; Stevenson, M. A.; Calderwood, S. K. Targeting the oncogene and kinome chaperone Cdc37. *Nat. Rev. Cancer* **2008,** 8, 491-495.

157.   Smith, J. R.; Workman, P. Targeting Cdc37: an alternative, kinase-directed strategy for disruption of oncogenic chaperoning. *Cell Cycle* **2009,** 8, 362-372.

158.   Gray, P. J. J.; Stevenson, M. A.; Calderwood, S. K. Targeting Cdc37 inhibits multiple signaling pathways and induces growth arrest in prostate cancer cells. *Cancer Res.* **2007,** 67, 11942-11950.

159.   Smith, J. R.; Clarke, P. A.; Billy, E. d.; Workman, P. Silencing the cochaperone Cdc37 destabilizes kinase clients and sensitizes cancer cells to Hsp90 inhibitors. *Oncogene* **2008,** 28, 157-169.

160.   Setty, A. R.; Sigal, L. H. Herbal medications commonly used in the practice of rheumatology: mechanisms of action, efficacy, and side effects. *Semin. Arthritis Rheum.* **2005,** 34, 773-784.

161.   Sreeramulu, S.; Gande, S. L.; Gobel, M.; Schwalbe, H. Molecular mechanism of inhibition of the human protein complex Hsp90-Cdc37, a kinome chaperone-cochaperone, by triterpene celastrol. *Angew. Chem. Int. Ed.* **2009,** 48, 5853-5855.

162.   Trott, A.; West, J. D.; Klaic, L.; Westerheide, S. D.; Silverman, R. B.; Morimoto, R. I.; Morano, K. A. Activation of heat shock and antioxidant responses by the natural product celastrol: transcriptional signatures of a thiol-targeted molecule. *Mol. Biol. Cell* **2008,** 19, 1104-1112.

163.   Westerheide, S. D.; Bosman, J. D.; Mbadugha, B. N.; Kawahara, T. L.; Matsumoto, G.; Kim, S.; Gu, W.; Devlin, J. P.; Silverman, R. B.; Morimoto, R. I. Celastrols as inducers of the heat shock response and cytoprotection. *J. Biol. Chem.* **204,** 279, 56053-56060.

164.   Lamb, J.; Crawford, E. D.; Peck, D.; Modell, J. W.; Blat, i. C.; Wrobel, M. J.; Lerner, J.; Brunet, J.-P.; Subramanian, A.; Ross, K. N.; Reich, M.; hieronymus, h.; Wei, G.; Armstrong, S. A.; Haggarty, S. J.; Clemons, P. A.; Wei, R.; Carr, S. A.; Lander, E. S.; Golub, T. R. The

connectivity map: using gene-expression signatures to connect small molecules, genes, and disease. *Science* **2006,** 313, 1929-1935.

165. Hieronymus, H.; Lamb, J.; Ross, K. N.; Peng, X. P.; Clement, C.; Rodina, A.; nieto, M.; Du, J.; Stegmaier, K.; Raj, S. M.; Maloney, K. N.; Clardy, J.; Hahn, W. C.; Chiosis, G.; Golub, t. R. Gene expression signature-based chemical genomic prediction identifies a novel class of Hsp90 pathway modulators. *Cancer Cell* **2006,** 10, 321-330.

166. Subapriya, R.; Nagini, S. Medicinal properties of neem leaves: a review. *Curr. Med. Chem. Anticancer Agents* **2005,** 5, 149-156.

167. Brahmachari, G. Neem--an omnipotent plant: a retrospection. *Chembiochem* **2004,** 5, 408-421.

168. Yang, H.; Chen, D.; Cui, Z. C.; Yuan, X.; Dou, W. P. Celastrol, a triterpene extracted from the chinese "thunder of god vine," is a potent proteasome inhibitor and suppresses human prostate cancer growth in nude mice. *Cancer Res.* **2006,** 66, 4758-4765.

169. Balick, M. J.; Lee, R. Digging in the herb garden: responding to a patient's query about thunder of god vine. *Altern. Ther. Health M.* **2001,** 7, 100-103.

170. Aladakatti, R. H.; Ahamed, R. N. Ultrastructural changes in leydig cells and cauda epididymal spematozoa induced by azadirachta indica leaves in albino rats. *Phytother. Res.* **2005,** 19, 756-766.

171. Brandt, G. E. L.; Schmidt, M. D.; Prisinzano, T. E.; Blagg, B. S. J. Gedunin, a novel Hsp90 inhibitor: semisynthesis of derivatives and preliminary structure-activity relationships. *J. Med. Chem.* **2008,** 51, 6495-6502.

172. Pedersen, P. L. Transport ATPases: structure, motors, mechanism and medicine: a brief overview. *J. Bioenerg. Biomembr.* **2005,** 37, 349-257.

173.   Gruber, G.; Wieczorek, H.; Harvey, W. R.; Muller, V. F1Fo, V1Vo and A1Ao enzymes are essential cellular energy converters which transduce the chemical energy of ATP hydrolysis into transmembrane ionic electrochemical potential differences. *J. Exp. Biol.* **2001,** 204, 2597-2605.

174.   Huttemann, M.; Lee, I.; Pecinova, A.; Pecina, P.; Przyklenk, K.; Doan, J. W. Regulation of oxidative phosphorylation, the mitochondrial membrane potential, and their role in human disease. *J. Bioenerg. Biomembr.* **2008,** 40, 445-456.

175.   Pedersen, P. L. Transport ATPases into the year 2008: a brief overview related to types, structures, functions and roles in health and disease. *J. Bioenerg. Biomembr.* **2007,** 39, 349-355.

176.   Grover, G. J.; Malm, J. Pharmacological profile of the selective mitochondrial F1F0 ATP hydrolase inhibitor BMS-199264 in myocardial ischemia. *Cardiovasc. Ther.* **2008,** 26, 287-296.

177.   Panfoli, I.; Ravera, S.; Brushi, M.; Candiano, G.; Morelli, A. Proteomics unravels the exportability of mitochondrial respiratory chains. *Expert. Rev. Proteomics* **2011,** 8, 231-239.

178.   Papathanassiu, A. E.; MacDonald, N. J.; Bencsura, A.; Vu, H. A. F1F0-ATP synthase functions as a co-chaperone of Hsp90-substrate protein complexes. *Biochem. Biophys. Res. Commun.* **2006,** 345, 419-429.

179.   Francis, B. R.; Thorsness, P. E. Hsp90 and mitochondrial proteases Yme1 and Yta10/12 participate in ATP synthase assembly in *Sarccharomyces cerevisiae. Mitochondrion* **2011,** 11, 587-600.

180.   Papathanassiu, A. E.; MacDonald, N. J.; Emlet, D. R.; Vu, H. A. Antitumor activity of efrapeptins, alone or in combination with 2-deoxyglucose, in breast cancer *in vitro* and *in vivo*. *Cell Stress Chaperones* **2011,** 16, 181-193.

181.	Boot, C. M.; Amagata, T.; Tenney, K.; Compton, J. E.; Pietraszkiewicz, H.; Valeriote, F. A.; Crews, P. Four classes of structurally unusual peptides from two marine-derived fungi: structures and bioactivities. *Tetrahedron* **2007,** 63, 9903-9914.

182.	Kunze, B.; Sasse, F.; Wieczorek, H.; Huss, M. Cruentaren A, a highly cytotoxic benzolactone from Myxobacteria is a novel selective inhibitor of F1-ATPases. *FEBS Lett.* **2007,** 581, 3523-3527.

183.	Kunze, B.; Steinmetz, H.; Hofle, G.; Huss, M.; Wieczorek, H.; Reichenbach, H. Cruentaren, a new antifungal salicylate-type macrolide from *Byssovorax cruenta* (myxobacteria) with inhibitory effect on mitochondrial ATPase activity. Fermentation and biological properties. *J. Antibiot.* **2006,** 59, 664-668.

184.	Jundt, L.; Steinmetz, H.; Luger, P.; Weber, M.; Kunze, B.; Reichenbach, H.; Hofle, G. Isolation and structure elucidation of cruentarens A and B - novel members of the benzolactone class of ATPase inhibitors from myxobacterium *Byssovorax cruenta*. *European J. Org. Chem.* **2006,** 2006, 5036-5044.

Chapter II

Chemical and Biological Investigation of Gedunin, a Novel Disruptor of the CDC37-Hsp90 Interaction

II.1   Targeting Hsp90 by Disrupting Association with CDC37 Co-Chaperone

The Hsp90 protein folding mechanism is a stepwise operation that progresses *via* a complex array of protein-protein interactions between homodimeric Hsp90 and several co-chaperones, immunophillins, and partner proteins.[1-5] Consensus has been reached on the general understanding of this process; however, a complete and detailed analysis remains elusive. While the requirement for specific co-chaperones for certain client proteins complicates such analysis, this individualized nature also represents a therapeutic opportunity for selective client protein degradation.

Many oncogenic kinases are Hsp90-dependent client proteins that, unlike non-kinase clients, require participation of the co-chaperone CDC37 within the super chaperone complex.[6, 7] Disruption of the Hsp90/CDC37 interaction is therefore a target for selective degradation of kinase client proteins without affecting the maturation of non-kinase substrates. Selective kinase client degradation is particularly attractive toward the management of oncogene-addicted cancers that are hypersensitive to perturbation of kinase activity.[8-10]

Selective kinase degradation by disruption of the Hsp90/CDC37 interaction has been confirmed experimentally.[11-16]   CDC37   siRNA   mediated

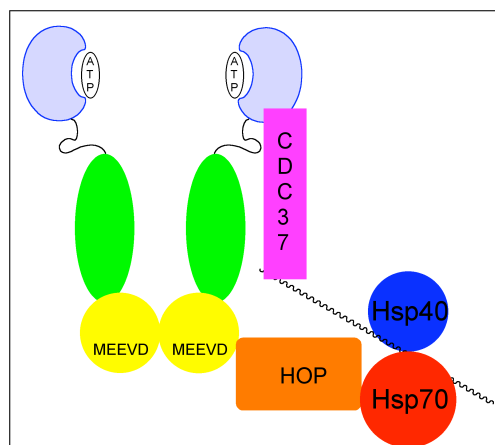**Figure 2.1**. Hsp90-dependent kinase client proteins are form multiple protein-protein interactions during the maturation process. Unlike non-kinase client protiens, however, stabilization of the heteroprotien complex by CDC37 is required for kinases.

knockdown in colon cancer cells induced the degradation of kinase clients (erbB2, cRAF, CDK4 and CDK6, as well as phosphorylated AKT) but not non-kinase clients (glucocorticoid receptor and survivin). Not only was selective kinase client degradation observed, Hsp90 and Hsp70 levels were unaffected by CDC37 knockdown and no heat shock response was produced. Therefore, disruption of Hsp90/CDC37 interactions is an attractive therapeutic strategy that is capable of addressing limitations that result from induction of the pro-survival heat shock response, which is observed for every Hsp90 inhibitor in clinical trials.

II.1.1 *Hsp90/CDC37 disrupting small molecules*

Hsp90 inhibitors that target the N- or C-terminus have been extensively investigated.[3, 17-22] Despite attractive features such as the absence of an induced heat shock response and the propensity for selectively targeting kinase clients for degradation, small molecule disruptors of Hsp90/CDC37 interactions remain largely underexplored. The lack of chemical leads that display such a biological profile has contributed to this current status.

The triterpenoid natural product celastrol was recently identified as a small molecule disruptor of Hsp90/CDC37 interactions and manifests anti-proliferative activity against pancreatic cancer cells.[23] Celastrol was originally identified as an Hsp90 inhibitor that exhibits a novel mechanism of action through the use of "Connectivity Map" screening.[24, 25] This same screen also identified the limonoid natural product gedunin as an Hsp90 inhibitor mechanistically similar to celastrol. This chapter will describe the semi-synthetic derivatization of gedunin for elucidation of structure-activity relationships, biological and mechanistic evaluation of such derivatives, and preliminary molecular docking studies that explore the Hsp90-gedunin interaction.[24, 25]

II.2 Semi-synthetic Modification of Gedunin

Gedunin (**1**, Figure 2.2), a tetranortriterpenoid isolated from the Indian neem tree (*Azadirachta Indica*), manifests anti-malarial, insecticidal, anti-spermatogenic, and most recently anti-cancer activity.[26, 27] The anti-tumor activity of gedunin was explored through the use of the Connectivity Map.[24, 25] Lamb *et*

Figure 2.2. Gedunin, **1**, and 7-desacetylgedunin, **2**.
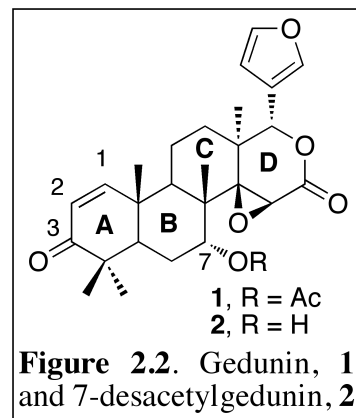
al. demonstrated, *via* high connectivity scores with GDA, 17-AAG, and 17-DMAG, that gedunin exhibited its anti-proliferative activity through Hsp90 modulation. In a subsequent report, these authors determined that the interaction of gedunin with Hsp90 occurred *via* a mechanism distinct from competitive inhibition of ATP, and therefore unlike known Hsp90 inhibitors such as GDA or RAD. While gedunin induces Hsp90-dependent client protein degradation similar to other Hsp90 inhibitors, the natural product was unable to displace GDA in a fluorescence polarization assay with purified Hsp90 at concentrations up to 100 μM. Conversely, similarity between the mechanism of action responsible for the anti-proliferative activity of celastrol, involving disruption of the interaction between Hsp90 and the co-chaperone CDC37, and that observed for gedunin suggests a common Hsp90 inhibitory mode. As a structurally and mechanistically distinct regulator of the Hsp90 protein folding machinery, gedunin represents a lead compound that may possess unique Hsp90 modulatory attributes.

Prior to the work described herein, no structure-activity relationships had been established between Hsp90 and gedunin. The ease of acquiring both gedunin and its 7-desacetyl derivative from bulk, commercially available neem oil make them well-suited for semi-synthetic derivatization for the development of more efficacious compounds. In addition, these limonoid natural products present a variety of chemical surfaces ideal for chemoselective manipulation to

Figure 2.3. Schematic depiction of isolation protocol.
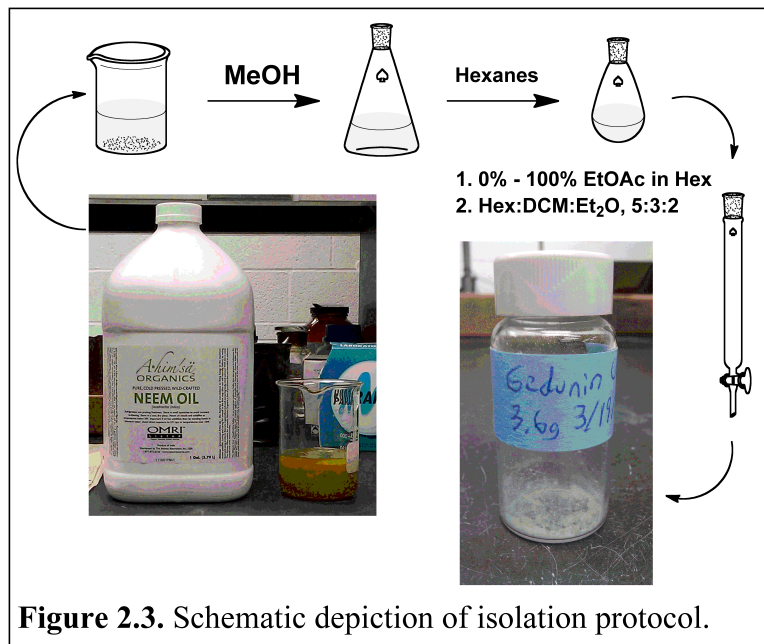
evaluate structure activity relationships at distinct locations. In total, 19 analogues of gedunin were prepared through semi-synthetic procedures aimed at elucidating the role of the α,β-unsaturated ketone, exploring the sensitivity of the ketone binding pocket to steric bulk, and the effects of various substituents at the 7-position. All analogues were evaluated for anti-proliferative activity against MCF-7 and SKBr-3 breast cancer cell lines, and a interesting compounds subsequently analyzed by Western blot analysis of Hsp90-dependent client proteins.[28]
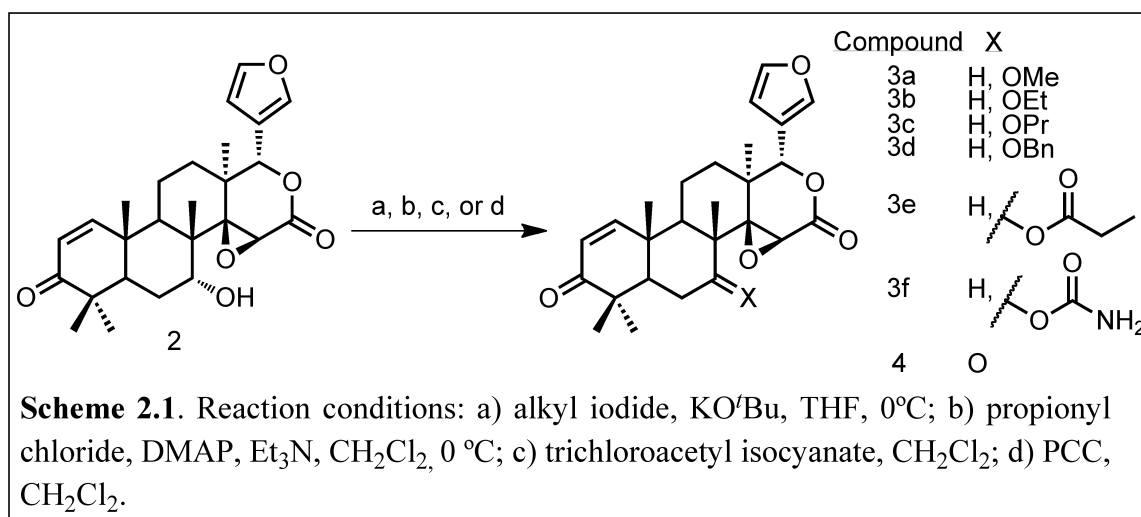
II.2.1 *Natural product isolation*

Commercially available neem oil presents an affordable resource for a rich supply of gedunin. Several commercial samples of neem oil derived from cold-pressed seeds of the tree were analyzed to determine the source that provided oil containing the highest concentration of gedunin. Samples were analyzed by TLC, ESI HRMS, and HPLC. Sample oil from Ahim'sa Organics was found to contain the most gedunin and the following studies were conducted with natural product isolated from neem oil supplied by this vendor.

Isolation of the natural product was straightforward (Figure 2.3). 1 Kg of neem oil from Ahim'sa was diluted with 1 L of methanol (MeOH) and vigorously stirred for 24 h. The alcohol and oil layers were then allowed to separate, and the alcoholic extract was collected and

concentrated under reduced pressure. After repeating this cycle for five iterations, all condensed alcoholic extracts were combined to afford a viscous, dark brown, translucent oil that was subsequently washed several times with ^{n}hexanes (Hex) under sonication in order to remove any remaining fatty oils. The resultant dark brown resin was subjected to flash column chromatography using a gradient of 100% Hex to 100% ethyl acetate (EtOAc). Fractions containing gedunin were pooled and subjected to successive columns, each using a tighter gradient of Hex and EtOAc, ultimately to afford a pale yellow resin that was crystallized from EtOAc by triteration with Hex to provide 3 g of a white crystalline solid, which contained 2 products by TLC and HPLC. ^{1}H and ^{13}C NMR data depicted all peaks previously described for gedunin and 7-desacetylgedunin.[13] These two compounds were obtained in their pure forms by a final isocratic purification using Hex:dichloromethane (DCM):diethyl ether (Et$_2$O) in a ratio of 5:3:2.

II.2.2 *Design and synthesis of gedunin semi-synthetic derivatives*

Compounds **3a**–**3f** and **4** were synthesized from 7-desacetylgedunin (**2**) (Scheme 2.1) as a series of derivatives to probe the steric and electronic tolerance of replacements at C-7.   7-desacetylgedunin (**2**) was treated with 2eq.uivalents of 1 M potassium tert-butoxide (KO^{t}Bu) in

Scheme 2.1. Reaction conditions: a) alkyl iodide, KO^{t}Bu, THF, 0°C; b) propionyl chloride, DMAP, Et$_3$N, CH$_2$Cl$_2$, 0 °C; c) trichloroacetyl isocyanate, CH$_2$Cl$_2$; d) PCC, CH$_2$Cl$_2$.

tetrahydrofuran (THF) and subsequently reacted with the requisite alkyl halide to afford ethers **3a–3d**. Standard acylation procedures were used to generate **3e**.

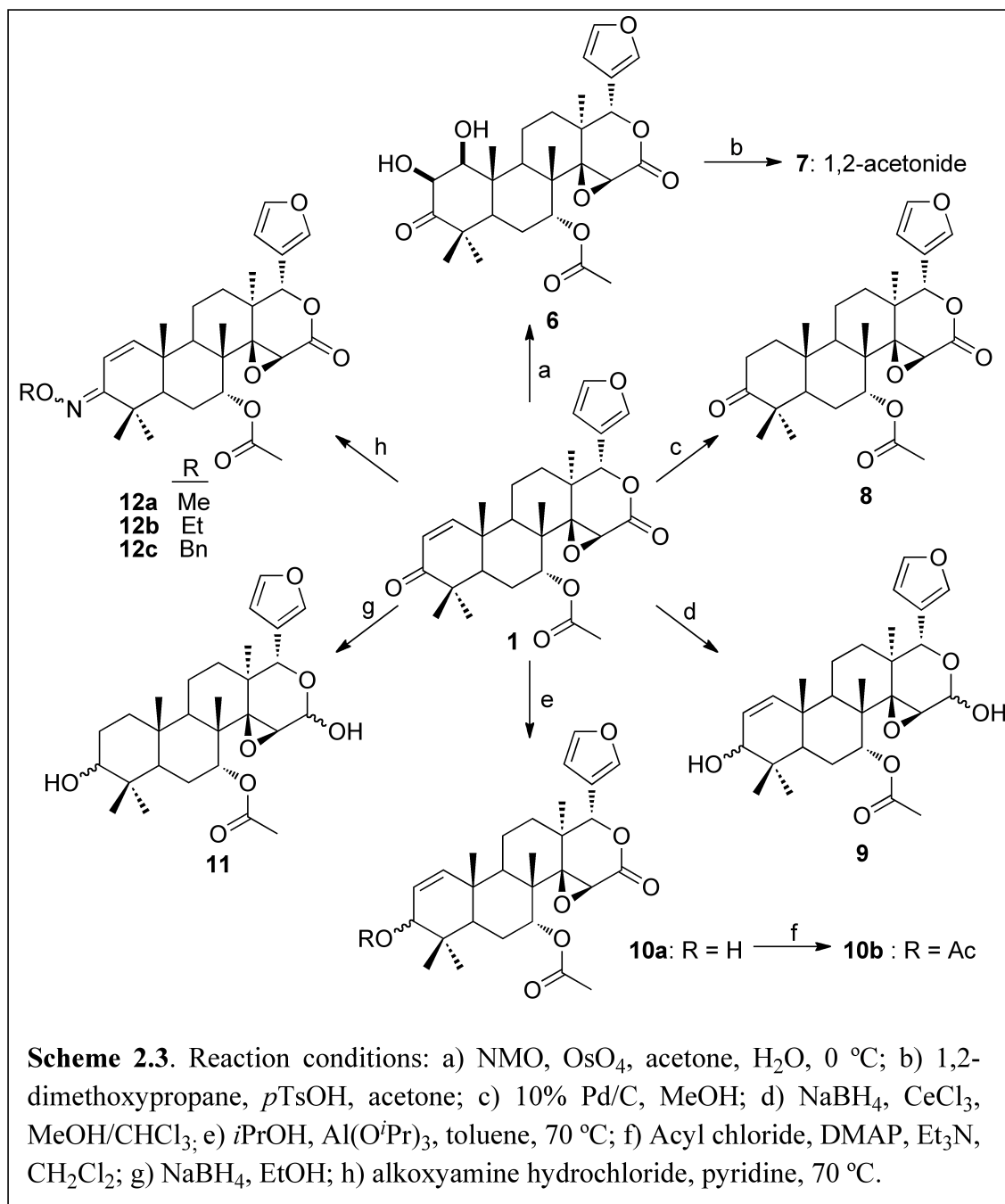**Scheme 2.2**. Reaction conditions: a) NaOH, H$_2$O$_2$, acetone.
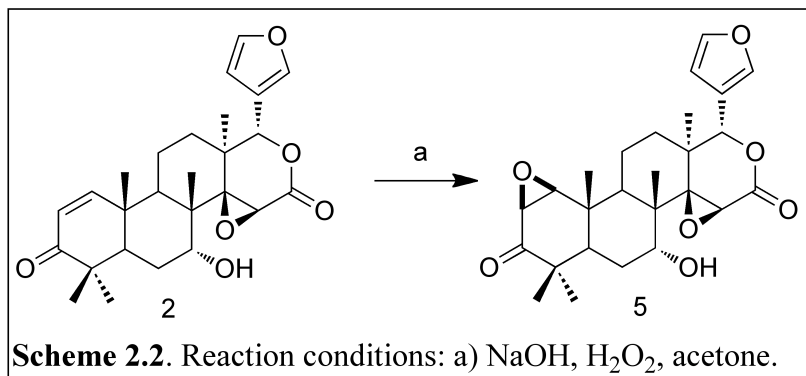
Compound **3f** was produced by treatment of 7-desacetylgedunin with trichloroacetyl isocyanate followed by basic aqueous workup. Pyridinium chlorochromate (PCC) oxidation of 7-desacetylgedunin gave the corresponding ketone, **4**.

The synthesis of compounds **5–13** are provided in Schemes 2.2, 2.3, and 2.4. This series of derivatives was pursued to evaluate the effects of altering the Michael accepting ability of the α,β-unsaturated ketone and to probe the steric and electronic limitations of the A-ring binding domain of Hsp90.

Treatment of 7-desacetylgedunin with sodium hydroxide and hydrogen peroxide afforded epoxide **5** (Scheme 2.2). Dihydroxylation of the olefin in **1** using osmium tetroxide (OsO$_4$) and *N*-methylmorpholine-*N*-oxide (NMO) gave vicinal diol **6**, which upon treatment with 2,2-dimethoxypropane (DMP) and *p*-toluenesulfonic acid (TsOH) yielded the corresponding acetonide, **7**. Hydrogenation of the double bond was accomplished by the use of 10 % palladium on carbon (Pd/C) and hydrogen gas to afford **8**. Standard Luche conditions surprisingly gave hemi-lactol product **9**, presumably as a result of the increased electrophillic character of the D-ring lactone induced by the α,β–epoxide moiety. Chemoselective reduction of the ketone was accomplished *via* Merwein-Pondorf-Verley conditions with aluminum isopropoxide and isopropanol to afford **10a**. The allylic alcohol **10a** was acetylated under standard conditions to

give **10b.** Treatment of gedunin with excess sodium borohydride (NaBH₄) without a lanthanide

gave the corresponding alcohol, **11** (Scheme 2.3).

Scheme 2.3. Reaction conditions: a) NMO, OsO₄, acetone, H₂O, 0 °C; b) 1,2-dimethoxypropane, *p*TsOH, acetone; c) 10% Pd/C, MeOH; d) NaBH₄, CeCl₃, MeOH/CHCl₃; e) *i*PrOH, Al(O*i*Pr)₃, toluene, 70 °C; f) Acyl chloride, DMAP, Et₃N, CH₂Cl₂; g) NaBH₄, EtOH; h) alkoxyamine hydrochloride, pyridine, 70 °C.

Oxime ether derivatives of gedunin, **12a–c**, were synthesized by the treatment of the

natural product with the appropriately substituted hydroxylamine. Compound **13** (Scheme 2.4),

the product resulting from the treatment of gedunin with hydroxylamine, further demonstrates the

Scheme 2.4. Reaction conditions: a) hydroxylamine hydrochloride, pyridine, 70 °C.
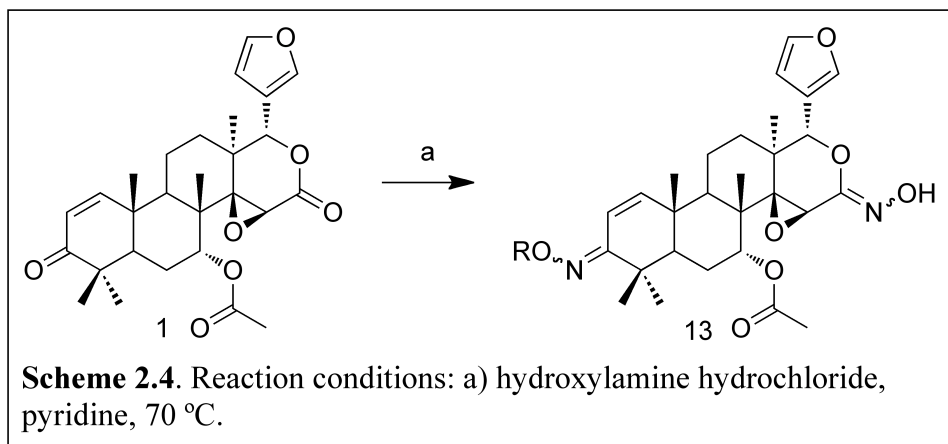
increased electrophillic nature of the lactone moiety of gedunin.

II.3   Biological Evaluation of Gedunin Derivatives

With no prior knowledge of the site to which gedunin binds Hsp90, the 19 semi-synthetic derivatives were designed to elucidate the importance of specific functional groups on the tetracyclic core, as well as to probe the chemical space surrounding these ring systems. Because the goal of this project was to generate preliminary structure-activity relationships, products of non-stereospecific reactions were not separated into their diastereomerically pure forms. Compounds were tested for anti-proliferative activity against two breast cancer cell lines. The most active compounds were subjected to Western blot analysis to confirm the disruption of Hsp90 kinase client activity. Additionally, experiments were conducted to determine the effects of gedunin on the Hsp90/CDC37 interaction and the heat shock response.

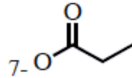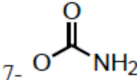### II.3.1   *Anti-proliferative activity*
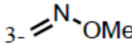
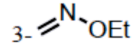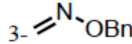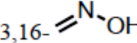Compounds **1**, **2**, **3a–f**, **4**, **5**, **6**, **7**, **8**, **9**, **10a–b**, **11**, **12a–c**, and **13** were evaluated for anti-proliferative activity against MCF-7 and SKBr3 cells using GDA as a positive control. Rates of cellular proliferation in the presence of increasing analogue concentrations were measured using the Promega MTS/PMS assay system. Reductase enzymes present within living cells catalyze

MTS tetrazolium reduction to a colored formazan product that can be quantified by measuring absorbance at 490 nm. Degree of absorbance is directly related to cell count and therefore rate of proliferation. Results from these studies are listed in Table 2.1. While many of the prepared compounds retain activity, none of the derivatives is more active than the natural product, however, some important preliminary structure-activity relationships have been identified.

Substituents at the 7-position are placed in an environment that is sensitive to the effects of increasing and decreasing steric bulk away from that presented by the native ligand. From compounds **3a** through **3e,** a pronounced decrease in anti-proliferative activity resulted upon decreasing or increasing the size of the substituent from an ethyl ether (**3b**) to either a methyl ether or an *n*-propyl ether (**3a** and **3c**) and complete loss in activity was produced by incorporation of the benzyl ether as evidenced by compound **3d**. A complete loss in activity was also noted upon incorporation of the propionate ester as in **3e**. The *n*-propyl ether in **3c** may retain activity due to its less rigid nature as compared to the propionate ester, **3e**. Also, preliminary molecular modeling results suggest that the carbonyl oxygen present on the propionate is tilted out of alignment with the carbonyl oxygen of the natural product suggesting that this moiety, when present, is important for binding.

From the initial data set, it also appears that the binding site for substituents at the 7-position is not sensitive to a change in the electronic nature of the substituent. Compound **3f**, which incorporates a carbamate as a non-bulky hydrogen bond acceptor/donor, exhibited an IC_{50} value almost identical to that of the natural product. The most active analogue found in the 7-position series is compound **4**, the 7-oxo derivative, further demonstrating the tolerance of this binding site to small, hydrogen bond acceptors, rather than small hydrophobic moieties as in **3a**.

Table 2.1. IC_{50} values with standard deviations of Gedunin Analogs in MCF-7 and SKBr3 Breast Cancer Cell Lines[a]

Compound	Functionality	MCF-7	SKBr3
1	7-OAc	8.84 ± 0.03	3.22 ± 0.6
2	7-OH	28.96 ± 4.48	21.09 ± 5.95
3a	7-OMe	38.88 ± 0.36	12.99 ± 0.85
3b	7-OEt	14.79 ± 0.87	12.06 ± 1.27
3c	7-OPr	37.27 ± 2.20	18.14 ± 0.99
3d	7-OBn	>100	>100
3e	7-O (propanoyl ester)	>100	>100
3f	7-O (carbamate, NH_2)	9.79 ± 0.69	7.05 ± 1.00
4	7-Oxo	10.90 ± 0.41	4.49 ± 0.98
5	1,2-Epoxide	>100	>100
6	1,2-Diol	>100	>100
7	1,2-Acetonide	>100	>100
8	1,2-Dihydro	>100	>100
9	3-OH/Lactol	47.72 ± 1.59	82.38 ± 17.62
10a	3-OH	54.31 ± 6.78	47.70 ± 1.61
10b	3-OAc	>100	>100
11	1,2-Dihydro-3-OH/Lactol	>100	>100
12a	3- (N-OMe)	>100	>100
12b	3- (N-OEt)	>100	>100
12c	3- (N-OBn)	>100	>100
13	3,16- (N-OH)	33.17 ± 2.18	26.49 ± 0.93

[a] IC_{50} values (μM) determined from non-linear dose-response curve (GraphPad Prism) based on data from standard MTS/PMS antiproliferative assay repeated in triplicate.

These results support two reasonable conclusions in regards to the effect of differing substituents at the 7-position: (1) the binding site complementary to substituents at this position may provide a hydrogen bond donor that resides in a shallow pocket. This would explain why hydrogen bond acceptors exhibit the best anti-proliferative activities, while decreasing or increasing steric bulk from that presented by the native ligand without the presence of a hydrogen bond acceptor at this position decreases activity; (2) substituents placed at the 7-position of gedunin are positioned in an region critical to the overall conformation of the molecule, thereby exhibiting significant impact on binding. This latter observation explains why even small changes in the size of substituents, e.g. the additional methyl group of **3e** compared to **1**, cause a substantial decrease in anti-proliferative activity.

The anti-proliferative activity of the α,β-unsaturated ketone series also provides key information regarding the importance of this functional group. Compounds lacking the 1,2-olefin of gedunin manifest IC_{50} values greater than 100 μM (i.e. **6**, **7**, **8**, and **11**). At first inspection, this data might suggest that the α,β-unsaturated ketone is acting as a Michael acceptor, however, anti-proliferative activity of related compounds in this series suggest otherwise. For example, compound **9**, which contains the reduced ketone and lactone moieties, retains anti-proliferative activity. Although **9** exhibits activity five to ten fold less potent than the natural product, evidence suggests that the α,β-unsaturated ketone is not acting as a Michael acceptor, as a far less potent compound would be expected. The biological activity observed for compounds **10a** and **12a** provides additional support for a non-covalent mechanism of action for gedunin. Compound **10a** manifests anti-proliferative activity five times less potent than gedunin in both MCF-7 and SKBr3 cells. Compound **12a** also retains some activity, and is only 3-4 times less
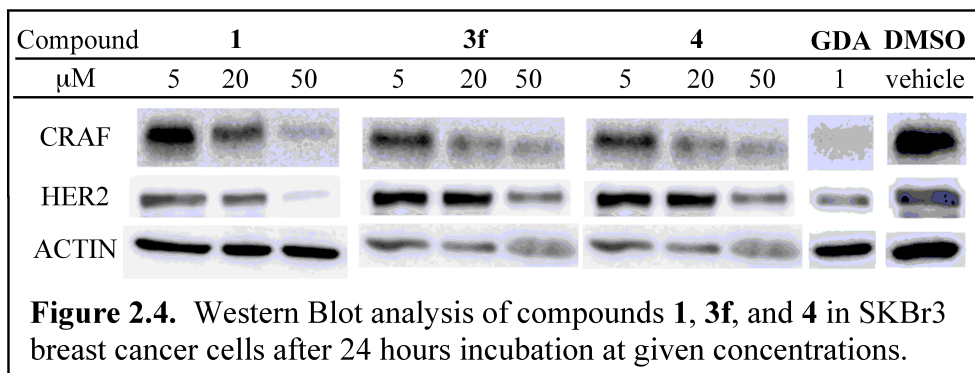
potent than the natural product and incorporates an electron-rich oxime, which serves as a poor Michael acceptor.

Compounds **10b**, **12a-12c**, and **13** also provide valuable insight into the binding site of the α,β-unsaturated ketone. This binding pocket appears sensitive to steric bulk and/or intolerant to hydrophobic moieties. Compound **10b**, the acetylated version of **10a**, exhibits no activity. Compound **12a**, the *O*-methyl oxime, also manifests no anti-proliferative activity. This is interesting, because aside form the additional projection of steric bulk and the increase in hydrophobicity from the methyl group on the oxime ether, **12a** appears to include the requirements for successful binding at other positions of the molecule, including the α,β-olefin, a hydrogen bond acceptor at the 3-position, and the appropriately fitting substituent at the 7-position. Neither **12b** nor **12c** exhibited anti-proliferative activity and also parallel this trend.
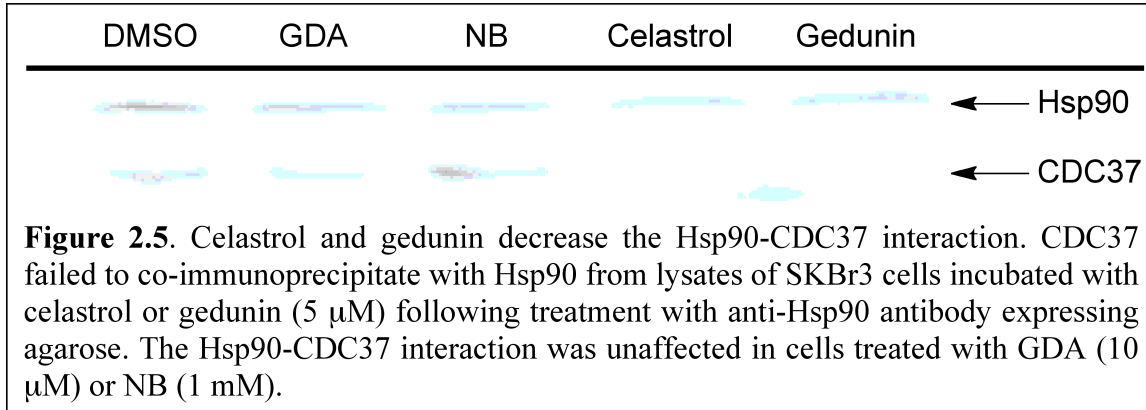
II.3.2 *Western blot analysis of Hsp90 client protein*

Compound		**1**			**3f**			**4**			GDA	DMSO
μM	5	20	50	5	20	50	5	20	50	1	vehicle
CRAF												
HER2												
ACTIN												

Figure 2.4. Western Blot analysis of compounds **1**, **3f**, and **4** in SKBr3 breast cancer cells after 24 hours incubation at given concentrations.
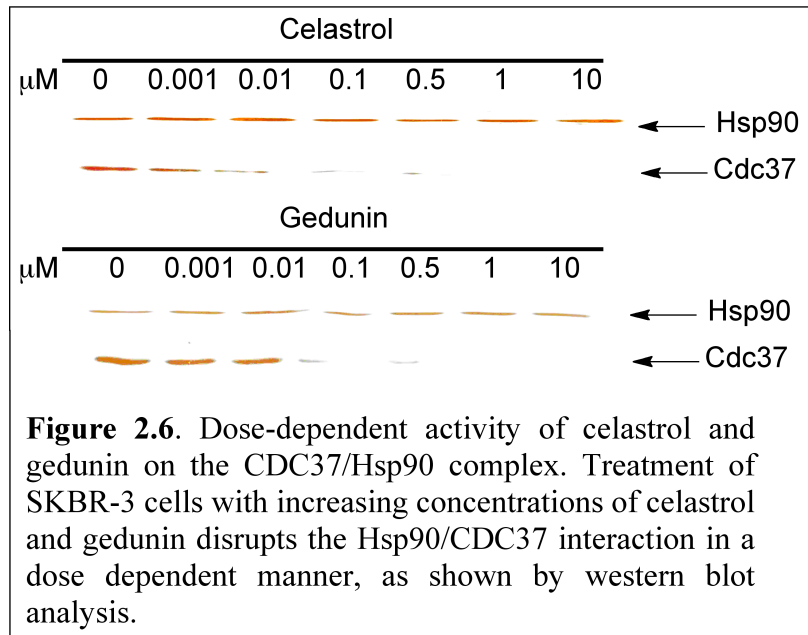
In order to demonstrate the retention of Hsp90 inhibition, despite structural manipulation, the most active compounds in this series were evaluated to determine their ability to induce Hsp90-dependent client protein degradation. **1**, **3f**, and **4** were subjected to Western blot analysis for the detection of two known Hsp90 client proteins, Raf and HER2 (Figure 2.4). Both compounds **3f** and **4** demonstrate client protein degradation similar to **1** and GDA, which further supports their activity, stems from modulation of the Hsp90 molecular chaperone.

Figure 2.5. Celastrol and gedunin decrease the Hsp90-CDC37 interaction. CDC37 failed to co-immunoprecipitate with Hsp90 from lysates of SKBr3 cells incubated with celastrol or gedunin (5 μM) following treatment with anti-Hsp90 antibody expressing agarose. The Hsp90-CDC37 interaction was unaffected in cells treated with GDA (10 μM) or NB (1 mM).

II.3.3 *Effects on Hsp90/CDC37 interaction*

To determine whether gedunin causes disassembly of the Hsp90/CDC37 complex, co-immunoprecipitation experiments were conducted. SKBr3 breast cancer cells were incubated for 24 hours with concentrations of celastrol, gedunin, NB, and GDA and then lysed with NP-40 lysis buffer (Figure 2.5).

Lysates were immunoprecipitated with an anti-Hsp90 antibody and Protein G agarose. Protein was submitted to SDS-PAGE and analyzed by immunoblot, using the Hsp90 and CDC37 antibodies. The control compounds, GDA and NB,
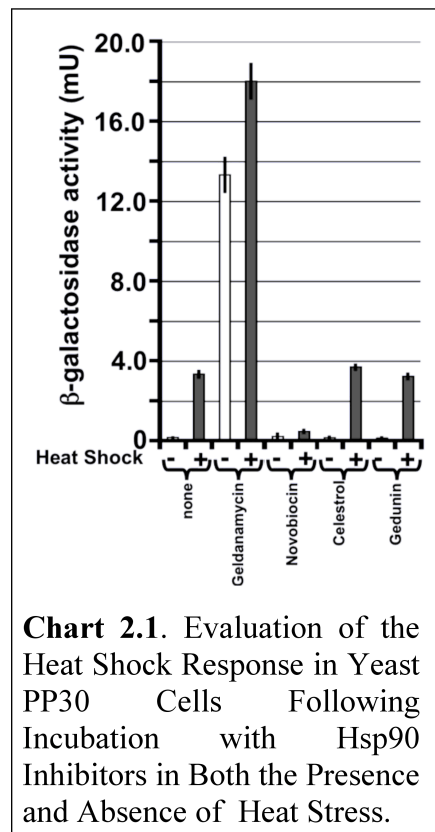

Figure 2.6. Dose-dependent activity of celastrol and gedunin on the CDC37/Hsp90 complex. Treatment of SKBR-3 cells with increasing concentrations of celastrol and gedunin disrupts the Hsp90/CDC37 interaction in a dose dependent manner, as shown by western blot analysis.

exhibited no effect on the concentrations of CDC37 following Hsp90 immunoprecipitation, in agreement with previously reported data,[39] as these compounds are unable to disrupt the CDC37/Hsp90 complex. However, celastrol and gedunin decreased the levels of CDC37 in a concentration-dependent manner (Figure 2.6), supporting the hypothesis that all three

compounds manifest a similar mechanism of action that results from disruption of the Hsp90/CDC37 complex.

II.3.4 *Comparison of heat shock response induction by several Hsp90 modulators*

Heat shock transcription factor 1 (HSF1) is an Hsp90-dependent client protein that, when displaced from Hsp90, results in the heat shock response upon transcriptional activation of the heat shock genes by binding to the heat shock-binding element. Previous work has shown that human Hsp90 is functional in yeast lacking endogenous Hsp90. Therefore; we examined the effects of celastrol and gedunin on HSF activity. PP30 cells

Chart 2.1. Evaluation of the Heat Shock Response in Yeast PP30 Cells Following Incubation with Hsp90 Inhibitors in Both the Presence and Absence of Heat Stress.

expressing hHsp90a (as the only copy of Hsp90) and containing the HSF-*lac*Z reporter (Heat Shock Binding Element, HSE-*lac*Z) were treated with 100μM of the above compounds for 3 hours. In addition, these cells were subsequently stressed upon heat shock (39˚C) for 1 hour. Celastrol, and gedunin exhibited no altered effect on the heat shock response in yeast, suggesting these inhibitors do not interfere with Hsp90/HSF1 interactions (Chart 2.1).

II.4   Concluding Remarks

Preliminary structure-activity relationships between gedunin and Hsp90 were elucidated through this work. We have shown that the α,β-unsaturated ketone, while required for anti-proliferative activity, does not behave as a Michael acceptor, and may therefore evade toxicity associated with this type of motif. We have also shown that the anti-proliferative activity of this series of compounds is drastically reduced by a decrease or increase in steric bulk at the 7-

position from the native ligand, suggesting that the natural product has optimized the steric effects at this position. Also, it appears that the activity of compounds within the 7-position series is not affected by a change in the electronic characteristics of substituents at this location.

Of further note, the most active compounds, **3f** and **4**, may present scaffolds that exhibit advantages over the natural product, **1**. The acetate moiety present in **1** is quite labile in physiological systems, as it may be rapidly cleaved by endogenous and promiscuous esterases. Naturally derived 7-desacylgedunin exhibits significantly lower anti-proliferative activity, and this may prevent derivatives of gedunin containing the acetate moiety from producing clinical significance. Conversely, the carbamate of **3f** and the ketone of **4** represent more stable functional groups that can withstand robust physiological environments. The carbamate of **3f** also has the added feature of lowering the lipophilicity of the natural product, which also increases its solubility and perhaps, physiological relevance.

Results obtained from this work also provide support for the hypothesis that the anti-proliferative effects of gedunin are a consequence of disrupting the Hsp90/CDC37 interaction. Co-immunoprecipitation experiments confirmed that efficient protein-protein interactions between Hsp90 and CDC37 are prevented by the administration of gedunin and celastrol, but not by GDA or NB. Additionally, evidence supporting a lack of the heat shock response following Hsp90/CDC37 interaction disruption was also observed.

II.5   Methods and Experimentals

General Methods. Unless otherwise indicated, all reagents were purchased from commercial suppliers and are used without further purification. Commercial solvents were purified by activated alumina prior to use. All stir bars and glassware were flame dried and glassware was flushed with Argon immediately prior to use. The ^{1}H and ^{13}C NMR spectra were

recorded at 500 and 125 MHz respectively, on a Bruker DRX 500 using CDCl$_3$ as solvent, chemical shift values are reported in ppm (TMS as internal standard), and coupling constants (J) are reported in Hz. Column chromatography was performed with silica gel (40-63 m particle size) from Sorbent Technologies (Atlanta, GA). Analytical HPLC was carried out on an Agilent 1100 Series Capillary HPLC system with diode array detection at 254 nm (compounds 5–8, 10a, and 11 were detected at 214.15 nm) on an Agilent Eclipse XDB-C18 column (4.6 × 150 mm, 5 mm) with isocratic elution in 70% acetonitrile (ACN) and 30% H$_2$O at a flow rate of 5.0 mL/min.
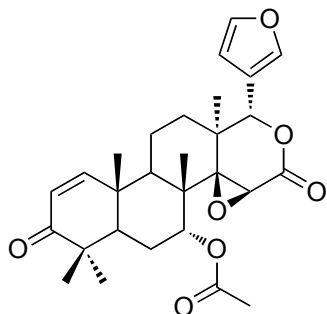

Gedunin (1). Spectral data match what was previously reported in the literature. ^{1}H NMR (500 MHz, CDCl$_3$) δ 7.35 (s, 2H), 7.03 (d, J = 10.2 Hz, 1H), 6.28 (s, 1H), 5.80 (d, J = 10.2 Hz, 1H), 5.55 (s, 1H), 4.49 (s, 1H), 3.46 (s, 1H), 2.42 (dd, J = 12.7, 6.0 Hz, 1H), 2.10 (d, J = 13.2 Hz, 1H), 2.04 (s, 3H), 2.00 – 1.85 (m, 2H), 1.84 – 1.62 (m, 3H), 1.53 (dd, J = 13.3, 11.2 Hz, 1H), 1.18 (s, 3H), 1.16 (s, 3H), 1.09 (s, 3H), 1.01 (s, 3H), 1.00 (s, 3H). ^{13}C NMR (126 MHz, CDCl$_3$) δ 204.01, 169.92, 167.48, 156.98, 143.11, 141.21, 126.03, 120.42, 109.88, 78.27, 73.23, 69.80, 56.91, 46.04, 44.07, 42.62, 40.04, 39.52, 38.73, 27.19, 25.99, 23.27, 21.22, 21.11, 19.78, 18.34, 17.74, 14.99.
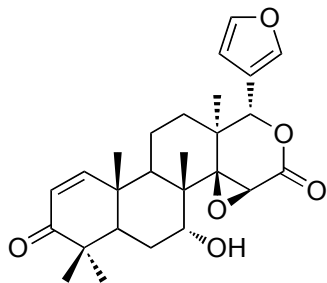
Desacetylgedunin (2). Spectral data match what was previously reported in the literature. ^{1}H NMR (500 MHz, CDCl$_3$) δ 7.43 – 7.25 (m, 2H), 7.04 (d, J = 10.2 Hz, 1H), 6.28 (dd, J = 1.7, 0.8 Hz, 1H), 5.78 (d, J = 10.2 Hz, 1H), 5.53 (s, 1H), 3.84 (s, 1H), 3.51 (d, J = 1.5 Hz, 1H), 2.45 (dd, J = 13.0, 6.5 Hz, 1H), 2.41 (dd, J = 13.5, 2.7 Hz, 1H), 1.96 – 1.80 (m, 2H), 1.81 – 1.69 (m, 1H), 1.70 – 1.55 (m, 2H), 1.52 – 1.44 (m, 1H), 1.40 (d, J = 3.1 Hz, 1H), 1.17 (s, 3H), 1.13 (s, 3H), 1.08 (s, 3H), 1.03 (s, 3H), 1.02 (s, 3H). ^{13}C NMR (126 MHz, CDCl$_3$) δ 203.49, 167.14, 156.68, 141.94, 140.14, 124.76, 119.62, 108.95, 77.40, 68.96, 68.74, 56.84, 52.41, 43.56, 43.15, 42.61, 39.17, 37.31, 36.93, 26.31, 25.34, 20.48, 18.92, 17.67, 16.76, 14.02.

General Procedure A. A solution of **2** (20 mg, 0.045 mmol, 1eq..) in anhydrous THF (450 μL) was stirred at 0 ºC under argon atmosphere. KO′Bu (45 μL, 0.09 mmol, 2eq.) was added dropwise and the mixture stirred for 30 min before alkyl iodide (10eq) was added. The resulting mixture was stirred at 0 ºC for 1.5 h and then quenched by the addition of H$_2$O (1mL). The organic layer was removed and the aqueous layer extracted with DCM (3 × 5mL). The combined organic layers were dried (Na$_2$SO$_4$), filtered, and concentrated. The residue was purified *via* SiO$_2$ chromatography (5:3:2, Hex:DCM:Et$_2$O) to yield the desired compound.
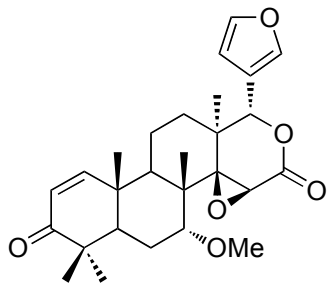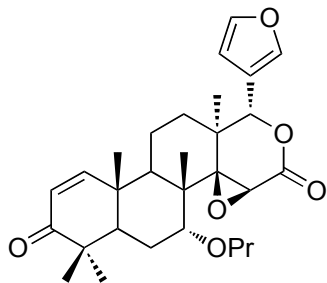
(1S,3aS,41R,4a1S,5R,10aR,12aS)-1-(furan-3-yl)-5-methoxy-4a1,7,7,10a,12a-pentamethyl-4a1,5,6,6a,7,10a,10b,11,12,12a-decahydronaphtho[2,1-f]oxireno[2,3-d]isochromene-3,8(1H,3aH)-dione (3a).

Compound **3a** was synthesized from **2** using general procedure A and iodomethane to afford 13 mg (64%) as a colorless solid. ^{1}H NMR (500 MHz, CDCl$_3$): δ 1.01 (s, 3H), 1.04 (s, 3H), 1.10 (s, 3H), 1.13 (s, 3H), 1.13 (s, 3H), 1.44-1.52 (m, 2H), 1.67-1.75 (m, 2H), 1.82-1.90 (m, 2H), 2.23 (dd, J = 2.1, 13.2 Hz, 1H), 2.38 (dd, J = 5.9, 12.7 Hz, 1H), 2.85 (d, J = 2.1 Hz, 1H), 3.25 (s, 3H), 3.55 (s, 1H), 5.52 (s, 1H), 5.76 (d, J = 10.2 Hz, 1H), 6.27 (d, J = 0.6 Hz, 1H), 7.01 (d, J = 10.2, 1H), 7.30-7.35 (m, 2H): ^{13}C NMR (125 MHz, CDCl$_3$);δ14.1, 16.7, 17.5, 18.9, 19.2, 20.5, 25.4, 26.4, 37.3, 37.7, 39.0, 43.1, 43.2, 43.5, 54.6, 56.4, 69.1, 77.4, 78.2, 108.9, 119.7, 124.7, 140.1, 141.9, 156.8, 167.1, 203.5; HRMS (*ESI +pos.) (*m/z*): [M+H] calcd. for C$_{27}$H$_{35}$O$_6$, 455.2434; found, 455.2419; HPLC t_R = 10.09 min; Purity = > 99 %.
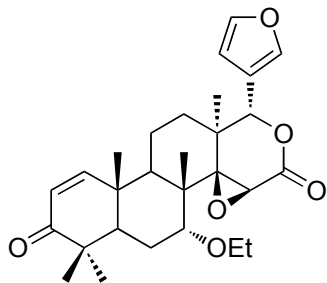
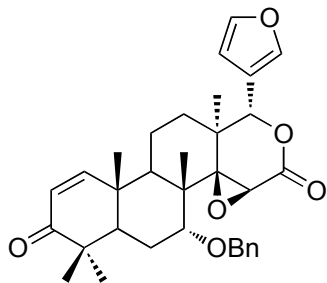**(1*S*,3a*S*,41*R*,4a1*S*,5*R*,10a*R*,12a*S*)-5-ethoxy-1-(furan-3-yl)-4a1,7,7,10a,12a-pentamethyl-4a1,5,6,6a,7,10a,10b,11,12,12a-decahydronaphtho[2,1-f]oxireno[2,3-d]isochromene-3,8(1H,3aH)-dione (3b)**.

Compound **3b** was synthesized from **2** using general procedure A and 1-iodoethane to afford 7 mg (33%) as a colorless solid. ^{1}H NMR (500 MHz, CDCl$_3$): δ 1.00 (s, 3H), 1.03 (s, 3H), 1.08 (s, 3H), 1.12 (s, 3H), 1.15 (s, 3H), 1.15 (t, *J* = 12.7 Hz, 3H), 1.46-1.50 (m, 1H), 1.53-1.57 (m, 1H), 1.61-1.65 (m, 1H), 1.69-1.73 (m, 1H), 1.81-1.89 (m, 2H), 2.24 (dd, *J* = 2.2, 13.1 Hz, 1H), 2.26 (dd, *J* = 5.8, 12.8 Hz, 1H), 2.95 (d, *J* = 2.1 Hz, 1H), 3.14 (dq *J* = 7.0, 8.7 Hz, 1H), 3.55 (s, 1H), 3.57 (dq, *J* = 7.0, 8.7 Hz, 1H), 5.53 (s, 1H), 5.77 (d, *J* = 10.2 Hz, 1H), 7.02 (d, *J* = 10.3 Hz, 1H), 7.31-7.35 (m, 2H); ^{13}C NMR (125 MHz, CDCl$_3$): δ 14.0, 14.5, 16.8, 17.4, 18.9, 20.0, 20.5, 25.4, 26.4, 37.3, 37.8, 39.0, 43.0, 43.2, 43.7, 56.4, 62.8, 69.2, 77.1, 77.4, 109.0, 119.7, 124.7, 140.1, 141.9, 156.8, 167.1, 203.6; HRMS (*ESI +pos.) (*m/z*): [M+H] calcd. for C$_{28}$H$_{37}$O$_6$, 469.2590; found, 469.2581; HPLC t_R = 12.71 min; Purity = > 99 %.

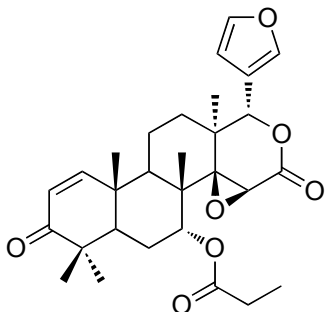**(1S,3aS,41R,4a1S,5R,10aR,12aS)-1-(furan-3-yl)-4a1,7,7,10a,12a-pentamethyl-5-propoxy-4a1,5,6,6a,7,10a,10b,11,12,12a-decahydronaphtho[2,1-f]oxireno[2,3-d]isochromene-3,8(1H,3aH)-dione (3c)**.

Compound **3c** was synthesized from **2** using general procedure A and 1-iodopropane to afford 5 mg (23%) as a colorless solid. ^{1}H NMR (500 MHz, CDCl$_3$): δ 0.86 (t, J = 7.4 Hz, 3H), 1.01 (s, 3H), 1.04 (s, 3H), 1.08 (s, 3H), 1.13 (s, 3H), 1.16 (s, 3H), 1.46-1.50 (m, 1H), 1.50-1.61 (m, 3H), 1.62-1.67 (m, 1H), 1.70-1.74 (m, 1H), 1.84-1.88 (m, 1H), 1.90-1.95 (m, 1H), 2.25 (dd, J = 2.2, 13.1 Hz, 1H), 2.42 (dd, J = 6.0, 12.8 Hz, 1H), 2.94 (d, J = 2.2 Hz, 1H), 3.10 (dt, J = 2.3, 6.2 Hz, 1H), 3.42 (dt, J = 1.6, 6.5 Hz, 1H), 3.55 (s, 1H), 5.52 (s, 1H), 5.77 (d, J = 10.2 Hz, 1H), 6.27-6.29 (m 1H), 7.02 (d, J = 10.2 Hz, 1H), 7.31-7.35 (m, 2H). ^{13}C NMR (125 MHz, CDCl$_3$): δ 10.1, 14.0, 16.8, 17.5, 18.9, 19.9, 20.5, 22.3, 25.4, 26.5, 37.3, 37.8, 39.0, 43.0, 43.2, 43.7, 56.4, 68.9, 69.1, 76.8, 77.4, 108.9, 119.7, 124.7, 140.1, 141.9, 156.9, 167.0, 203.6; HRMS ([*]ESI +pos.) (*m/z*): [M+H] calcd. for C$_{29}$H$_{39}$O$_6$, 483.2747; found, 483.2737; HPLC t_R = 15.90 min; Purity = > 99 %.

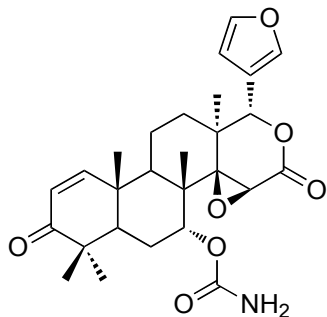**(1S,3aS,41R,4a1S,5R,10aR,12aS)-5-(benzyloxy)-1-(furan-3-yl)-4a1,7,7,10a,12a-pentamethyl-4a1,5,6,6a,7,10a,10b,11,12,12a-decahydronaphtho[2,1-f]oxireno[2,3-d]isochromene-3,8(1H,3aH)-dione (3d)**.

Compound **3d** was synthesized from **2** using general procedure A and benzyl bromide and catalytic tetrabutylammonium iodide to afford 14 mg (59%) as a colorless solid. ^{1}H NMR (500 MHz, CDCl$_3$): δ 1.02 (s, 3H), 1.04 (s, 3H), 1.07 (s, 3H), 1.12 (s, 3H), 1.14 (s, 3H), 1.42-1.46 (m, 1H), 1.59-1.68 (m, 2H), 1.68-1.72 (m, 1H), 1.80-1.85 (m, 1H), 2.02 (dt, J = 3, 14.7 Hz, 1H), 2.32 (dd, J = 2.2, 13.1 Hz), 2.41 (dd, J = 5.9, 12.7 Hz, 1H), 3.14 (d, J = 2.2 Hz, 1H), 3.67 (s, 1H), 4.25 (d, J = 10.2 Hz, 1H), 4.45 (d, J = 10.2 Hz, 1H), 5.51 (s, 1H), 5.75 (d, J = 10.2 Hz, 1H), 6.25 (d, J = 1.0 Hz, 1H), 6.99 (d, J = 10.2 Hz, 1H), 7.24-7.30 (m, 2H), 7.35-7.21 (m, 5H); ^{13}C NMR (125 MHz, CDCl$_3$): δ 14.0, 16.9, 17.6, 19.1, 19.9, 20.5, 25.5, 26.6, 37.3, 37.7, 39.1, 43.2, 43.3, 43.7, 56.3, 69.0, 69.6, 76.4, 77.3, 109.0, 119.6, 124.7, 127.1, 127.5, 127.5, 127.7, 127.7, 135.8, 140.1, 141.9, 156.9, 166.9, 203.4; HRMS ([*]ESI +pos.) (*m/z*): [M+H] calcd. for C$_{33}$H$_{39}$O$_6$, 531.2747; found, 531.2762; HPLC t_R = 16.08 min; Purity = 97.8%.

(1S,3aS,41R,4a1S,5R,10aR,12aS)-1-(furan-3-yl)-4a1,7,7,10a,12a-pentamethyl-3,8-dioxo-1,3,3a,4a1,5,6,6a,7,8,10a,10b,11,12,12a-tetradecahydronaphtho[2,1-f]oxireno[2,3-d]isochromen-5-yl propionate (3e).
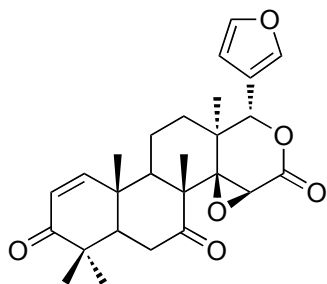
A solution of **2** (20 mg, 0.045 mmol, 1eq.), DMAP (catalytic), and Et$_3$N (35 µL, 0.248 mmol, 5.5eq.) in 450 µL anhydrous DCM was stirred under argon atmosphere at 0 ºC until completely dissolved. Propionyl chloride (20 µL, 0.225 mmol, 5eq.) was added dropwise to the solution and then stirred for 5 h before the reaction was quenched by addition of H$_2$O (1mL). The organic layer was removed and the aqueous layer extracted with DCM (3 × 5mL). The combined organic layers were dried (Na$_2$SO$_4$), filtered, and concentrated. The resulting yellow oil was purified *via* SiO$_2$ chromatography (4:3:3, Hex:DCM:Et$_2$O) to yield 17 mg (76%) **3e** as a colorless solid. ^{1}H NMR (500 MHz, CDCl$_3$): δ 0.98 (s, 3H), 1.00 (t, *J* = 7.6 Hz, 3H), 1.00 (s, 3H), 1.12 (s, 3H), 1.17 (s, 3H), 1.36 (s, 3H), 1.66-1.97 (m, 4H), 2.09 (dd, *J* = 2.4, 13.4 Hz, 1H), 2.20-2.38 (m, 1H), 2.30 (dq, *J* = 2.6, 7.7 Hz, 1H), 2.40-2.46 (m, 2H), 2.42 (dq, *J* = 2.6, 7.7 Hz, 1H), 3.48 (s, 1H), 4.52 (m, 1H), 5.52 (s, 1H), 5.79 (d, *J* = 10.2 Hz, 1H), 6.26 (m, 1H), 7.02 (d, *J* = 10.2 Hz, 1H), 7.34 (m, 1H); ^{13}C NMR (125 MHz, CDCl$_3$): δ 10.5, 14.1, 15.2, 17.7, 18.9, 19.9, 21.3, 23.3, 25.3, 27.3, 38.9, 39.6, 40.2, 42.8, 44.1, 46.1, 57.6, 69.4, 72.7, 78.0, 110.0, 114.0, 120.5, 126.0, 141.2, 143.1, 157.0, 165.1, 166.9, 204.1; HRMS (*ESI +pos.) (*m/z*): [M+H] calcd. for C$_{29}$H$_{37}$O$_7$, 497.2539; found, 497.2542; HPLC t_R = 13.66 min; Purity = 97.1%.

(1S,3aS,41R,4a1S,5R,10aR,12aS)-1-(furan-3-yl)-4a1,7,7,10a,12a-pentamethyl-3,8-dioxo-1,3,3a,4a1,5,6,6a,7,8,10a,10b,11,12,12a-tetradecahydronaphtho[2,1-f]oxireno[2,3-d]isochromen-5-yl carbamate (3f).
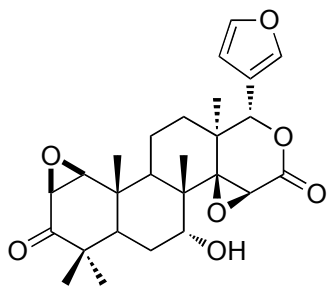
A solution of **2** (20 mg, 0.045 mmol, 1eq.) in 450 μL anhydrous DCM under argon atmosphere was stirred at 0 ºC. Trichloroacetyl isocyanate (10.7 μL, 0.09 mmol, 2eq.) was added drop-wise, and the solution was allowed to warm up to room temperature and stirred for 3 h, at which point the reaction was quenched by the addition of H_2O (1mL). The organic layer was collected and the aqueous layer extracted with DCM (3 × 5mL). The combined organic extracts were concentrated and then dissolved in 1mL 0.1M K_2CO_3 in MeOH, and stirred for 1.5 h at ambient temperature. The reaction was quenched by the addition of H_2O (1mL). The reaction mixture was extracted with DCM (3 × 5mL). The combined organic layers were dried (Na_2SO_4), filtered, and concentrated. The resulting colorless oil was purified *via* SiO_2 chromatography (4:3:3, Hex:DCM:Et_2O) to yield 21 mg (97%) **3f** as a colorless solid. ^1H NMR (500 MHz, $CDCl_3$): δ 1.01 (s, 3H), 1.03 (s, 3H), 1.09 (s, 3H), 1.16 (s, 6H), 1.49-1.53 (m, 1H), 1.65-1.68 (m, 1H), 1.778-1.81 (m, 2H), 1.85-1.93 (m, 2H), 2.15 (dd, J = 2.5, 12.7 Hz, 1H), 2.37 (dd, J = 6.1, 12.7 Hz, 1H), 3.66 (s, 1H), 4.45 (s, 1H), 4.67 (br s, 2H), 5.54 (s, 1H), 5.79 (d, J = 10.2 Hz, 1H), 6.25-6.27 (m, 1H), 7.02 (d, J = 10.2 Hz, 1H), 7.32-7.35 (m, 2H); ^{13}C NMR (125 MHz, $CDCl_3$): δ 15.0, 18.0, 18.5, 19.8, 21.3, 23.6, 26.0, 27.2, 38.6, 39.5, 40.0, 42.9, 44.1, 45.9, 56.9, 69.7, 73.5,

78.2, 109.9, 120.5, 126.0, 141.2, 143.1, 155.1, 157.1, 167.4, 204.2; HRMS (*ESI +pos.) (*m/z*): [M+H] calcd. for $C_{27}H_{34}N_1O_7$, 484.2335; found, 484.2320; HPLC t_R = 3.59 min; Purity = 98.7%.
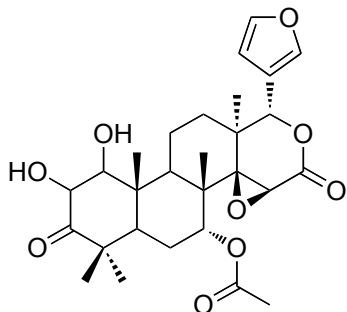

(1*S*,3a*S*,41*R*,4a1*R*,10a*S*,12a*S*)-1-(furan-3-yl)-4a1,7,7,10a,12a-pentamethyl-6,6a,7,10a,10b,11,12,12a-octahydronaphtho[2,1-f]oxireno[2,3-d]isochromene-3,5,8(1H,3aH,4a1H)-trione (4).

A solution of **2** (20 mg, 0.045 mmol, 1eq.) in 450 μL anhydrous DCM was stirred at ambient temperature. PCC (29.1 mg, 0.135 mmol, 3eq.) was added in one portion and the reaction mixture was stirred overnight before the solution was filtered through a plug of silica using Et2O as eluent. The colorless solution was dried (Na_2SO_4), filtered, and concentrated. The resulting colorless oil was purified *via* SiO_2 chromatography (5:3:2, Hex:DCM:Et$_2$O) to yield 19 mg (96%) **4** as a colorless solid. ^{1}H NMR (500 MHz, CDCl$_3$): δ 1.07 (s, 3H), 1.07 (s, 3H), 1.09 (s, 3H), 1.15 (s, 3H), 1.29 (s, 3H), 1.41 (dt, *J* = 3.9, 9.8 Hz, 1H), 1.71-1.77 (m, 2H), 1.91-1.95 (m, 1H), 2.10-2.17 (m, 2H), 2.34 (dd, *J* = 3.2, 14 Hz, 1H), 2.86 (t, *J* = 14.4 Hz, 1H), 3.80 (s, 1H), 5.4 (s, 1H), 5.85 (d, *J* = 10.2 Hz, 1H), 6.29 (dd, *J* = 0.7, 1.8 Hz, 1H), 7.03 (d, *J* = 10.2 Hz, 1H), 7.32-7.34 (m, 1H), 7.34-7.36 (m, 1H); ^{13}C NMR (125 MHz, CDCl$_3$): δ 16.2, 16.4, 18.8, 19.6, 19.9, 25.7, 31.2, 35.7, 36.7, 35.7, 36.7, 38.6, 44.2, 46.6, 52.4, 52.6, 53.5, 64.5, 77.0, 108.8, 119.2, 125.4, 140.0, 142.1, 154.9, 165.8, 202.2, 207.1; HRMS (*ESI +pos.) (*m/z*): [M+H] calcd. for $C_{26}H_{31}O_6$, 439.2121; found, 439.2129; HPLC t_R = 5.45 min; Purity = > 99 %.

(1*S*,3a*S*,41*R*,4a1*S*,5*R*,10a*R*,12a*S*)-1-(furan-3-yl)-5-hydroxy-4a1,7,7,10a,12a-pentamethyl-4a1,5,6,6a,7,10a,10b,11,12,12a-decahydronaphtho[2,1-f],[9,10]dioxireno[2,3-d]isochromene-3,8(1H,3aH)-dione (5).

A solution of **2** (20 mg, 0.045 mmol, 1eq.) in 450 μL acetone was stirred at 0 ºC. A solution of 8% aqueous sodium hydroxide (85 μL) and a solution of 30% aqueous hydrogen peroxide (52 μL) were added. The reaction mixture was allowed to warm to room temperature. After stirring overnight, 2N hydrochloric acid (1mL) was added. The reaction mixture was extracted with DCM (3 × 5 mL), and the combined organic layers were dried (Na_2SO_4), filtered, and concentrated. The resulting colorless oil was purified *via* SiO_2 chromatography (5:3:2, Hex:DCM:Et_2O) to yield 14 mg (68%) **5** as a colorless solid. ^{1}H NMR (500 MHz, CDCl$_3$): δ 0.92 (s, 3H), 0.96 (s, 3H), 1.00 (s, 3H), 1.04 (s, 3H), 1.22 (s, 3H), 1.45-1.52 (m, 2H), 1.63 (dd, *J* = 4.1, 8.1 Hz, 1H), 1.71-1.77 (m, 2H), 1.92-1.96 (m, 1H), 2.64 (dd, *J* = 2.6, 13.7 Hz, 1H), 2.72 (dd, *J* = 6.6, 12.7 Hz, 1H), 3.32 (d, *J* = 4.6 Hz, 1H), 3.46 (s, 1H), 3.48 (d, *J* = 4.5 Hz, 1H), 3.85 (s, 1H), 5.53 (s, 1H), 6.29 (s, 1H), 7.33 (s, 1H), 7.32-7.34 (m, 2H); ^{13}C NMR (125 MHz, CDCl$_3$): δ 14.5, 14.8, 16.4, 17.7, 19.8, 25.0, 26.0, 26.5, 35.9, 36.1, 37.4, 38.2, 42.2, 43.2, 55.6, 57.0, 62.1, 68.5, 68.9, 77.4, 109.0, 119.6, 140.2, 141.9, 167.2, 210.7; HRMS ([*]ESI +pos.) (*m/z*): [M+H] calcd. for $C_{26}H_{33}O_7$, 457.2226; found, 457.2220; HPLC t_R = 6.40 min; Purity = 98.6%.

(1S,3aS,41R,4a1S,5R,10aR,12aS)-1-(furan-3-yl)-9,10-dihydroxy-4a1,7,7,10a,12a-pentamethyl-3,8-dioxohexadecahydronaphtho[2,1-f]oxireno[2,3-d]isochromen-5-yl acetate (6).

A solution of **1** (100 mg, 0.21 mmol, 1eq.) in 1.78 mL fully degassed acetone was stirred under argon atmosphere at 0 ºC. A 4% solution of osmium tetroxide in water (72 μL, 0.011 mmol, 0.05eq.) and a 1 M solution of N-methylmorpholine N-oxide in deionized water (315 μL, 0.315 mmol, 1.5eq.) were added. After stirring overnight, saturated aqueous sodium sulfite was added (4 mL) and the reaction mixture was stirred for 1 hour at room temperature. The reaction mixture was extracted 4 times with EtOAc. The combined organics were dried (Na$_2$SO$_4$), filtered, and concentrated. The resulting black oil was purified *via* SiO$_2$ chromatography (7:6:6, Hex:DCM:Et$_2$O) to yield 97 mg (89%) **6** as a colorless solid. ^{1}H NMR (500 MHz, CDCl$_3$): δ 0.99 (s, 3H), 1.02 (s, 3H), 1.07 (s, 3H), 1.18 (s, 3H), 1.19 (s, 3H), 1.48-1.51 (m, 1H), 1.60-1.63 (m, 2H), 1.79-1.82 (m, 2H), 2.03 (s, 3H), 2.16 (dd, *J* = 4.1, 11.5 Hz, 1H), 2.48 (s, 1H), 2.96 (dd, *J* = 6.4, 12.1 Hz, 1H), 3.42 (s, 1H), 3.86 (d, *J* = 2.3 Hz, 1H), 3.89 (d, *J* = 2.8 Hz, 1H), 4.44 (br s, 1H), 4.60-4.62 (m, 1H), 5.54 (s, 1H), 6.25-6.27 (m, 1H), 7.32-7.34 (s, 1H). ^{13}C NMR (125 MHz, CDCl$_3$): δ 13.5, 15.3, 15.7, 17.5, 19.9, 20.1, 22.0, 22.8, 24.6, 35.7, 37.9, 40.2, 40.8, 41.0, 45.5, 55.7, 69.0, 70.2, 72.5, 75.9, 77.5, 109.0, 119.6, 140.1, 141.9, 166.6, 169.1, 213.0; HRMS (*ESI

+pos.) (*m/z*): [M+H] calcd. for $C_{28}H_{37}O_9$, 517.2438; found, 517.2421; HPLC t_R = 4.71 min; Purity = > 99 %.
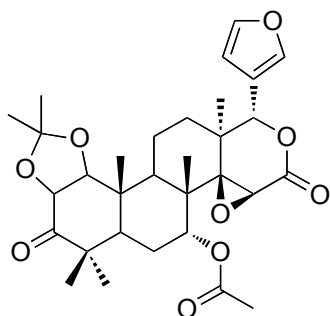
(1*S*,3a*S*,41*R*,4a1*S*,5*R*,10a*R*,12a*S*)-1-(furan-3-yl)-9,10-dihydroxy-4a1,7,7,10,10,10a,12a-heptamethyl-3,8-dioxohexadecahydronaphtho-9,11-dioxol-[2,1-f]oxireno[2,3-d]isochromen-5-yl acetate (7).

A solution of **6** (10.5 mg, 0.02 mmol, 1eq.) in 100 μL of acetone was stirred at room temperature. 2,2-dimethoxypropane (11 μL, 0.088 mmol, 4.4eq.) was added followed by the addition of catalytic *p*-Toluenesulfonic acid. After stirring for 3 h, solvent was blown dry, and residue was taken up in 300 μL of DCM and washed with sodium bicarbonate and brine. The organic layer was dried (Na_2SO_4), filtered, and concentrated. The resulting colorless oil was purified *via* SiO_2 chromatography (5:3:2, Hex:DCM:Et_2O) to yield 10 mg (90%) **7** as a colorless solid. ^{1}H NMR (500 MHz, CDCl$_3$): δ 0.98 (s, 3H), 1.02 (s, 3H), 1.13 (s, 3H), 1.22 (s, 3H), 1.23 (s, 3H), 1.48 (s, 3H), 1.48-1.51 (m, 1H), 1.50 (s, 3H), 1.56-1.63 (m, 3H), 1.71-1.73 (m, 1H), 1.83 (dt, *J* = 3.7, 14.9 Hz, 1H), 2.05 (s, 3H), 2.42 (dd, *J* = 3.6, 13.7 Hz, 1H), 2.95 (dd, *J* = 6.2, 12.4 Hz, 1H), 3.48 (s, 1H), 4.05 (d, *J* = 7.5 Hz, 1H), 4.31 (d, *J* = 7.5 Hz, 1H), 4.45 (dd, *J* = 1.9, 3.4, 1H), 5.55 (s, 1H), 6.27 (d, *J* = 1.0 Hz, 1H), 7.32-7.35 (m, 2H); ^{13}C NMR (125 MHz, CDCl$_3$): δ 13.8, 14.5, 15.7, 16.9, 20.1, 20.4, 22.5, 22.9, 24.5, 24.9, 28.4, 32.6, 36.7, 37.8, 39.5, 40.4, 44.0, 52.4, 55.7, 69.1, 72.3, 77.4, 81.1, 109.0, 109.4, 119.6, 140.1, 141.9, 166.7, 168.9, 210.9; HRMS

(*ESI +pos.) (m/z): [M+Na] calcd. for $C_{31}H_{40}O_9Na$, 579.2570; found, 579.2548; HPLC t_R = 14.17 min; Purity = 96.1%.
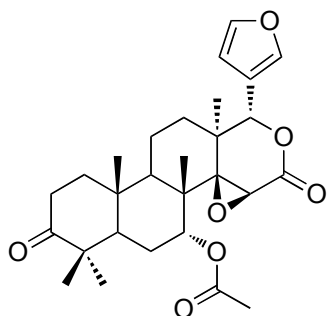
(1S,3aS,41R,4a1S,5R,10aR,12aS)-1-(furan-3-yl)-4a1,7,7,10a,12a-pentamethyl-3,8-dioxohexadecahydronaphtho[2,1-f]oxireno[2,3-d]isochromen-5-yl acetate (8).

A solution of **1** (20 mg, 0.041 mmol, 1eq.) and 10% Pd/C (2 mg) in 1 mL of methanol was stirred at room temperature under an atmosphere of argon. The reaction flask was purged with H_2 repeatedly. The fully H_2 purged flask was stirred at room temperature for 5 h after which, the solution was run through a plug of silica using ether as eluent. The organic filtrate was dried (Na_2SO_4), filtered, and concentrated. The resulting colorless oil was purified *via* SiO_2 chromatography (5:3:2, Hex:DCM:Et$_2$O) to yield 7 mg (35%) **8** as a colorless solid. ^{1}H NMR (500 MHz, CDCl$_3$): δ 0.96 (s, 3H), 1.00 (s, 3H), 1.05 (s, 3H), 1.17 (s, 3H), 1.42 (s, 3H), 1.48-1.53 (m, 2H), 1.63-1.71 (m, 4H), 1.77-1.81 (m, 1H), 1.81-1.83 (m, 1H), 1.84-1.86 (m, 1H), 2.24 (dd, J = 6.9, 12.1 Hz, 1H), 2.38-2.40 (m, 1H), 2.50-2.52 (m, 1H), 3.45 (s, 1H), 4.44-4.47 (m, 1H), 5.54 (s, 1H), 6.25-6.26 (m, 1H), 7.31-7.33 (m, 2H); ^{13}C NMR (125 MHz, CDCl$_3$): δ 14.0, 14.7, 16.4, 17.0, 19.9, 20.1, 22.7, 24.8, 25.0, 32.7, 36.3, 37.8, 37.9, 40.9, 43.0, 45.6, 46.7, 55.7, 68.78, 72.7, 77.3, 108.9, 119.5, 140.1, 142.0, 166.6, 169.0, 214.9; HRMS (*ESI +pos.) (m/z): [M+H] calcd. for $C_{28}H_{37}O_7$, 485.2539; found, 485.2549; HPLC t_R = 6.35 min; Purity = 97.6%.
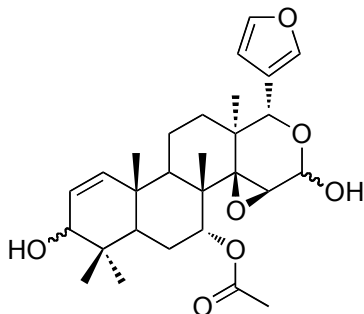
(1*S*,3a*S*,41*R*,4a1*S*,5*R*,10a*S*,12a*S*)-1-(furan-3-yl)-3,8-dihydroxy-4a1,7,7,10a,12a-pentamethyl-1,3,3a,4a1,5,6,6a,7,8,10a,10b,11,12,12a-tetradecahydronaphtho[2,1-f]oxireno[2,3-d]isochromen-5-yl acetate (9).

A solution of **1** (500 mg, 1.04 mmol, 1eq.) in 4 mL of a 2:1 mixture of methanol and chloroform was stirred under argon atmosphere at 0 ºC. Cerium trichloride hexahydrate (740 mg, 2.08 mmol, 2 eq) was added followed by the slow addition of sodium borohydride (39.33 mg, 1.04 mmol, 1eq). The reaction mixture was stirred for 3 minutes and quenched by the addition of a solution of 1% acetic acid in water. The reaction mixture was extracted 3 times with dichloromethane. The combined organic layers were dried (Na_2SO_4), filtered, and concentrated. The resulting colorless crystals were dissolved in minimal DCM and purified *via* SiO_2 chromatography (6:7:7, Hex:DCM:Et_2O) to yield 473 mg (93%) **9** as a colorless solid. Major Diastereomer: ^{1}H NMR (500 MHz, CDCl$_3$): δ 0.74 (s, 3H), 0.83 (s, 3H), 0.95 (s, 3H), 1.02 (s, 3H), 1.16 (s, 3H), 1.45-1.80 (m, 7H), 2.05 (s, 3H), 2.30 (dd, *J* = 5.4, 12.9 Hz, 1H), 3.00-3.10 (m, 2H), 3.21 (d, *J* = 1.8 Hz, 1H), 3.84 (bs, 1H), 4.56-4.60 (m, 1H), 4.92 (s, 1H), 5.05 (d, *J* = 10.2 Hz, 1H), 5.28 (d, *J* = 10.2, 1H), 5.80 (m, 1H), 6.20 (m, 1H), 7.23 (m, 1H), 7.27 (m, 1H); ^{13}C NMR (125 MHz, CDCl$_3$): δ 14.6, 16.1, 17.2, 18.5, 18.7, 20.3, 22.2, 25.6, 26.5, 35.6, 35.7, 338.4, 40.9, 41.9, 45.0, 57.5, 68.5, 71.4, 73.4, 73.4, 76.2, 86.8, 109.2, 121.9, 125.1, 136.3, 125.1, 136.3,

139.6, 141.3, 168.8; HRMS (*ESI +pos.) (m/z): [M+Na] calcd. for $C_{28}H_{38}O_7Na$, 509.2515; found, 509.2500; HPLC t_R = 6.12 min; Purity = > 99 %.
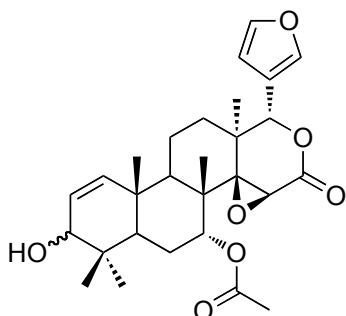
(1S,3aS,41R,4a1S,5R,10aS,12aS)-1-(furan-3-yl)-8-hydroxy-4a1,7,7,10a,12a-pentamethyl-3-oxo-1,3,3a,4a1,5,6,6a,7,8,10a,10b,11,12,12a-tetradecahydronaphtho[2,1-f]oxireno[2,3-d]isochromen-5-yl acetate (10a).

A solution of **1** (500mg, 1.04 mmol, 1eq.) in 1.3 mL toluene was stirred at ambient temperature under argon atmosphere. Isopropyl alcohol (687 mg, 11.44 mmol, 11eq.) and aluminum triisopropoxide (127.5 mg, 0.624, 0.6eq.) were added, and the reaction mixture was heated at 70°C for 20h. After being allowed to cool to ambient temperature, the reaction mixture was quenched by the addition of 1 N HCl (4 mL) and EtOAc (4 mL) and stirred for 1.5h. The organic layer was washed with water and concentrated. The resulting colorless oil was purified *via* SiO_2 chromatography (3:1:1, Hex:DCM:Et$_2$O) to yield 284 mg (56%) of **10a** as a colorless solid. ^{1}H NMR (500 MHz, CDCl$_3$): δ 0.75 (s, 3H), 0.83 (s, 3H), 1.02 (s, 3H), 1.04 (s, 3H), 1.16 (s, 3H), 1.44-1.48 (m, 1H), 1.57-1.61 (m, 1H), 1.59-1.63 (m, 1H), 1.66-1.69 (m, 2H), 1.82-1.86 (m, 1H), 1.90 (dd, J = 2.6, 11.7 Hz, 1H), 2.05 (s, 3H), 2.29 (dd, J = 6.4, 12.6 Hz, 1H), 3.42 (s, 1H), 3.84 (d, J = 8.3, 1H), 4.45 (bs, 1H), 5.29 (d, J = 10.5 Hz, 1H), 5.53 (s, 1H), 5.78 (d, J = 10.6 Hz, 1H), 6.26 (s, 1H), 7.33 (s, 2H); ^{13}C NMR (125 MHz, CDCl$_3$): δ 15.4, 17.3, 17.5, 18.5, 19.6, 21.2, 22.6, 26.0, 27.4, 36.5, 38.8, 39.7, 42.0, 42.7, 45.8, 56.8, 65.9, 69.9, 73.9, 78.4, 109.9, 120.6,

126.5, 136.7, 141.2, 143.0, 167.8, 170.0; HRMS (*ESI +pos.) (*m/z*): [M+H] calcd. for $C_{28}H_{37}O_7$, 485.2539; found, 485.2540; HPLC t_R = 4.31 min; Purity = 98.1%.
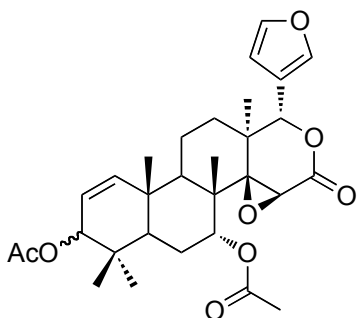
(1*S*,3a*S*,41*R*,4a1*S*,5*R*,10a*S*,12a*S*)-1-(furan-3-yl)-4a1,7,7,10a,12a-pentamethyl-3-oxo-1,3,3a,4a1,5,6,6a,7,8,10a,10b,11,12,12a-tetradecahydronaphtho[2,1-f]oxireno[2,3-d]isochromene-5,8-diyl diacetate (10b).

A solution of **10a** (10 mg, 0.0206 mmol, 1eq), DMAP (catalytic), and Et_3N (15 µL, 0.103 mmol, 5eq.) in anhydrous THF (250 µL) was stirred under argon atmosphere at 0 ºC. Acetyl chloride (8 µL, 0.103 mmol, 5eq.) was added drop-wise, and the reaction mixture was stirred overnight while allowing to warm to ambient temperature. The reaction mixture was quenched by the addition of water (500 µL), and the organic layer was collected and the aqueous layer was washed with DCM (3 × 5mL). The combined organic layers were dried (Na_2SO_4), filtered, and concentrated. The resulting yellow oil was purified *via* SiO_2 chromatography (5:3:2, Hex:DCM:Et$_2$O) to yield 9 mg (83%) **10b** as a colorless solid. ^1H NMR (500 MHz, CDCl$_3$): δ 0.74 (s, 3H), 0.83 (s, 3H), 1.02 (s, 3H), 1.07 (s, 3H), 1.15 (s, 3H), 1.46-1.50 (m, 1H), 1.59-1.61 (m, 1H), 1.66-1.72 (m, 2H), 1.81 (m, 2H), 1.90 (d, *J* = 15.0 Hz, 1H), 2.03 (s, 3H), 2.05 (s, 3H), 2.31 (dd, *J* = 6.4, 12.7 Hz, 1H), 3.42 (s, 1H), 4.45 (bs, 1H), 5.07 (d, *J* = 1.8 Hz, 1H), 5.17 (dd, *J* = 1.4, 9.7 Hz, 1H), 5.52 (s, 1H), 5.82 (d, *J* = 10.5 Hz, 1H), 6.26 (s, 1H), 7.33 (s, 2H). ^{13}C NMR (125 MHz, CDCl$_3$): δ 14.4, 16.4, 17.3, 17.4, 18.4, 20.2, 21.4, 25.0, 26.4, 34.5, 37.7, 38.7, 41.0,

41.6, 44.8, 55.7, 68.8, 72.7, 77.4, 77.7, 108.9, 119.5, 121.8, 136.6, 140.1, 142.0, 166.6, 169.0, 170.4; HRMS (*ESI +pos.) (m/z): [M+H] calcd. for $C_{30}H_{39}O_8$, 527.2645; found, 527.2654; HPLC t_R = 16.63 min; Purity = 96.2%.
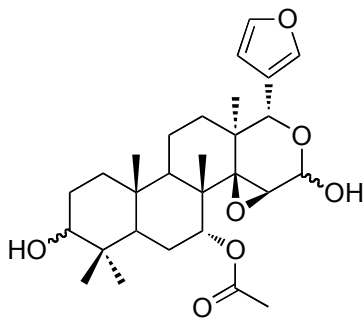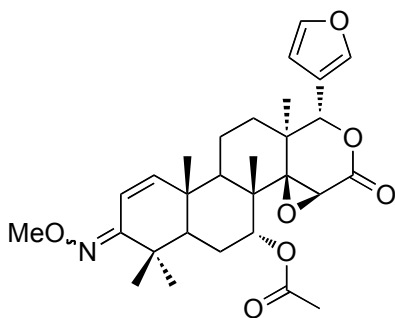

(1S,3aS,41R,4a1S,5R,10aS,12aS)-1-(furan-3-yl)-3,8-dihydroxy-4a1,7,7,10a,12a-pentamethylhexadecahydronaphtho[2,1-f]oxireno[2,3-d]isochromen-5-yl acetate (11).

A solution of **1** (20 mg, 0.041 mmol, 1eq.) in 450 µL ethanol was stirred at ambient temperature under argon atmosphere. Sodium borohydride (10 mg, 0.25 mmol, 6eq.) was added in one portion and reaction mixture was stirred for 45 minutes. The reaction mixture was quenched by the addition of 1% aqueous acetic acid. The reaction mixture was extracted 3 times with chloroform. The combined organic layers were dried (Na_2SO_4), filtered, and concentrated. The resulting colorless oil was purified *via* SiO_2 chromatography (4:3:3, Hex:DCM:Et$_2$O) to yield 17 mg (85%) **11** as a colorless solid. Major Diasteromer: ^{1}H NMR (500 MHz, CDCl$_3$): δ 0.69 (s, 3H), 0.81 (s, 3H), 0.85 (s, 3H), 0.94 (s, 3H), 1.18 (s, 3H), 1.15-1.36 (m, 2H), 1.45-1.75 (m, 9H), 2.05 (s, 3H), 2.10-2.21 (m, 1H), 2.96 (d, J = 10.4, 1H), 3.17-3.20 (m, 1H), 3.22 (s, 1H), 4.56-4.59 (m, 1H), 4.92 (s, 1H), 5.06 (d, J = 10.4, 1H), 6.21 (m, 1H), 7.22-7.26 (m, 1H), 7.26-7.28 (m, 1H); ^{13}C NMR (125 MHz, CDCl$_3$): δ 14.2, 16.8, 17.2, 18.5, 20.4, 22.3, 25.4, 25.7, 26.5, 26.7, 26.5, 26.7, 35.7, 36.8, 37.3, 37.4, 43.3, 45.0, 47.0, 52.4, 57.8, 72.2, 73.8, 77.5, 86.8, 109.3, 122.4,

139.6, 141.3, 168.9; HRMS (*ESI +pos.) (*m/z*): [M+Na] calcd. for $C_{28}H_{40}O_7Na$, 511.2672; found, 511.2681; HPLC t_R = 4.23 min; Purity = 98.3%.

General Procedure B. A solution of **1** (20 mg, 0.041 mmol, 1eq.) was stirred in pyridine (450 μL) at room temperature. Hydroxylamine or appropriate hydroxylamine derivative (2eq.) was added and the reaction mixture was stirred at 70 ºC in a sealed tube overnight. The reaction mixture was diluted with toluene and solvents were condensed *in vacuo*. The co-evaporation procedure was repeated 2 more times. The resulting oil was dissolved in DCM and washed with saturated aqueous sodium bicarbonate (2 × 5 mL). The organic layer was collected, and the aqueous layer was re-extracted with dichloromethane (2 × 5 mL). The combined organic layers were dried (Na_2SO_4), filtered, and concentrated. The resulting oil was purified *via* SiO_2 chromatography (eluent: Hex:DCM:Et_2O) to yield the desired oxime.

(1S,3aS,41R,4a1S,5R,10aS,12aS)-1-(furan-3-yl)-8-(methoxyimino)-4a1,7,7,10a,12a-pentamethyl-3-oxo-1,3,3a,4a1,5,6,6a,7,8,10a,10b,11,12,12a-tetradecahydronaphtho[2,1-f]oxireno[2,3-d]isochromen-5-yl acetate (12a).

Compound **12a** was synthesized from **1** using general procedure B and methoxyhydroxylamine hydrochloride to afford 13 mg (62%) as a colorless solid. ^{1}H NMR (500 MHz, CDCl$_3$): δ 1.05 (s, 3H), 1.06 (s, 3H), 1.07 (s, 3H), 1.08 (s, 3H), 1.16 (s, 3H), 1.46-1.50 (m, 1H), 1.63-1.65 (m,

1H), 1.67-1.71 (m, 1H), 1.77 (dd, *J* = 1.8, 13.4, 1H), 1.76-1.78 (m, 1H), 1.90 (dd, *J* = 2.2, 12.7, 1H), 1.89-1.93 (m, 1H), 2.32 (dd, *J* = 6.0, 12.8 Hz, 1H), 3.45 (s, 1H), 3.79 (s, 3H), 4.45-4.49 (m, 1H), 5.54 (s, 1H), 6.24-6.28 (m, 1H), 6.33 (d, *J* = 10.4 Hz, 1H), 6.49 (d, *J* = 10.4, 1H), 7.32-7.34 (m, 1H); ^{13}C NMR (125 MHz, CDCl$_3$): δ 14.0, 16.7, 17.2, 18.0, 20.1, 21.9, 23.2, 25.0, 28.7, 36.3, 37.7, 38.8, 38.9, 41.5, 45.4, 55.8, 60.6, 68.9, 72.5, 77.3, 108.9, 113.3, 119.5, 140.1, 142.0, 145.4, 157.4, 166.6, 168.9; HRMS (*ESI +pos.) (*m/z*): [M+H] calcd. for C$_{29}$H$_{38}$N$_1$O$_7$, 512.2649; found, 512.2635; HPLC t_R = 21.37 min; Purity = > 99 %.
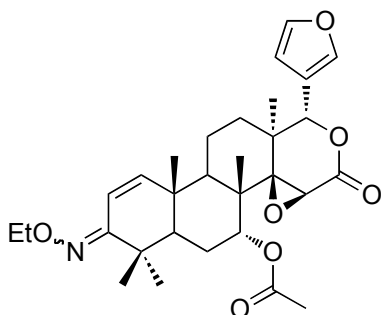
(1*S*,3a*S*,41*R*,4a1*S*,5*R*,10a*S*,12a*S*)-8-(ethoxyimino)-1-(furan-3-yl)-4a1,7,7,10a,12a-pentamethyl-3-oxo-1,3,3a,4a1,5,6,6a,7,8,10a,10b,11,12,12a-tetradecahydronaphtho[2,1-f]oxireno[2,3-d]isochromen-5-yl acetate (12b).

Compound **12b** was synthesized from **1** using general procedure B and ethoxyhydroxylamine hydrochloride to afford 17 mg (79%) as a colorless solid. ^{1}H NMR (500 MHz, CDCl$_3$): δ 1.05 (s, 3H), 1.06 (s, 3H), 1.08 (s, 3H), 1.16 (s, 3H), 1.18 (s, 3H), 1.18 (t, *J* = 6.9 Hz, 3H), 1.60-1.75 (m, 5H), 1.75-1.92 (m, 2H), 2.02 (s, 3H), 2.33 (dd, *J* = 5.9, 12.8 Hz, 1H), 3.45 (s, 1H), 4.03 (q, *J* = 7 Hz, 2H), 4.47 (s, 1H), 5.54 (s, 1H), 6.26 (m, 1H), 6.32 (d, *J* = 10.3 Hz, 1H), 6.52 (d, *J* = 10.3 Hz, 1H), 7.33 (m, 2H); ^{13}C NMR (125 MHz, CDCl$_3$): δ 14.6, 15.0, 17.7, 18.2, 19.1, 21.1, 22.9, 24.2, 26.1, 29.6, 37.4, 38.7, 39.9, 40.0, 42.5, 46.5, 56.9, 69.4, 70.0, 73.6, 78.3, 109.9, 114.5,

120.5, 141.2, 143.0, 146.0, 158.1, 163.1, 164.0; HRMS (*ESI +pos.) (m/z): [M+Na] calcd. for C$_{30}$H$_{39}$NO$_7$Na, 548.2624; found, 548.2616; HPLC t_R = 28.90 min; Purity = > 99 %.
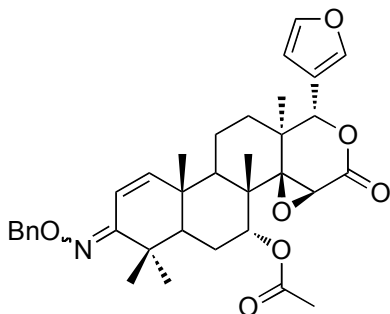
(1S,3aS,41R,4a1S,5R,10aS,12aS)-8-(benzyloxyimino)-1-(furan-3-yl)-4a1,7,7,10a,12a-pentamethyl-3-oxo-1,3,3a,4a1,5,6,6a,7,8,10a,10b,11,12,12a-tetradecahydronaphtho[2,1-f]oxireno[2,3-d]isochromen-5-yl acetate (12c).
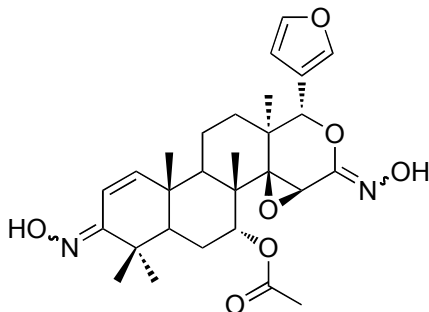
Compound **12c** was synthesized from **1** using general procedure B and benzyloxyhydroxylamine hydrochloride to afford 10 mg (42%) as a colorless solid. ^{1}H NMR (500 MHz, CDCl$_3$): δ 1.05 (s, 6H), 1.06 (s, 3H), 1.07 (s, 3H), 1.15 (s, 3H), 1.60-1.75 (m, 5H), 1.78-1.88 (m, 2H), 2.02 (s, 3H), 2.31 (dd, J = 6.05, 12.8 Hz, 1H), 3.45 (s, 1H), 4.46 (t, J = 1.6 Hz, 1H), 5.02 (s, 2H), 5.53 (s, 1H), 6.26 (m, 1H), 6.32 (d, J = 10.4 Hz, 1H), 6.55 (d, J = 10.4 Hz, 1H), 7.25-7.28 (m, 5H), 7.28-7.29 (m, 2H); ^{13}C NMR (125 MHz, CDCl$_3$): δ 14.0, 16.7, 17.2, 18.1, 20.1, 21.9, 23.2, 24.5, 28.6, 36.4, 37.6, 38.8, 38.9, 41.4, 45.3, 55.8, 68.9, 72.5, 74.9, 77.3, 108.9, 113.5, 119.4, 126.6, 126.8, 127.2, 127.2, 127.3, 137.0, 140.1, 142.0, 145.3, 157.8, 166.6, 169.0; HRMS (*ESI +pos.) (m/z): [M+H] calcd. for C$_{35}$H$_{42}$N$_1$O$_7$, 588.2961; found, 588.2915; HPLC t_R = 15.06 min; Purity = 96.3%.

(1S,3aS,41R,4a1S,5R,10aS,12aS)-1-(furan-3-yl)-3,8-bis(hydroxyimino)-4a1,7,7,10a,12a-pentamethyl-1,3,3a,4a1,5,6,6a,7,8,10a,10b,11,12,12a-tetradecahydronaphtho[2,1-f]oxireno[2,3-d]isochromen-5-yl acetate (13).

Compound **13** was synthesized from **1** using general procedure B and hydroxylamine hydrochloride to afford 7 mg (34%) as a colorless solid. ^{1}H NMR (500 MHz, CDCl$_3$): δ 1.06 (s, 3H), 1.07 (s, 3H), 1.07 (s, 6H), 1.18 (s, 3H), 1.38-1.40 (m, 1H), 1.59 (m, 1H), 1.72 (m, 2H), 1.82 (dd, J = Hz, 1H), 1.89 (m, 2H), 2.03 (s, 3H), 2.34 (dd, J = 6.1, 12.8 Hz, 1H), 3.48 (s, 1H), 4.50 (m, 1H), 5.37 (s, 1H), 6.31 (m, 1H), 6.41 (d, J = 10.4 Hz, 1H), 6.60 (d, J = 10.4 Hz, 1H), 6.66 (br. s, 1H), 7.34 (m, 1H), 7.38 (m, 1H); ^{13}C NMR (125 MHz, CDCl$_3$): δ 14.1, 16.8, 17.0, 18.1, 20.2, 22.0, 23.1, 25.0, 28.6, 29.3, 36.4, 37.8, 39.0, 41.2, 45.3, 55.1, 66.5, 72.5, 76.5, 109.0, 112.4, 120.0, 140.3, 141.9, 146.1, 149.2, 158.8, 169.0; HRMS (*ESI +pos.) (m/z): [M+H] calcd. for C$_{28}$H$_{37}$N$_2$O$_7$, 513.2595; found, 513.2509; HPLC t_R = 4.26 min; Purity = > 99 %.

Anti-proliferation Assay. MCF-7 and SKBr3 cells were maintained in a 1:1 mixture of Advanced DMEM/F12 (Gibco) supplemented with non-essential amino acids, L-glutamine (2 mM), streptomycin (500 mg/mL), penicillin (100 units/mL), and 10% FBS. Cells were grown to confluence in a humidified atmosphere (37 °C, 5% CO$_2$), seeded (2000/well, 100 μL) in 96-well plates, and allowed to attach overnight. Compound or GDA at varying concentrations in DMSO

(1% DMSO final concentration) was added, and cells were returned to the incubator for 72 h. At 72 h, the number of viable cells was determined using an MTS/PMS cell proliferation kit (Promega) per the manufacturer's instructions. Cells incubated in 1% DMSO were used as 100% proliferation, and values were adjusted accordingly. IC_{50} values were calculated from separate experiments performed in triplicate using GraphPad Prism.

Western Blot Assay. SKBr3 cells were maintained in a 1:1 mixture of Advanced DMEM/F12 (Gibco) supplemented with non-essential amino acids, L-glutamine (2 mM), streptomycin (500 mg/mL), penicillin (100 units/mL), and 10% FBS. Cells were grown to confluence in a humidified atmosphere (37 °C, 5% CO_2), seeded (1000000/dish, 5 mL) in sterile culture dishes, and allowed to attach overnight. Compounds or GDA at varying concentrations in DMSO (1% DMSO final concentration) was added, and cells were returned to the incubator for 24 h. Cells were washed once with cold phosphate buffered saline (pH 7.0) and lysed by scraping in TMNS (50 mM Tris- HCl, pH 7.5, 20 mM Na_2MoO_4, 0.1% NP-40, 150 mM NaCl) supplemented with 20 mg/mL aprotinin, 20 mg/mL leupeptin, and 1 mM phenylmethanesulfonyl fluoride. Cell lysate was clarified by centrifugation at 14,000 rpm at 4 °C for 15 min, and protein concentration was determined using the BCA method (Pierce, Rockford, IL). Twenty micrograms of total protein from cell lysates was separated by 4-20% gradient SDS-PAGE (Bio-Rad, Hercules, CA). Western blotting for ErbB2 was performed as described previously.[18] Blotting for actin was used to verifyeq.ual loading of lanes. Antibodies for R-tubulin and HER2 were from Calbiochem (La Jolla, CA). Antibodies for Actin, HER2 and Raf were from Calbiochem (La Jolla, CA).

Hsp90 Co-immunoprecipitation: SKBr-3 cells were treated with vehicle, celastrol and gedunin. GDA and NB were used as control. Cells were lysed in 20 mM Tris HCl (pH 7.4), 25 mM NaCl, 2 mM DDT, 20 mM Na_2MoO_4, 0.1 % NP-40, and protein inhibitors. Lysates were incubated for 2 hr at 4°C while rotating, and then centrifuged at 14,000 rpm for 10 min. Protein (500 μg) was incubated with anti-Hsp90 antibody for 2 hrs at 4°C. Protein G agarose (40 μl) was added to each sample, and samples were then incubated overnight at 4°C. The beads were washed with the same lysis buffer. Bound proteins were isolated by boiling in sample buffer, and subjected to SDS-PAGE. Co-immunoprecipitating proteins were analyzed by western blot analysis.

β-Galactosidase Assay: PP30 yeast strain expressing Hsp90a as their sole Hsp90[43] was transformed with the centromeric *URA3* vector, pHSE,[44] constitutively expressing β-galactosidase (encoded by *lacz*) as a reporter gene under control of a promoter bearing 3× Heat Shock Element (HSE) response elements.[44] Transformants were selected by DO medium (dropout 2% glucose medium) supplemented with appropriate amino acids without uracil.[45] Yeast cells were grown overnight to exponential phase with a cell density of $2-3\times10^6$ cells per ml in 50ml of the same medium at 30°C. Then, appropriate compounds were added to a final concentration of 30μM, followed by incubation at 30°C for 2h. Cells were additionally heat shocked at 39°C for 1h, collected by centrifugation (2000×g; 5 minutes), washed once with ddH$_2$O, and frozen at -80°C. The proteins were extracted as previously described,[46] except for exclusion of EDTA in the extraction buffer. β-Galactosidase activities of HSE were measured as previously described.[47] Cell lysate (10μl) was mixed witheq.ual volume of 2×buffer Z (0.12 M $Na_2HPO_4.7H_2O$, 0.08 M $NaH_2PO_4.H_2O$, 0.02 M KCl, 0.002 M $MgSO_4$) pH 7.0. The mixture was

added to 700μl of 2mg/ml ONPG solution in 1×buffer Z pre-warmed at 30°C and incubated at 30°C for 5-30 minutes. The reaction was stopped by adding 500 μL of 1 M Sodium Carbonate. The optical density at 420nm (OD_{420}) of each reaction mixture was determined. The protein concentration of the lysate was determined by the BioRad assay (BioRad). The β-galactosidase activity was calculated using the following formula: Enzyme Activity = $1000 \times OD_{420}$/minute/[10μl×protein concentration (μg/μl)].

II.6   References

1.   Brandt, G. E. L.; Blagg, B. S. J. Alternate strategies of Hsp90 modulation for the treatment of cancer and other diseases. *Curr. Top. Med. Chem.* **2009,** 9, 1447-1461.

2.   Banerji, U. Heat shock protein 90 as a drug target: some like it hot. *Clin. Cancer Res.* **2009,** 15, 9-14.

3.   Bishop, S. C.; Burlison, J. A.; Blagg, B. S. J. Hsp90: a novel target for the disruption of multiple signaling cascades. *Curr. Cancer Drug Targets* **2007,** 7, 369-388.

4.   Caplan, A. J. What is a co-chaperone? *Cell Stress and Chaperones* **2003,** 8, 105-107.

5.   Chadli, A.; Bruinsma, E. S.; Stensgard, B.; Toft, D. Analysis of Hsp90 cochaperone interactions reveals a novel mechanism for TPR protein recognition. *Biochemistry* **2008,** 47, 2850-2857.

6.   Caplan, A. J.; Ayan, A. M.; Wilis, I. M. Multiple kinases and system robustness: a link between Cdc37 and genome integrity. *Cell Cycle* **2007,** 6, 3145-3147.

7.   Caplan, A. J.; Mandal, A. K.; Theodoraki, M. A. Molecular chaperones and protein kinase quality control. *Trends Cell. Biol.* **2007,** 17, 87-92.

8.   Yuan, T. L.; Cantley, L. C. PI3K pathway alterations in cancer: variations on a theme. *Oncogene* **2008,** 27, 5497-5510.

9.   Di Nicolantonio, f.; Bardelli, A. Kinase mutations in cancer: chinks in the enemy's armour? *Curr. Opin. Oncol.* **2006,** 18, 69-76.

10.   Stella, G. M.; Benvenuti, S.; Comoglio, P. M. Targeting the MET oncogene in cancer and metastases. *Expert Opin. Investig. Drugs* **2010,** 19, 1381-1394.

11.   Pearl, L. H. Hsp90 and Cdc37 - a chaperone cancer conspiracy. *Curr. Opin. Genet. Dev.* **2005,** 15, 55-61.

12.   Smith, J. R.; Clarke, P. A.; Billy, E. d.; Workman, P. Silencing the cochaperone Cdc37 destabilizes kinase clients and sensitizes cancer cells to Hsp90 inhibitors. *Oncogene* **2008,** 28, 157-169.

13.   Smith, J. R.; Workman, P. Targeting Cdc37: an alternative, kinase-directed strategy for disruption of oncogenic chaperoning. *Cell Cycle* **2009,** 8, 362-372.

14.   Hartson, S. D.; Irwin, A. D.; Shao, J.; Scroggins, B. T.; Volk, L.; Huang, W.; Matts, R. L. p50cdc37 is a nonexclusive Hsp90 cohort which participates intimately in Hsp90-mediated folding of immature kinase molecules. *Biochemistry* **2000,** 39, 7631-7644.

15.   Roe, S. M.; Ali, M. M.; Meyer, P.; Vaughan, C. K.; Panaretou, B.; Piper, P. W. The mechanism of Hsp90 regulation by the protein kinase-specific cochaperone p50cdc37. *Cell* **2004,** 11, 87-98.

16.   Sreeramulu, S.; Gande, S. L.; Gobel, M.; Schwalbe, H. Molecular mechanism of inhibition of the human protein complex Hsp90-Cdc37, a kinome chaperone-cochaperone, by triterpene celastrol. *Angew. Chem. Int. Ed.* **2009,** 48, 5853-5855.

17.   Amolins, M. W.; Blagg, B. S. J. Natural product inhibitors of Hsp90: potential leads for drug discovery. *Mini Rev. Med. Chem* **2009,** 9, 140-152.

18.   Blagg, B. S. J.; Kerr, T. D. Hsp90 inhibitors: small molecules that transform the Hsp90 protein folding machinery into a catalyst for protein degradation. *Med. Res. Rev.* **2006,** 26, 310-338.

19.   Brandt, G. E. L.; Blagg, B. S. Alternate strategies of Hsp90 modulation for the treatment of cancer and other diseases. *Curr. Top. Med. Chem.* **2009,** 9, 1447-1461.

20.   Chaudhury, S.; Welch, T. R.; Blagg, B. S. J. Hsp90 as a target for drug development. *ChemMedChem* **2006,** 1, 1331-1340.

21.   Donnelly, A.; Blagg, B. S. J. Novobiocin and additional inhibitors of the Hsp90 C-terminal nucleotide-binding pocket. *Curr. Med. Chem.* **2008,** 15, 2702-2717.

22.   Peterson, L. B.; Blagg, B. S. J. To fold or not to fold: modulation and consequences of Hsp90 inhibition. *Future Medicinal Chemistry* **2009,** 1, 267-283.

23.   Yang, H.; Chen, D.; Cui, Z. C.; Yuan, X.; Dou, W. P. Celastrol, a triterpene extracted from the chinese "thunder of god vine," is a potent proteasome inhibitor and suppresses human prostate cancer growth in nude mice. *Cancer Res.* **2006,** 66, 4758-4765.

24.   Hieronymus, H.; Lamb, J.; Ross, K. N.; Peng, X. P.; Clement, C.; Rodina, A.; nieto, M.; Du, J.; Stegmaier, K.; Raj, S. M.; Maloney, K. N.; Clardy, J.; Hahn, W. C.; Chiosis, G.; Golub, t. R. Gene expression signature-based chemical genomic prediction identifies a novel class of Hsp90 pathway modulators. *Cancer Cell* **2006,** 10, 321-330.

25.   Lamb, J.; Crawford, E. D.; Peck, D.; Modell, J. W.; Blat, i. C.; Wrobel, M. J.; Lerner, J.; Brunet, J.-P.; Subramanian, A.; Ross, K. N.; Reich, M.; hieronymus, h.; Wei, G.; Armstrong, S. A.; Haggarty, S. J.; Clemons, P. A.; Wei, R.; Carr, S. A.; Lander, E. S.; Golub, T. R. The connectivity map: using gene-expression signatures to connect small molecules, genes, and disease. *Science* **2006,** 313, 1929-1935.

26.   Nathan, S. S.; Kalaivani, K.; Chung, P. G.; Murugan, K. Effect of neem limonoids on lactate dehydrogenase (LDH of the rice leafholder, *Cnaphalocrocis medinalis* (Guenee) (Insecta: lepidoptera: Pyralidae). *Chemosphere* **2006,** 62, 1388-1393.

27.   Uddin, S. J.; Nahar, L.; Shilpi, J. A.; Shoeb, M.; Borkowski, T.; Gibbons, S.; Middleton, M.; Byres, M.; Sarker, S. D. Gedunin, a limonoid from *Xylocarpus granatum*, inhibits the growth of CaCo-2 colon cancer cell line *in vitro*. *Phytother. Res.* **2007,** 2007, 757-761.

28.   Brandt, G. E. L.; Schmidt, M. D.; Prisinzano, T. E.; Blagg, B. S. J. Gedunin, a novel Hsp90 inhibitor: semisynthesis of derivatives and preliminary structure-activity relationships. *J. Med. Chem.* **2008,** 51, 6495-6502.

<center>**Chapter III**</center>

<center>**Total Synthesis of Cruentaren A, Selective F_1F_o ATP Synthase Inhibitor Isolated from**</center>

<center>***Byssovorax cruenta.***</center>

III.1   Targeting F_1F_o ATP Synthase for Cancer Chemotherapy

F_1F_o-ATP Synthase (FAS) is a ubiquitously expressed macromolecular machine (Figure 3.1).[1-7] Under normal conditions, FAS provides 90% of cellular energy in the form ATP by catalyzing the oxidative phosphorylation of ADP.[8] The proton motive force that exists across the innermitochondrial membrane where FAS is bound drives this process.[9] The precise role of this mitochondrial protein in cancer cells is currently under dispute. Nevertheless, the biological effects that result from FAS inhibition make it an attractive target for cancer chemotherapy.
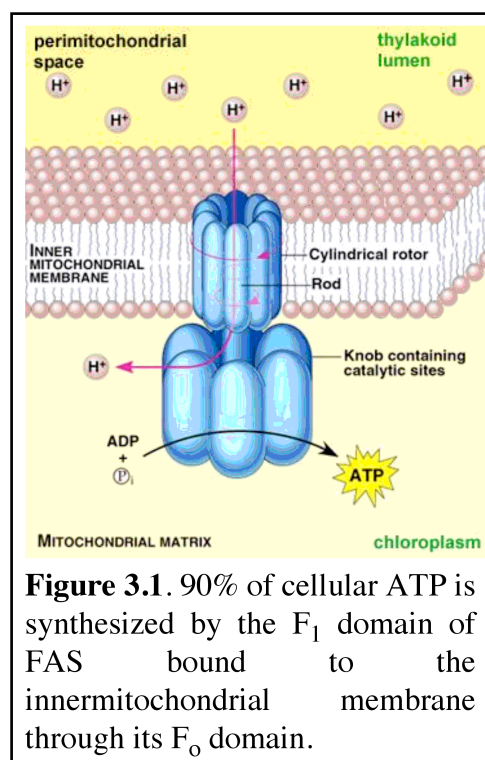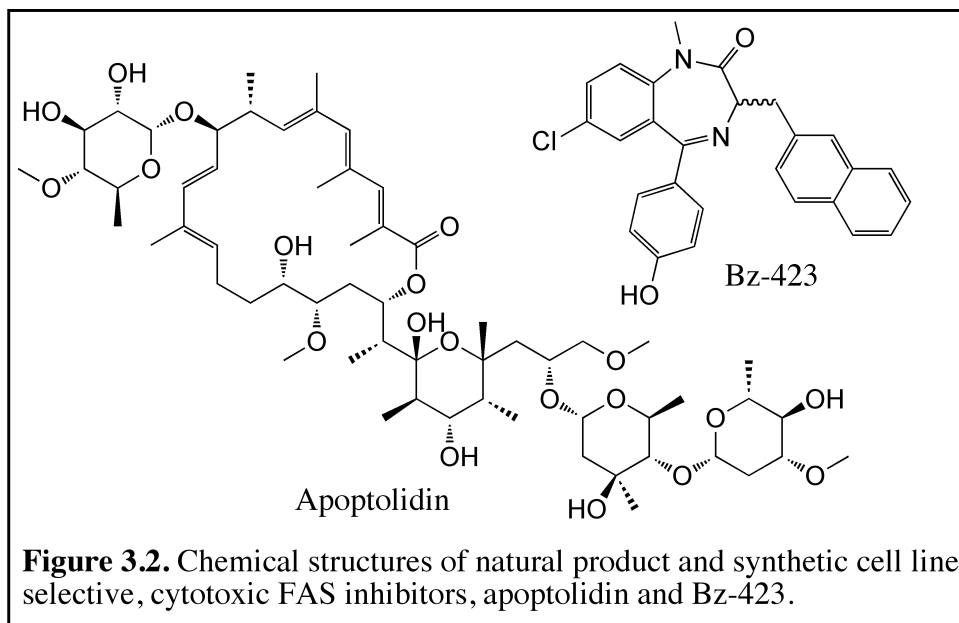

Figure 3.1. 90% of cellular ATP is synthesized by the F_1 domain of FAS bound to the innermitochondrial membrane through its F_o domain.

III.1.1 *Therapeutic effects of FAS inhibition*

The therapeutic potential of FAS as a target for cancer chemotherapy is delineated from an experimentally observed distinguishing characteristic of inhibition. Examples of both small molecule and antibody derived FAS inhibitors display remarkable differential selectivity. While normal cells display an inherent resistance to FAS inhibition, potent cytotoxic and apoptotic effects are observed in cancer cells following the administration of FAS inhibitors.

Biological effects of three known FAS inhibitors, apoptolidin, Bz-423, and mAb6F2C4, demonstrate the selectivity observed for FAS inhibition. Apoptolidin, a complex polyketide FAS

Figure 3.2. Chemical structures of natural product and synthetic cell line selective, cytotoxic FAS inhibitors, apoptolidin and Bz-423.

inhibitor isolated from a strain of actinomycete bacteria, is a potent, yet selective, cytotoxin. All nontransformed cell lines screened against apoptolidin demonstrate an inherent resistance to its cytotoxicity.[10, 11] Additionaly, this selective cytotoxic behavior is observed among the NCI-60 cancer cell lines. Of the roughly 37,000 compounds that had been screened against the NCI-60 at the time, apoptolidin was found to be among the top 0.1% most selective cytotoxic agents.[12, 13] Pathogenic cell selective effects are also observed following the administration of a synthetic 1,4-benzodiazepine FAS inhibitor, BZ-423, which is completely non-toxic in normal cell lines.[14-16] Likewise, these observations extend to several FAS inhibiting antibodies, as exemplified by mAb6F2C4, a murine derived antibody that targets FAS at the β subunit of the F_1 domain. Once again, potent cytotoxic effects are observed following both *in vivo* and *in vitro* administration of this antibody in cancer cells, while normal cells remain unaffected.[17, 18]

III.1.2 *FAS and cancer cell metabolism*

The favorable attributes of targeting FAS for cancer chemotherapy appear to contradict a generally accepted metabolic phenotype of cancer, known as "The Warburg Effect" (Otto Heinrich Warburg was the first to observe this effect and was subsequently awarded The Nobel

Prize in 1931).[19, 20] The underlying premise of "The Warburg Effect" suggests that tumor cells acquire an almost exclusive dependence on "aerobic glycolysis" for ATP synthesis rather than mitochondrial oxidative phosphorylation. This phenotype is expressed independent of the abundance of molecular oxygen. Biological consequences of "The Warburg Effect" are clinically applied during tumor excision, by administering "lactate ringers" during surgery, and in positron emission topography scanning for cancer diagnosis, which relies on tumor's increased glucose uptake.[21-25]

"The Warburg Effect" was highly controversial at the time it was proposed.[22] A vast collection of experimental observations relating to tumor metabolism has resulted in almost a dogmatic status for "The Warburg Effect" (Table 1).[20, 22] Nevertheless, cancer cell metabolism remains under intense investigation. The mechanisms thought to be responsible for cancer's acquisition of this phenotype involve a complicated milieu of transcriptional changes that result in distinct protein expression profiles (Table 1).[26-28] However, recent experimental re-evaluation of these mechanisms has lead to controversy in our understanding of cancer cell metabolism once again, specifically regarding the role of FAS, oxidative phosphorylation, and mitochondrial function.

Table 3.1. Aberant protein activity and the effects on cancer cell metabolism in support of "The Warburg Effect."

Observation in Cancer	Metabolic Consequence
reduced GSK3 activity	increased glycogen synthesis
decreased CD147 function	increased lactate production
dysfunctional SDH	sustained HIF-1 activation
UCP2 overexpression	decreased mitochondrial oxidative phosphorylation
PFKFB3 overexpression	increased glycolysis
dysfunctional IDH1	decreased oxygen consumption

Contradictions regarding the state of oxidative phosphorylation in cancer cells are abundant in the literature.[29, 30] A number of prior studies reported repressed oxidative phosphorylation and mitochondrial function in cancer cells,[6, 20, 21, 24, 27, 28] while more recent studies report overactive mitochondrial function.[23, 31-33] The cause of this discrepancy may be related to differences in experimental technique. The earlier reports, in which repressed mitochondria function was found, were largely based on experiments conducted *in vitro*. Results from these studies were based on isolated cancer cell lines in non-physiological conditions. In contrast, more recent reports, in which increased mitochondrial function was observed in cancer, are based on a physiologically relevant model. These studies were conducted on cancer cells supported by associated fibroblasts. A new model for cancer cell metabolism, "The Reverse Warburg Effect," has now been proposed to support these clinically relevant studies.[30, 31, 34-36]

"The Reverse Warburg Effect" suggests that "aerobic glycolysis" is a phenomenon isolated to cancer associated fibroblasts, not cancer cells themselves. It is interesting to point out, that "The Reverse Warburg Effect" does not negate conclusions derived from "The Warburg Effect," when the entire tumor is considered in a physiological context, not individual cells.[19, 25] In this model, cancer cells induce "The Warburg Effect" in surrounding stromal cells and rapidly absorb the highly energetic chemical by-products of "aerobic glycolysis" (e.g. pyruvate, lactate, 3-hydroxybutyrate) as a fuel source for mitochondrial oxidative phosphorylation.[30-32] A similar phenomenon is observed during neuron-glial coupling, in which astrocytes functionally "feed" associated neurons. In fact, several of the same glycolysis associated enzymes are overexpressed in the "support" cells for both of these processes.[19, 25, 30-33, 35-39]

Clearly, a complete description of the cancer metabolic phenotype will require significant investigation. Regardless of the available data concerning the expression levels of competent

FAS in transformed cells, the cancer selective cytotoxic effects that result from FAS inhibition remains undisputed.

III.1.3 *FAS activity and cancer cell biology*

While FAS expression was traditionally considered exclusively localized to the innermitochondrial membrane, the ectopic expression of FAS is now generally accepted.[29] Modern proteomic techniques have enabled the discovery of FAS in several extramitochondrial compartments including the plasma membrane, endoplasmic reticulum, and cytosol.[9, 23] These observations have prompted the investigation of possible biological roles for FAS that extend beyond ATP synthesis. Furthermore, differences between FAS expression in normal vs. cancer cell lines may provide additional insight toward elucidating its disputed role in cancer.[9]

The ectopic overexpression of FAS has been observed in several cancer cell lines and this overrepression is implicated in cancer cell biology.[17, 40] Plasma membrane bound FAS, where the F_o domain is rooted within lipid rafts and the F_1 domain is projected extracellularly, represents a significant region of ectopic expression. Additionally, FAS was recently identified as a co-chaperone component of the super chaperone complex required for a select group of Hsp90 client proteins.[41, 42]

Plasma membrane bound FAS

FAS overexpression and translocation to the plasma membrane is associated with highly metastatic tumors and increased angiogenic potential.[29, 34] This implies a role for FAS in facilitating metastasis and angiogenesis. FAS localized to the cell surface demonstrates catalytic competency.[29, 40] The hydrophobic F_o domain is membrane bound and oriented to project the catalytically active F_1 domain extracellularly.[43, 44] Because plasma membrane bound FAS is hyperactive in cancer cells, ATP concentrations are dramatically increased in the tumor

microenvironment.[21] Cell surface purinergic receptors, such as P2Y and P2X, play a role in cell proliferation and angiogenesis and are overexpressed in many cancers.[9] By supplying abundant ATP, overexpressed and catalytically active membrane-bound FAS is directly related to the maintenance of cancer cell hyper-proliferation and recruitment of vasculature to primary and metastatic tumors.[9, 23, 29]

While undergoing the catalytic cycle of ATP synthesis, the orientation of membrane bound FAS creates a shuttle that pumps protons out of the cytosol and into the extracellular space. FAS is likely a key regulator of intracellular pH within cancer cells, and may be responsible for the acidic environment that surrounds tumors. Experiments employing confocal microscopy confirmed that plasma membrane bound FAS is targeted by the antibody derived FAS inhibitor mAb6F2C4. The cancer specific cytoxic effects of this FAS inhibitor have been attributed to cancer cell acidosis, supporting FAS's role as a regulator of intracellular pH. Normal cell lines that manifest plasma membrane FAS expression maintain typical physiological pH ranges and are resistant to mAb6F2C4 induced cytoxicity due to a lack of appreciable intracellular proton accumulation.[40]
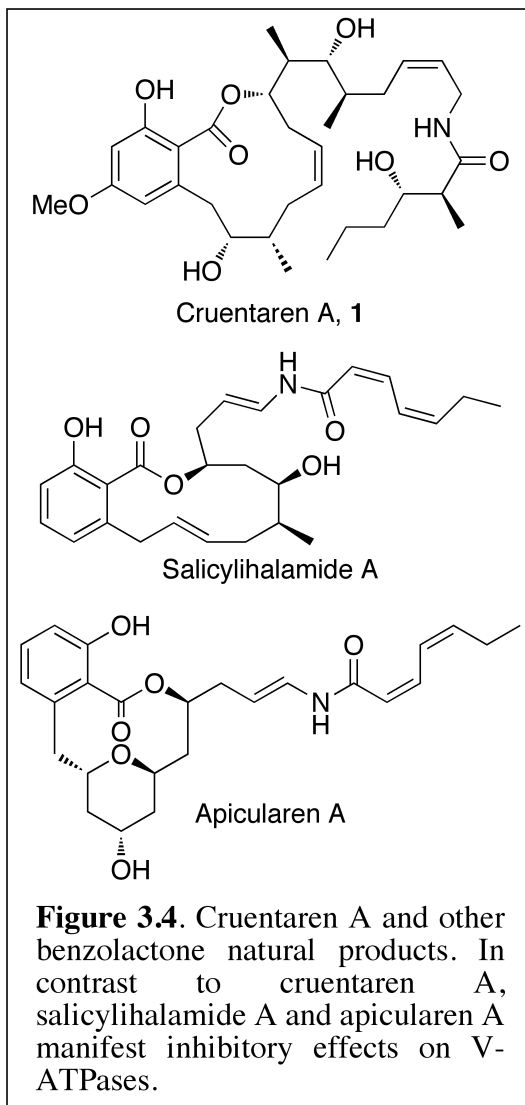
FAS, Hsp90 co-chaperone

Indirect inhibition of the Hsp90 super-chaperone complex by targeting FAS is a novel therapeutic strategy with anticancer potential. FAS was recently identified as an Hsp90 associated co-chaperone component of the super chaperone complex.[41, 42, 45] The evidence supporting a FAS-Hsp90 association is described in Chapter I. Succinctly, FAS co-immunoprecipitated with Hsp90 and other members of the super chaperone complex, including several client proteins. Small molecule FAS inhibitors prevented this immunoprecipitation,

Figure 3.3. Cruentarens A and B, novel isolates from myxobacterial sp. *Byssovorax cruenta*.
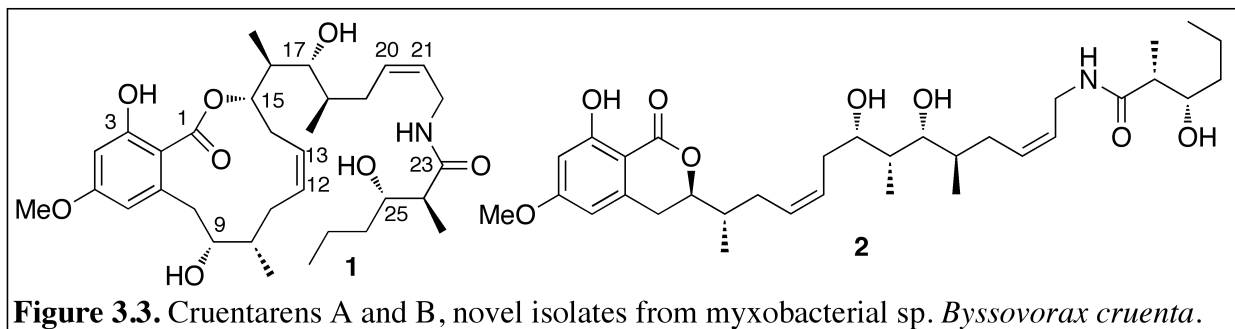
manifested anti-proliferative effects against various cancer cell lines, elicited Hsp90-dependent client protein degradation, and operated independent of cellular ATP concentrations.[42, 45]

Two effects exhibited by FAS-derived Hsp90 inhibition are of particular significance: 1) FAS inhibitors demonstrated selective Hsp90 client protein degradation. While FAS inhibitors caused the degradation of ERα, mutant p53, and caspase-3, Raf-1 levels remained constant.[42, 45] This suggests a role for FAS as a specific co-chaperone of non-kinase Hsp90 clients, although further investigation is required to define the specific subset of FAS-dependent clients. 2) FAS inhibitors elicited anti-proliferative activities against cancer cells without concomitant induction of the pro-survival, heat shock response. In fact, the opposite effect was observed wherein Hsp70 levels decreased in a dose-dependent manner. This unique activity has the potential to address limitations associated with every clinically evaluated Hsp90 inhibitor to date.[42, 45]

A caveat to these studies relates to the experimental use of non-selective ATPase inhibitors. All of the FAS inhibitors evaluated, including efrapeptin, oligomycin, and 7-chloro-4-nitrobenzo-2-oxa-1,3-diazole, demonstrate inhibitory effects on several other ATPases. The application of a FAS-selective inhibitor is needed to confirm the observed biological effects are not a result of multiple ATPase inhibition. In an effort to conduct the first experiments investigating the FAS-Hsp90 relationship with a selective FAS inhibitor, this chapter describes the total synthesis of cruentaren A (**1**, Figure 3.3), a benzolactone macrocyclic myxobacterial isolate that exhibits potent anticancer effects by selective inhibition of FAS catalytic activity.[46-48]

Figure 3.4. Cruentaren A and other benzolactone natural products. In contrast to cruentaren A, salicylihalamide A and apicularen A manifest inhibitory effects on V-ATPases.
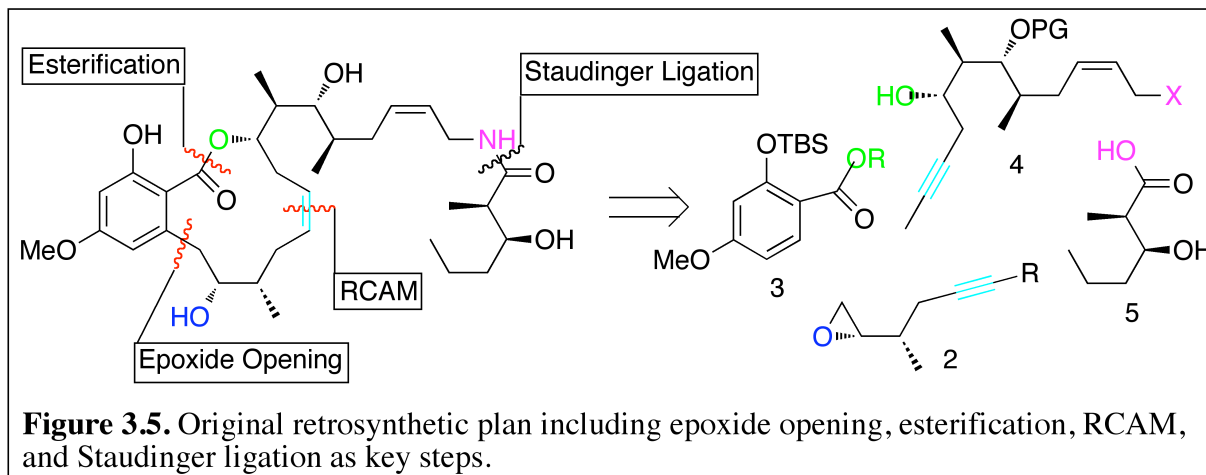
III.2 Identification of Cruentaren A as a FAS Selective Inhibitor

The laboratory of Gerhard Hofle identified cruentaren A and its isomeric analogue cruentaren B as the first novel basic structures isolated from the fermentation broths of *Byssovorax cruenta* in 2006. Cruentaren A, **1**, was the major component, isolated through bioassay guided fractionation[46, 48] focused on identifying novel antifungal and cytotoic agents. While cruentaren A demonstrated potent cytotoxic effects (IC_{50} of 8.3 nM against L929 mouse fibroblasts), cruentaren B, **2**, was only marginally toxic (no IC_{50} value reported).[47]

Cruentaren A is a member of the growing class of benzolactone natural products that incorporates a resorcinol containing, 12-membered macrocyclic lactone and *N*-acylallylamine side chain (Figure 3.4). Despite the structural similarities to other natural products of this class, cruentaren A possesses a unique mechanism of action. This natural product induces cytoxicity through selective inhibition of FAS, but is devoid of inhibitory effects against other ATPases. Due to this unique biological activity, a strategy for the total synthesis of cruentaren A was developed with the ultimate goal of evaluating the effects of selective FAS inhibition on the super chaperone complex. The total synthesis of cruentaren A is described in detail below.[46-48]

Figure 3.5. Original retrosynthetic plan including epoxide opening, esterification, RCAM, and Staudinger ligation as key steps.

III.3 Total Synthesis of Cruentaren A

At the outset of this synthetic endeavor, no total synthesis of cruentaren A had been reported. However, during the course of this work, three total syntheses were described. All three of the published syntheses followed a similar retrosynthetic scheme to what was originally conceived for this work and involved ring-closing alkyne metathesis (RCAM) as a key step for selective introduction of the *cis*-olefin present within the macrocyclic ring.[49-55] These similarities prompted a re-evaluation of the original strategy and led to the design of an alternate approach that involved ring-closing olefin metathesis (RCM). Progress toward the original strategy is described below, followed by a detailed account of the alternate approach and subsequent completion of the total synthesis.[56]

III.3.1 *Initial approach*

The original retrosynthetic strategy led to disassembly of the natural product into four fragments (Figure 3.5). Bond disconnections were designed to provide a convergent synthesis to rapidly assess SAR for cruentaren A analogues by manipulating functional and stereochemical attributes of these fragments. The macrocycle was expected to be assembled from fragments **2** – **5** through a stepwise process. The product resulting from nucleophillic attack of epoxide **2** by the ortholithiated species of **3** and subsequent hydrolysis would be esterified by alcohol **4**. Next, the

product of RCAM and *cis*-selective alkyne reduction would be converted to the corresponding allylazide, which would be elaborated to the natural product following Staudinger ligation with acid **5** and global deprotection.

The synthetic strategy for epoxide **2** was envisioned to include asymmetric crotylation and Sharpless asymmetric dihydroxylation, followed by transformation to the epoxide. Synthesis of secondary alcohol fragment **4** involved the use of Myers' pseudoephedrine chiral auxiliary,[56] asymmetric crotylation, iodolactonization, and Grignard-mediated epoxide opening. The use of Myers' pseudoephedrine chiral auxiliary was also chosen for the construction of acid **5** *via* alkylation of butyraldehyde (Figure 3.6).[57]
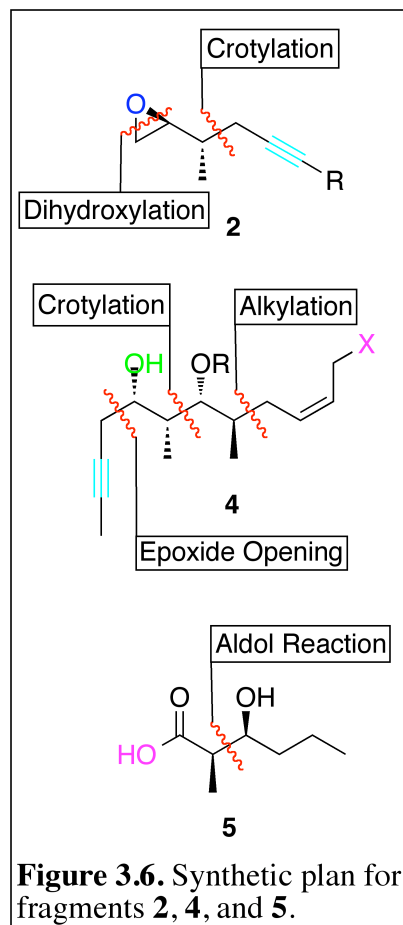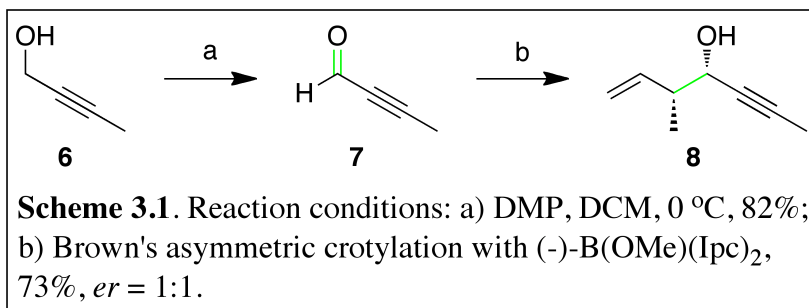

Figure 3.6. Synthetic plan for fragments **2**, **4**, and **5**.

The Rationale for employing Myers' pseudoephedrine instead of more popular chiral auxiliaries was governed by several unique chemical attributes. Products from these chiral auxiliaries manifest consistently high diastereomeric ratios independent of scale, are readily available from inexpensive

Figure 3.7. Synthetic utility of Myers' pseudoephedrine chiral auxiliary. a) lithium amidotrihydroborate (LAB) reduction to alcohols; b) hydrolysis to acids; c) LiAl(OEt)$_3$H reduction to aldehydes; d) organolithium mediated alkylation to ketones; e) LAB reduction followed by halogenation to alkyl halides.
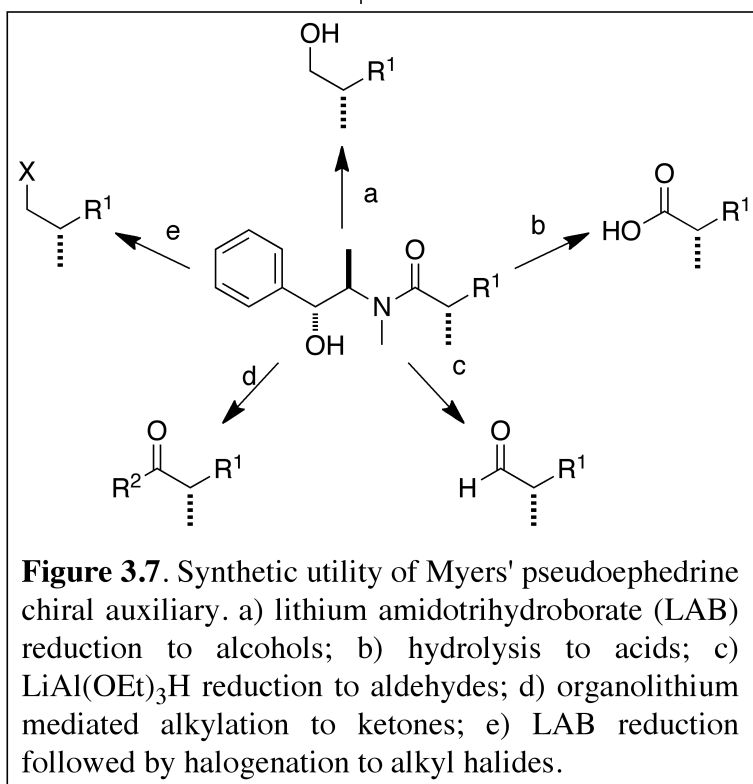
commercially available reagents *via* a simple, one step process, are isolated in high purity following crystalization from toluene,

Scheme 3.1. Reaction conditions: a) DMP, DCM, 0 °C, 82%; b) Brown's asymmetric crotylation with (-)-B(OMe)(Ipc)$_2$, 73%, *er* = 1:1.
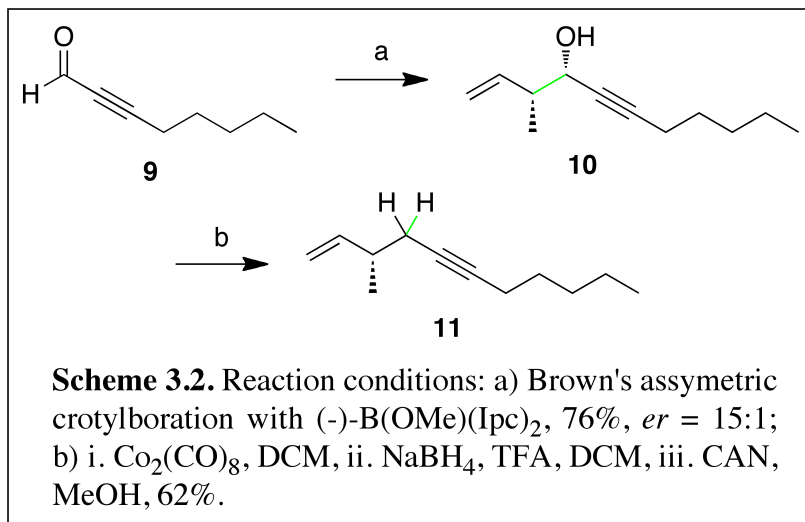
and can be recycled for application in subsequent stereoselective alkylations without loss of activity. Furthermore, these chiral auxiliaries can be elaborated into a variety of useful chemical entities (ketones, alcohols, aldehydes, carboxylic acids, alkyl halides) through well-defined synthetic protocols (Figure 3.7).[55]

Progress toward epoxide fragment 2

The initial strategy for the synthesis of epoxide **2** was met with several complications. Because successful RCAM has only been applied to non-terminal, methyl acetylenes, the initial approach to **2** involved the asymmetric crotylation of 2-butynal, **7** (Scheme 3.1). Oxidation of 2-butyn-1-ol (**6**) was surprisingly resistant to efficient conversion. Several oxidants were investigated including pyridinium chlorochromate (PCC), pyridinium dichromate (PDC), tetrapropylammonium perruthenate (TPAP) and manganese dioxide (MnO$_2$), but all proved ineffective. Eventual application of the Dess-Martin periodinane[58] at low temperature in DCM resulted in complete conversion to desired product and enabled a simple isolation protocol. Filtration through celite and distillation of the solvent provided pure **7**. However, elaboration of **7** to alcohol **8** under Brown's asymmetric crotylation failed to induce enantiofacial selectivity.[59]
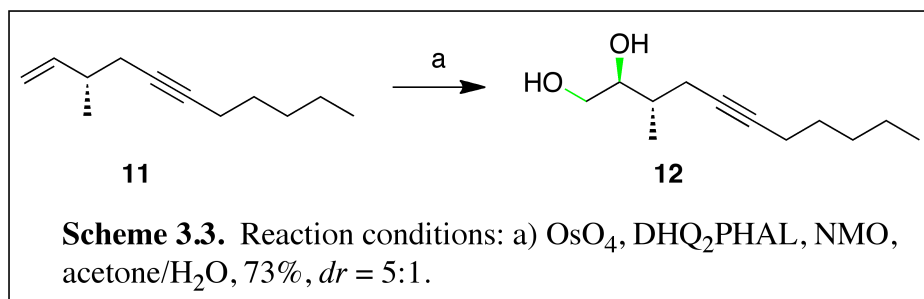
To circumvent this issue, the bulkier, commercially available 2-octynal **9** was subjected to Brown's conditions. Despite no literature precedent describing extended alkyl gains present on non-terminal alkynes participating in RCAM, optimizing conditions for such an alkyne could
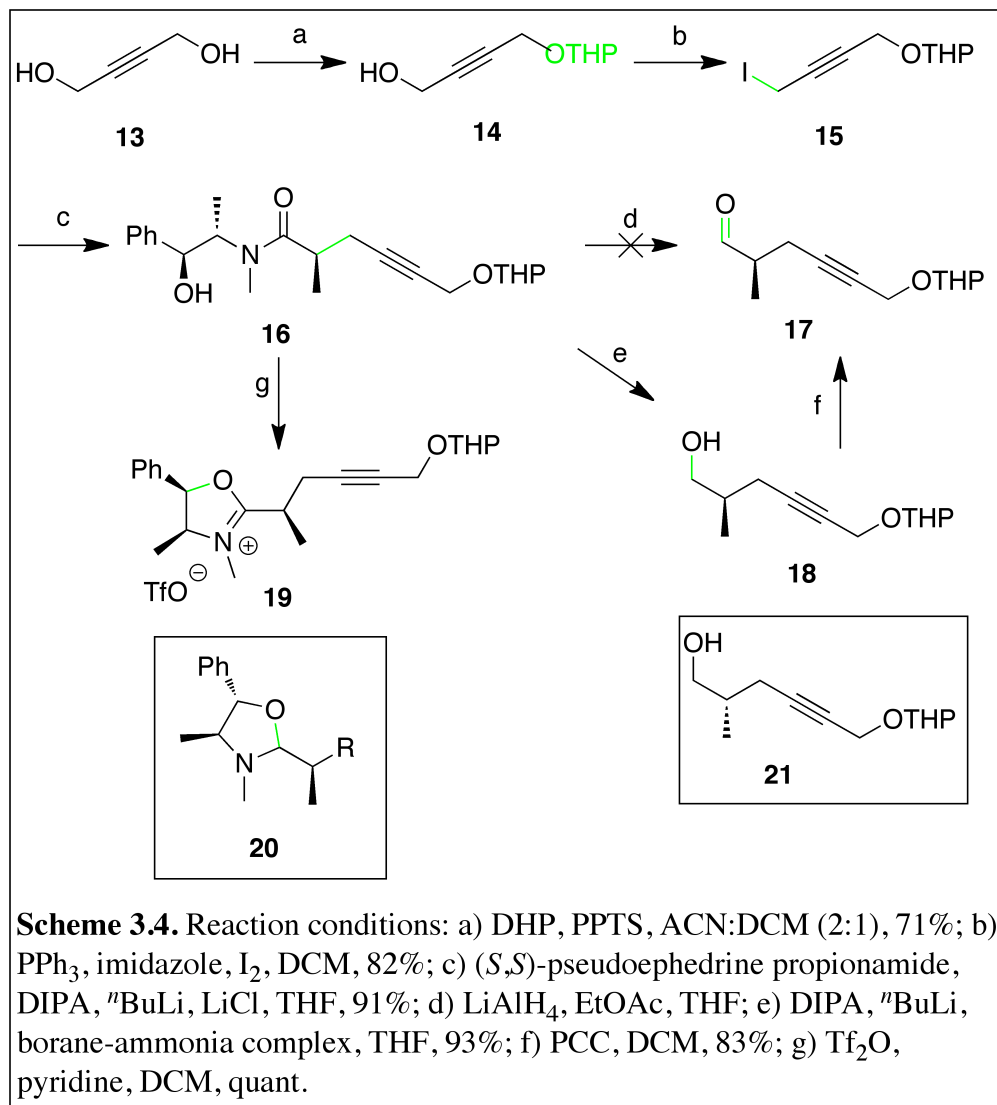
expand the practical utility of
RCAM. Under the same
reaction conditions,
stereoselective crotylation of
9 generated homoallylic
alcohol **10** in good yield with
an acceptable enantiomeric
ratio (15:1). Deoxygenation of

Scheme 3.2. Reaction conditions: a) Brown's assymetric crotylboration with (-)-B(OMe)(Ipc)$_2$, 76%, *er* = 15:1; b) i. Co$_2$(CO)$_8$, DCM, ii. NaBH$_4$, TFA, DCM, iii. CAN, MeOH, 62%.

10 was accomplished *via* a Nicholas reaction upon treatment of the Co-complexed alkyne with

NaBH$_4$ and TFA, followed by CAN mediated decomplexation to afford unsaturated hydrocarbon

11 (Scheme 3.2).[60]

Although terminal olefins undergo dihydroxylation with low stereoselectivity, an attempt

was made to overcome this potential problem.[61] Unfortunately, treatment of **11** with

commercially available AD-Mix α, in the presence or absence of additives, failed to induce

acceptable diastereoselectivity. However, treatment of **11** with catalytic osmium tetroxide (OsO$_4$)

in the presence of an enatiomerically enriched cinchona alkaloid ligand, DHQ$_2$PHAL, and *N*-

methylorpholine oxide (NMO) proved useful, resulting in a 5:1 diastereomeric ratio (Scheme

3.3).

Scheme 3.3. Reaction conditions: a) OsO$_4$, DHQ$_2$PHAL, NMO, acetone/H$_2$O, 73%, *dr* = 5:1.

Scheme 3.4. Reaction conditions: a) DHP, PPTS, ACN:DCM (2:1), 71%; b) PPh$_3$, imidazole, I$_2$, DCM, 82%; c) (*S,S*)-pseudoephedrine propionamide, DIPA, ^{n}BuLi, LiCl, THF, 91%; d) LiAlH$_4$, EtOAc, THF; e) DIPA, ^{n}BuLi, borane-ammonia complex, THF, 93%; f) PCC, DCM, 83%; g) Tf$_2$O, pyridine, DCM, quant.

Progress toward 1,3-diol fragment 4

Synthesis of 1,3-diol fragment **4** commenced with the mono-tetrahydropyran (THP) protection of 2-butyne-1,4-diol (**13**) by reaction with dihydropyran and catalytic pyridinium *p*-tuluenesulfonate (PPTS) in acetonitrile (ACN) and DCM (2:1) followed by iodination of propargyl alcohol **14** upon treatment with triphenylphosphine (PPh$_3$), imidazole, and I$_2$ in DCM. Alkylation of the corresponding (Z)-enolate of (S,*S*)-pseudoephedrine propionamide from the unhindered α-face (Figure 3.8) by propargyl iodide **15** gave α-methyl amide product **16**, in both excellent yield and diastereomeric ratio (> 20:1 as determined by Myer's NMR based analysis of

4,5-disubstituted oxazolium, **19**; this is the method of choice for all subsequent stereochemical

analyses of pseudoephedrine amide products) (Scheme 3.4).

Reduction of **16** to aldehyde **17** with

Li(OEt)$_3$BH was unsuccessful, presumably due to loss

of the THP protecting group during acidic work-up.

The initial product of Li(OEt)$_3$BH-mediated reduction

of pseudoephedrine amides is aminal **20**, which

requires treatment with strong acid (10 equiv of

trifluoroaceitc acid in 1 N aqueous hydrochloric acid)

Figure 3.8. Proposed reactive conformation of pseudoephedrine amide enolates
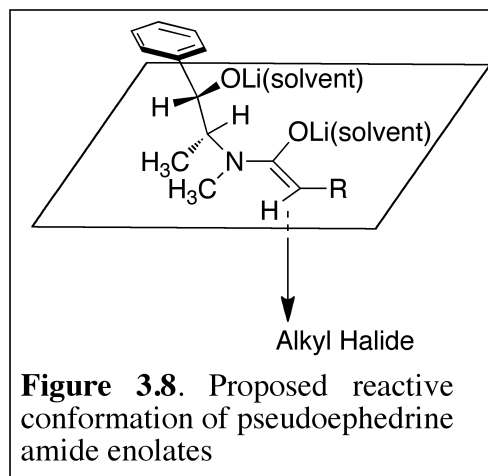
for conversion to the desired aldehyde. Attempts to avoid THP-deprotection by employing

weakly acidic conditions at reduced temperature were unsuccessful. However, conversion of **16**

to the corresponding alcohol **18**, following treatment of *in situ* generated lithium

amidotrihydroborate (LAB), proved effective. Alcohol **21**, the enatiomer of **18**, was synthesized

in the same fashion from (*R,R*)-pseudoephedrine propionamide for stereochemical comparison.

Mosher's ester products of alcohol **18** and its enantiomer **21**, analyzed using ^{19}F NMR

spectroscopy, showed the presence of a single enantiomer. PCC mediated oxidation of alcohol

**18** provided optically active aldehyde **17** (Scheme 3.4) in significant quantities.

The accessibility of aldehyde **17** enabled the investigation of chemical methods to

establish the desired stereochemistry at C-16 and C-17. Several procedures were investigated in

order to determine an optimal method, however, aldehyde **17** proved ill suited for application in

published asymmetric crotylation transformations. The first strategy considered involved

crotylstannane and chiral acyloxy borane (CAB), **21**, Lewis acid catalysis for alkylation (Figure

3.9).[62] Standard reaction conditions were effective for generating the desired stereochemical

Figure 3.9. A) Chemical structure of CAB (chiral acyloxy borane) catalyst **22**. B) CAB coordination to aldehyde results in β-attack of crotylstannane due α-face blocking 2,6-dimethyoxy benzoate ester.
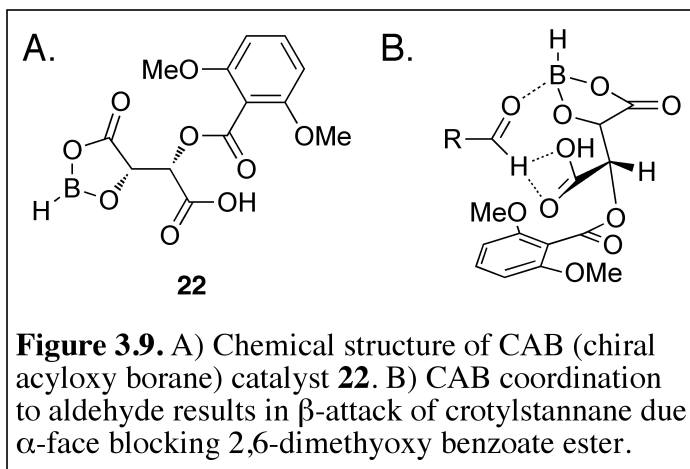
outcome, however, only with concomitant THP-deprotection (Scheme 3.5). Undesired diol **24** was the only isolable product from this procedure. Subsequent attempts to affect successful asymmetric crotylation were also unsuccessful.

Aldehyde **17** failed to react under conditions developed by Brown or Soderquist.[59, 63] The lack of reactivity under these conditions may be attributed to the sequestration of the Lewis acidic boron of the chiral auxiliaries.

Further development of either proposed synthetic routes toward fragments **2** or **4** was not pursued due to the

Scheme 3.5. Reaction conditions: a) **22**, crotylstannane, TFAA, propionitrile.
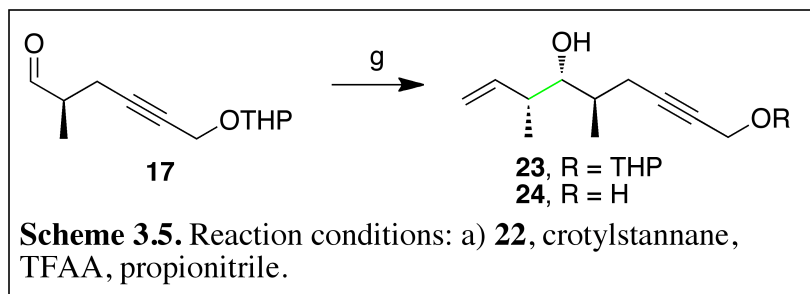
publication of cruentaren A total syntheses by two competing laboratories.[50, 52, 53] Both of these reports employed RCAM as a synthetic strategy, which prompted the re-evaluation of the synthetic approach described above.

III.3.2 *Design and implementation of RCM strategy for the total synthesis of cruentaren A*

A synthetic approach toward construction of the *cis*-olefin containing 12-membered lactone of cruentaren A by RCM questioned whether the sequence of RCAM/selective reduction was required. Implementation of RCM manifests the inherent risk that the conformational contraint of the metathesis substrate could lead to the undesired *trans*-macrocyclic product.

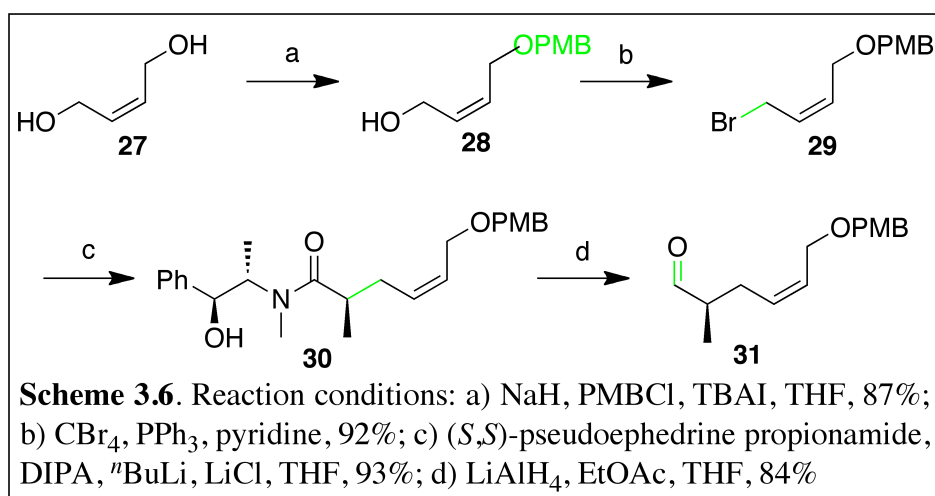**Figure 3.10**. Retrosynthetic strategy employing RCM as a key step
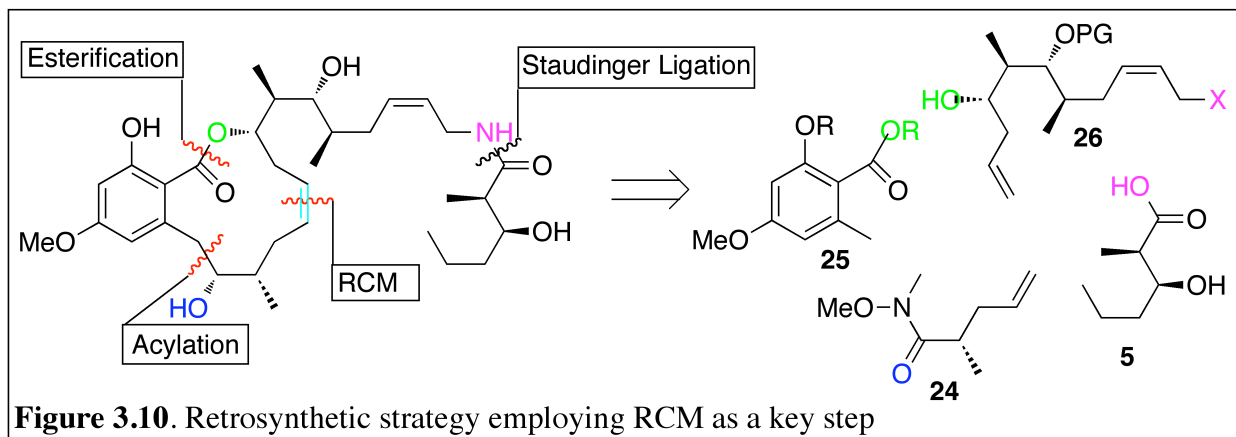
Nevertheless, a synthetic strategy employing RCM for construction of the desired *cis*-macrocyclic product was devised (Figure 3.10).

The retrosynthetic analysis of cruentaren A incorporating RCM for synthesis of the 12-membered lactone provided fragments **24**, **25**, **26**, and **5** as synthetic targets. As opposed to the RCAM approach, Weinreb amide **24** was targeted in lieu of epoxide **2**. Subsequent acylation of **24** with the benzylic anion of **25** would provide a ketone synthetic intermediate that would allow investigation of distinct metathesis substrates. The ketone product was conceived to evaluate the role of C-9 oxidation state during the metathesis step. Esterification of secondary alcohol **26** would provide the metathesis substrate and after RCM, the macrocycle. Staudinger ligation between allylazide and acid **5**, followed by global deprotection would provide the natural product. The successful stereochemical induction observed for Myers' pseudoephedrine chiral auxiliary in the original proposal led to the application of this strategy at several stages of the synthesis.


Figure 3.11. Synthetic strategy for targeted fragments **24**, **26**, and **5**.
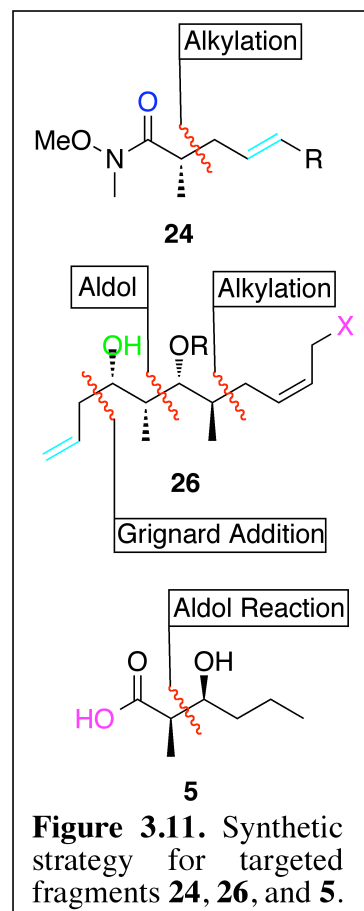
Synthesis of secondary alcohol **26** was envisioned to proceed through the use of Myers'

psueodoephedrine to construct three tertiary stereocenters through sequential reactions. After

transformation of the acid product to the Weinreb amide, alkylation with allylmagnesium

bromide and subsequent stereoselective reduction of the resulting ketone, **26** would be provided.

Access to fragment **5** through the employment of Myers' chiral auxiliary was envisioned in the

RCM strategy as in the RCAM strategy. Finally, Weinreb amide **24** was the target of

pseudoephedrine mediated stereochemical induction (Figure 3.11).

Synthesis of secondary alcohol fragment 26

Scheme 3.6. Reaction conditions: a) NaH, PMBCl, TBAI, THF, 87%; b) CBr$_4$, PPh$_3$, pyridine, 92%; c) (*S*,*S*)-pseudoephedrine propionamide, DIPA, ^{n}BuLi, LiCl, THF, 93%; d) LiAlH$_4$, EtOAc, THF, 84%

Fragment **26** was constructed in 11 steps from *cis*-2-butene-1,4-diol (**27**) with an overall yield of 44 %. Mono-*p*-methoxybenzyl ether

(PMB) protection of *cis*-2-butene-1,4-diol (**27**) under Finkelstein conditions employing sodium

hydride (NaH), PMB chloride, and tetrabutylammonium iodide (TBAI). Treatment of **28** with

carbon tetrabromide (CBr$_4$) and PPh$_3$ gave allyl bromide **29**. Alkylation of (*S*,*S*)-

pseudoephedrine propionamide by **29** proceeded smoothly under Myers' optimized conditions to

provide a scalable synthesis of diastereomerically enriched α-methyl amide **30** (> 20:1). The use

of PMB as a protecting group allowed the successful reduction of **30** to the corresponding

aldehyde **31**, although weaker acidic conditions (0.5 N aqueous HCl at 0 ºC) were required

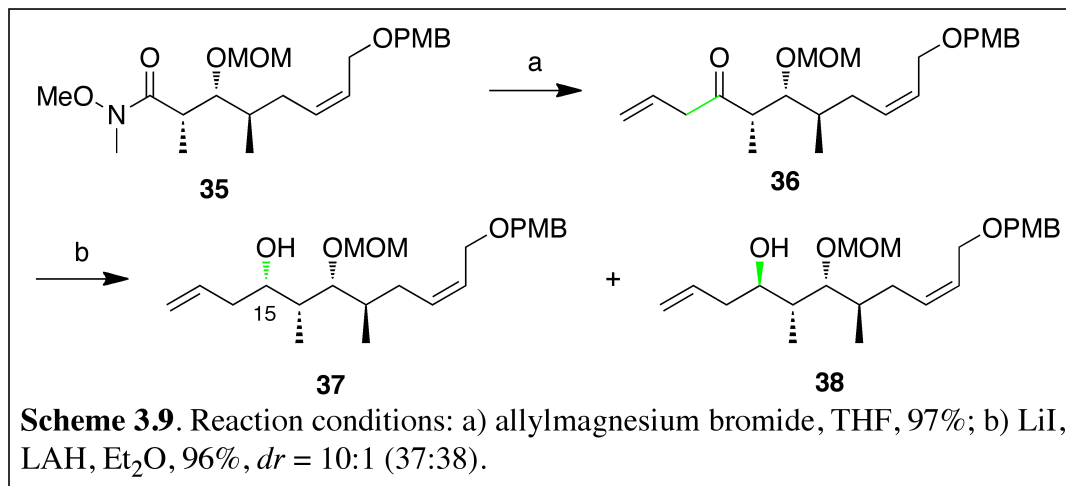during work-up to prevent PMB-deprotection (Scheme 3.6).

Scheme 3.7. Reaction conditions: a) DIPA, ^{n}BuLi, $Zr(Cp)_2(Cl)_2$, (R,R)-pseudoephedrine propionamide, THF, 88%.
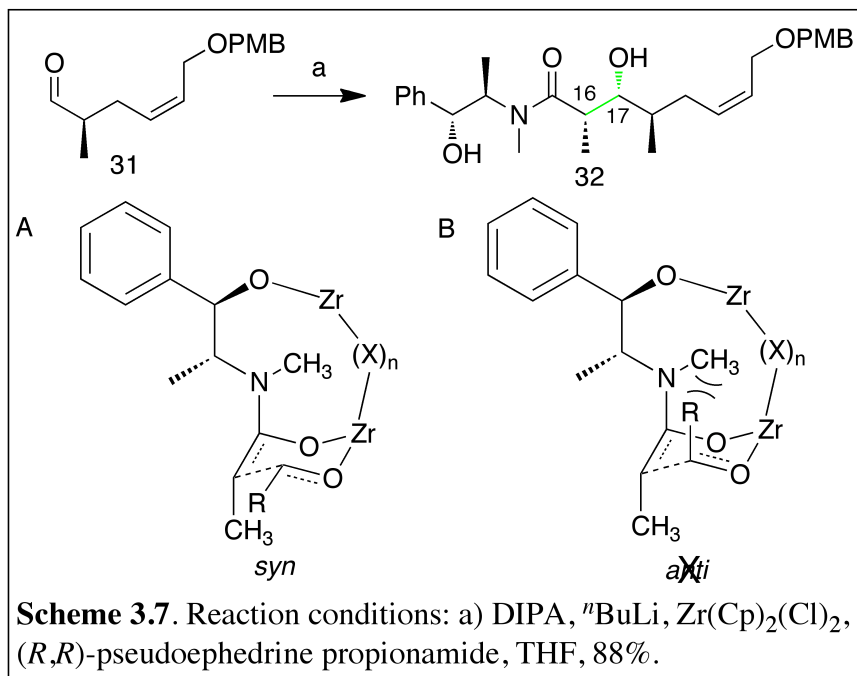
Induction of the required stereochemistry at C-16 and C-17 was accomplished using a bis(cyclopentadienyl)zirconium(IV) dichloride $(ZrCp_2Cl_2)$ Lewis acid-mediated aldol reaction between the corresponding (Z)-enolate of (R,R)-pseudoephedrine propionamide and enantiomerically enriched aldehyde **31**. Diastereomerically pure **32** was the only product observed when addition of aldehyde **31** was conducted at -116 ºC (stereohemical confirmation was conducted at a later stage), in spite of the potential for four possible diastereomeric products. Although the application of pseudoephedrine chiral auxiliaries for aldol chemistry is underappreciated (a Scifinder search reported only seven reactions from two references), the remarkable diastereoselectivity observed within this example highlights its synthetic utility. In fact, the pseudoephedrine-mediated aldol reaction described herein is the first reported case that extends the scope of this reaction to α-substituted, chiral aldehydes. The diastereoselectivity remained consistent on both milligram and multi-gram scales, although the requirement of the reaction to be conducted at such a low temperature renders any further increase in scale impractical. Enatiofacial selectivity is controlled by coordination of two Zr-complexes to the oxyanions of the (Z)-pseudoephedrine enolate. Metal coordination favors the chair-like, Zimmerman-Traxler transition state, A, with an axially positioned R group, which

Scheme 3.8. Reaction conditions: a) $^{n}Bu_4NOH$, $^{t}BuOH$, H_2O, 95%; b) COMU, DIPEA, *N,O*-dimethylhydroxylammonium chloride, DMF, 93%; c) MOMCl, DIPEA, DCM, 96%.
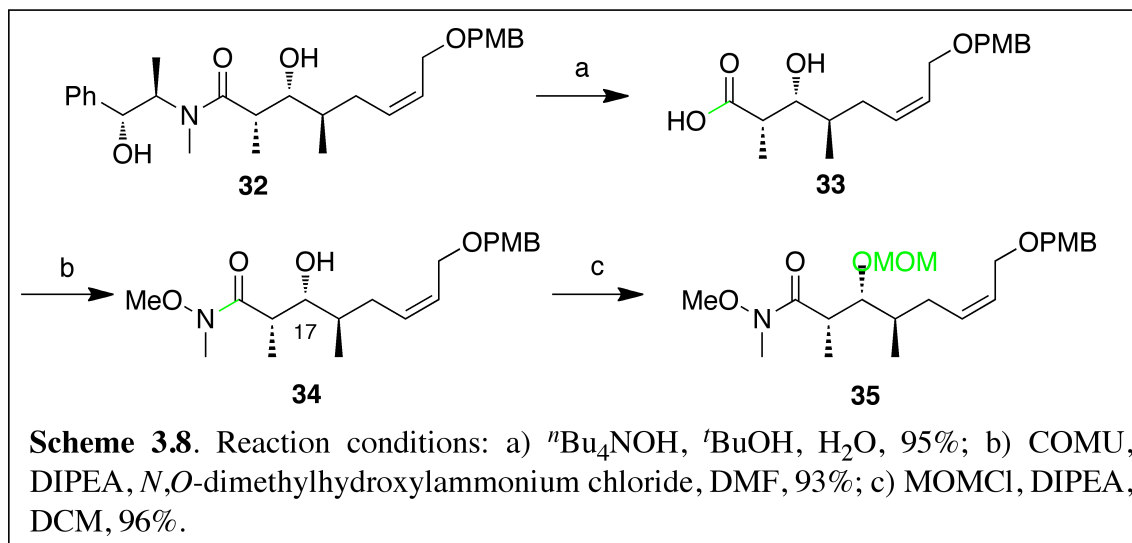
leads to generation of the *syn*-product (Scheme 3.7A). Transition state B, which would provide the *anti*-product, requires an equatorially positioned R group and is highly disfavored due to steric clash with *N*-CH$_3$ of the chiral auxiliary (B, Scheme 3.7).
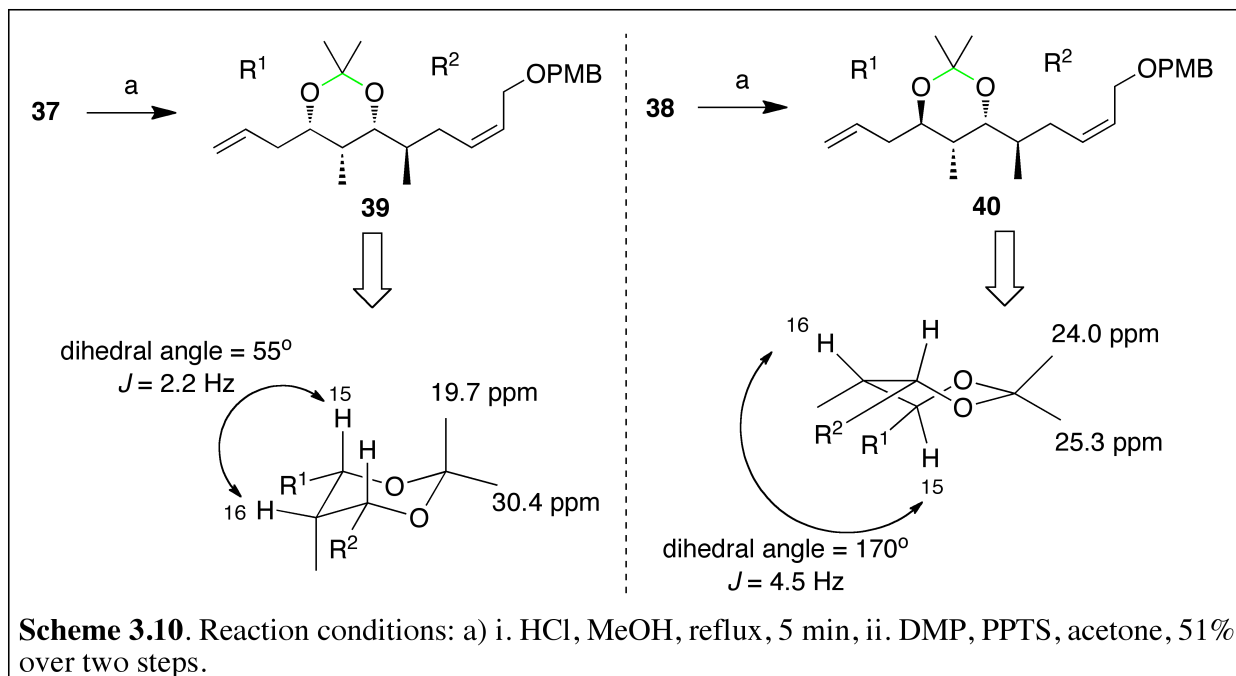
Robust methods developed by Myers *et al.* enabled rapid transformation of pseudoproionamide **32** to Weinreb amide **35**. Carboxylic acid **33** was accessed by treatment of **32** tetrabutylammonium hydroxide ($^{n}Bu_4NOH$) in aqueous *tert*-butylalcohol ($^{t}BuOH$) with no loss of diastereoselectivity. Generation of Weinreb amide **34** was similarly straightforward, and occurred by subjecting acid **33** to standard peptide coupling conditions with (1-Cyano-2-ethoxy-2-oxoethylidenaminooxy)dimethylamino-morpholino-carbenium hexafluorophosphate (COMU), *N,N*-diisopropylethylamine (DIPEA), and the hydrochloride salt of *N,O*-dimethylhydroxylamine in dimethylformamide (DMF). The COMU reagent was recently developed, and represents a significant advancement in peptide chemistry. This coupling reagent does not promote α-stereocenter racemization, and unlike other common reagents is highly stable and not sensitive to aqueous contamination. Mosher's ester analysis confirmed the stereochemical assignment of the β-carbonyl-alcohol, and confirmed the presence of desired (17*R*)-isomer of **34**.[64] Protection of

Scheme 3.9. Reaction conditions: a) allylmagnesium bromide, THF, 97%; b) LiI, LAH, Et$_2$O, 96%, *dr* = 10:1 (37:38).

secondary alcohol of **37** with methoxymethyl chloride (MOMCl) and DIPEA in DCM gave methoxymethyl ether containing Weinreb amide **35** in excellent yield (Scheme 3.8).

Weinreb amide **35** was efficiently converted to compound **38**, the structurally defined synthon related to fragment **26**. Treatment of **35** with allylmagnesium bromide in THF converted the Weinreb amide into the corresponding homoallylic ketone, **36**. While several reagents for the stereoselective reduction of ketones have been developed, the strategic use of MOM for the protection of the alcohol component of the β-hydroxy ketone negated the requirement for these more expensive reagents. Subjection of **36** to standard Suzuki reduction conditions with lithium iodide (LiI) and lithium aluminum hydride (LAH) provided *syn*-1,3-diol **37** in high yield and diastereomeric ratio (10:1). Simple flash chromatography enabled removal of the minor undesired epimeric product, **38** (Scheme 3.9).

Stereochemical assignment of advanced intermediate **37** (corresponding to fragment **26**, Figure 3.10) was accomplished through several methods. Mosher's ester analysis previously confirmed the proper stereochemical orientation of alcohol **34**, and was again employed to validate the proper stereochemistry of 1,3-diol **37** C-15. To determine the relative stereochemical relationship of the C-16 methyl group, acid-mediated MOM deprotection and subsequent

Scheme 3.10. Reaction conditions: a) i. HCl, MeOH, reflux, 5 min, ii. DMP, PPTS, acetone, 51% over two steps.

acetonide protection of the resultant 1,3-diol enabled the application of Rychnovsky's method to this system.[65] Confirmation of the *syn*-orientation of the C-16 methyl group was obtained by comparison of the coupling constant, *J* in Hz, between the C-16 and C-15 hydrogens of both **39** and **40**. Consideration of both the conformation of 1,3-*syn*- and 1,3-*anti*-acetonide 6-membered ring systems as described by Rychnovsky, and observation of the effects that dihedral torsion angle between vicinal protons manifests upon coupling constants expected from the Karplus curve, are critical for this assignment. According to Rychnovsky, 1,3-*syn*-acetonide 6-membered rings adopt a stable chair conformation, which results in a dihedral torsion angle between the hydrogens of approximately 55º. In contrast, 1,3-*anti*-acetonide 6 membered rings adopt a twist-boat conformation, which results in a dihedral torsion angle between the hydrogens of approximately 170º. According to the Karplus equation, larger coupling constants are expected for dihedral torsion angles as they approach 0º or 180º, but as the angle deviates toward 90º, the coupling constant also decreases. Therefore, the observation of a smaller coupling constant in **39** than the analogous coupling constant of **40** would provide evidence for the desired

118

stereochemical relationship in **37**. Spectral assignment and subsequent analysis of the coupling constants of the ^{1}H NMR spectra acquired at a frequency of 500 MHz in d_6-benzene of both epimers demonstrated that for **39**, $J = 2.2$ Hz, and that for **40**, $J = 4.5$ Hz. The relationship between the epimeric coupling constants is in direct agreement with predictions based on the Karplus equation, and confirms the proper stereochemical orientation of **37** (Scheme 3.10).
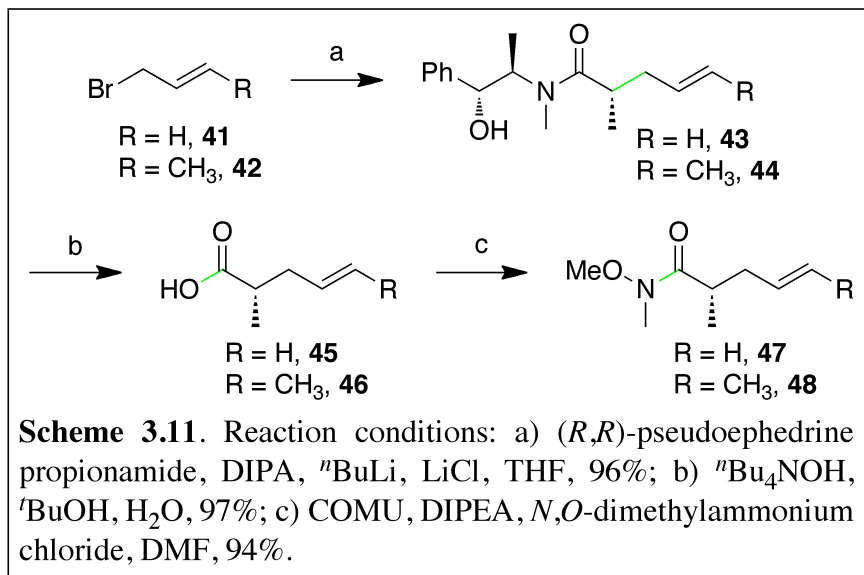
Rychnovsky analysis also provided corroborating evidence with the Mosher's ester analysis that the major product of the Suzuki reduction is a 1,3-diol, as depicted in **37**. Analysis of the ^{13}C NMR spectrum in d_6-benzene of both epimers provided a simple method to differentiate the 1,3-*syn*-acetonide from the 1,3-*anti*-acetonide, due to differences in chemical shift values of the dimethyl groups as a result of conformation. The ^{13}C NMR spectrum of **39** displayed peaks at 19.7 ppm and 30.4 ppm, which corresponded to the axial and equatorial methyl carbons respectively. This phenomenon is typically observed for six-membered rings in the chair conformation, indicating a 1,3-*syn* relationship for the corresponding diol, **37**. Conversely, the ^{13}C NMR spectrum of **40** displayed peaks at 24.0 ppm and 25.3 ppm which corresponded to the nearly identical environment of the methyl groups forced by the adoption of a twist-boat conformation, and a 1,3-*anti* relationship for the corresponding diol, **38**.

Synthesis of Weinreb amide fragment 24

The synthetic route to provide Weinreb amide fragment **24** was straightforward and provided a rapid means to generate significant quantities of this intermediate for subsequent optimization. To determine the appropriate olefin required in the RCM step, both the terminal olefin **47** and *trans*-methyl olefin **48** containing Weinreb amides were prepared through similar chemical routes. Alkylation of (*R,R*)-pseudoephedrine propionamide with allyl or *trans*-crotyl bromide under Myers' conditions generated α-methyl amides **43** and **44** in excellent yield and

diastereoselectivity.

Hydrolysis and subsequent COMU-mediated coupling produced Weinreb amides **47** and **48** without loss of enantioenrichment (Scheme 3.11).
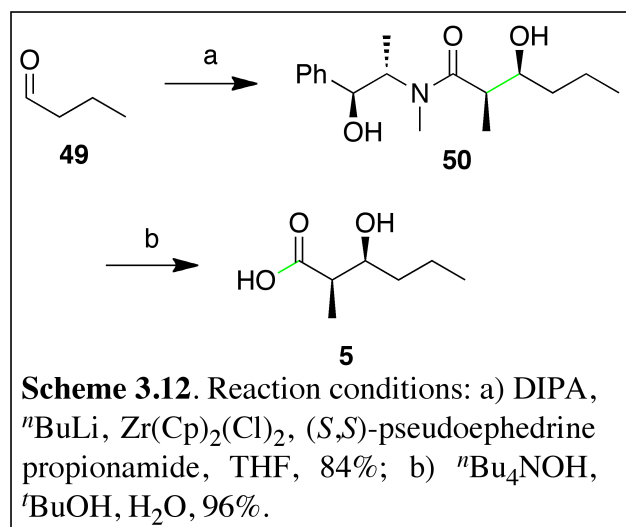

Scheme 3.11. Reaction conditions: a) (*R*,*R*)-pseudoephedrine propionamide, DIPA, ^{n}BuLi, LiCl, THF, 96%; b) ^{n}Bu$_4$NOH, ^{t}BuOH, H$_2$O, 97%; c) COMU, DIPEA, *N*,*O*-dimethylammonium chloride, DMF, 94%.

Synthesis of carboxylic acid 5

A similar Lewis acid-mediated aldol reaction between (*S*,*S*)-pseudoephedrine propionamide and butanal as described above provided amide **50** as the sole diastereomeric product (Scheme 3.12). Hydrolysis of **50** gave carboxylic acid **5** without diastereomeric loss. The successful COMU-mediated coupling reaction *en route* to Weinreb amide **34** suggested that the hydroxyl group of compound **5** did not require a protecting group. Therefore, the free alcohol of **5** was left unprotected.

Comparison of present synthetic route to those reported in the literature

Synthesis of individual fragments was designed for optimal efficiency. A comparison of published synthetic methods for analogous synthons demonstrates that both step- and chemical-economy were improved over prior reports (Figure 3.12).
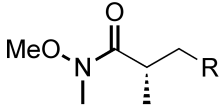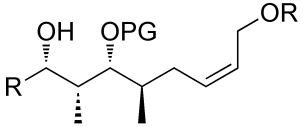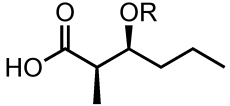

Scheme 3.12. Reaction conditions: a) DIPA, ^{n}BuLi, Zr(Cp)$_2$(Cl)$_2$, (*S*,*S*)-pseudoephedrine propionamide, THF, 84%; b) ^{n}Bu$_4$NOH, ^{t}BuOH, H$_2$O, 96%.

Figure 3.12. Comparison of the published total syntheses of cruentaren A with the present work. (NA: not applicable to synthetic strategy; NR: synthesis not reported.

Construction of the macrocycle

According to the retrosynthetic plan, the first step toward construction of the macrocyclic

scaffold of cruentaren A involved alkylation of Weinreb amide **47** or **48** by the benzylic anion

generated from methyl benzoate **51**. Lithium diisopropylamide (LDA) proved to be ineffective

toward this objective. Despite attempts to optimize these conditions, only poor yields were

obtained. However, replacement of LDA with 1.1 equiv *tert*-butyllithium (*t*BuLi) provided

ketone **52** in unexpectedly high yields (Scheme 3.13).

Scheme 3.13. Reaction conditions: a) *t*BuLi, THF, 87%
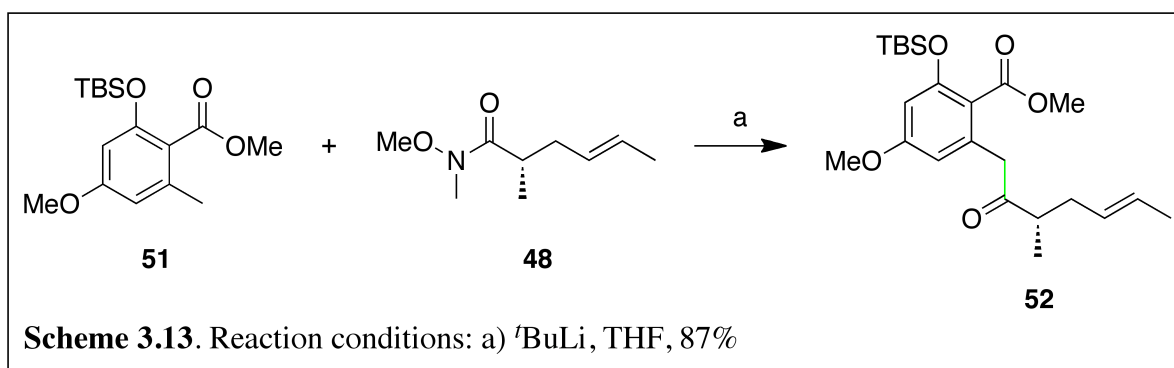
In one published synthesis of cruentaren A, the authors report successful reduction of a

similar ketone, **55**, under conditions of the Corey-Bakshi-Shibata (CBS) reaction.[66] While

stoichiometric quantites of CBS catalyst, rather than a catalytic amount, were required for this

reduction, high diastereomeric-enrichment was achieved. These results served as a starting point

Scheme 3.14. Reaction conditions: a) (*R*)-*B*-Bu-CBS, catecholborane, toluene, 84%; b) MOMCl, DIPEA, DCM, 94%.
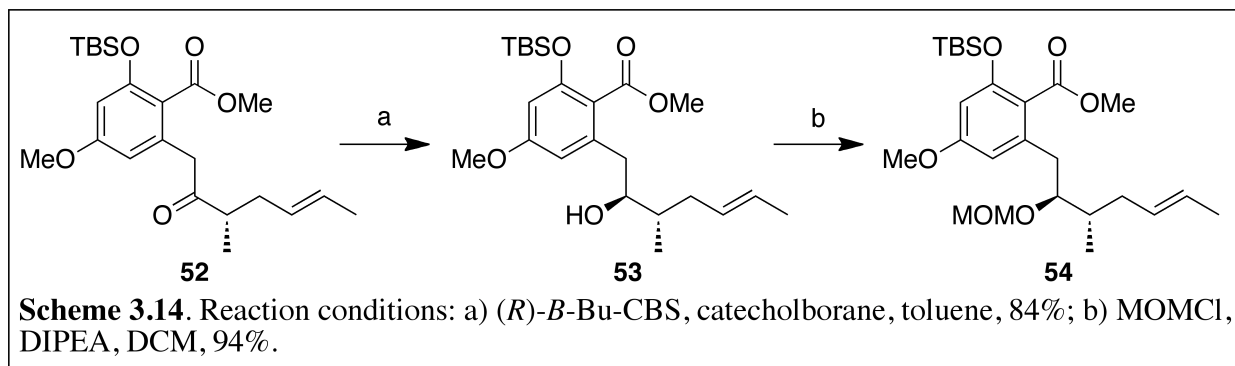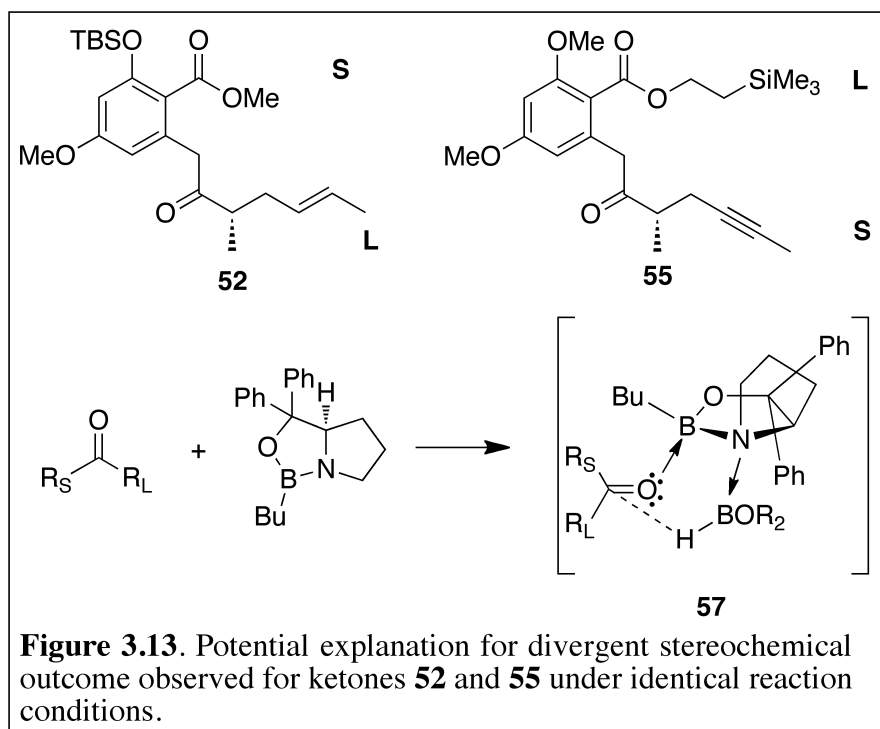
for the investigation of conditions to achieve the stereoselective reduction of ketone **52**. Fortuitously, under identical reaction conditions, treatment of ketone **52** with stoichiometric (*R*)-(+)-2-butyl-CBS-oxazaborolidine and catecholborane in toluene resulted in complete reduction to a single diastereomeric alcohol product, **53**. To prevent lactone formation, the alcohol was quickly treated with MOMCl and DIPEA in DCM to provide MOM-protected product **54** (Scheme 3.14).

To evaluate the stereochemical outcome of the CBS reduction, during the scale up process, a sample of the alcohol product was subjected to Mosher's analysis. Surprisingly, despite identical conditions, spectral analysis of the Mosher's ester analogues suggested the product was the undesired epimer (as drawn in Scheme 3.14). This analysis was repeated three times with different batches of commercially available catalyst in order to rule out the potential for experimental or human error. The presence of undesired epimeric product was consistently observed. Therefore, ketone **53** was subjected to CBS reduction with the corresponding enantiomeric catalyst in hopes of providing the desired diastereomer. (*S*)-(-)-2-butyl-CBS-oxazaborolidine-mediated reduction of ketone **53** proved highly inefficient in terms of both chemical yield and diastereomeric ratio. Attempts to overcome this result by the investigation of various CBS catalysts, solvent effects, and boranes were similarly dismal.

Scheme 3.15. Reaction conditions: a) (R)-B-Bu-CBS, catecholborane, toluene.
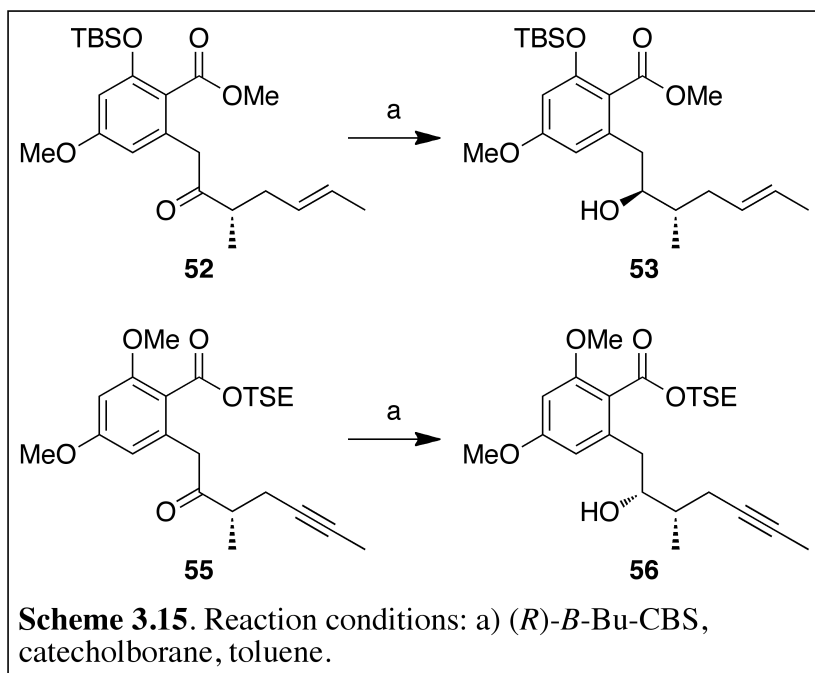
The observation of opposing stereochemical outcomes on highly similar ketones with enantiomerically identical catalysts is curious (Scheme 3.15). One potential explanation involves differences in protecting groups between the compounds **52** and **55** (Figure 3.13). A phenolic methyl ether and (trimethylsilyl)ethoxy (TSE) ester were incorporated into the published ketone **55**, while a phenolic TBS ether and methyl ester are present in ketone **52**. The CBS reduction proceeds *via* transition state **57**, with the more sterically bulky substituent distal to the *B*-butyl group. The stereochemical results indicate that the TSE ester of **55** functions as the bulky substituent, while in

Figure 3.13. Potential explanation for divergent stereochemical outcome observed for ketones **52** and **55** under identical reaction conditions.

the case of **52**, the bulky substituent corresponds to the hydrocarbon chain.

Fortunately, an alternate synthetic route toward the metathesis substrate was simultaneously under consideration. Construction of the macrocyclic architecture under this strategy involved esterification of **37** with commercially available benzoic acid **58**. Synthesis of ester **59** proved significantly challenging. The published syntheses of cruentaren A describe similar difficulties (Figure 3.14).[50, 52, 53] Vintonyak and Maier found that esterification was inaccessible in the presence of protecting groups. Successful esterification only proceeded upon treatment of unprotected 1,3-diol **62** with imidazolidine **61**, following conversion of acid **58** with carbonyl diimidazole (CDI) in DMF at 50 ºC for 4 h. The authors reported that the major product observed was indeed the desired alcohol. However, Furstner *et al*. were unable to repeat these experimental results in the course of their total synthesis. These authors reported that successful esterification could only be achieved through isolation of an acyl fluoride intermediate, **65**, and subsequent nucleophillic attack by the corresponding sodium alkoxide of compound **66**. These and several other esterification conditions were attempted in the present work with disappointing results. After significant investment, synthesis of ester **59** was realized upon treatment of acid **58** with oxalyl bromide [$(COBr)_2$], DIPEA, and catalytic DMF in DCM at 0 ºC for 30 min, followed by the addition of alcohol **37** and 4-(dimethylamino)pyridine (DMAP) (Scheme 3.16). Complete conversion to the desired ester **59** occurred within 5 min in nearly quantitative yield. These reaction conditions proved effective up to 500 mg scale. An extensive review of the available literature regarding esterification, acyl halide synthesis, and chemical utility of $(COBr)_2$ suggested that this is the first description of acyl bromide mediated esterification.
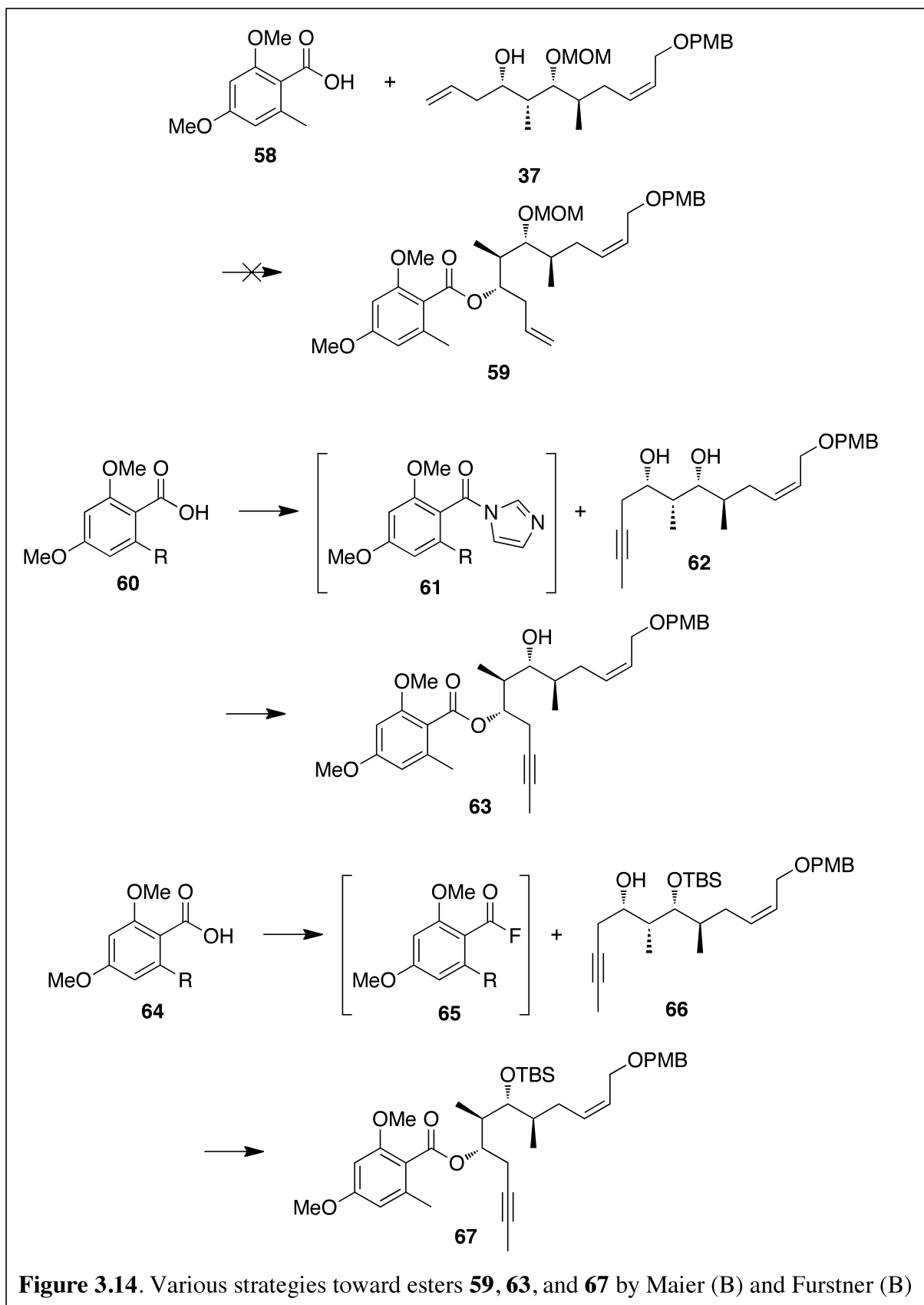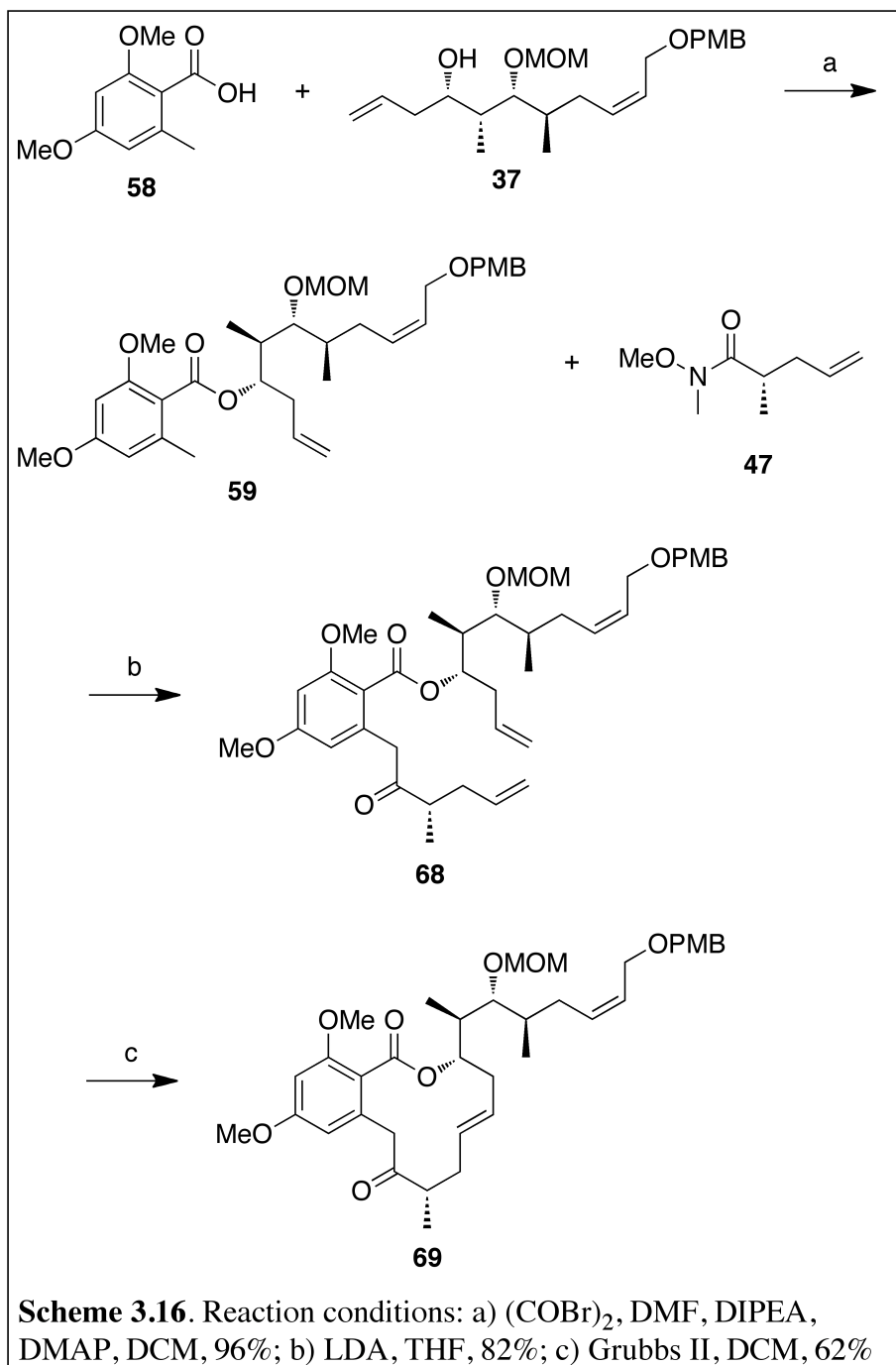
**Figure 3.14**. Various strategies toward esters **59**, **63**, and **67** by Maier (B) and Furstner (B)
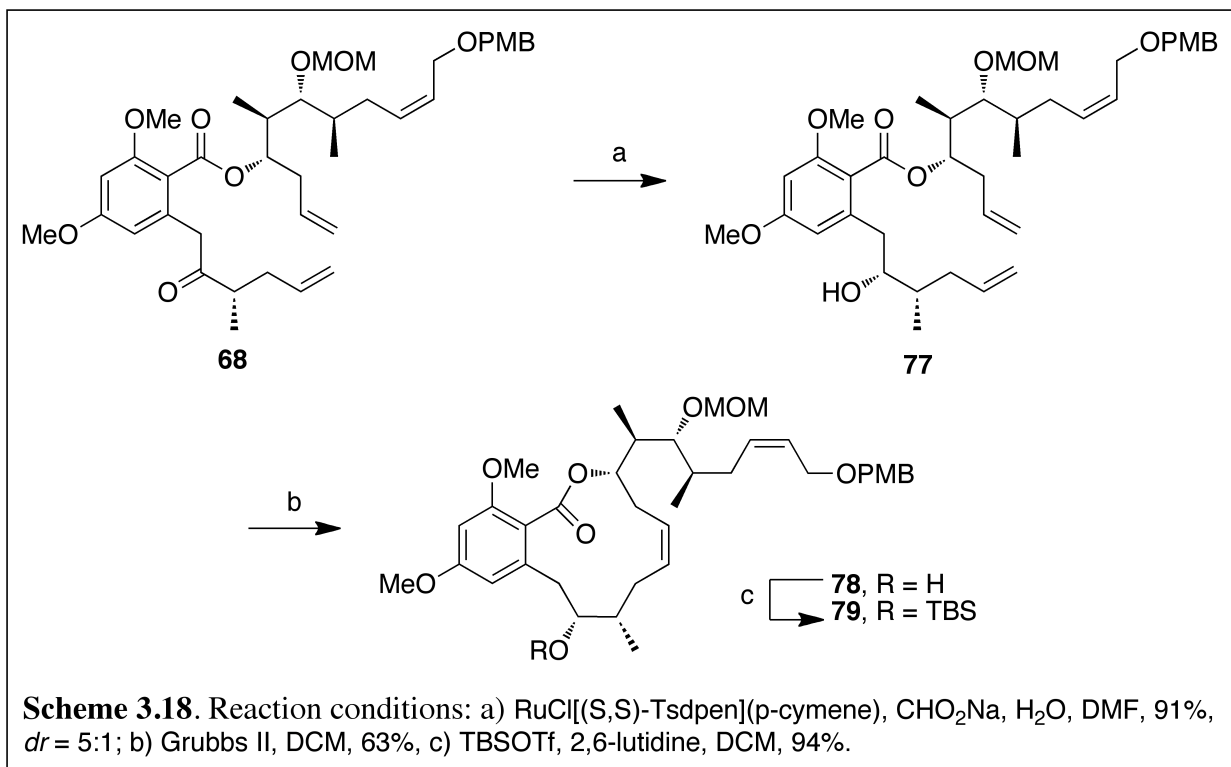
Unlike methyl benzoate **51**, alkylation of Weinreb amide **47** by the benzylic anion of **59** was effectively mediated by LDA to produce advanced intermediate **68** in appreciable yield. Synthesis of **68** provided the first metathesis substrate. Successful RCM of substrate **68** to selectively produce the *cis*-macrocyclic product have provided the inherent benefit of

Scheme 3.16. Reaction conditions: a) (COBr)$_2$, DMF, DIPEA, DMAP, DCM, 96%; b) LDA, THF, 82%; c) Grubbs II, DCM, 62%

potentially overcoming issues associated with asymmetric reduction of ketone **53**. In this case, the ketone would be conformationally constrained by the ring to elicit higher enantiofacial selectivity. Unfortunately, variations in solvent, concentration, temperature, catalyst, and catalyst loading were unsuccessful, as the major product was *trans*-macrocycle **69** along with minor

126

traces of acyclic dimer and unreacted starting material. Several factors influence the *cis*:*trans* ratio of RCM products, including ring strain, steric bulk surrounding the alkene, and rate of productive vs. unproductive metallocyclobutane elimination for *cis* and *trans* ruthenium metallocycle intermediates.[67, 68] Macrocycle **69** contains six sp^2 hybridized carbon atoms. Exclusive production of the *trans* macrocycle suggests that product ring strain favors a dramatic increase in productive elimination for *trans*-metallocyclobutane compared to the *cis*-metallocyclobutane.

During the investigation of RCM with ketone **69**, a novel approach toward the selective synthesis of *cis*-olefin containing macrocycles *via* RCM was described by Wang *et al*.[69] This work reported that the incorporation of a removable vinylsiloxane at the internal position of a single terminal olefin proved to be an effective method for producing *cis*-olefin macrocyclization products. This publication prompted synthesis of Weinreb amide **73**, which contained a terminal alkyne, in similar fashion to the related Weinreb amides **47** and **48**. LDA mediated alkylation of **73** with ester **59** provided access to advanced intermediate **74**, which subsequently underwent hydrosilylation in the presence of triethyoxysilane and catalytic pentamethylcyclopentadienyltris (acetonitrile)ruthenium(II) hexafluorophosphate to furnish vinylsiloxane **75**.[70] Subjection of this metathesis substrate to the published reaction conditions led to **76** as the only product. In hindsight, this result is not surprising considering the unreactive nature of 1,1-disubstituted olefins in RCM catalysis.[71] In accordance with the published observations, variations in solvent, concentration, temperature, catalyst, and catalyst loading were incapable of generating the desired 12-membered macrocycle (Scheme 3.17).
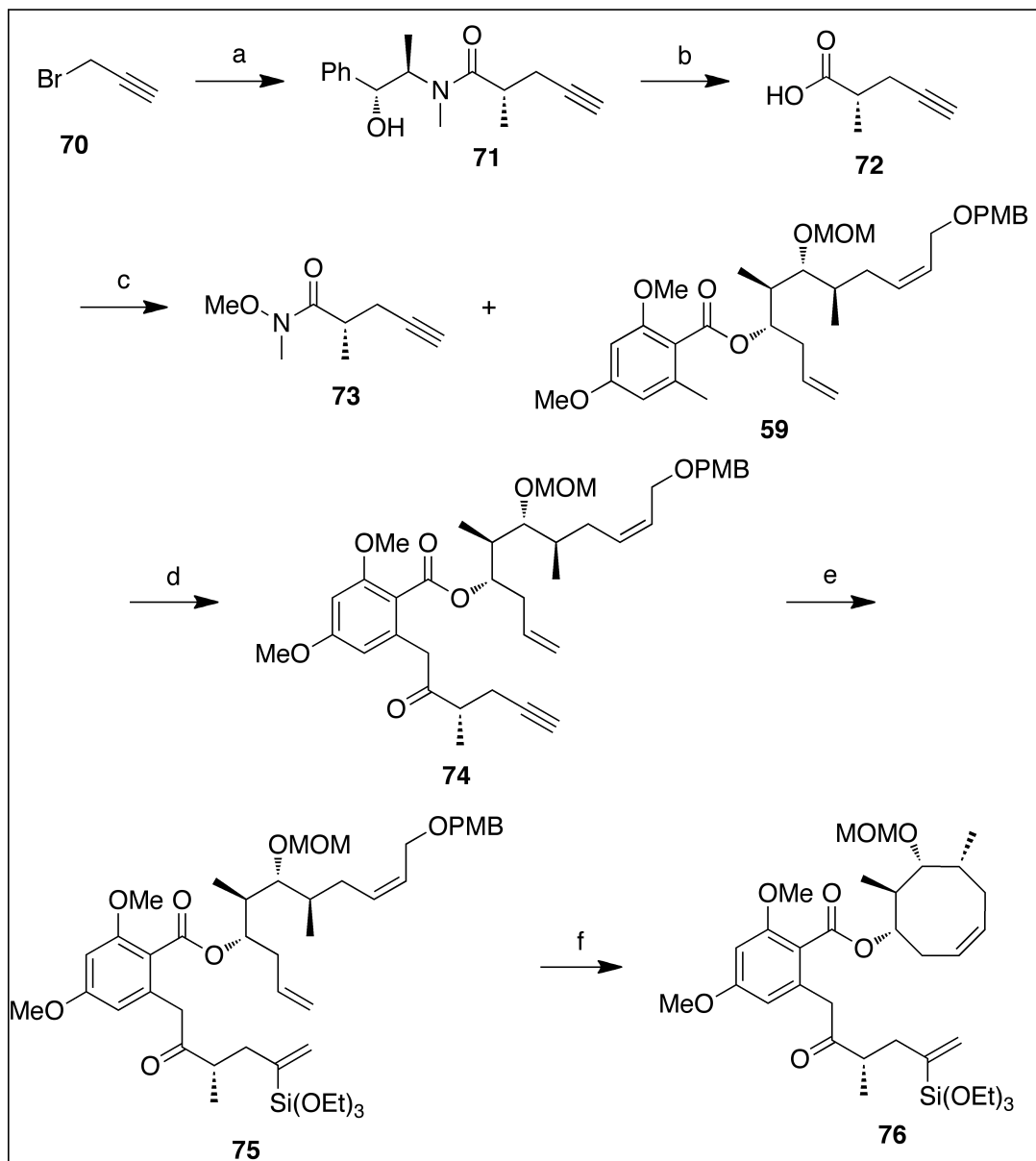
Scheme 3.17. Reaction conditions: a) (R,R)-pseudoephedrine propionamide, DIPA, "BuLi, LiCl, THF, 95%; b) "Bu₄NOH, ᵗBuOH, H₂O, 96%; c) COMU, DIPEA, N,O-dimethylammonium chloride, DMF, 94%, d) LDA, THF, 74%; e) triethoxysilane, pentamethylcyclopentadienyltris(acetonitrile)ruthenium(II) hexafluorophosphate, DCM, 97%; f) [1,3-bis(2-methylphenyl)-2-imidazolidinylidene](benzylidene)(tricyclohexylphosphine)ruthenium(II), toluene, 69%.

Scheme 3.18. Reaction conditions: a) RuCl[(S,S)-Tsdpen](p-cymene), CHO$_2$Na, H$_2$O, DMF, 91%, *dr* = 5:1; b) Grubbs II, DCM, 63%, c) TBSOTf, 2,6-lutidine, DCM, 94%.

Prior to attempting the RCM on 1-substituted terminal olefin synthons, the stereoselective reduction of ketone **8** was considered. Attempts to affect the stereoselective reduction of ketone **68** under various conditions of CBS reduction were less successful than previous attempts on compound **52**. Ketone **68** was highly resistant to reduction under CBS conditions. However, reduction of ketone **68** under conditions of Noyori asymmetric transfer hydrogenation was fruitful.[72, 73] Owing to the complications encountered in prior attempts at asymmetric reduction, both enantiomers of Noyori's Ru catalyst were tested. Following Mosher's analysis of the corresponding products, RuCl[(*S,S*)-Tsdpen](*p*-cymene) was identified as the catalyst that induced the required stereochemical outcome (Scheme 3.18). Treatment of ketone **68** with sodium formate and catalytic RuCl[(*S,S*)-Tsdpen](*p*-cymene) in DMF and deionized water proved to be optimal for generation of alcohol **77** in good yield and acceptable diastereomeric ratio (~5:1). Unfortunately, the epimeric products were not separable *via* column chromatography.

Consequently, alcohol **77** was subjected to RCM catalysis, and gratifyingly, the *cis*-olefin containing macrocycles were obtained in diastereomerically pure forms, as the alcohol epimers were readily separable *via* column chromatography (Scheme 3.18). While the desired epimer was amenable to column

Figure 3.15. Potential vinyl PMB ether byproduct
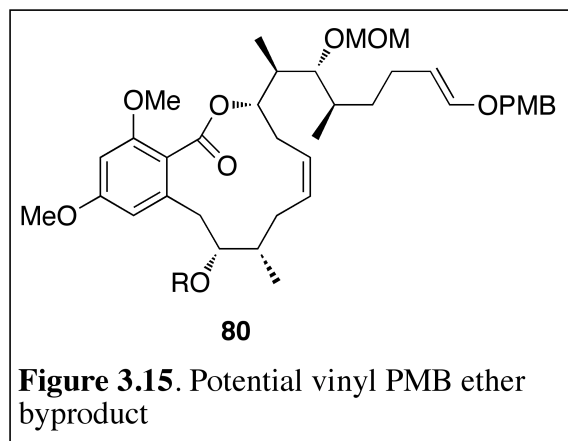
chromatography, the undesired epimer was not. Minor undesired product impurities, with an exact mass corresponding to acyclic homodimers, could not be removed from the minor epimeric product during initial attempts. Subsequent attempts at purification were not pursued.

The selective nature of the metathesis reaction between the terminal olefins is somewhat surprising. Previous attempts employing vinylsiloxane **75** demonstrated the high propensity for metathesis reaction between the terminal olefin and *cis*-allylic ether. However, the potential eight-membered cyclic product was not observed in this case. An additional concern arising from incorporation of the *cis*-allylic ether was the potential for isomerization to the corresponding vinyl ether **80** (Figure 3.15). This type of isomerization is hypothesized to be the result of a catalytically incompetent Ru hydride complex.[74] In spite of the likelihood for side reactions, no vinyl ether formation was observed. Unfortunately, an unexpected side reaction did occur, in which *cis* to *trans* isomerization of the side chain olefin was observed.

Initial conditions, addition of 20 mol % Grubbs' II at rt to a 2 mM solution of alcohol **77** in toluene followed by stiring at 50 ºC overnight, resulted in a 1:2 (*cis:trans*) mixture of olefin isomers that were inseparable *via* column chromatography. A variety of conditions were surveyed to increase yield and decrease isomerization. The effects of solvent, concentration,

temperature, catalyst, and catalyst loading were examined alongside various alcohol protecting groups. Interestingly, the RCM reaction of MOM protected substrate resulted in several uncharacterizable products, while TBS protected substrate elicited an increased rate of isomerization. The effects of various solvents on the RCM reaction should also be noted. Several solvents, including THF, benzene, and methanol (MeOH) were screened, but the most dramatic decrease in isomerization was observed in DCM. Grubbs' catalysts are known to be less stable in DCM than other solvents such as toluene, and additionally less reactive. This observation is in line with the experimental results. By decreasing the stability and reactivity of Grubbs II, DCM effectively disrupted catalyst complexation and subsequent formation of the ruthenocyclobutane intermediate with the *cis*-1,2-disubstituted olefin of the side chain, but had no effect on catalyst complexation and ruthenocyclobutane formation with the less hindered terminal olefins.

The optimized reaction conditions included the addition of 5 mol% Grubbs II at 0 ºC to a 0.5 mM solution of alcohol **77** in DCM, followed by warming to 20 ºC. RCM was complete after 3.5 h, but required treatment with saturated aqueous potassium carbonate (K_2CO_3) for catalyst deactivation in order to prevent additional isomerization during work-up. These reaction conditions furnished epimerically pure *cis*-macrocyclic product, **78**, in 63% yield from a 5:1 mixture of alcohol epimers as a 3:1 (*cis*:*trans*) mixture of side chain olefin isomers. TBS protection of macrocycle **78** with TBSOTf and 2,6-lutidine in DCM afforded intermediate **79** in high yield.

Upon successful construction of the macrocyclic core of cruentaren A, the final synthetic steps were pursued. Deprotection of the allylic PMB ether was accomplished by treating intermediate **79** with 2,3-Dichloro-5,6-dicyano-1,4-benzoquinone (DDQ) at room temperature in a 16:1 respective mixture of DCM and deionized water (Scheme 3.19). Next, conversion of

Scheme 3.19. Reaction conditions: a) DDQ, DCM, H_2O, 86%; b) $Zn(N_3)_2(pyr)_2$, DIAD, PPh_3, toluene, 89%; c) i. PPh_3, THF, ii. COMU, DIPEA, **5**, DMF, 72%.
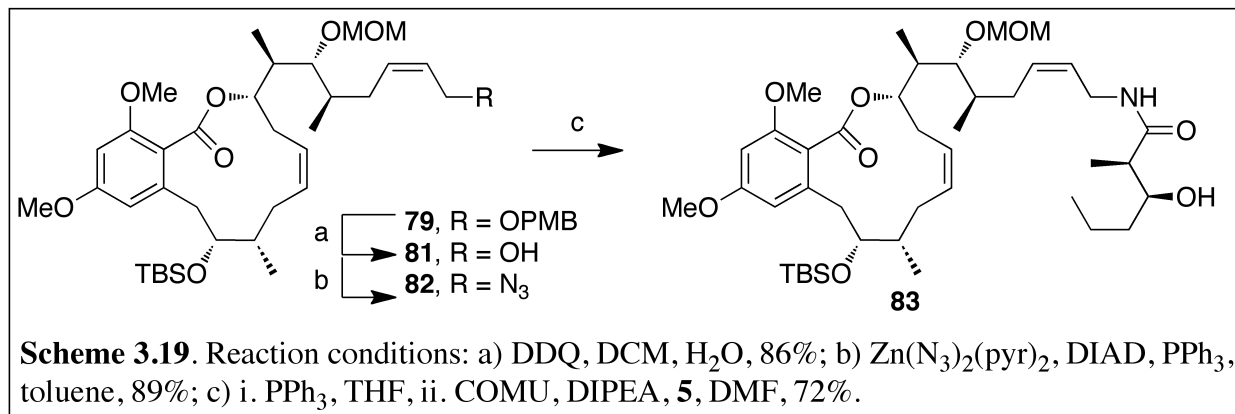
allylic alcohol **81** to the corresponding allylic azide **82** for application in the Staudinger ligation was attempted. Tosylation of this alcohol, with the ultimate goal of nucleophillic displacement by azide, resulted only in an undesired product. Analysis of the ^1H NMR spectrum of this product suggested the presence of a terminal olefin, presumably the result of secondary, S_N2' reaction of chloride anion (mass spectral analysis confirmed this hypothesis). Mitsunobu conditions were then investigated. Treatment of allylic alcohol **81** with diphenylphosphoryl azide, PPh_3, and diisopropylazodicarboxylate (DIAD) in THF surprisingly afforded an undesired DIAD adduct. Evaluation of different batches of diphenylphosphoryl azide and DIAD resulted in the same undesired product. An alternate method for conversion of activated alcohols to the corresponding azide under Mitsunobu conditions involved the use of $Zn(N_3)_2(pyridine)_2$ as an azide source.[75]

No commercial source for this reagent was located and this azide donor surrogate is only available by warming a stirred solution of $Zn(NO_3)_2$ in deionized water to 50 °C followed by the addition of an aqueous solution of 2 equiv of NaN_3 and subsequent addition of 2 equiv of pyridine according to literature reports. This protocol provided the desired Zn complex, although in low yield and high water content, which would adversely effect its application to the Mitsunobu reaction. An optimized protocol was developed that involved combining all three reagents in minimal deionized water and subsequent sonication that, after 10 min, resulted in

rapid precipitation of the Zn complex. The aqueous solvent was decanted and any remaining water was removed by azeotroping with toluene. Gratifyingly, application of the Zn complex from this protocol to Mitsunobu conditions (DIAD and PPh$_3$ in toluene) with allylic alcohol **81** afforded allylic azide **82** in excellent yield. Surprisingly, no optimization was required for the application of allylic azide **82** to the Staudinger ligation with acid **5**. Allylic azide was stirred with PPh$_3$ in THF at 50 ºC for 2 h followed by cooling to rt. Acid **5** was then activated by COMU and DIPEA in DMF in a separate flask and subsequently added to the *in situ* generated iminophosphorane. Two products, corresponding to the *cis* and *trans*-olefinic side chain isomers, **83**, were isolated as a chromatographically inseparable mixture (Scheme 3.19).

Advanced intermediate **83** required the removal of three protecing groups, the C-3 methyl ether, C-17 MOM ether, and the C-8 silyl ether. All of these functional groups demonstrate lability to acidic conditions, and, therefore, global deprotection was expected upon treatment with boron trichloride. Following the treatment of **83** with boron trichloride in DCM at -78 ºC, four products were isolated and identified: desired *cis*-olefin product **84**, *trans*-olefin isomer **85**, and an inseparable mixture of cruentaren A and its *trans*-olefin isomer **86** (Scheme 3.20). Because desired product **84** and undesired isomeric **85** could be separated, reaction conditions were sought that could avoid TBS-deprotection and provide **84** and **85** as the major products. Optimization involved a simple decrease in reaction time with **84** and **85** being the only products observed in excellent overall yield. Unfortunately, penultimate intermediate **84** was unexpectedly unstable.
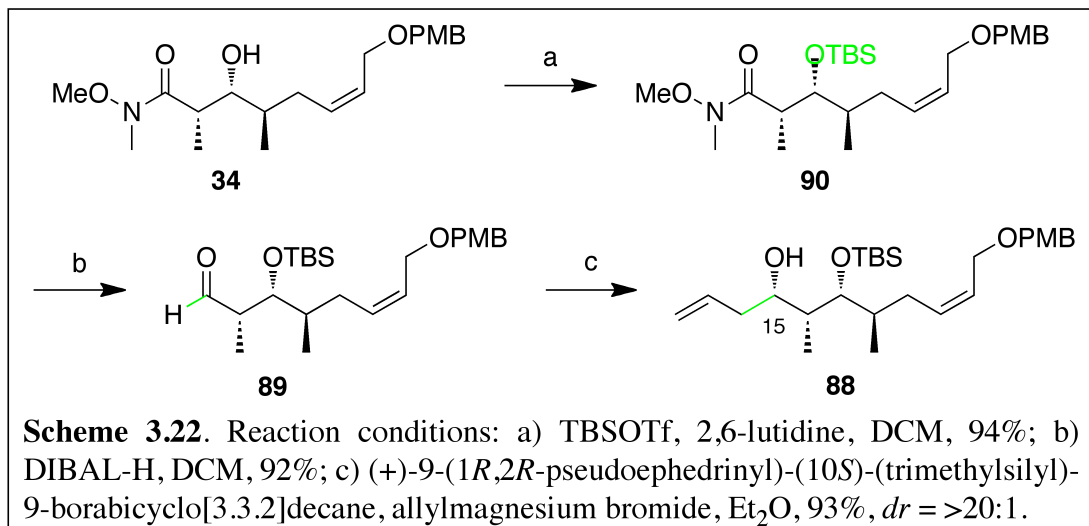
Scheme 3.20. Reaction conditions: a) BCl$_3$, DCM, -78 °C, 4 h; b) BCl$_3$, DCM, -78 °C, 1 h
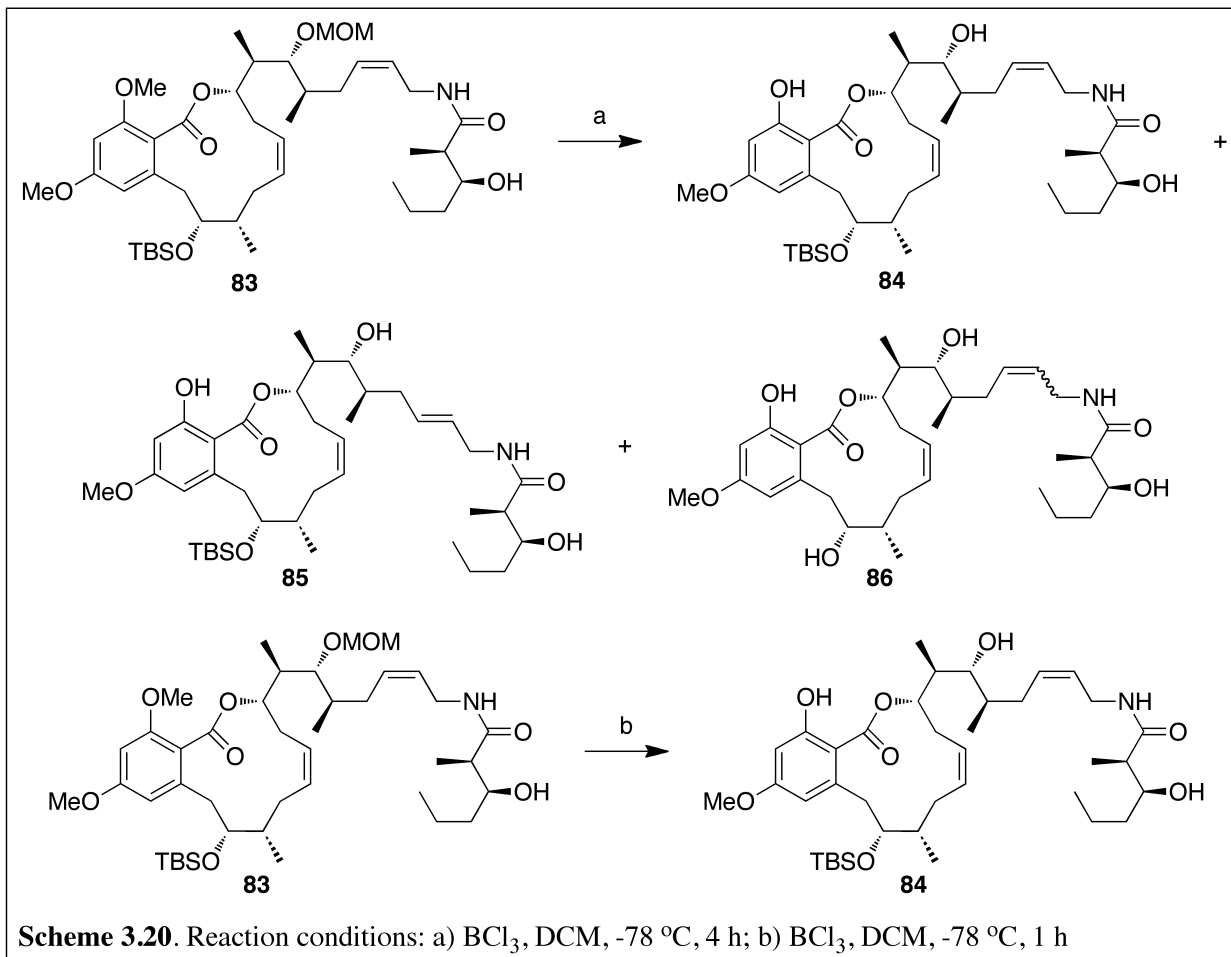
Despite the appearance of a single peak in the high-resolution mass spectrum (HRMS) corresponding to the [M+Na]$^+$ ion adduct of **84**, a trace impurity was observed in the ^{1}H and ^{13}C NMR spectra. Attempts to chromatographically remove this impurity surprisingly lead to the isolation of a single component. Purified material was identical to **84** in HRMS, but surprisingly corresponded to what was previously present as a trace impurity in the ^{1}H and ^{13}C NMR spectra. Upon further analysis, this impurity was identified as the ring-expanded product **87**, which was presumably the result of transesterification and ring-expansion of **84** apparently catalyzed by the weakly acidic nature of SiO$_2$ (Scheme 3.21).

Scheme 3.21. Ring-expansion of **84** to **87**.
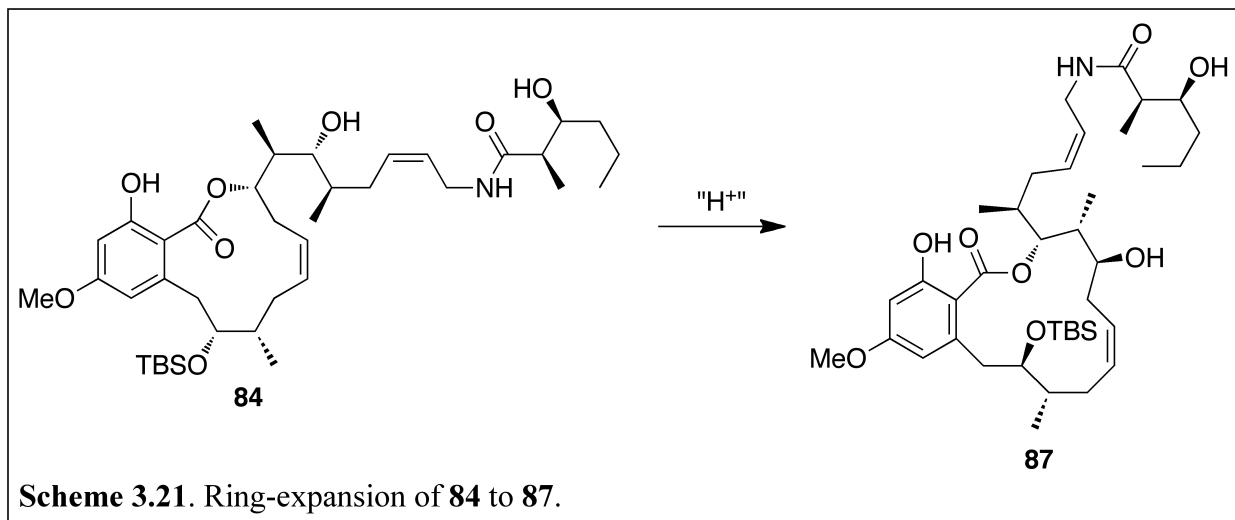
The rearrangement of **84** to ring-expanded **87** was completely unexpected. No such rearrangement was observed during the isolation of cruentaren or reported in the published total syntheses of this natural product. Ring expansion of **84** to form **87** might arise from perturbation of macrocycle conformation and subsequent reorientation of the unprotected C-17 alcohol as an unintended consequence of the TBS protection of the C-8 alcohol. Therefore, a new synthetic route was devised that involved replacement of the C-17 MOM ether protecting group with TBS. Such a protecting group swap prevents application of the Suzuki reduction previously employed for the construction of the desired *syn*-1,3-diol moiety at C-15 and C-17 of compound **37**. This expectation necessitated an alternate strategy for stereochemical induction at C-15. Therefore, the novel synthetic target **88** was envisioned to be acquired by stereoselective allylation of aldehyde **89**, which could be accessed from advanced intermediate **34** (Figure 3.16).

Figure 3.16. Novel synthetic strategy to access **88** from advanced intermediate **34**.

Scheme 3.22. Reaction conditions: a) TBSOTf, 2,6-lutidine, DCM, 94%; b) DIBAL-H, DCM, 92%; c) (+)-9-(1*R*,2*R*-pseudoephedrinyl)-(10*S*)-(trimethylsilyl)-9-borabicyclo[3.3.2]decane, allylmagnesium bromide, Et$_2$O, 93%, *dr* = >20:1.
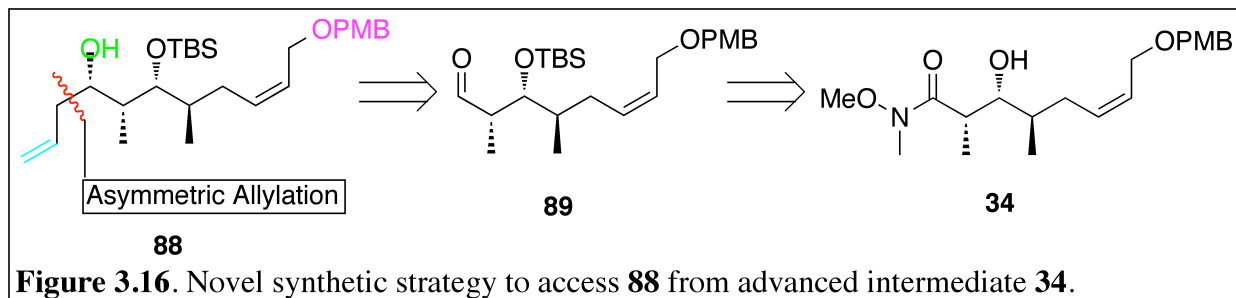
Treatment of Weinreb amide **34** with TBSOTf and 2,6-lutidine in DCM afforded **90**, which was subsequently transformed to aldehyde **89** by DIBAL-H mediated reduction. Soderquist allylation of aldehyde **89**, using (+)-9-(1*R*,2*R*-pseudoephedrinyl)-(10*S*)-(trimethylsilyl)-9-borabicyclo[3.3.2]decane and allylmagnesium bromide proceeded in high yield and *dr*, furnishing homoallylic alcohol **88** without the need for reaction condition optimization (Scheme 3.22).[63]

Asymmetric allylboration is a powerful chemical tool for the stereoselective construction of carbon-carbon bonds.[76] Several advancements since the pioneering studies of Brown and co-workers have lead to increases in chemical efficiency, reaction yield, and enantio- and diastereoselectivity. The development of 10-trimethylsilyl-9-borabicyclo[3.3.2]decane for the asymmetric allylation of a variety of carbonyl species by Soderquist and co-workers is particularly exciting. The *in situ* generated allylborane intermediate **92** demonstrates increased yields and facial selectivity for the production of highly enantio-enriched homoallylic alcohols. This stereoselectivity is a result of the rigid, bicyclic nature of the borabicycle (Figure 3.17). Additionally, Soderquist's allylboranes can be easily synthesized from racemic starting
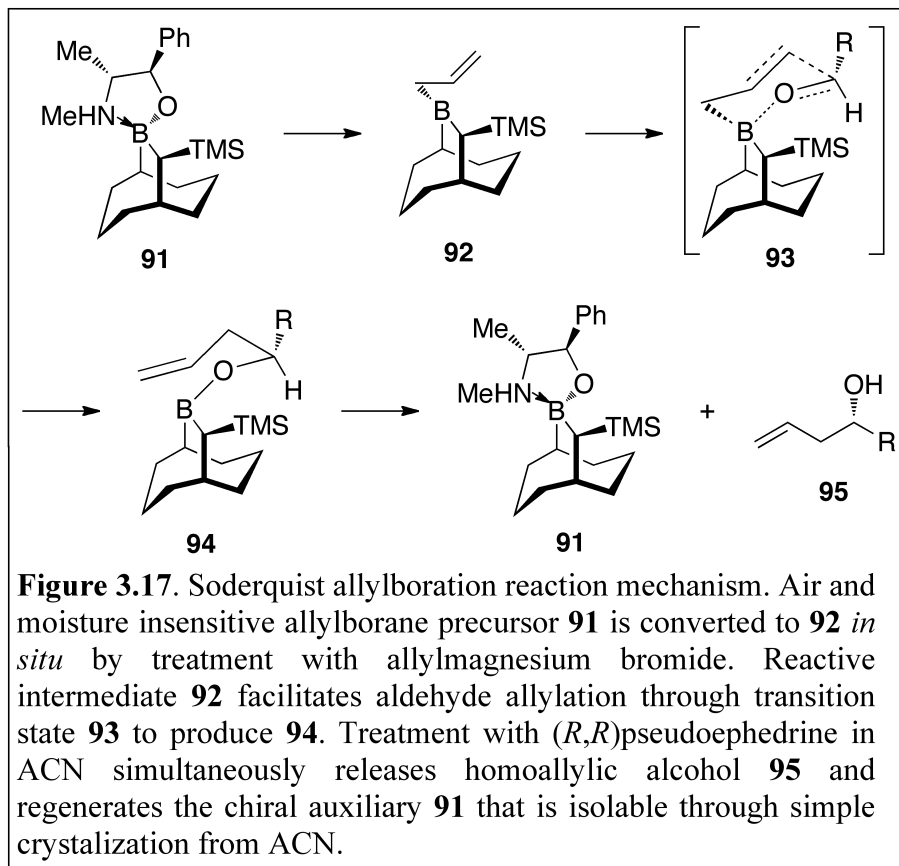
Figure 3.17. Soderquist allylboration reaction mechanism. Air and moisture insensitive allylborane precursor **91** is converted to **92** *in situ* by treatment with allylmagnesium bromide. Reactive intermediate **92** facilitates aldehyde allylation through transition state **93** to produce **94**. Treatment with (*R*,*R*)pseudoephedrine in ACN simultaneously releases homoallylic alcohol **95** and regenerates the chiral auxiliary **91** that is isolable through simple crystalization from ACN.

materials, are recyclable, and are air and moisture insensitive for prolonged storage (as **91**), rendering it synthetically practical. Furthermore, due to the rigid nature of this bicyclic structure,

Soderquist's allylboranes are less

temperature dependent than previously developed reagents, providing high levels of stereoselectivity even at rt. Finally, the mild, non-oxidative work-up procedure allows for a wide substrate scope that includes chemical entities incompatible with the harsh work-up conditions of other allylboration strategies.[63]

Elaboration of **88** for completion of the formal synthesis of cruentaren A proceeded in an identical fashion as previously described (Scheme 3.23). Oxalyl bromide mediated esterification of **88** lead to **96**, which was subsequently treated with LDA and Weinreb amide **47** to provide **97**. Noyori asymmetric transfer hydrogenation of **97** to form **98** was accomplished with catalytic RuCl[(*S*,*S*)-Tsdpen](*p*-cymene) and sodium formate in aqueous DMF. Bis-terminal olefin **98** underwent RCM to exclusively provide *cis*-olfein containing macrocycle **99**, which was then
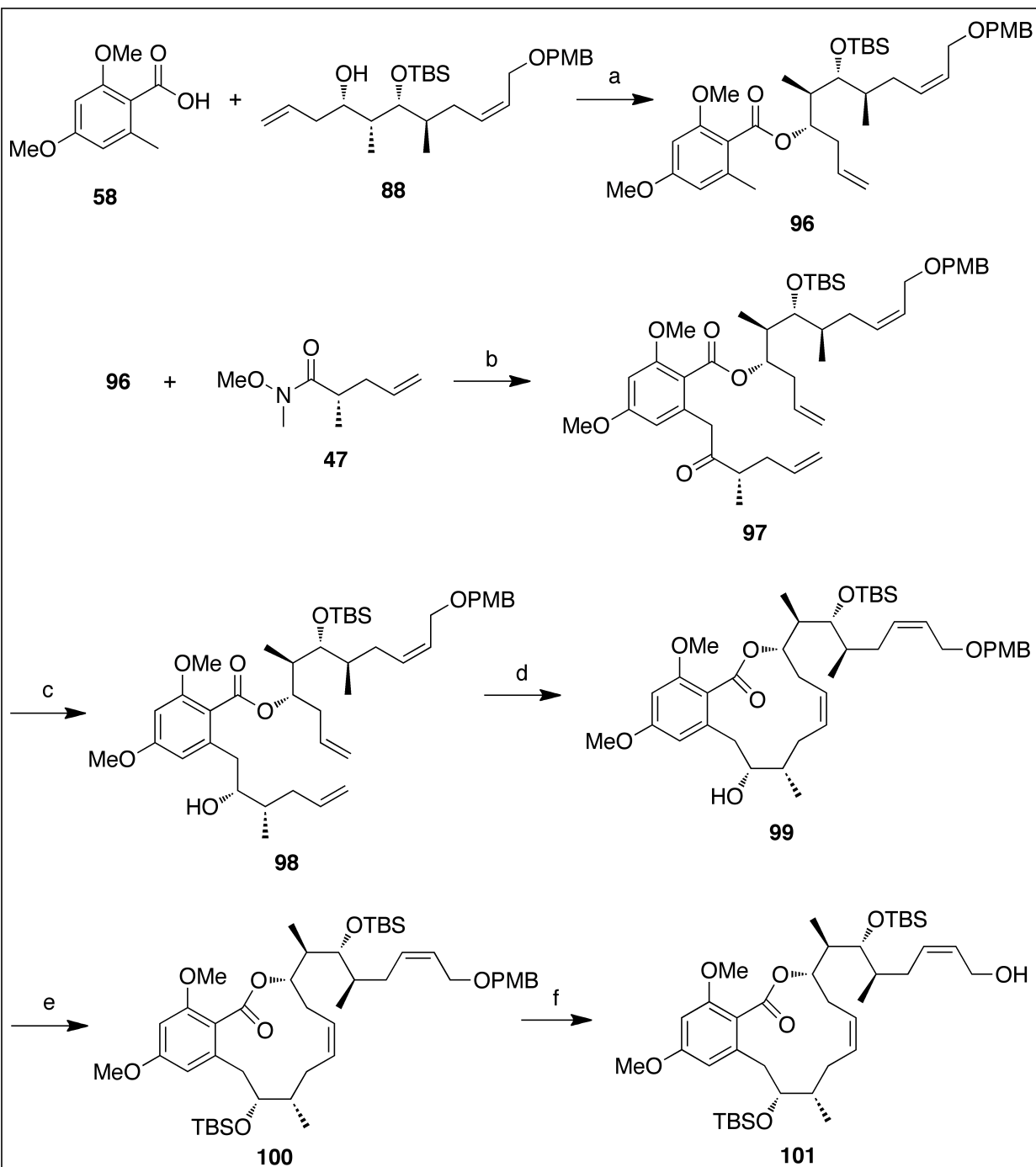
Scheme 3.23. Reaction conditions: a) (COBr)$_2$, DMF, DIPEA, DMAP, DCM, 93%; b) LDA, THF, 81%; c) RuCl[(S,S)-Tsdpen](p-cymene), CHO$_2$Na, H$_2$O, DMF, 74%, *dr* = 9:1; d) Grubbs II, DCM, 79%; e) TBSOTf, 2,6-lutidine, DCM, 91%; f) DDQ, H$_2$O, DCM, 99%

sequentially TBS-protected at C-8 to generate **100** and PMB-deprotected to lead to **101** and

completion of the formal synthesis.

Elaboration of compound **101** to cruntaren A, and completion of the total synthesis involved four additional manipulations (Scheme 3.24). The allylic alcohol of **101** converted to the allyl-azide **102** following treatment with $Zn(N_3)_2(pyridine)_2$, DIAD, and PPh_3. One-pot azide reduction and amide formation was achieved *via* Staudinger ligation conditions in order to provide protected cruentaren A, compound **103**. Methyl ether deprotection commenced by subjecting compound **103** to BCl_3 in DCM at low temperature to afford **104**. Treatment of the disilyl ether with HF in ACN and deionized water provided the final product cruentaren A (**1**).
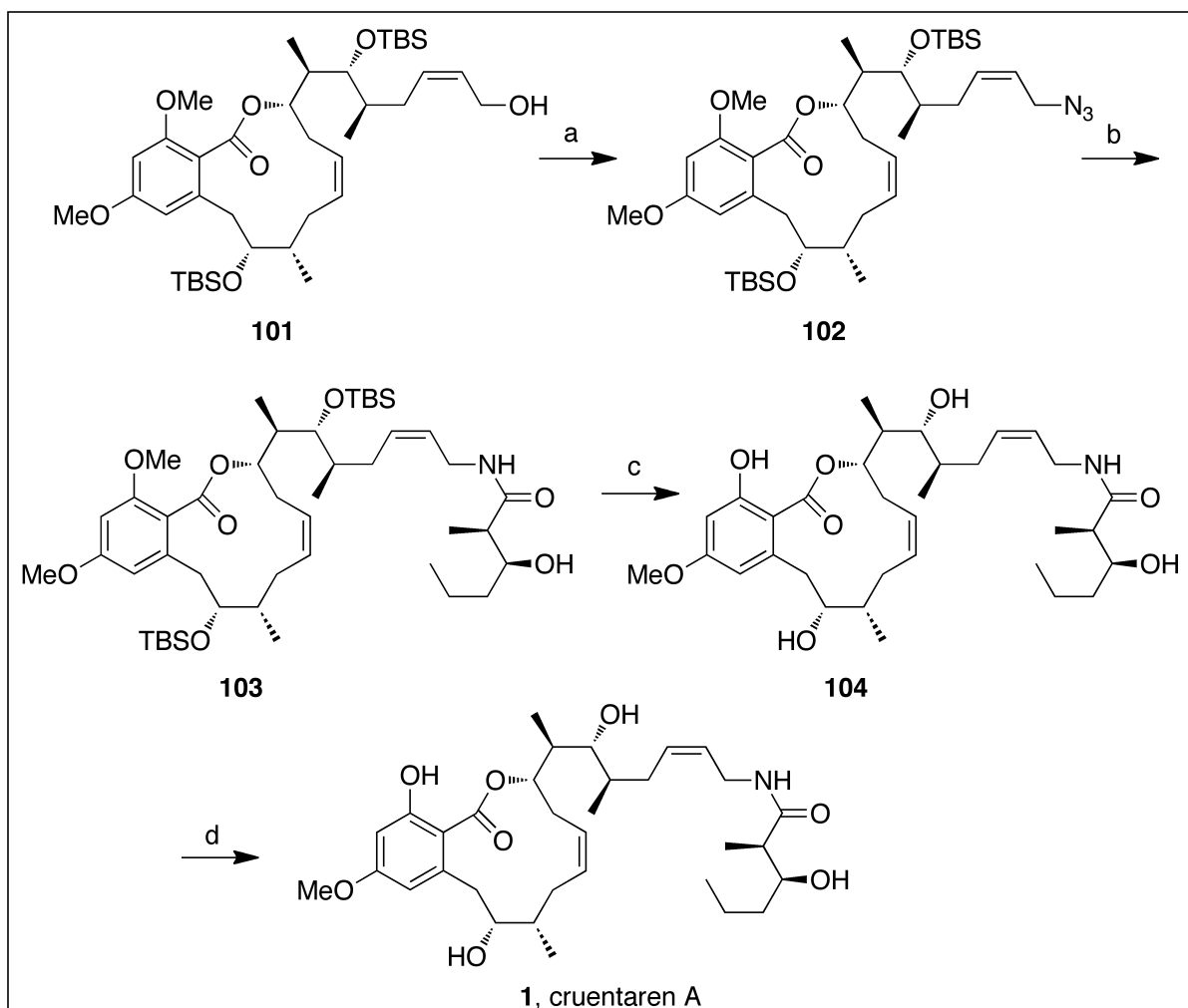
Scheme 3.24. Reaction conditions: a) $Zn(N_3)_2(pyridine)_2$, DIAD, PPh_3, toluene, 89%; b) i. PPh_3, THF, ii. **5**, DIPEA, COMU, DMF, 79%; c) BCl_3, DCM, 93%; d) HF, H_2O, ACN, 87%.

III.4 Concluding Remarks

Successful completion of the formal synthesis of cruentaren A by the route described herein will facilitate the first investigation into the effects of a selective FAS inhibitor on the super chaperone complex. This realm of Hsp90 research remains uninvestigated, and provides incredible opportunities to further delineate the mechanisms manifested by the Hsp90 protein folding process. Furthermore, by approaching this synthetic endeavor from a medicinal chemistry standpoint, the route described above will also facilitate the investigation of cruentaren A SAR. Of particular interest is the potential to deconvolute structural features of cruentaren A that are responsible for its selectivity for FAS over other ATPases. Specific areas of interest include the macrocyclic olefin, stereochemistry at C-16, C-17, and C-18, bio-isosteric replacement of the macrocyclic lactone, and the potential for non-macrocyclic, constrained analogues. Additionally, precise identification of the FAS structural domain to which cruentaren A binds using natural product based chemical probes may lead to previously unknown inhibitory regions of this macromolecular machine.

While the synthetic route described above provides a stereoselective means for the production of cruentaren A, several aspects of this strategy require refinement in a second generation synthesis. Further screening of recently developed, tethered Ru catalysts should be evaluated for their ability to increase diastereoselectivity of the Noyori asymmetric transfer hydrogenation. Ru catalysts such as **105** demonstrate improved diastereocontrol by constraining the chiral elements of the ligand and the η^6-aryl group in an optimized orientation for the transition state of the transfer hydrogenation reaction (Figure 3.18). Also, additional Ru metathesis catalysts should be screened in an effort to limit side chain olefin isomerization. The presence more sterically demanding NHC substituents, *e.g.* **106**, may prove effective toward this

Figure 3.18. Examples of alternate catalysts for improving Noyori asymmetric transfer hydrogenation (**105**) and RCM (**106**).
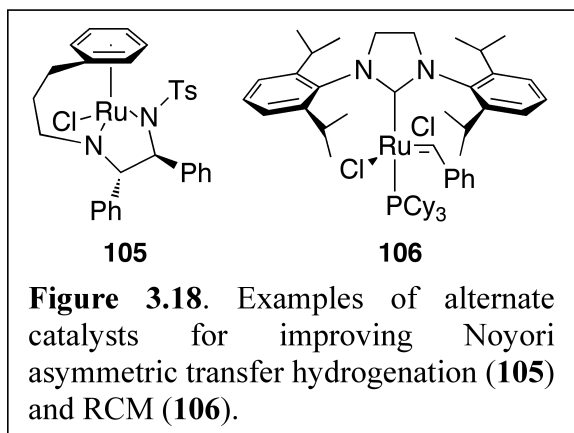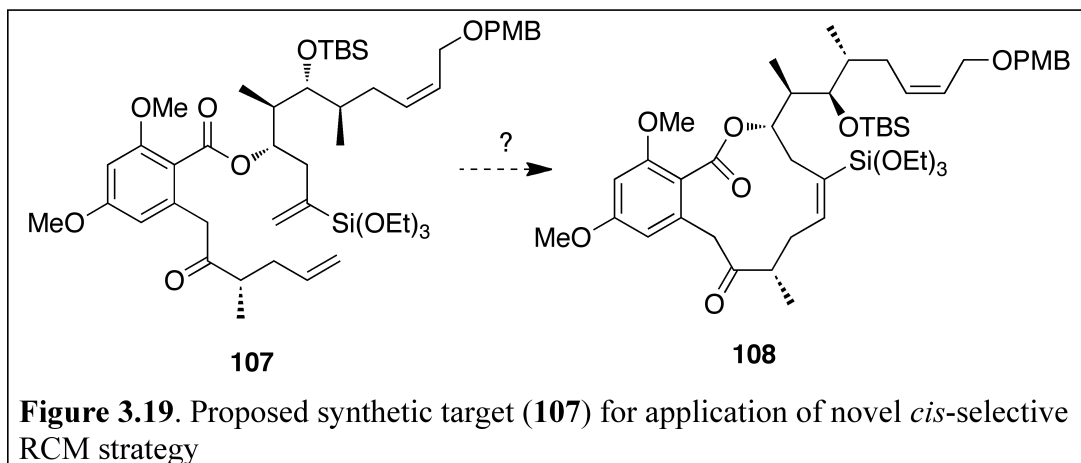
goal by occluding efficient metal complexation between catalyst and 1,2-disubstituted olefin at C-20 and C-21 while still allowing terminal olefin metathesis (Figure 3.18).

Aside from optimization of reaction conditions, one aspect of the synthetic strategy should be re-evaluated. In the recently published description of macrocycle geometrical control through incorporation of a vinylsiloxane by Trost *et al.*, the authors note that varying vinylsiloxane location between terminal olefins dramatically impacts reaction outcome. Both yield and isomeric ratio were affected depending on which of the two terminal olefins were functionalized with the vinylsiloxane. An effort should be made toward the synthesis of metathesis substrate **107** to assess its reactivity in RCM. A likely finding is that increased reaction rate and temperature will be required to induce cyclization, and this may lead to increased side chain olefin isomerization (Figure 3.19). Nevertheless, unpredictable reactivity in spite of the predictable has been a common theme during the course of these studies.

In summation, a convergent and efficient total synthesis of cruentaren A has been described herein with a total overall yield of 5.2 % for the longest linear sequence of 19 steps,

Figure 3.19. Proposed synthetic target (**107**) for application of novel *cis*-selective RCM strategy

and 23 steps overall. Completion of the total synthesis and subsequent biological evaluation of this natural product is in the capable hands of the Blagg laboratory and is primed for initiation.

III.5   Methods and Experimentals

General Methods. All reactions were carried out in flame dried glassware under argon atmosphere unless otherwise stated. Dichloromethane (DCM), diethyl ether, tetrahydrofuran (THF), and toluene were purchased from Sigma Aldrich and were passed through a column of activated alumina prior to use. Anhydrous methanol, acetonitrile, DMF (DMF), and dimethoxyethane (DME) were purchased from Sigma Aldrich and used without further purification. All reagents and other solvents [ethyl acetate (EtOAc) and hexanes (Hex)] were purchased from Sigma Aldrich and were used without further purification unless otherwise stated. Flash column chromatography was performed using silica gel (40 – 63 μm particle size) from Sorbent Technologies. The ^{1}H and ^{13}C-NMR (proton decoupled) spectra were recorded at 500 and 126 MHz, respectively, on a Bruker AM 500 using CDCl$_3$ or benzene-D$_6$ purchased from Cambridge Isotope Laboratories, Inc., using solvent as an internal standard (CDCl$_3$ at 7.260 ppm for ^{1}H and 77.160 ppm for ^{13}C, benzene-D$_6$ at 7.160 ppm for ^{1}H and 128.060 ppm for ^{13}C) or tetramethylsilane (0.00 ppm) unless otherwise stated. Data are reported as h = hextet, p = pentet, q = quartet, t = triplet, d = doublet, s = singlet, bs = broad singlet, m = multiplet; coupling constant(s) in Hz. ^{19}F-NMR spectra were recorded at 376 MHz on a Bruker DRX 400 in C$_6$D$_6$ using (*R*)-3,3,3-trifluoro-2-methoxy-2-phenylpropanoic acid as an internal standard unless otherwise stated. Two-dimensional NMR experiments were run on a Bruker AM 500 at 500 MHz. High resolution mass spectral data were obtained on a Ribermag R10-10 quadrupole, VG

Analytical ZA. Optical rotations were recorded with a Perkin Elmer polarimeter at 589 nm at 25 °C with concentration reported as g/mL.

Experimentals:
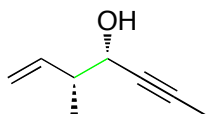
(3*R*,4*S*)-3-methylhept-1-en-5-yn-4-ol, 8

A 500 mL flask was flame dried and flushed with argon before DCM (250 mL) and 2-butyne-1-ol (4 g, 58.0 mmol, 1 eq.) were added. DMP (31 g, 146.0 mmol, 2.5 eq.) was then slowly added and the reaction mixture was stirred at 0°C for 5 h. A 1:1 solution of diethyl ether and pentane (200 mL) was added to the reaction mixture, and the slurry was filtered through a plug of celite and additional 1:1, diethyl ether:pentane (500 mL) was used to wash the SiO$_2$. Solvent was evaporated at 40 °C at 1 atm to afford aldehyde **7**, which was subsequently used without further purification. A 250 mL flask was flame dried and flushed with argon before THF (38 mL) and potassium *tert*-butoxide (1 M in THF, 19 mL, 19 mmol, 1.3 eq.) were added. The solution was cooled to -78 °C, and *cis*-2-butene (3.2 mL, 36 mmol, 2.5 eq.) was added followed by the dropwise addition of butyllithium (2.5 M in hexanes, 7.6 mL, 19 mmol, 1.3 eq.). The suspension was warmed to -42 °C and stiring was continued for 30 min at which point the suspension was cooled back to -78 °C. A solution of (−)-*B*-methoxydiisopinocampheylborane (7 g, 22 mmol, 1.5 eq.) in THF (20 mL) cooled to 0 °C was added, and the reaction mixture was allowed to warm to -42 °C and stirred for 1 h and then cooled back to -78 °C. Boron trifluoride diethyl etherate (3.02 mL, 24 mmol, 1.7 eq.) was added followed by the addition of a solution of aldehyde **7** (1 g, 14.6

mmol, 1 eq.) in THF (10 mL) cooled to 0 °C. Stirring was continued for 4 h at -78 °C, at which point the reaction was quenched by the addition of ethanolamine (1.8 g, 29.2 mmol, 2 eq.) and deionized water (5 mL). Stirring was continued as the suspension was allowed to warm to rt over 1 h. The resulting suspension was filtered through a pad of celite, and the filtrate was collected, dried over anhydrous sodium sulfate, and solvent was removed under reduced pressure to afford a colorless oil that was purified by SiO_2 flash chromatography (5 % – 20 % EtOAc in hexanes) to provide alcohol **8**, 1:1 enantiomeric mixture, as a colorless liquid (1.5 g, 82 %). $[\alpha]^{25}_D = 0.01°$ (c = 0.135, DCM). ^{1}H NMR (500 MHz, CDCl$_3$) δ 5.83 – 5.69 (m, 1H), 5.18 – 5.07 (m, 2H), 4.64 (m, 1H), 4.03 (m, 1H), 2.35 – 2.25 (m, 1H), 1.85 (d, J = 2.1 Hz, 3H), *1.06 (d, J = 4.5 Hz, 3H). ^{13}C NMR (126 MHz, CDCl$_3$) δ 140.39, 140.29, 116.04, 116.01, 81.51, 79.99, 74.58, 72.44, 62.94, 61.46, 44.04, 43.88, 14.75, 14.72, 3.76, 3.72. HRMS (ESI, *m/z*): calcd for $[C_8H_{12}O]^+$, ($[M + Na]^+$): 147.0786, found 147.0785.
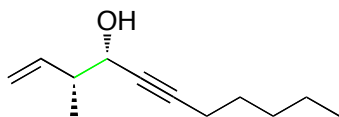
(3*R*,4*S*)-3-methylundec-1-en-5-yn-4-ol, 10

A 250 mL flask was flame dried and flushed with argon before THF (38 mL) and potassium *tert*-butoxide (1 M in THF, 19 mL, 19 mmol, 1.3 eq.) were added. The solution was cooled to -78 °C, and *cis*-2-butene (3.2 mL, 36 mmol, 2.5 eq.) was added followed by the dropwise addition of butyllithium (2.5 M in hexanes, 7.6 mL, 19 mmol, 1.3 eq.). The suspension was warmed to -42 °C and stiring was continued for 30 min at which point the suspension was cooled back to -78 °C. A solution of (−)-*B*-methoxydiisopinocampheylborane (7 g, 22 mmol, 1.5 eq.) in THF (20 mL) cooled to 0 °C was added, the reaction mixture was allowed to warm to -42 °C, stirred for 1 h and then cooled back to -78 °C. Boron trifluoride diethyl etherate (3.02 mL, 24 mmol, 1.7 eq.)

was added followed by the addition of a solution of aldehyde **9** (1.8 g, 14.6 mmol, 1 eq.) in THF (10 mL) cooled to 0 °C. Stirring was continued for 4 h at -78 °C, at which point reaction was quenched by the addition of ethanolamine (1.8 g, 29.2 mmol, 2 eq.) and deionized water (5 mL). Stirring was continued as the suspension was allowed to warm to rt over 1 h. The resulting suspension was filtered through a pad of celite, filtrate was dried over anhydrous sodium sulfate, and solvent was removed under reduced pressure to afford a colorless oil that was purified by SiO$_2$ flash chromatography (5 % – 20 % EtOAc in hexanes) to provide alcohol **10**, 15:1 diastereomeric mixture, as a colorless liquid (2.3 g, 86 %). $[\alpha]^{25}_D$ = -27.4° (c =0.018 , DCM). (*Denotes minor diastereomeric peak) ^{1}H NMR (500 MHz, CDCl$_3$) δ 5.86 (ddd, J = 8,1, 9.8, 17.9 Hz, 1H), *5.85 – 5.77 (m, 1H), 5.19 – 5.11 (m, 2H), 4.26 (dt, J = 2.4, 4.7 Hz, 1H), *4.19 (dt, J = 6.3, 1.9 Hz, 1H), 2.48 – 2.39 (m, 1H), 2.21 (td, J = 7.1, 2.1 Hz, 2H), 1.55 – 1.46 (m, 2H), 1.41 – 1.28 (m, 4H), *1.12 (d, J = 6.8 Hz, 3H), 1.10 (d, J = 6.9 Hz, 3H), 0.90 (t, J = 7.1 Hz, 3H). ^{13}C NMR (126 MHz, CDCl$_3$) δ *139.69, 139.27, 117.07, *116.66, 86.91, *86.76, *79.53, 79.22, *66.53, 66.38, *44.88, 44.64, 31.15, 28.49, 22.31, 18.78, 15.79, *15.43, 14.13. HRMS (ESI, m/z): calcd for $[C_{12}H_{20}O]^+$, $([M + Na]^+)$: 203.1412, found 203.1412.
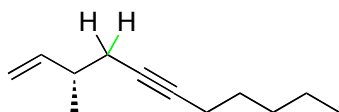
(*S*)-3-methylundec-1-en-5-yne, 11

A 500 mL flask was flame dried and flushed with argon before DCM (140 mL) and alcohol **10** (6.3 g, 35 mmol, 1 eq.) were added. Solid cobalt carbonyl (12 g, 35 mmol, 1 eq.) was added. After stirring for 8 h, the solution was cooled to 0 °C and solid sodium borohydride (4 g, 105 mmol, 3 eq.) was added followed by the dropwise addition of trifluoroacetic acid (35 mL, 454 mmol, 13 eq.) over 1 h, and stirring was continued at 0 °C for 3 h. Reaction was quenched at 0

°C by the careful addition of saturated aqueous sodium bicarbonate (200 mL). The organic layer was collected and the aqueous layer was extracted with DCM (3 X, 100 mL). The combined organic layers were dried over anhydrous sodium sulfate and solvent was removed under reduced pressure to afford a dark red oil that was diluted with methanol (50 mL). Ceric ammonium nitrate (76.8 g, 140 mmol, 4 eq.) was carefully added portionwise over several minutes. After complete addition of ceric ammonium nitrate, the reaction mixture was diluted with saturate aqueous sodium bicarbonate (100 mL) and organic solvent was removed under reduced pressure. The resultant slurry was diluted with diethyl ether (150 mL). The organic layer was collected and the aqueous layer was extracted by diethyl ether (2 X, 100 mL). The combined organic layers were dried over anhydrous sodium sulfate and solvent was removed under reduced pressure at 10 °C to afford an orange oil that was purified by SiO_2 flash chromatography (5 % diethyl ether in pentane) to provide hydrocarbon **11** as a colorless oil (3.6 g, 62 %). $[\alpha]^{25}_D$ = -13.2° (c = 0.006, DCM). ^{1}H NMR (500 MHz, CDCl$_3$) δ 5.82 (ddd, J = 17.2, 10.4, 6.8 Hz, 1H), 5.02 (ddd, J = 17.2, 1.7, 1.4 Hz, 1H), 4.97 (ddd, J = 10.4, 1.7, 1.2 Hz, 1H), 2.37 – 2.28 (m, 1H), 2.24 – 2.09 (m, 4H), 1.53 – 1.44 (m, 2H), 1.40 – 1.24 (m, 4H), 1.08 (d, J = 6.7 Hz, 3H), 0.90 (t, J = 7.2 Hz, 3H). ^{13}C NMR (126 MHz, CDCl$_3$) δ 143.22, 113.20, 81.72, 78.45, 37.29, 31.19, 28.98, 26.36, 22.37, 19.22, 18.86, 14.17.
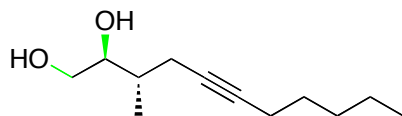
(2S,3S)-3-methylundec-5-yne-1,2-diol, 12

A 10 mL flask was charged with deionized water (0.38 mL), acetone (1.74 mL), hydrocarbon **11** (454 mg, 2.76 mmol, 1 eq.), NMO (388 mg, 3.3 mmol, 1.2 eq.), and DHQ2PHAL (430 mg, 0.55 mmol, 0.2 eq.). The solution was cooled to 0 °C and osmium tetroxide (25 mg per mL solution in

toluene, 0.056 mL, 0.0055 mmol, 0.002 eq.) was added. The reaction mixture was stirred for 23

h at which point the reaction was quenched by the addition of saturate aqueous sodium bisulfite

(2 mL). Organic solvent was removed under reduced pressure and the resultant aqueous slurry

was extracted with DCM (4 X, 3 mL). The combined organic layers were dried over anhydrous

sodium sulfate and solvent was removed under reduced pressure to afford a black oil that was

purified by SiO_2 flash chromatography (30 % – 40 % EtOAc in hexanes) to provide diol **12**, 5:1

mixture of diastereomers, as a colorless oil (400 mg, 73 %). (*Denotes minor diastereomeric

peak) ^{1}H NMR (500 MHz, CDCl$_3$) δ 3.79 – 3.72 (m, 1H), 3.70 – 3.51 (m, 2H), 2.36 – 2.18 (m,

2H), 2.14 (tt, J = 7.1, 2.5 Hz, 2H), 1.82 – 1.74 (m, 1H), 1.54 – 1.43 (m, 2H), 1.40 – 1.26 (m, 4H),

*1.02 (d, J = 6.9 Hz, 3H), 0.99 (d, J = 6.9 Hz, 3H), 0.89 (t, J = 7.1 Hz, 3H). ^{13}C NMR (126 MHz,

CDCl$_3$) δ 82.65, *82.47, *78.10, 77.99, 75.64, *74.99, *65.05, 64.97, 35.49, *35.40, 31.23,

28.88, *28.87, *23.22, 22.64, 22.34, 18.85, *18.83, 16.17, *14.79, 14.16. HRMS (ESI, *m/z*):

calcd for $[C_{12}H_{22}O_2]^+$, $([M + Na]^+)$: 221.1518, found 221.1514.

4-((tetrahydro-2*H*-pyran-2-yl)oxy)but-2-yn-1-ol, 14

A 2 liter round bottom flask was charged with acetonenitrile, (500 mL), DCM (500 mL), 1,4-

butynediol (10g, 116 mmol, 1 eq.), and dihydropyran (10.7 g, 127.6 mmol, 1.1 eq.). *p*-

toluenesulfonic acid (304 mg, 1.16 mmol, 0.01 eq.) was added and the reaction mixture was

stirred at rt for 10 hrs, at which point saturated, aqueous sodium bicarbonate (500 mL) was added

to quench. The organic layers were collected and the aqueous layer was extracted with DCM

(3X, 300 mL). The organic layers were combined, dried over anhydrous sodium sulfate, filtered,

and solvent was removed to afford a green oil, which was purified by SiO_2 flash chromatography

(60% EtOAc in hexanes). Mono-tetrahydropyran protected alcohol **14** was isolated as a colorless

oil (14 g, 71%). ^{1}H NMR (500 MHz, CDCl$_3$) δ 4.81 (t, J = 3.4 Hz, 1H), 4.39 – 4.24 (m, 4H), 3.89 – 3.81 (m, 1H), 3.59 – 3.50 (m, 1H), 1.90 – 1.79 (m, 1H), 1.79 – 1.71 (m, 1H), 1.70 – 1.60 (m, 3H), 1.60 – 1.50 (m, 2H). ^{13}C NMR (126 MHz, CDCl$_3$) δ 96.96, 84.18, 81.88, 62.12, 54.26, 51.18, 30.24, 25.37, 19.12. HRMS (ESI, m/z): calcd for [C$_9$H$_{14}$O$_3$]+ ([M+H]+): 170.0943, found 170.0947.
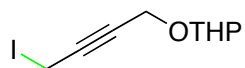
2-((4-iodobut-2-yn-1-yl)oxy)tetrahydro-2H-pyran, 15

THP-protected alcohol **14** (9.0 g, 52.9 mmol, 1 eq.), triphenylphosphine (27.8 g, 105.8 mmol, 2 eq.), and imidazole (7.2 g, 105.8 mmol, 2 eq.) were dissolved in DCM (300 mL) under argon and cooled to 0 °C. Iodine (26.9 g, 105.8 mmol, 2 eq.) was added slowly over twenty minutes, and the reaction mixture was stirred for 30 minutes. Solvent was removed and the resulting slurry was purified by SiO$_2$ chromatography (40% EtOAc in hexanes) to afford alkyl iodide **15** as a colorless oil (12.2 g, 82%). ^{1}H NMR (500 MHz, CDCl$_3$) δ 4.72 (t, J = 3.4 Hz, 1H), 4.20 (qt, J = 15.8, 2.2 Hz, 2H), 3.79 – 3.73 (m, 1H), 3.67 (t, J = 2.2 Hz, 2H), 3.50 – 3.45 (m, 1H), 1.81 – 1.71 (m, 1H), 1.71 – 1.64 (m, 1H), 1.59 – 1.52 (m, 2H), 1.52 – 1.43 (m, 2H). ^{13}C NMR (126 MHz, CDCl$_3$) δ 96.88, 82.68, 81.29, 61.98, 54.43, 30.19, 25.31, 19.00. HRMS (ESI, m/z): calcd for [C$_9$H$_{13}$IO$_2$]+ ([M+H]+): 279.9960, found 279.9962.
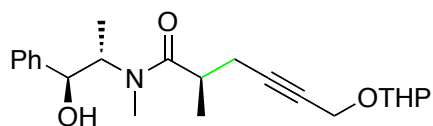

(2R)-N-((1S,2S)-1-hydroxy-1-phenylpropan-2-yl)-N,2-dimethyl-6-((tetrahydro-2H-pyran-2-yl)oxy)hex-4-ynamide, 16

A 1 L round bottom flask was flame dried and flushed with argon before tetraydrofuran (82 mL), anhydrous lithium chloride (15.4 g, 363 mmol, 7.8 eq.), and DIPA (17.54 mL, 124 mmol, 2.67

eq.) were added. The solution was cooled to -78 °C and *n*-butyllithium (2.5 M in hexanes, 46.1 mL, 115 mmol, 2.48 eq.) was added slowly to maintain temperature. The reaction mixture was briefly warmed to 0 °C and subsequently cooled back to -78 °C. *N*-((1*S*,2*S*)-1-hydroxy-1-phenylpropan-2-yl)-*N*-methylpropionamide (13.31 g, 60.4 mmol, 1.3 eq.) was then added in anhydrous THF (192 mL) *via* cannula. The reaction mixture was stirred at -78 °C for 1 hr, 0 °C for 20 min, rt for 5 min, and then cooled to 0 °C before 2-((4-iodobut-2-yn-1-yl)oxy)tetrahydro-2*H*-pyran (13.0 g, 46.5 mmol, 1 eq.) was added in one portion. Stirring was continued for 2 hr at 0 °C, at which point the reaction was quenched by the careful addition of half-saturated, aqueous ammonium chloride (100 mL). The organic layer was collected, and the aqueous layer was extracted with EtOAc (3 X, 150 mL). The combined organic layers were collected, dried over anhydrous sodium sulfate, and solvent was removed under reduced pressure to afford a yellow oil that was purified by SiO_2 flash chromatography (30 % – 50 % EtOAc in hexanes) to provide pure **16** as a colorless oil (17.6 g, 92%). $[\alpha]^{25}_D = 74.3°$ (c = 0.023, DCM). (Isolated as a mixture of amide rotamers with two THP diastereomers, *denotes minor rotamer peak) ^{1}H NMR (500 MHz, CDCl$_3$) δ 7.37 – 7.21 (m, 5H), *4.89 (t, *J* = 3.1 Hz, 1H), *4.79 (t, *J* = 3.4 Hz, 1H), 4.75 (t, *J* = 3.4 Hz, 1H), 4.69 – 4.56 (m, 1H), 4.55 (d, *J* = 8.5 Hz, 1H), *4.51 (d, *J* = 7.6 Hz, 1H), 4.49 – 4.34 (m, 1H), 4.31 – 3.93 (m, 1H), 3.88 – 3.70 (m, 1H), 3.55 – 3.41 (m, 1H), *3.27 (bs, 1H), *3.25 – 3.14 (m, 1H), *3.14 – 3.05 (m, 1H), *2.88 (s, 3H), 2.88 (m, 1H), 2.87 (s, 3H), *2.68 – 2.56 (m, 2H), 2.49 – 2.39 (m, 1H), 2.39 – 2.23 (m, 1H), 1.89 (bs, 1H), 1.85 – 1.73 (m, 1H), 1.73 – 1.64 (m, 1H), 1.63 – 1.40 (m, 4H), 1.14 (d, *J* = 6.8 Hz, 3H), 1.08 (d, *J* = 6.8 Hz, 3H), *0.99 (d, *J* = 6.8 Hz, 3H), *0.96 (d, *J* = 6.8 Hz, 3H). ^{13}C NMR (126 MHz, CDCl$_3$) δ 177.27, *176.30, 142.44, *141.26, *128.79, 128.47, 127.78, *127.05, *127.04, 126.47, 96.81, *96.73, *95.61, *86.22, *85.40, 84.54, 84.53, *77.07, 76.48, 76.46, *75.47, *75.21, 62.07, *61.94, *61.67,

*58.43, *58.21, *54.83, 54.65, 54.63, *54.46, 36.60, *36.22, *35.95, 30.35, 30.34, *30.11, *27.27, *27.14, *25.49, 25.43, *23.67, *23.56, 23.51, 19.17, *19.07, *18.80, *17.81, 17.06, *15.78, *15.62, 14.50. HRMS (ESI, *m/z*): calcd for $[C_{22}H_{31}NO_4]^+$, $([M + Na]^+)$: 396.2151, found 396.2149.
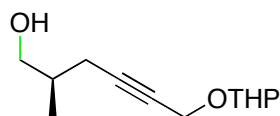
**(2R)-2-methyl-6-((tetrahydro-2H-pyran-2-yl)oxy)hex-4-yn-1-ol, 18**

A 1 L flask was flame dried and flushed with argon before anhydrous THF (180 mL) and DIPA (36.8 mL, 260.4 mmol, 4.2 eq.) were added. The solution was cooled to -78 °C followed by the careful addition of *n*-butyllithium (2.5 M in hexanes, 97 mL, 241.8 mmol, 3.9 eq.). The reaction mixture was allowed to warm to 0 °C and ammonia-borane complex (8.5 g, 248 mmol, 4 eq.) was slowly added. Vigorous stirring was continued, and the reaction mixture was allowed to warm to rt and then cooled back to 0 °C at which point **16** (23.2 g, 62 mmol, 1 eq.) was added in anhydrous THF (120 mL) *via* cannula. The reaction mixture was stirred for 3 hr at 0 °C or until the starting material was observed to be consumed by thin-layer chromatography. 3 N aqueous hydrochloric acid was then added dropwise until pH between 4.5 and 5 was attained. The organic layer was collected, and the aqueous layer was extracted with EtOAc (5 X, 80 mL) followed by sequential washing of the combined organic extracts with 2 N aqueous hydrochloric acid (2 X, 50 mL) 2 N aqueous sodium hydroxide (2 X, 50 mL), and saturated aqueous sodium chloride (2 X, 50 mL). The organic layer was then dried over anhydrous sodium sulfate and solvent was removed under reduced pressure to afford a colorless oil that was purified by SiO_2 flash chromatography (15 % – 40 % EtOAc in hexanes) to provide pure **18** (12.2 g, 93%). $[\alpha]^{25}_D$ = 4.2° (c = 0.150, DCM). (Mixture of THP diastereomers) ^1H NMR (500 MHz, CDCl$_3$) δ 4.78

(dd, J = 6.6, 3.2 Hz, 1H), 4.58 – 4.52 (m, 1H), 4.28 – 4.14 (m, 2H), 3.86 – 3.76 (m, 1H), 3.63 – 3.54 (m, 1H), 3.54 – 3.43 (m, 2H), 3.28 – 3.20 (m, 1H), 2.46 (s, 1H), 2.40 – 2.10 (m, 2H), 1.98 – 1.88 (m, 1H), 1.87 – 1.73 (m, 2H), 1.74 – 1.62 (m, 1H), 1.62 – 1.43 (m, 4H), 0.97 (d, J = 6.8 Hz, 3H), 0.95 (d, J = 6.8 Hz, 3H). ^{13}C NMR (126 MHz, CDCl$_3$) δ 96.79, 84.75, 77.29, 67.06, 62.13, 54.70, 35.18, 30.38, 25.46, 22.79, 19.20, 16.37. HRMS (ESI, m/z): calcd for [C$_{12}$H$_{20}$O$_3$]$^+$, ([M + Na]$^+$): 235.1310, found 235.1313.
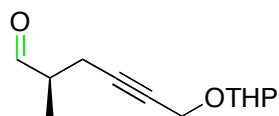
(2R)-2-methyl-6-((tetrahydro-2H-pyran-2-yl)oxy)hex-4-ynal, 17

A 500 mL flask was flame dried and flushed with argon before DCM (200 mL) and alcohol **18** (10 g, 47 mmol, 1 eq.) were added. The solution was cooled to 0 °C and pyridinium chlorochromate (25.3 g, 118 mmol, 2.5 eq.) was slowly added over 20 minutes. Stirring was continued and the reaction mixture was allowed to warm to rt overnight at which point a 1:1 mixture of hexanes and diethyl ether (250 mL) was added. The suspension was passed through a plug of SiO$_2$ with a 1:1 mixture of hexanes and diethyl ether (500 mL) as eluent. The organic filtrate was collected and solvent was removed under reduced pressure to provide pure aldehyde **17** as a colorless oil (8.2 g, 83%). [α]^{25}$_D$ = 3.1° (c = 0.012, DCM). ^{1}H NMR (500 MHz, CDCl$_3$) δ 4.81 (t, J = 3.4 Hz, 1H), 4.28 (dt, J = 15.4, 2.1 Hz, 1H), 4.21 (dt, J = 15.4, 1.8 Hz, 1H), 3.84 (ddd, J = 11.5, 9.5, 5.0 Hz, 1H), 3.58 – 3.47 (m, 1H), 2.73 – 2.64 (m, 1H), 2.64 – 2.57 (m, 1H), 2.46 – 2.38 (m, 1H), 1.87 – 1.77 (m, 1H), 1.77 – 1.69 (m, 1H), 1.65 – 1.48 (m, 4H), 1.29 (d, J = 7.0 Hz, 3H). ^{13}C NMR (126 MHz, CDCl$_3$) δ 180.53, 96.77, 83.39, 77.83, 62.16, 54.59, 30.38, 25.48, 22.91, 19.21, 16.41, 16.40. HRMS (ESI, m/z): calcd for [C$_{12}$H$_{18}$O$_3$]$^+$, ([M + H]$^+$): 211.1334, found 211.1333.
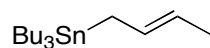
(*E*)-but-2-en-1-yltributylstannane

THF (50 mL) and saturated aqueous ammonium chloride (50 mL) were added to a 250 mL flask followed by tributyltin chloride (1.0 g, 3.1 mmol, 1 eq.) and *trans*-crotyl bromide (0.42 g, 3.1 mmol, 1 eq.). The solution was vigorously stirred at rt and zinc dust (2.0 g, 31 mmol, 10 eq.) was added in 0.2 g portions very slowly over 30 min (zinc must be added cautiously as the reaction is highly exothermic). The biphasic reaction mixture was then vigorously stirred for 2 h at which point deionized water (50 mL) was added. The organic layer was removed and the aqueous layer was extracted with EtOAc (3 X, 20 mL). The combined organic layers were dried over anhydrous sodium sulfate and solvent was removed under reduced pressure to afford a colorless oil that was purified by SiO$_2$ flash chromatography (Hex) to provide pure tributyl(crotyl)stannane as a colorless liquid (1.0 g, 96%). Characterization matched literature data. ^{1}H NMR (400 MHz, CDCl$_3$) δ 5.64 – 5.46 (m, 1H), 5.17 (m, 1H), 1.72 (d, *J* = 9.1 Hz, 3H), 1.76 – 1.37 (m, 12H), 1.58 (d, *J* = 6.8 Hz, 2H), 1.37 – 1.20 (m, 1H), 0.89 (t, *J* = 7.2 Hz, 9H), 0.95 – 0.76 (m, 6H).
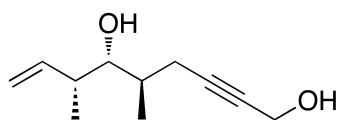

(5R,6R,7R)-5,7-dimethylnon-8-en-2-yne-1,6-diol, 24

A 5 mL flask was flame dried and flushed with argon before anhydrous propionitrile (0.5 mL) and chiral acyloxy borane catalyst (79 mg, 0.25 mmol, 0.5 eq.) were added. The solution was cooled to 0 °C followed by dropwise addition of borane THF complex (1 M solution in THF, 0.375 mL, 0.375 mmol, 0.75 mmol). Stirring was continued for 1 h at 0 °C at which point the solution was further cooled to -78 °C followed by sequential addition of aldehyde **17** (105 mg,

0.5 mmol, 1 eq.) in anhydrous propionitrile (0.5 mL), trifluoacetic anhydride (0.140 mL, 1 mmol, 2 eq.), and crotyl tributyltin (173 mg, 0.5 mmol, 1 eq.) in anhydrous propionitrile (0.5 mL) and the resultant reaction mixture was stirred for 10 h at -78 °C. Reaction was quenched at -78 °C by the addition of saturated aqueous sodium bicarbonate (1 mL). The organic layer was collected and the aqueous layer was extracted with diethyl ether (4 X, 1 mL). The combined organic layers were dried over anhydrous sodium sulfate and solvent was removed under reduced pressure to afford a yellow amorphous solid that was dissolved in minimal methanol and saturated with potassium carbonate. The heterogenous mixture was vigorously stirred for 2 h and subsequently diluted with deionized water (10 mL) and diethyl ether (4 mL). The organic layer was collected and the aqueous layer was extracted with diethyl ether (4 X, 4 mL). The combined organic layers were dried over anhydrous sodium sulfate and solvent was removed under reduced pressure to afford a colorless oil that was diluted with saturated aqueous potassium fluoride (5 mL) and diethyl ether and stirred for 5 h. The organic layer was collected and the aqueous layer was extracted with diethyl ether (4 X, 5 mL). The combined organic layers were dried over anhydrous sodium sulfate and solvent was removed under reduced pressure to afford a colorless oil that was purified by SiO_2 flash chromatography (20 % – 30 % EtOAc in hexanes) to provide THP deprotected alcohol **24** as a colorless oil (50 mg, 54 %). $[\alpha]^{25}_D = 3.1°$ (c = 0.012, DCM). (isolated as a ~3.5:1 inseparable mixture of α,β diastereomers at C-6 and C-7, *denotes minor diastereomer peak) ^{1}H NMR (500 MHz, CDCl$_3$) δ 5.90 – 5.81 (m, 1H), *5.68 (m, 1H), 5.16 – 5.08 (m, 2H), *5.07 – 5.00 (m, 2H), 4.26 (bs, 2H), *3.45 (dd, J = 8.0, 3.5 Hz, 1H), 3.36 (dd, J = 7.8, 4.2 Hz, 1H), 2.49 – 2.19 (m, 3H), *1.93 – 1.84 (m, 1H), 1.85 – 1.77 (m, 1H), *1.08 (d, J = 6.7 Hz, 3H), 1.03 (d, J = 6.9 Hz, 3H), 1.00 (d, J = 6.8 Hz, 3H), *0.96 (d, J = 6.8 Hz, 3H). ^{13}C NMR (126 MHz, CDCl$_3$) δ 141.79, *141.05, 115.41, *115.12, *85.14, 85.11, 79.97, *79.91,

77.10, *77.06, 51.55, *51.50, *41.94, 39.78, 35.11, *34.92, *24.09, 22.12, *16.36, 16.28, *12.87, 11.97. HRMS (ESI, *m/z*): calcd for $[C_{11}H_{18}O_2]^+$, $([M + K]^+)$: 221.0944, found 221.0940.
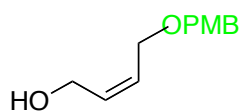
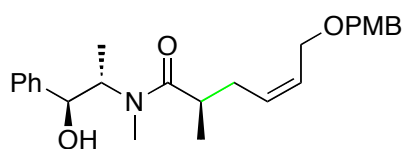## (Z)-4-((4-methoxybenzyl)oxy)but-2-en-1-ol, 28

A 1 L round bottom flask was flame dried and flushed with argon before THF (500 mL) and sodium hydride (3.2 g, 80 mmol, 0.5 eq.) were added. The solution was cooled to 0 °C and 1,4-butenediol (7.1 g, 80 mmol, 0.5 eq.) was added. The reaction mixtured was stirred at 0 °C for 1 hr, at which point *p*-methoxybenzyl chloride (25 g, 160 mmol, 1 eq.) and sodium iodide (5.9 g, 16 mmol, .1 eq.) were added. The reaction mixture was warmed to rt and stirred for 5 hr, and then quenched by the careful addition of saturated aqueous ammonium chloride. The organic layer was collected, and the aqueous layer was extracted with EtOAc (3 X 200 mL). The combined organic layers were dried over anhydrous sodium sulfate and solvent was removed to afford a yellow oil that was purified by SiO$_2$ chromatography (30% – 50% EtOAc in hexanes). Mono PMB-protected alcohol **28** was obtained as a colorless oil (14.5 g, 87%). ^{1}H NMR (500 MHz, CDCl$_3$) δ 7.26 (d, *J* = 8.7 Hz, 2H), 6.88 (d, *J* = 8.7 Hz, 2H), 5.81 – 5.75 (m, 1H), 5.73 – 5.67 (m, 1H), 4.44 (s, 2H), 4.12 (s, 1H), 4.05 (d, *J* = 6.3 Hz, 2H), 3.79 (s, 3H). ^{13}C NMR (126 MHz, CDCl$_3$) δ 159.29, 132.45, 129.91, 129.54, 128.04, 113.84, 72.10, 65.31, 58.49, 55.27. HRMS (ESI, *m/z*): calcd for $[C_{12}H_{16}O_3]^+$, $([M + Na]^+)$: 231.0997, found 231.0999.
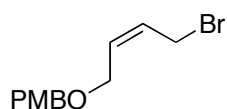
(Z)-1-(((4-bromobut-2-en-1-yl)oxy)methyl)-4-methoxybenzene, 29

A 500 mL flask was flame dried and flushed with argon before pyridine (150 mL), alcohol **28** (10 g, 48.0 mmol, 1 eq.), and tetrabromomethane (19.1 g, 57.6 mmol, 1.2 eq.) were added. The

solution was cooled to 0 °C and triphenylphospine (13.5 g, 52.8 mmol, 1.1 eq.) was added 1 g at a time over 1 h. The reaction mixture was allowed to warm to rt and stiring was continued for 1 h when toluene (100 mL) was added. Solvent was removed under reduced pressure to afford an orange amorphous solid that was purified by SiO$_2$ chromatography (2.5 % – 10 % EtOAc in hexanes) to provide pure allylic bromide **29** as a colorless oil (12 g, 92%). ^{1}H NMR (500 MHz, CDCl$_3$) δ 7.19 (d, J = 8.6 Hz, 1H), 6.80 (d, J = 8.6 Hz, 1H), 5.86 – 5.74 (m, 1H), 5.73 – 5.61 (m, 1H), 4.37 (s, 1H), 4.03 (dd, J = 6.4, 1.4 Hz, 1H), 3.89 (d, J = 8.4 Hz, 1H), 3.71 (s, 2H). ^{13}C NMR (126 MHz, CDCl$_3$) δ 159.31, 131.27, 129.48, 128.34, 113.86, 72.15, 64.61, 55.29, 26.63. HRMS (ESI, m/z): calcd for [C$_{12}$H$_{15}$BrO$_2$]$^+$, ([M + H]$^+$): 271.0334, found 271.0333.

(R,Z)-N-((1S,2S)-1-hydroxy-1-phenylpropan-2-yl)-6-((4-methoxybenzyl)oxy)-N,2-dimethylhex-4-enamide, 30

A 1 L round bottom flask was flame dried and flushed with argon before tetraydrofuran (82 mL), anhydrous lithium chloride (15.4 g, 363 mmol, 7.8 eq.), and DIPA (17.54 mL, 124 mmol, 2.67 eq.) were added. The solution was cooled to -78 °C and *n*-butyllithium (2.5 M in hexanes, 46.1 mL, 115 mmol, 2.48 eq.) was added slowly to maintain temperature. The reaction mixture was briefly warmed to 0 °C and subsequently cooled back to -78 °C. *N*-((1*S*,2*S*)-1-hydroxy-1-phenylpropan-2-yl)-*N*-methylpropionamide (13.31 g, 60.4 mmol, 1.3 eq.) was then added in anhydrous THF (192 mL) *via* cannula. The reaction mixture was stirred at -78 °C for 1 hr, 0 °C for 20 min, rt for 5 min, and then cooled to 0 °C before (*Z*)-1-(((4-bromobut-2-en-1-yl)oxy)methyl)-4-methoxybenzene (12.6 g, 46.5 mmol, 1 eq.) was added in one portion. Stirring was continued for 2 hr at 0 °C, at which point the reaction was quenched by the careful addition

of half-saturated, aqueous ammonium chloride (100 mL). The organic layer was collected, and

the aqueous layer was extracted with EtOAc (3 X, 150 mL). The combined organic layers were

collected, dried over anhydrous sodium sulfate, and solvent was removed under reduced pressure

to afford a yellow oil that was purified by SiO_2 flash chromatography (30 % – 50 % EtOAc in

hexanes) to provide pure **30** as a colorless oil (17.6 g, 92%). $[\alpha]^{25}_D$ = 71.3° (c = 0.093, DCM).

(*Denotes minor rotamer peak) ^{1}H NMR (500 MHz, CDCl$_3$) δ 7.39 – 7.29 (m, 5H), 7.29 – 7.23

(m, 2H), 6.93 – 6.79 (m, 2H), 5.72 – 5.55 (m, 1H), 5.50 – 5.40 (m, 1H), 4.67 – 4.51 (m, 1H),

4.44 (s, 2H), *4.44 (s, 2H), 4.44 (m, 2H), 4.15 – 3.97 (m, 4H), 3.80 (s, 3H), *3.79 (s, 3H), 2.83

(s, 3H), 2.87 – 2.76 (m, 1H), *2.81 (s, 3H), 2.68 – 2.59 (m, 1H), 2.51 (m, 1H), 2.38 – 2.26 (m,

1H), *2.17 – 2.06 (m, 1H), 1.15 – 1.11 (m, 3H), 1.09 (d, J = 6.8 Hz, 3H), *1.00 (d, J = 6.8 Hz,

3H). ^{13}C NMR (126 MHz, CDCl$_3$) δ 178.38, *176.45, 159.33, 142.66, *141.16, *130.52, 130.45,

129.57, *128.54, 128.49, *127.81, 127.75, *127.07, 127.05, *126.51, 126.44, 113.92, 77.37,

76.61, 72.20, *72.14, *65.81, 65.71, 55.43, 36.98, 32.04, 27.76, 17.22, *14.66, 14.60. HRMS

(ESI, *m/z*): calcd for $[C_{25}H_{33}NO_4]^+$, $([M + Na]^+)$: 434.2307, found 434.2306.
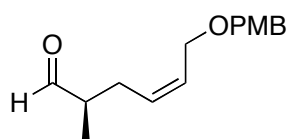
(*R*,*Z*)-6-((4-methoxybenzyl)oxy)-2-methylhex-4-enal, 31

A 1 L flask was flame dried and flushed with argon before anhydrous hexanes (170 mL) and

solid lithium aluminum hydride (95%, 2.95 g, 73.9 mmol, 2.30 equiv) were added. The

suspension was cooled to 0 °C and EtOAc (10.7 mL, 110 mmol, 3.41 equiv) was added by

addition funnel over a period of 1.5 h followed by cooling to -78 °C. A solution of amide **30**

(10.0 g, 32.1 mmol, 1 equiv) in anhydrous THF (110 mL) was added via cannula over 5 min, and

the reaction mixture was warmed to 0 °C. After being stirred for 1 h at 0 °C, the reaction mixture

was transferred by cannula to a solution of trifluoroacetic acid (5 mL, 65 mmol, 2 equiv) in 0.5 N aqueous hydrochloric acid solution (400 mL) at 0 °C. The resulting biphasic mixture was stirred at 0 °C for 20 min and then diluted with 0.1 N aqueous hydrochloric acid solution (700 mL) when the layers were separated. The aqueous layer was extracted with EtOAc (3 X, 150 mL). The combined organic layers were neutralized by the cautious addition of saturated aqueous sodium bicarbonate (250 mL). The aqueous layer (pH 7-8) was separated and extracted with EtOAc (100 mL). The combined organic extracts were dried over anhydrous sodium sulfate and solvent was removed under reduced pressure to afford a yellow oil that was purified by SiO_2 flash chromatography (5 % – 10 % EtOAc in hexanes) to afford aldehyde **31** as a colorless oil (6.7 g, 84 %). $[\alpha]^{25}_D$ = -4.6° (c = 0.021, DCM). ^{1}H NMR (500 MHz, CDCl$_3$) δ 9.54 (s, 1H), 7.20 – 7.15 (m, 2H), 6.82 – 6.74 (m, 2H), 5.66 – 5.57 (m, 1H), 5.51 – 5.42 (m, 1H), 4.36 (s, 2H), 3.96 (dd, J = 6.5, 1.4 Hz, 2H), 3.70 (s, 3H), 2.46 – 2.26 (m, 2H), 2.17 – 1.98 (m, 1H), 1.00 (d, J = 7.1 Hz, 3H). ^{13}C NMR (126 MHz, CDCl$_3$) δ 204.37, 159.24, 130.24, 129.47, 129.45, 128.72, 113.80, 71.97, 65.29, 55.26, 46.23, 28.43, 13.07. HRMS (ESI, *m/z*): calcd for $[C_{15}H_{20}O_3]^+$, $([M + Na]^+)$: 271.1310, found 271.1310.
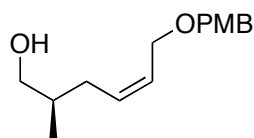
(R,Z)-6-((4-methoxybenzyl)oxy)-2-methylhex-4-en-1-ol, 30a

A 1 L flask was flame dried and flushed with argon before anhydrous THF (180 mL) and DIPA (36.8 mL, 260.4 mmol, 4.2 eq.) were added. The solution was cooled to -78 °C followed by the careful addition of *n*-butyllithium (2.5 M in hexanes, 97 mL, 241.8 mmol, 3.9 eq.). The reaction mixture was allowed to warm to 0 °C and ammonia-borane complex (8.5 g, 248 mmol, 4 eq.) was slowly added. Vigorous stirring was continued, and the reaction mixture was allowed to

warm to rt and then cooled back to 0 °C at which point **30** was added in anhydrous THF (120 mL) *via* cannula. The reaction mixture was stirred for 3 hr at 0 °C or until the starting material was observed to be consumed by thin-layer chromatography. 3 N aqueous hydrochloric acid was then added dropwise until pH between 3.5 and 4 was attained. The organic layer was collected, and the aqueous layer was extracted with EtOAc (5 X, 80 mL) followed by sequential washing of the combined organic extracts with 2 N aqueous hydrochloric acid (2 X, 50 mL) 2 N aqueous sodium hydroxide (2 X, 50 mL), and saturated aqueous sodium chloride (2 X, 50 mL). The organic layer was then dried over anhydrous sodium sulfate and solvent was removed under reduced pressure to afford a colorless oil that was purified by SiO_2 flash chromatography (15 % – 40 % EtOAc in hexanes) to provide pure **30a** (14.4 g, 93%). $[\alpha]^{25}_D$ = -11.4° (c = 0.043, DCM). ^{1}H NMR (500 MHz, CDCl$_3$) δ 7.30 – 7.25 (m, 2H), 6.91 – 6.85 (m, 2H), 5.73 – 5.61 (m, 2H), 4.46 (s, 2H), 4.07 – 3.94 (m, 2H), 3.81 (s, 3H), 3.45 (ddd, *J* = 25.4, 10.9, 5.8 Hz, 2H), 2.17 (dt, *J* = 13.7, 6.8 Hz, 1H), 2.04 – 1.97 (m, 1H), 1.79 – 1.68 (m, 1H), 0.93 (d, *J* = 6.8 Hz, 3H). ^{13}C NMR (126 MHz, CDCl$_3$) δ 159.40, 132.73, 130.27, 129.71, 127.10, 113.94, 72.26, 67.10, 65.23, 55.42, 35.92, 31.14, 16.71. HRMS (ESI, *m/z*): calcd for $[C_{15}H_{22}O_3]^+$, $([M + Na]^+)$: 273.1467, found 273.1466.
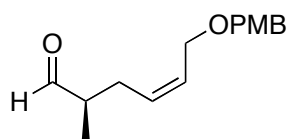
(*R,Z*)-6-((4-methoxybenzyl)oxy)-2-methylhex-4-enal, 31

A flame dried 500 mL flask was flame dried and flushed with argon before DCM (200 mL), 2.5 Å activated molecular sieves (500 mg), alcohol **30a** (10 g, 40.0 mmol, 1 eq.), and *N*-Methylmorpholine-*N*-oxide (5.2 g, 44.0 mmol, 1.1 eq.) were added. The solution was cooled to 0 °C, tetrapropylammonium perruthenate (703 mg, 2 mmol, 0.05 eq.) was add, and stirring was

continued for 1 h and the reaction mixture was allowed to warm to rt. DCM (200 mL) was added

to the reaction mixture followed by sequential washing with saturated aqueous sodium sulphite

(100 mL), saturate aqueous sodium chloride (100 mL), and saturated aqueous copper(II) sulphate

(100 mL). The organic layer was collected and dried over sodium sulphate. Solvent was removed

under reduced pressure to afford a colorless oil that was eluted through a SiO_2 plug with 40 %

EtOAc in hexanes. Solvent was removed under reduced pressure to provide pure aldehyde **31** as

a colorless oil (84 %, 8.3 g). $[\alpha]^{25}_D$ = -4.6° (c = 0.021, DCM). ^{1}H NMR (500 MHz, CDCl$_3$) δ

9.54 (s, 1H), 7.20 – 7.15 (m, 2H), 6.82 – 6.74 (m, 2H), 5.66 – 5.57 (m, 1H), 5.51 – 5.42 (m, 1H),

4.36 (s, 2H), 3.96 (dd, J = 6.5, 1.4 Hz, 2H), 3.70 (s, 3H), 2.46 – 2.26 (m, 2H), 2.17 – 1.98 (m,

1H), 1.00 (d, J = 7.1 Hz, 3H). ^{13}C NMR (126 MHz, CDCl$_3$) δ 204.37, 159.24, 130.24, 129.47,

129.45, 128.72, 113.80, 71.97, 65.29, 55.26, 46.23, 28.43, 13.07. HRMS (ESI, m/z): calcd for

$[C_{15}H_{20}O_3]^+$, $([M + Na]^+)$: 271.1310, found 271.1305.
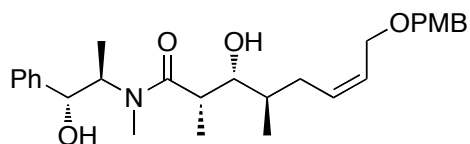
(2S,3R,4R,Z)-3-hydroxy-N-((1R,2R)-1-hydroxy-1-phenylpropan-2-yl)-8-((4-

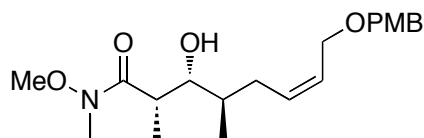**methoxybenzyl)oxy)-N,2,4-trimethyloct-6-enamide, 32**

A 500 mL flask was flame dried and flushed with argon before anhydrous THF (45 mL) and

DIPA (4.78 mL, 33.8 mmol, 2.1 eq.) were added. The solution was cooled to -78 °C and *n*-

butyllithium (2.5 M in hexanes, 13.2 mL, 33 mmol, 2.05 eq.) was slowly added. Stirring was

continued as the solution was allowed to warm to 0 °C and then cooled back to -78 °C at which

point a solution of (*R,R*)-pseudoephedrine propionamide (3.56 g, 16.1 mmol, 1 eq.) in anhydrous

THF (45 mL) was added slowly *via* cannula. Stirring was continued at -78 °C for 2 hr, 0 °C for

30 min, and rt for 10 min. The reaction mixture was cooled back to -78 °C followed by the

addition of a solution of Bis(cyclopentadienyl)zirconium(IV) dichloride (10.34 g, 35.4 mmol, 2.2 eq.) in anhydrous THF (100mmL). The deep orange solution was stirred at -78 °C for 3 hr and then cooled to -116 °C when a solution of aldehyde **31** (4 g, 16.1 mmol, 1 eq.) in anhydrous THF (10 mL) was added dropwise. Stirring was continued at -116 °C for 3 hr at which point the reaction was quenched by the addition of saturated aqueous ammonium chloride (50 mL). The biphasic reaction mixture was warmed to rt and filtered through a pad of celite using EtOAc (300 mL) to rinse. The organic layer was collected, and the aqueous layer was extracted with EtOAc (3 X, 100 mL). The combined organic layers were dried over anhydrous sodium sulfate and solvent was removed under reduced pressure to afford an orange oil that was purified by SiO_2 flash chromatography (40 % – 70%) to provide pure **32** as a colorless oil (6.7 g, 88 %). $[\alpha]^{25}_D = -45.6°$ (c = 0.123, DCM). (*Denotes minor rotamer peak) ^1H NMR (500 MHz, CDCl$_3$) δ 7.39 – 7.31 (m, 5H), *7.30 – 7.28 (m, 5H), 7.28 – 7.24 (m, 2H), 6.89 – 6.84 (m, 2H), 5.71 – 5.54 (m, 2H), 5.07 (d, J = 0.7 Hz, 1H), 4.63 (bs, 1H), 4.68 – 4.56 (m, 1H), *4.54 (d, J = 8.2 Hz, 1H), *4.50 (d, J = 1.4 Hz, 1H), 4.43 (s, 2H), *4.42 (s, 2H), 4.07 (d, J = 6.4 Hz, 2H), *4.04 – 3.97 (m, 1H), 3.79 (s, 3H), *3.77 (s, 3H), 3.45 (dd, J = 16.7, 7.7 Hz, 1H), *3.07 – 2.99 (m, 1H), 2.91 (s, 3H), *2.87 (s, 3H), 2.76 – 2.69 (m, 1H), 2.50 – 2.38 (m, 1H), 2.01 (m, 1H), 1.70 – 1.58 (m, 1H), *1.09 (d, J = 6.5 Hz, 3H), 1.07 (d, J = 7.1 Hz, 3H), 1.06 (d, J = 7.3 Hz, 3H), *1.00 (d, J = 7.0 Hz, 3H), 0.78 (d, J = 5.6 Hz, 3H), *0.77 (d, J = 5.7 Hz, 3H). ^{13}C NMR (126 MHz, CDCl$_3$) δ 179.68, *179.61, 159.22, *159.17, 142.13, *141.45, 131.87, 131.59, *130.71, *130.64, *129.56, 129.55, 128.99, *128.62, 128.57, *127.99, 127.92, *127.74, 126.74, 126.46, 113.85, 76.28, *75.57, 74.65, 71.96, 71.89, 65.84, *58.02, 55.38, 36.77, *35.56, 35.39, 35.37, *30.97, 30.75, *27.31, *15.75, 15.42, *15.23, 14.30, *9.80, 9.26. HRMS (ESI, *m/z*): calcd for $[C_{28}H_{39}NO_5]^+$, ($[M + K]^+$): 508.2465, found 508.2466.
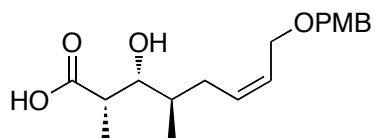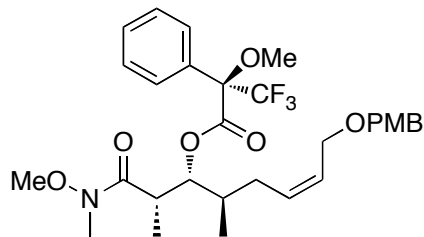
(2S,3R,4R,Z)-3-hydroxy-8-((4-methoxybenzyl)oxy)-2,4-dimethyloct-6-enoic acid, 33

A 500 mL flask was charged with amide **32** (8.4 g, 18 mmol, 1 eq.), *t*-Butylalcohol (55 mL), and deionized water (180 mL). A 1.5 M aqueous solution of tetrabutylammonium hydroxide (60 mL, 90 mmol, 5 eq.) was added and the reaction mixture was heated at reflux for 20 hr. After cooling to rt, the reaction mixture was partitioned between 0.5 N aqueous sodium hydroxide (2.3 L) and diethyl ether (320 mL). The organic layer was removed, and the aqueous layer was extracted with diethyl ether (3 X, 320 mL). The aqueous layer was collected, cooled to 0 °C, acidified to pH 3, saturated with sodium chloride, and then extracted with dietyl ether (6 X, 300 mL). The organic extracts were collected, dried over anhydrous sodium sulfate, and solvent was removed under reduced pressure to afford pure acid **33** (5.5 g, 95 %). $[\alpha]^{25}_D$ = -3.7° (c = 0.172, DCM). ^{1}H NMR (500 MHz, CDCl$_3$) δ 10.09 (s, 1H), 7.30 – 7.22 (m, 2H), 6.92 – 6.82 (m, 2H), 5.81 – 5.67 (m, 2H), 4.46 (s, 2H), 4.10 (dd, *J* = 11.0, 6.3 Hz, 1H), 3.95 (dd, *J* = 11.1, 6.0 Hz, 1H), 3.81 (s, 3H), 3.68 (dd, *J* = 9.5, 2.6 Hz, 1H), 2.67 (qd, *J* = 7.2, 2.7 Hz, 1H), 2.39 – 2.30 (m, 1H), 2.21 (dt, *J* = 9.1, 4.3 Hz, 1H), 1.83 – 1.72 (m, 1H), 1.19 (d, *J* = 7.2 Hz, 3H), 0.88 (d, *J* = 6.9 Hz, 3H). ^{13}C NMR (126 MHz, CDCl$_3$) δ 178.59, 159.57, 132.65, 129.87, 127.07, 114.04, 77.37, 73.84, 72.56, 65.10, 55.45, 41.26, 35.39, 31.00, 15.86, 9.62. HRMS (ESI, *m/z*): calcd for [C$_{18}$H$_{26}$O$_5$]$^-$, ([2M + Na – 2H]$^+$): 665.3302, found 665.3301.
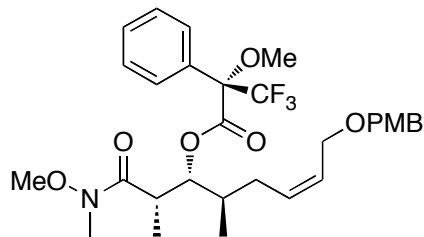
(2*S*,3*R*,4*R*,*Z*)-3-hydroxy-*N*-methoxy-8-((4-methoxybenzyl)oxy)-*N*,2,4-trimethyloct-6-enamide, 34

A 250 mL flask was flame dried and flushed with argon before DMF (40 mL), acid **33** (5.50 g, 17.1 mmol, 1 eq.), and DIPEA (6.3 mL, 36 mmol, 2.1 eq.) were added. COMU (8.14 g, 1.9 mmol, 1.1 eq.) was then added in one portion and the reaction mixture was stirred at rt for 45 min at which point *N*,*O*-Dimethylhydroxylamine hydrochloride (3.35 g, 34.2 mmol, 2 eq.) was added. Stirring was continued for 1 hr and the reaction was quenched by the careful addition of saturated aqueous sodium bicarbonate (30 mL). The resulting slurry was then extracted with EtOAc (5 X, 50 mL) and the combined organic portions were dried over anhydrous sodium sulfate. Solvent was removed under reduced pressure to afford a red oil that was purified by SiO_2 flash chromatography (25 % – 45% EtOAc in hexanes) to provide pure amide **34** as a yellow oil (5.8 g, 93 %). $[\alpha]^{25}_D$ = -2.1° (c = 0.010, DCM). ^{1}H NMR (500 MHz, CDCl$_3$) δ 7.29 – 7.21 (m, 2H), 6.88 – 6.83 (m, 2H), 5.71 – 5.55 (m, 2H), 4.43 (s, 2H), 4.11 (bs, 1H), 4.07 (d, *J* = 6.0 Hz, 2H), 3.78 (s, 3H), 3.68 (s, 3H), 3.50 (dd, *J* = 9.2, 1.9 Hz, 1H), 3.18 (s, 3H), 3.10 – 3.03 (m, 1H), 2.48 – 2.39 (m, 1H), 2.05 (dt, *J* = 14.0, 8.5 Hz, 1H), 1.67 (tqd, *J* = 13.6, 6.9, 3.5 Hz, 1H), 1.13 (d, *J* = 7.1 Hz, 3H), 0.81 (d, *J* = 6.8 Hz, 3H). ^{13}C NMR (126 MHz, CDCl$_3$) δ 178.66, 159.20, 131.50, 130.64, 129.50, 127.94, 113.82, 77.36, 74.82, 71.93, 65.82, 61.62, 55.34, 35.50, 32.00, 30.69, 15.32, 9.57. HRMS (ESI, *m/z*): calcd for $[C_{20}H_{31}NO_5]^+$, $([M + K]^+)$: 404.1839, found 404.1839.
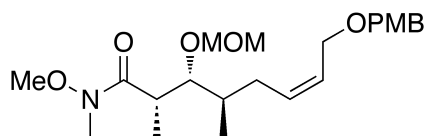
(*R*)-(2*S*,3*R*,4*R*,*Z*)-1-(methoxy(methyl)amino)-8-((4-methoxybenzyl)oxy)-2,4-dimethyl-1-oxooct-6-en-3-yl 3,3,3-trifluoro-2-methoxy-2-phenylpropanoate, 34a

A 5 mL flas was flame dried and flushed with argon before anhydrous DCM (0.5 mL) and (*R*)-3,3,3-trifluoro-2-methoxy-2-phenylpropanoic acid (12 mg, 0.051 mmol, 2 eq,) were added. The solution was cooled to 0 °C and oxalyl chloride (5 μL, 0.054 mmol, 2.1 eq.) and DMF (2 drops) were added. The reaction mixture was allowed to warm to rt and stirring was continued for 2 h at which point DIPEA (20 μL, 0.11 mmol, 4.3 eq.), amide **34** (10 mg, 0.026 mmol, 1 eq.), and DMAP (6.5 mg, 0.051 mmol, 2 eq.) were added. The reaction mixture was stirred for 1 h at which point solvent was removed to afford a yellowish-brown oil that was purified by SiO$_2$ flash chromatography (5 % – 10 % EtOAc in hexanes) to afford pure R-Mosher's ester **34a** as a colorless oil (13 mg, 86 %). ^{1}H NMR (500 MHz, Acetone) δ 7.66 – 7.58 (m, 2H), 7.50 – 7.41 (m, 3H), 7.30 – 7.23 (m, 2H), 6.96 – 6.88 (m, 2H), 5.59 – 5.48 (m, 1H), 5.45 – 5.33 (m, 1H), 5.36 (dd, *J* = 6.9, 5.0 Hz, 1H), 4.37 (s, 2H), 3.87 (d, *J* = 5.6 Hz, 2H), 3.79 (s, 3H), 3.78 (s, 3H), 3.65 (s, 3H), 3.42 – 3.31 (m, 1H), 3.15 (s, 3H), 1.96 – 1.89 (m, 1H), 1.82 (m, 1H), 1.65 (m, 1H), 1.12 (d, *J* = 6.9 Hz, 3H), 0.86 (d, *J* = 6.8 Hz, 3H). ^{13}C NMR (126 MHz, Acetone) δ 175.24, 166.82, 160.14, 133.18, 131.71, 130.73, 130.55, 129.99, 129.44, 129.15, 128.39, 114.41, 80.89, 72.25, 66.14, 61.94, 56.34, 55.48, 37.44, 36.16, 30.24, 29.94, 15.97, 11.90. HRMS (ESI, *m/z*): calcd for [C$_{30}$H$_{38}$F$_3$NO$_7$]$^+$, ([M + H]$^+$): 582.2679, found 582.2678.

(*S*)-(2*S*,3*R*,4*R*,*Z*)-1-(methoxy(methyl)amino)-8-((4-methoxybenzyl)oxy)-2,4-dimethyl-1-oxooct-6-en-3-yl 3,3,3-trifluoro-2-methoxy-2-phenylpropanoate, 34b

A 5 mL flas was flame dried and flushed with argon before anhydrous DCM (0.5 mL) and (*S*)-3,3,3-trifluoro-2-methoxy-2-phenylpropanoic acid (12 mg, 0.051 mmol, 2 eq,) were added. The solution was cooled to 0 °C and oxalyl chloride (5 µL, 0.054 mmol, 2.1 eq.) and DMF (2 drops) were added. The reaction mixture was allowed to warm to rt and stirring was continued for 2 h at which point DIPEA (20 µL, 0.11 mmol, 4.3 eq.), amide **34** (10 mg, 0.026 mmol, 1 eq.), and DMAP (6.5 mg, 0.051 mmol, 2 eq.) were added. The reaction mixture was stirred for 1 h at which point solvent was removed to afford a yellowish-brown oil that was purified by SiO_2 flash chromatography (5 % – 10 % EtOAc in hexanes) to afford pure R-Mosher's ester **34b** as a colorless oil (13 mg, 86 %). ^{1}H NMR (500 MHz, Acetone) δ 7.66 – 7.58 (m, 2H), 7.50 – 7.41 (m, 3H), 7.25 (dd, *J* = 5.1, 3.6 Hz, 2H), 6.91 – 6.88 (m, 2H), 5.68 – 5.63 (m, 1H), 5.55 – 5.51 (m, 1H), 5.36 (dd, *J* = 6.9, 5.0 Hz, 1H), 4.41 (s, 2H), 4.02 (d, *J* = 6.3 Hz, 2H), 3.78 (s, 3H), 3.76 (s, 3H), 3.53 (s, 3H), 3.37 – 3.31 (m, 1H), 3.15 (s, 3H), 2.30 – 2.27 (m, 1H), 1.93 – 1.90 (m, 2H), 0.98 (d, *J* = 6.9 Hz, 3H), 0.95 (d, *J* = 6.5 Hz, 3H). ^{13}C NMR (126 MHz, Acetone) δ 175.22, 166.83, 160.14, 132.97, 131.68, 130.97, 130.63, 130.00, 129.57, 129.23, 128.86, 114.41, 81.41, 72.30, 66.19, 62.00, 56.02, 55.47, 37.45, 36.52, 30.25, 29.94, 16.36, 12.78. HRMS (ESI, *m/z*): calcd for $[C_{30}H_{38}F_3NO_7]^+$, $([M + H]^+)$: 582.2679, found 582.2681.

**(2S,3R,4R,Z)-N-methoxy-8-((4-moethoxybenzyl)oxy)-3-(methoxymethoxy)-N,2,4-trimethyloct-6-enamide**, **35**

A 250 mL flask was flame dried and flushed with argon before anhydrous DCM (100 mL), amide **34** (4.0 g, 11.0 mmol, 1 eq.), and DIPA (1.2 mL, 69 mmol, 6.3 eq.) were added. The solution was cooled to 0 °C and MOMCl (6.0 M in dimethoxymethane, 11 mL, 66 mmol, 6 eq.) were added dropwise. Stiring was continued at 0 °C for 1 hr, at which point the reaction was quenched by the addition of saturated aqueous sodium bicarbonate (50 mL). The organic layer was collected and the aqueous layer was extracted with DCM (3 X, 35 mL). The combined organic layers were dried over anhydrous sodium sulfate and solvent was removed under reduced pressure to afford a yellow oil that was purified by SiO$_2$ flash chromatography (15 % – 30 % EtOAc in hexanes) to provide pure amide **35** as a colorless oil (4.1 g, 91 %). $[\alpha]^{25}_D = 2.2°$ (c = 0.065, DCM). ^{1}H NMR (500 MHz, Acetone) δ 7.29 – 7.22 (m, 2H), 6.92 – 6.87 (m, 2H), 5.64 – 5.50 (m, 2H), 4.60 (dd, J = 10.2, 6.7 Hz, 2H), 4.42 (s, 2H), 4.09 – 4.00 (m, 2H), 3.78 (s, 3H), 3.73 (s, 3H), 3.64 (dd, J = 7.1, 4.4 Hz, 1H), 3.32 (s, 1H), 3.19 – 3.04 (m, 1H), 3.12 (s, 3H), 2.29 – 2.20 (m, 1H), 1.96 – 1.86 (m, 1H), 1.68 – 1.58 (m, 1H), 1.12 (d, J = 6.9 Hz, 3H), 0.92 (d, J = 6.9 Hz, 3H). ^{13}C NMR (126 MHz, Acetone) δ 176.78, 160.09, 132.46, 131.75, 129.98, 128.61, 114.38, 98.86, 84.81, 72.20, 66.24, 61.88, 56.17, 55.46, 38.69, 37.79, 30.37, 29.53, 16.86, 14.01. HRMS (ESI, m/z): calcd for $[C_{22}H_{35}NO_6]^+$, ($[M + Na]^+$): 432.2362, found 432.2365.
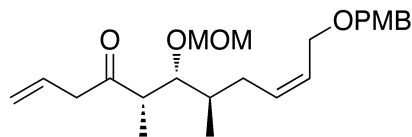
(5S,6R,7R,Z)-11-((4-methoxybenzyl)oxy)-6-(methoxymethoxy)-5,7-dimethylundeca-1,9-dien-4-one, **36**

A 250 mL flask was flame dried and flushed with argon before anhydrous THF (90 mL) and amide **35** (3.6 g, 9 mmol, 1 eq.) were added. The solution was cooled to -78 °C and allyl magnesium bromide (1 M in diethyl ether, 11 mL, 11 mmol, 1.2 eq.) was added dropwise. Stirring was continued at -78 °C for 30 min at which point the reaction was quenched by the addition of saturated aqueous ammonium chloride (30 mL). The solution was allowed to warm to rt, the organic layer was collected, and the aqueous layer was extracted with EtOAc (3 X, 30 mL). The combined organic layers were dried over anhydrous sodium sulfate and solvent was removed under reduced pressure to afford a yellow oil that was purified by SiO$_2$ flash chromatography (5 % – 10 % EtOAc in hexanes) to provide pure **36** as a colorless oil (3.3 g, 94 %). $[\alpha]^{25}_D$ = 11.1° (c = 0.023, DCM). ^{1}H NMR (500 MHz, CDCl$_3$) δ 7.30 – 7.22 (m, 2H), 6.87 (d, J = 8.6 Hz, 2H), 5.91 (ddt, J = 17.1, 10.1, 6.9 Hz, 1H), 5.71 – 5.60 (m, 1H), 5.60 – 5.51 (m, 1H), 5.17 (dd, J = 10.2, 1.1 Hz, 1H), 5.12 (dd, J = 17.2, 1.4 Hz, 1H), 4.56 (dd, J = 10.2, 6.8 Hz, 2H), 4.44 (s, 2H), 4.03 (d, J = 6.4 Hz, 2H), 3.79 (s, 3H), 3.69 (dd, J = 6.3, 4.6 Hz, 1H), 3.30 (s, 3H), 3.39 – 3.18 (m, 1H), 2.83 – 2.73 (m, 1H), 2.40 – 2.22 (m, 1H), 1.90 (dt, J = 13.9, 9.0 Hz, 1H), 1.75 – 1.59 (m, 1H), 1.12 (d, J = 7.0 Hz, 3H), 0.89 (d, J = 6.8 Hz, 3H). ^{13}C NMR (126 MHz, CDCl$_3$) δ 210.50, 159.29, 131.81, 131.00, 130.51, 129.52, 127.82, 118.80, 113.87, 98.14, 83.37, 72.03, 65.66, 56.27, 55.37, 48.49, 46.41, 37.04, 30.41, 16.53, 11.10. HRMS (ESI, *m/z*): calcd for [C$_{23}$H$_{34}$O$_5$]$^+$, ([M + Na]$^+$): 413.2304, found 413.2303.
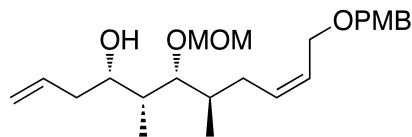
(4S,5R,6R,7R,Z)-11-((4-methoxybenzyl)oxy)-6-(methoxymethoxy_5,7-dimethylundeca-1,9-dien-4-ol, 37
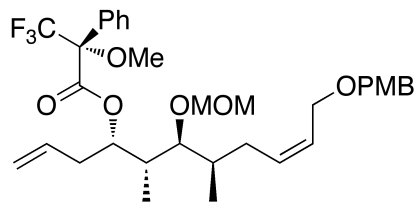
A 500 mL flask was flame dried and flushed with argon before anhydrous diethyl ether (200 mL) and ketone **36** (3.0 g, 7.7 mmol, 1 eq.) were added. The solution was cooled to -42 °C and lithium iodide (10.3 g, 77 mmol, 10 eq.) was added. Vigorous stiring was continued for 2 h or until the solution became a deep yellow color and lithium iodide was completely dissolved. The solution was cooled to -78 °C and lithium aluminum hydride (2.93 g, 77 mmol, 10 eq.) was slowly added. The reaction mixture was stirred at -78 °C for 30 min at which point deionized water (50 mL) was added dropwise *via* addition funnel over 20 min. The reaction mixture was allowed to warm to rt and a half saturated solution of aqueous sodium potassium tartrate added. Stiring was continued until the resultant emulsion became biphasic. The organic layer was collected, and the aqueous layer was extracted with EtOAc (6 X, 50 mL). The combined organic layers were dried over anhydrous sodium sulfate and solvent was removed under reduced pressure to afford a colorless oil consisting of a 10:1 mixture of alcohol epimers that was purified by SiO$_2$ flash chromatography (5 % – 10 % EtOAc in hexanes) to provide pure **37** as a colorless oil (2.6 g, 87 %). Stereochemistry of the major product was confirmed by Mosher's analysis (*vide infra*). [α]^{25}$_D$ = -12.9° (c = 0.006, DCM). ^{1}H NMR (500 MHz, CDCl$_3$) δ 7.26 (d, *J* = 8.5 Hz, 2H), 6.87 (d, *J* = 8.6 Hz, 2H), 5.81 (ddt, *J* = 17.2, 10.1, 7.1 Hz, 1H), 5.66 (dt, *J* = 12.6, 6.4 Hz, 1H), 5.57 (ddd, *J* = 9.7, 8.0, 6.7 Hz, 1H), 5.18 – 5.06 (m, 2H), 4.67 (dd, *J* = 26.0, 6.2 Hz, 2H), 4.44 (s, 2H), 4.03 (d, *J* = 6.4 Hz, 2H), 3.80 (s, 3H), 3.76 – 3.72 (m, 1H), 3.39 (s, 3H), 3.35 (dd, *J* = 6.8, 2.7 Hz, 1H), 2.92 (s, 1H), 2.32 – 2.16 (m, 3H), 1.92 – 1.82 (m, 1H), 1.82 – 1.76 (m,

1H), 1.76 – 1.66 (m, 2H), 0.95 (d, J = 7.0 Hz, 3H), 0.85 (d, J = 6.7 Hz, 3H). ^{13}C NMR (126

MHz, CDCl$_3$) δ 159.31, 135.62, 132.05, 130.49, 129.54, 127.60, 117.46, 113.89, 98.86, 88.12,

74.68, 72.03, 65.62, 56.17, 55.39, 39.81, 38.72, 37.06, 30.75, 16.25, 7.47. HRMS (ESI, m/z):

calcd for [C$_{23}$H$_{36}$O$_5$]$^+$, ([M + K]$^+$): 431.2200, found 431.2198.
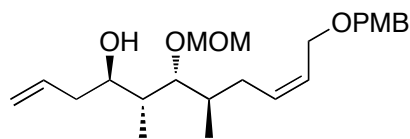
(4S,5R,6S,7R,Z)-11-((4-methoxybenzyl)oxy)-6-(methoxymethoxy_5,7-dimethylundeca-1,9-

dien-4-ol, **38**

Alcohol **38** was isolated as a minor product from the Suzuki reduction of ketone **36** as a colorless

oil (270 mg, 9 %). [α]^{25}$_D$ = 16.4° (c = 0.031, DCM). ^{1}H NMR (500 MHz, CDCl$_3$) δ 7.27 (d, J =

7.5 Hz, 2H), 6.91 – 6.84 (m, 2H), 5.99 – 5.88 (m, 1H), 5.71 – 5.63 (m, 1H), 5.62 – 5.55 (m, 1H),

5.17 – 5.06 (m, 2H), 4.69 – 4.64 (m, 2H), 4.44 (s, 2H), 4.03 (d, J = 6.4 Hz, 2H), 3.80 (s, 3H),

3.61 (dd, J = 9.1, 1.9 Hz, 1H), 3.50 (bs, 2H), 3.41 (s, 3H), 2.45 (m, 1H), 2.30 (m, 1H), 2.14 (dt, J

= 7.8, 14.4 Hz, 1H), 1.87 (dt, J = 14.1, 9.1 Hz, 1H), 1.79 – 1.70 (m, 1H), 1.70 – 1.62 (m, 1H),

0.85 (d, J = 6.9 Hz, 3H), 0.80 (d, J = 6.8 Hz, 3H). ^{13}C NMR (126 MHz, CDCl$_3$) δ 159.32,

135.91, 132.12, 130.55, 129.56, 127.69, 117.19, 113.91, 99.18, 84.26, 72.09, 72.04, 65.68, 56.34,

55.42, 40.27, 39.39, 36.70, 31.41, 15.91, 10.22. HRMS (ESI, m/z): calcd for [C$_{23}$H$_{36}$O$_5$]$^+$, ([M +

K]$^+$): 431.2200, found 431.2198.

(R)-(4S,5R,6S,7R,Z)-11-((4-methoxybenzyl)oxy)-6-(methoxymethoxy)5,7-dimethylundeca-1,9-dien-4-yl 3,3,3-trifluoro-2-methoxy-2-phenylpropanoate, 37a

A 5 mL flas was flame dried and flushed with argon before anhydrous DCM (0.5 mL) and (*R*)-3,3,3-trifluoro-2-methoxy-2-phenylpropanoic acid (12 mg, 0.051 mmol, 2 eq.) were added. The solution was cooled to 0 °C and oxalyl chloride (5 μL, 0.054 mmol, 2.1 eq.) and DMF (2 drops) were added. The reaction mixture was allowed to warm to rt and stirring was continued for 2 h at which point DIPEA (20 μL, 0.11 mmol, 4.3 eq.), alcohol **37** (10 mg, 0.026 mmol, 1 eq.), and DMAP (6.5 mg, 0.051 mmol, 2 eq.) were added. The reaction mixture was stirred for 1 h solvent was then removed under reduced pressure to afford a yellow-brown oil that was purified by SiO_2 flash chromatography (5 % – 10 % EtOAc in hexanes) to afford pure R-Mosher's ester as a colorless oil (14 mg, 86 %). ^{1}H NMR (500 MHz, Acetone) δ 7.62 – 7.55 (m, 2H), 7.51 – 7.43 (m, 3H), 7.30 – 7.23 (m, 2H), 6.92 – 6.87 (m, 2H), 5.83 (dddd, *J* = 16.5, 10.2, 7.9, 6.2 Hz, 1H), 5.66 – 5.53 (m, 2H), 5.32 (td, *J* = 6.6, 5.0 Hz, 1H), 5.18 (ddd, *J* = 17.1, 3.2, 1.6 Hz, 1H), 5.14 – 5.10 (m, 1H), 4.59 (d, *J* = 6.8 Hz, 1H), 4.53 (d, *J* = 6.8 Hz, 1H), 4.42 (s, 2H), 4.04 (d, *J* = 5.9 Hz, 2H), 3.78 (s, 3H), 3.59 (q, *J* = 1.2 Hz, 3H), 3.36 (s, 3H), 3.18 (dd, *J* = 6.0, 4.6 Hz, 1H), 2.68 – 2.53 (m, 2H), 2.27 – 2.16 (m, 1H), 2.02 – 1.97 (m, 1H), 1.91 (m, 1H), 1.79 – 1.70 (m, 1H), 0.83 (d, *J* = 7.6 Hz, 3H), 0.82 (d, *J* = 6.9 Hz, 3H). ^{13}C NMR (126 MHz, Acetone) δ 166.69, 160.13, 134.48, 133.22, 132.23, 131.73, 130.57, 130.02, 129.27, 128.75, 128.22, 124.53 (q, *J* = 289 Hz, C-F$_3$), 118.89, 114.40, 99.45, 84.99, 78.57, 72.21, 66.17, 56.15, 55.47, 38.56, 37.13, 37.06,

30.54, 16.82, 10.15. HRMS (ESI, *m/z*): calcd for $[C_{33}H_{43}F_3O_7]^+$, $([M + Na]^+)$: 631.2859, found 631.2858.
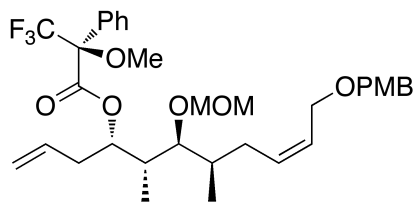
(S)-(4*S*,5*R*,6*S*,7*R*,*Z*)-11-((4-methoxybenzyl)oxy)-6-(methoxymethoxy)5,7-dimethylundeca-1,9-dien-4-yl 3,3,3-trifluoro-2-methoxy-2-phenylpropanoate, 37b

A 5 mL flas was flame dried and flushed with argon before anhydrous DCM (0.5 mL) and (*S*)-3,3,3-trifluoro-2-methoxy-2-phenylpropanoic acid (12 mg, 0.051 mmol, 2 eq,) were added. The solution was cooled to 0 °C and oxalyl chloride (5 μL, 0.054 mmol, 2.1 eq.) and DMF (2 drops) were added. The reaction mixture was allowed to warm to rt and stirring was continued for 2 h at which point DIPEA (20 μL, 0.11 mmol, 4.3 eq.), alcohol **37** (10 mg, 0.026 mmol, 1 eq.), and DMAP (6.5 mg, 0.051 mmol, 2 eq.) were added. The reaction mixture was stirred for 1 h solvent was then removed under reduced pressure to afford a yellow-brown oil that was purified by SiO_2 flash chromatography (5 % – 10 % EtOAc in hexanes) to afford pure S-Mosher's ester as a colorless oil (14 mg, 86 %). ^{1}H NMR (500 MHz, Acetone) δ 7.60 – 7.54 (m, 2H), 7.51 – 7.45 (m, 3H), 7.29 – 7.24 (m, 2H), 6.92 – 6.87 (m, 2H), 5.70 – 5.53 (m, 3H), 5.31 (td, *J* = 6.6, 4.8 Hz, 1H), 5.05 (ddd, *J* = 17.1, 3.1, 1.6 Hz, 1H), 5.00 (dd, *J* = 10.2, 0.8 Hz, 1H), 4.66 (d, *J* = 6.9 Hz, 1H), 4.62 (d, *J* = 6.8 Hz, 1H), 4.42 (s, 2H), 4.05 (d, *J* = 7.1 Hz, 2H), 3.78 (s, 3H), 3.54 (q, *J* = 1.0 Hz, 3H), 3.38 (s, 3H), 3.32 (dd, *J* = 6.3, 4.2 Hz, 1H), 2.60 – 2.42 (m, 2H), 2.29 – 2.23 (m, 1H), 2.10 – 2.01 (m, 1H), 2.01 – 1.91 (m, 1H), 1.82 (m, 1H), 0.99 (d, *J* = 6.9 Hz, 3H), 0.87 (d, *J* = 6.8 Hz, 3H). ^{13}C NMR (126 MHz, Acetone) δ 166.81, 160.13, 134.16, 132.86, 132.22, 131.74, 130.62, 130.02, 129.30, 128.79, 128.59, 124.51 (q, *J* = 289 Hz, C-F$_3$), 118.86, 114.40, 99.44,

84.99, 78.86, 72.21, 66.17, 56.16, 55.47, 38.40, 37.25, 36.91, 30.76, 16.75, 10.42. HRMS (ESI,

m/z): calcd for $[C_{33}H_{43}F_3O_7]^+$, $([M + Na]^+)$: 631.2859, found 631.2863.
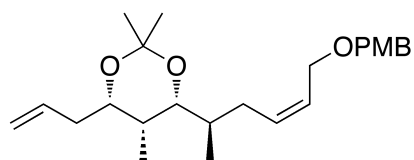
(4*S*,5*R*,6*R*)-4-allyl-6-((*R*,*Z*)-6-((4-methoxybenzyl)oxy)hex-4-en-2-yl)-2,2,5-trimethyl-1,3-

dioxane, 39

A 5 mL flask was charged with methanol (0.5 mL) before compound **37** (15 mg, 0.038 mmol, 1

eq.) was added. Concentrated hydrochloric acid (12 M in deionized water, 46 μL, 0.0038 mmol,

0.1 eq.) was added and the solution was heated at reflux for 5 min and then cooled to 0 °C at

which point saturated aqueous sodium bicarbonate (1 mL) was added to quench the reaction.

Organic solvent was removed under reduced pressure and the resultant slurry was diluted with

EtOAc (1 mL) and deionized water (1 mL). The organic layer was collected and the aqueous

layer was extracted with EtOAc (3 X, 1 mL). The combined organic layers were dried over

anhydrous sodium sulfate and solvent was removed under reduced pressure to afford a yellow oil

that was purified by SiO$_2$ flash chromatography (30 % – 50 % EtOAc in hexanes) to provide

pure diol as a colorless oil (7.5 mg, 57 %), which was used in the subsequent step without further

characterization. A 1/2 dram vial was charge with acetone (50 μL) before 2,2-dimethoxypropane

(52 mL, 0.44 mmol, 20 eq.) diol (7.5 mg, 0.022 mmol, 1 eq.), and pyridinium *p*-toluenesulfonate

(0.5 mg, 0.0022 mmol, 0.1 eq.) were added. The solution was stirred at rt for 4 h and the reaction

was quenched by the addition of saturated aqueous sodium bicarbonate (0.5 mL). Organic

solvent was removed under reduced pressure and the resultant slurry was diluted with EtOAc (1

mL) and deionized water (1 mL). The organic layer was collected and the aqueous layer was

extracted with EtOAc (4 X, 1 mL). The combined organic layers were dried over anhydrous

sodium sulfate and solvent was removed under reduced pressure to afford a colorless oil that was

purified by SiO$_2$ flash chromatography (10 % EtOAc in hexanes) to provide pure acetonide **39** as

a colorless oil. ^{1}H NMR (500 MHz, C$_6$D$_6$) δ 7.30 – 7.26 (m, 2H), 6.84 – 6.78 (m, 2H), 5.92 –

5.85 (m, 1H), 5.85 – 5.78 (m, 1H), 5.62 – 5.52 (m, 1H), 5.10 (ddd, *J* = 17.2, 3.4, 1.7 Hz, 1H),

5.07 – 5.03 (m, 1H), 4.46 – 4.39 (m, 2H), 4.13 (m, 2H), 3.71 (ddd, *J* = 8.0, 6.0, 2.2 Hz, 1H), 3.30

(s, 3H), 3.24 (dd, *J* = 9.9, 2.1 Hz, 1H), 2.49 – 2.35 (m, 2H), 2.10 – 1.98 (m, 2H), 1.74 – 1.64 (m,

1H), 1.49 (s, 3H), 1.29 (s, 3H), 1.26 – 1.19 (m, 1H), 0.88 (d, *J* = 6.8 Hz, 3H), 0.64 (d, *J* = 6.9 Hz,

3H). ^{13}C NMR (126 MHz, C$_6$D$_6$) δ 159.72, 135.37, 131.00, 129.50, 128.69, 128.35, 116.74,

114.09, 99.01, 76.94, 73.43, 72.10, 66.09, 54.76, 37.93, 34.82, 32.72, 31.18, 30.36, 19.71, 13.94,

4.80. HRMS (ESI, *m/z*): calcd for [C$_{24}$H$_{36}$O$_4$]$^+$, ([M + Na]$^+$): 411.2511, found 411.2515.
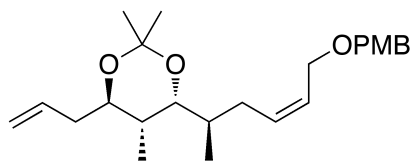
(4*R*,5*R*,6*R*)-4-allyl-6-((*R*,*Z*)-6-((4-methoxybenzyl)oxy)hex-4-en-2-yl)-2,2,5-trimethyl-1,3-

dioxane, 40

A 5 mL flask was charged with methanol (0.5 mL) before compound **38** (15 mg, 0.038 mmol, 1

eq.) was added. Concentrated hydrochloric acid (12 M in deionized water, 46 µL, 0.0038 mmol,

0.1 eq.) was added and the solution was heated at reflux for 5 min and then cooled to 0 °C at

which point saturated aqueous sodium bicarbonate (1 mL) was added to quench the reaction.

Organic solvent was removed under reduced pressure and the resultant slurry was diluted with

EtOAc (1 mL) and deionized water (1 mL). The organic layer was collected and the aqueous

layer was extracted with EtOAc (3 X, 1 mL). The combined organic layers were dried over

anhydrous sodium sulfate and solvent was removed under reduced pressure to afford a yellow oil

that was purified by SiO$_2$ flash chromatography (30 % – 50 % EtOAc in hexanes) to provide

pure diol as a colorless oil (7.5 mg, 57 %), which was used in the subsequent step without further characterization. A 1/2 dram vial was charge with acetone (50 μL) before 2,2-dimethoxypropane (52 mL, 0.44 mmol, 20 eq.) diol (7.5 mg, 0.022 mmol, 1 eq.), and pyridinium *p*-toluenesulfonate (0.5 mg, 0.0022 mmol, 0.1 eq.) were added. The solution was stirred at rt for 4 h and the reaction was quenched by the addition of saturated aqueous sodium bicarbonate (0.5 mL). Organic solvent was removed under reduced pressure and the resultant slurry was diluted with EtOAc (1 mL) and deionized water (1 mL). The organic layer was collected and the aqueous layer was extracted with EtOAc (4 X, 1 mL). The combined organic layers were dried over anhydrous sodium sulfate and solvent was removed under reduced pressure to afford a colorless oil that was purified by SiO_2 flash chromatography (10 % EtOAc in hexanes) to provide pure acetonide **40** as a colorless oil. ^{1}H NMR (500 MHz, C_6D_6) δ 7.30 – 7.25 (m, 2H), 6.84 – 6.78 (m, 2H), 5.97 (ddt, *J* = 17.1, 10.2, 6.9 Hz, 1H), 5.89 – 5.81 (m, 1H), 5.62 – 5.54 (m, 1H), 5.15 – 5.05 (m, 2H), 4.43 – 4.37 (m, 2H), 4.17 – 4.05 (m, 2H), 3.41 (dd, *J* = 10.6, 4.3 Hz, 1H), 3.35 – 3.30 (m, 1H), 3.30 (s, 3H), 2.62 – 2.53 (m, 1H), 2.33 – 2.18 (m, 2H), 1.89 (dtd, *J* = 14.1, 8.9, 0.9 Hz, 1H), 1.67 – 1.54 (m, 2H), 1.34 (s, 3H), 1.33 (s, 3H), 0.76 (d, *J* = 6.7 Hz, 3H), 0.66 (d, *J* = 6.7 Hz, 3H). ^{13}C NMR (126 MHz, C_6D_6) δ 159.70, 135.76, 131.40, 129.48, 128.54, 128.35, 116.69, 114.07, 100.81, 75.13, 72.96, 72.01, 66.02, 54.76, 39.69, 38.02, 33.59, 31.45, 25.29, 23.96, 14.96, 11.97. HRMS (ESI, *m/z*): calcd for $[C_{24}H_{36}O_4]^+$, $([M + Na]^+)$: 411.2511, found 411.2515.
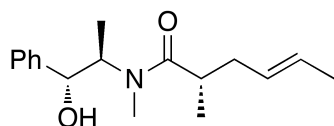

(S,E)-N-((1R,2R)-1-hydroxy-1-phenylpropan-2-yl)-N,2-dimethylhex-4-enamide, 44

A 250 mL flask was flame dried and flushed with argon before anhydrous THF (17 mL), anhydrous lithium chloride (3 g, 68 mmol, 5 eq.), and DIPA (4.4 mL, 31 mmol, 2.25 eq.) were

added. The suspension was cooled to -78 °C, butyllithium (2.5 M in hexanes, 11.3 mL, 28 mmol, 2.08 eq.) was added, and stirring was continued as the solution was briefly warmed to 0 °C and then cooled back to -78 °C. An ice cooled solution of amide *R,R*-pseudoephedrinepropionamide (3 g, 13.6 mmol, 1 eq.) in anhydrous THF (43 mL) was added *via* cannula followed by a wash with THF (5 mL). Stirring was continued at -78 °C for 2 h, 0 °C for 30 min, and rt for 5 min, before the reaction mixture was finally cooled to 0 °C. *trans*-crotyl bromide (2.80 g, 20.4 mmol, 1.5 eq.) was then added in one portion, and the reaction mixture was stirred for 2 h at 0 °C. Reaction was quenched at 0 °C by the addition of saturated aqueous ammonium chloride (2 mL) and the mixture was partitioned between saturated aqueous ammonium chloride (130 mL) and EtOAc (50 mL). The organic layer was collected and the aqueous layer was extracted with EtOAc (3 X, 50 mL). The combined organic layers were dried over anhydrous sodium sulfate and solvent was removed under reduced pressure to afford a yellow oil that was purified by SiO_2 flash chromatography (30 % EtOAc in hexanes) to provide pure **44** as a colorless oil (94 %). Diastereoselectivity (>20:1) was assessed using Myers oxazolium technique (*vide infra*). $[\alpha]^{25}_D$ = -76.6° (c = 0.068, DCM). (*Denotes minor rotamer peak) ^{1}H NMR (500 MHz, CDCl$_3$) δ 7.42 – 7.30 (m, 5H), *7.29 – 7.23 (m, 5H), *5.56 – 5.51 (m, 1H), 5.50 – 5.5 (m, 1H), 5.41 – 5.35 (m, 1H), *5.33 – 5.27 (m, 1H), 4.62 (dd, J = 8.6, 7.2 Hz, 1H), 4.58 (d, J = 8.7 Hz, 1H), *4.55 – 4.45 (m, 1H), 4.40 (bs, 1H), *4.12 – 4.04 (m, 1H), *2.91 (s, 3H), 2.84 (s, 3H), 2.67 – 2.58 (m, 1H), *2.49 – 2.40 (m, 1H), 2.26 (ddd, J = 14.0, 7.4, 6.5 Hz, 1H), *2.20 – 2.13 (m, 1H), *2.10 (m, 1H), 2.01 (ddd, J = 14.0, 7.7, 7.1 Hz, 1H), *1.66 (d, J = 6.3 Hz, 3H), 1.63 (dd, J = 6.4, 1.0 Hz, 3H), 1.13 (d, J = 6.9 Hz, 3H), *1.10 (d, J = 6.9 Hz, 3H), 1.09 (d, J = 6.7 Hz, 3H), *1.01 (d, J = 6.7 Hz, 3H). ^{13}C NMR (126 MHz, CDCl$_3$) δ 178.87, *177.57, 142.71, *141.05, *129.07, *128.89, 128.56, 128.48, 127.73, *127.46, 127.31, *127.10, 126.48, *126.04, 77.37, 76.70, *75.62,

*58.27, 37.21, 37.16, 37.13, *37.00, *36.38, *31.31, *18.16, 18.08, *17.75, 17.11, *15.62, 14.65.

HRMS (ESI, *m/z*): calcd for $[C_{17}H_{25}NO_2]^+$, $([M + Na]^+)$: 298.1783, found 298.1782.
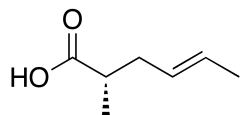
(*S,E*)-2-methylhex-4-enoic acid, 46

A 500 mL flask was charged with *tert*-butanol (42 mL) and deionized water (136 mL) before amide **44** (3.56 g, 13.6 mmol, 1 eq.) and tetrabutylammonium hydroxide (1.5 M in deionized water, 50 mL, 68 mmol, 5 eq.) were added. The solution was heated at reflux for 23 h. Once the reaction was complete, the solution was allowed to cool to rt and suspended between 0.5 M aqueous sodium hydroxide (1.76 L) and diethyl ether (250 mL). The organic layer was removed, and the aqueous layer was extracted with diethyl ether (3 X, 250 mL). The aqueous layer was cooled to 0 °C, saturated with sodium chloride, and acidified to pH 2 with 4 N aqueous hydrochloric acid. The acid solution was extracted with diethyl ether (4 X, 300 mL) and the combined organic extracts were dried over anhydrous sodium sulfate. Solvent was removed under reduced pressure to afford pure acid **46** as a colorless liquid (1.64 g, 94%). $[\alpha]^{25}_D = +9.7°$ (c = 0.031, DCM). ^{1}H NMR (500 MHz, CDCl$_3$) δ 10.68 (s, 1H), 5.53 – 5.45 (m, 1H), 5.41 – 5.33 (m, 1H), 2.53 – 2.45 (m, 1H), 2.40 – 2.31 (m, 1H), 2.17 – 2.08 (m, 1H), 1.64 (dd, *J* = 6.3, 1.3 Hz, 3H), 1.15 (d, *J* = 7.0 Hz, 3H). ^{13}C NMR (126 MHz, CDCl$_3$) δ 182.98, 127.90, 127.68, 39.73, 36.49, 18.04, 16.38. HRMS (ESI, *m/z*): calcd for $[C_7H_{12}O_2]^-$, $([2M + Na - 2H]^-)$: 277.1416, found 277.1415.
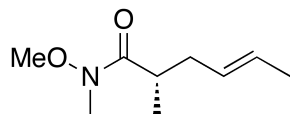
**(*S*,*E*)-*N*-methoxy-*N*,2-dimethylhex-4-enamide, 48**

A 100 mL flask was flame dried and flushed with argon before DMF (20 mL), acid **46** (1.34 g, 10.5 mmol, 1 eq.), and DIPEA (2.4 mL, 22.1 mmol, 2.1 eq.) were added. COMU (3.13 g, 11.6 mmol, 1.1 eq.) was then added in one portion and the reaction mixture was stirred at rt for 45 min at which point *N*,*O*-Dimethylhydroxylamine hydrochloride (1.3 g, 21 mmol, 2 eq.) was added. Stirring was continued for 1 hr and the reaction was quenched by the careful addition of saturated aqueous sodium bicarbonate (15 mL). The resulting slurry was then extracted with EtOAc (5 X, 30 mL) and the combined organic portions were dried over anhydrous sodium sulfate. Solvent was removed under reduced pressure to afford a red oil that was purified by SiO_2 flash chromatography (5 % – 15% EtOAc in hexanes) to provide pure amide **48** as a colorless oil (94 %). $[\alpha]^{25}_D$ = 30.4° (c = 0.004, DCM). ^{1}H NMR (500 MHz, CDCl$_3$) δ 5.50 – 5.42 (m, 1H), 5.41 – 5.32 (m, 1H), 3.67 (s, 3H), 3.17 (s, 3H), 2.88 (m, 1H), 2.36 – 2.29 (m, 1H), 2.08 – 2.00 (m, 1H), 1.63 (dd, *J* = 6.3, 1.1 Hz, 3H), 1.09 (d, *J* = 6.9 Hz, 3H). ^{13}C NMR (126 MHz, CDCl$_3$) δ 177.77, 128.73, 127.17, 61.59, 36.80, 18.07, 17.10. HRMS (ESI, *m/z*): calcd for $[C_9H_{17}NO_2]^+$, ($[M + Na]^+$): 194.1157, found 194.1156.
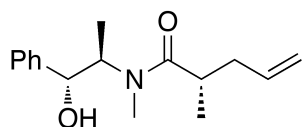
(*S*)-*N*-((1*R*,2*R*)-1-hydroxy-1-phenylpropan-2-yl)-*N*,2-dimethylpent-4-enamide, 43
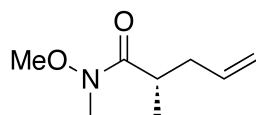
A 250 mL flask was flame dried and flushed with argon before anhydrous THF (17 mL), anhydrous lithium chloride (3 g, 68 mmol, 5 eq.), and DIPA (4.4 mL, 31 mmol, 2.25 eq.) were added. The suspension was cooled to -78 °C, butyllithium (2.5 M in hexanes, 11.3 mL, 28 mmol,

2.08 eq.) was added, and stirring was continued as the solution was briefly warmed to 0 °C and then cooled back to -78 °C. An ice cooled solution of *R,R*-pseudoephedrinepropionamide (3 g, 13.6 mmol, 1 eq.) in anhydrous THF (43 mL) was added *via* cannula followed by a wash with THF (5 mL). Stirring was continued at -78 °C for 2 h, 0 °C for 30 min, and rt for 5 min, before the reaction mixture was finally cooled to 0 °C. Allyl bromide (1.77 mL, 20.4 mmol, 1.5 eq.) was then added in one portion, and the reaction mixture was stirred for 2 h at 0 °C. Reaction was quenched at 0 °C by the addition of saturated aqueous ammonium chloride (2 mL) and the mixture was partitioned between saturated aqueous ammonium chloride (130 mL) and EtOAc (50 mL). The organic layer was collected and the aqueous layer was extracted with EtOAc (3 X, 50 mL). The combined organic layers were dried over anhydrous sodium sulfate and solvent was removed under reduced pressure to afford a yellow oil that was purified by SiO_2 flash chromatography (30 % EtOAc in hexanes) to provide pure **43** as a colorless oil (94 %). Diastereoselectivity (>20:1) was assessed using Myers oxazolium technique (*vide infra*). $[\alpha]^{25}_D =$ -71.5° (c = 0.142, DCM). (*Denotes minor rotamer peak) ^{1}H NMR (500 MHz, CDCl$_3$) δ 7.42 – 7.30 (m, 5H), *7.29 – 7.23 (m, 5H), *5.80 (ddt, *J* = 17.2, 10.0, 7.0 Hz, 1H), 5.70 (ddt, *J* = 17.2, 10.0, 7.0 Hz, 1H), 5.15 – 5.07 (m, 2H), 5.06 – 4.97 (m, 2H), 4.66 – 4.55 (m, 1H), *4.58 (d, *J* = 8.7 Hz, 1H), 4.52 – 4.24 (m, 1H), *4.13 – 4.02 (m, 1H), *2.92 (s, 3H), 2.86 (s, 3H), 2.74 – 2.63 (m, 1H), *2.58 – 2.47 (m, 1H), *2.47 – 2.40 (m, 1H), 2.40 – 2.28 (m, 1H), *2.24 – 2.13 (m, 1H), 2.14 – 2.01 (m, 1H), 1.11 (d, *J* = 6.8 Hz, 6H), *1.02 (d, *J* = 6.8 Hz, 1H). ^{13}C NMR (126 MHz, CDCl$_3$) δ 178.55, *177.26, 142.61, *141.12, *136.80, 136.14, *128.90, *128.62, 128.49, 127.76, *127.05, 126.50, *116.72, 116.68, 77.37, 76.66, *75.64, *58.22, *38.21, 38.18, 36.71, 35.95, *27.19, *17.75, 17.15, *15.67, 14.65. HRMS (ESI, *m/z*): calcd for $[C_{16}H_{23}NO_2]^+$, $([M + Na]^+)$: 284.1626, found 284.1623.
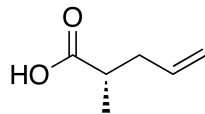
(*S*)-2-methylpent-4-enoic acid, 45

A 500 mL flask was charged with *tert*-butanol (42 mL) and deionized water (136 mL) before amide **43** (3.56 g, 13.6 mmol, 1 eq.) and tetrabutylammonium hydroxide (1.5 M in deionized water, 50 mL, 68 mmol, 5 eq.) were added. The solution was heated at reflux for 23 h. Once the reaction was complete, the solution was allowed to cool to rt and suspended between 0.5 M aqueous sodium hydroxide (1.76 L) and diethyl ether (250 mL). The organic layer was removed, and the aqueous layer was extracted with diethyl ether (3 X, 250 mL). The aqueous layer was cooled to 0 °C, saturated with sodium chloride, and acidified to pH 2 with 4 N aqueous hydrochloric acid. The acid solution was extracted with diethyl ether (4 X, 300 mL) and the combined organic extracts were dried over anhydrous sodium sulfate. Solvent was removed under reduced pressure to afford pure acid **45** as a colorless liquid (1.46 g, 94%). $[\alpha]^{25}_{D} = +9.6°$ (c = 0.047, DCM). ^{1}H NMR (500 MHz, CDCl$_3$) δ 5.77 (ddt, J = 17.1, 10.2, 7.0 Hz, 1H), 5.09 (ddt, J = 17.1, 1.7, 1.5 Hz, 1H), 5.06 (ddt, J = 10.2, 1.9, 1.0 Hz, 1H), 2.61 – 2.51 (m, 1H), 2.49 – 2.41 (m, 1H), 2.21 (m, 1H), 1.19 (d, J = 7.0 Hz, 3H). ^{13}C NMR (126 MHz, CDCl$_3$) δ 175.41, 135.29, 117.28, 39.17, 37.62, 16.46. HRMS (ESI, *m/z*): calcd for [C$_6$H$_{10}$O$_2$]$^-$, ([2M + Na – 2H]$^-$): 249.1103, found 249.1102.

(*S*)-*N*-methoxy-*N*,2-dimethylpent-4-enamide, 47

A 100 mL flask was flame dried and flushed with argon before DMF (20 mL), acid **45** (1.20 g, 10.5 mmol, 1 eq.), and DIPEA (2.4 mL, 22.1 mmol, 2.1 eq.) were added. COMU (3.13 g, 11.6

mmol, 1.1 eq.) was then added in one portion and the reaction mixture was stirred at rt for 45 min at which point *N,O*-Dimethylhydroxylamine hydrochloride (1.3 g, 21 mmol, 2 eq.) was added. Stirring was continued for 1 hr and the reaction was quenched by the careful addition of saturated aqueous sodium bicarbonate (15 mL). The resulting slurry was then extracted with EtOAc (5 X, 30 mL) and the combined organic portions were dried over anhydrous sodium sulfate. Solvent was removed under reduced pressure to afford a red oil that was purified by SiO_2 flash chromatography (5 % – 15% EtOAc in hexanes) to provide pure amide **47** as a colorless oil (94 %). $[\alpha]^{25}_D = 27.3°$ (c = 0.007, DCM). ^1H NMR (500 MHz, CDCl$_3$) δ 5.73 (ddt, *J* = 17.0, 10.2, 7.0 Hz, 1H), 5.03 (dd, *J* = 17.1, 1.4 Hz, 1H), 4.97 (dd, *J* = 10.2, 0.9 Hz, 1H), 3.65 (s, 3H), 3.15 (s, 3H), 2.91 (m, 1H), 2.39 (m, 1H), 2.09 (m, 1H), 1.09 (d, *J* = 6.9 Hz, 3H). ^{13}C NMR (126 MHz, CDCl$_3$) δ 177.41, 136.27, 116.47, 61.54, 37.91, 35.25, 17.09. HRMS (ESI, *m/z*): calcd for $[C_8H_{15}NO_2]^+$, ($[M + Na]^+$): 180.1000, found 180.1002.
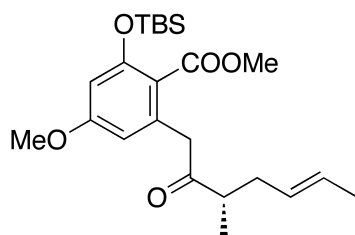
(*S,E*)-methyl-2-((*tert*-butyldimethylsilyl)oxy)-4-methoxy-6-(3-methyl-2-oxohept-5-en-1-yl)benzoate, 52

A flame dried 10 mL flask was flame dried and flushed with argon before THF (1.7 mL) and ester **51** (200 mg, 0.83 mmol, 1 eq.) were added. The solution was cooled to -78 °C and *tert*-butyllithium (1.7 M in pentane, 540 μL, 0.91 mmol, 1.1 eq.) was added dropwise over 5 min. The reaction mixture was stirred for 5 min at which point a solution of amide **48** (142 mg, 0.83 mmol, 1 eq.) in THF (100 μL) was added at once. Stirring was continued at -78 °C for 5 min at which point the reaction was quenched at -78 °C by the careful addition of saturated aqueous

ammonium chloride (2 mL) and the biphasic mixture was allowed warm to rt. The organic layer was collected and the aqueous layer was extracted with EtOAc (4 X, 1.5 mL). The combined organic layers were dried over anhydrous sodium sulfate and solvent was removed under reduced pressure to afford a light yellow oil that was purified by SiO_2 flash chromatography (5 % – 15 % EtOAc in hexanes) to provide pure ketone **52** as a colorless liquid (87 %). $[\alpha]^{25}_D =$ 15.8° (c = 0.011, DCM). ^{1}H NMR (500 MHz, CDCl$_3$) δ 6.31 (d, J = 2.3 Hz, 1H), 6.29 (d, J = 2.3 Hz, 1H), 5.48 – 5.40 (m, 1H), 5.34 – 5.26 (m, 1H), 3.79 (s, 3H), 3.85 – 3.67 (m, 1H), 3.76 (s, 3H), 2.70 – 2.61 (m, 1H), 2.35 – 2.27 (m, 1H), 2.06 – 1.98 (m, 1H), 1.63 (dd, J = 6.3, 1.3 Hz, 3H), 1.05 (d, J = 6.9 Hz, 3H), 0.96 (s, 9H), 0.21 (s, 6H). ^{13}C NMR (126 MHz, CDCl$_3$) δ 210.54, 168.57, 161.22, 155.09, 135.77, 128.20, 127.55, 109.21, 105.61, 104.65, 55.43, 52.03, 47.07, 45.59, 36.10, 26.11, 25.67, 18.07, 16.18, -4.23. HRMS (ESI, m/z): calcd for $[C_{23}H_{36}O_5Si]^+$, ($[M + Na]^+$): 443.2230, found 443.2231.
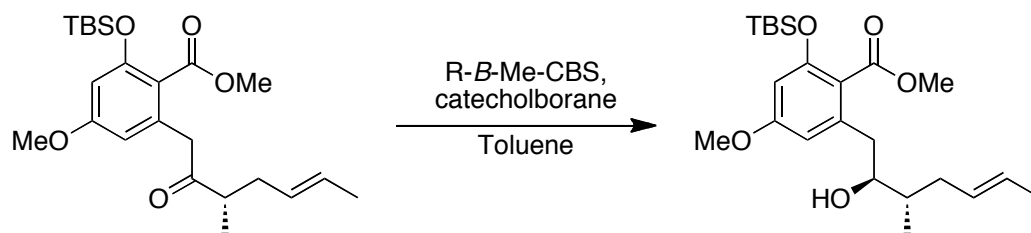
methyl 2-((*tert*-butyldimethylsilyl)oxy)-6-((2*S*,3*S*,*E*)-2-hydroxy-3-methylhept-5-en-1-yl)-4-methoxybenzoate, 53

A 5 mL flask was flame dried and flushed with argon before toluene (1.2 mL), ketone **52** (60 mg, 0.14 mmol, 1 eq.), and (*R*)-(+)-2-butyl-CBS-oxazaborolidine (1 M in toluene, 290 μL, 0.29 mmol, 2 eq.) were added. The solution was cooled to -78 °C and catecholborane (1 M in THF, 290 μL, 0.29 mmol, 2 eq.) was added dropwise over 5 h. Stirring was continued for an additional 12 h at which point the reaction was quenched at -78 °C by the addition of saturated aqueous sodium bicarbonate (2 mL) and the biphasic solution was allowed to warm to rt. The organic

layer was collected and the aqueous layer was extracted with EtOAc (4 X, 2 mL). The combined organic layers were dried over anhydrous sodium sulfate and solvent was removed under reduced pressure to afford a yellow oil that was purified by SiO$_2$ flash chromatography (10 % – 20 % EtOAc in hexanes) to provide pure alcohol **53** as a colorless oil (84 %). $[\alpha]^{25}_D$ = -35.7° (c = 0.008, DCM). ^{1}H NMR (500 MHz, CDCl$_3$) δ 6.41 (d, *J* = 2.2 Hz, 1H), 6.26 (d, *J* = 1.9 Hz, 1H), 5.51 – 5.38 (m, 2H), 3.84 (s, 3H), 3.77 (s, 3H), 3.72 – 3.65 (m, 1H), 2.73 (dd, *J* = 13.6, 3.1 Hz, 1H), 2.60 (dd, *J* = 13.6, 10.1 Hz, 1H), 2.57 (m, 1H), 2.26 – 2.17 (m, 1H), 1.95 – 1.86 (m, 1H), 1.66 (d, *J* = 5.3 Hz, 3H), 0.97 (s, 9H), 0.94 (d, *J* = 6.9 Hz, 3H), 0.23 (s, 3H), 0.20 (s, 3H). ^{13}C NMR (126 MHz, CDCl$_3$) δ 169.66, 161.39, 154.63, 140.80, 129.99, 126.53, 119.39, 108.28, 104.03, 75.60, 55.44, 52.28, 39.31, 39.05, 36.73, 25.67, 18.21, 18.11, 13.92, -4.17, -4.29. HRMS (ESI, *m/z*): calcd for $[C_{23}H_{38}O_5Si]^+$, ($[M + Na]^+$): 445.2386, found 445.2386.
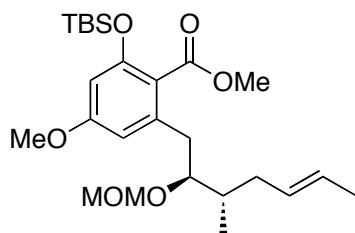

methyl 2-((tert-butyldimethylsilyl)oxy)-4-methoxy-6-((2S,3S,E)-2-(methoxymethoxy)-3-methylhept-5-en-1-yl)benzoate, 54

A 250 mL flask was flame dried and flushed with argon before DCM (100 mL), **53** (4 g, 9.5 mmol, 1 eq.). and DIPEA (12 mL, 64 mmol, 6.5 eq.) were added. The solution was cooled to 0 °C and MOMCl (6 M, 9.6 mL, 58 mmol, 6 eq.) was added and the reaction mixture was stirred for 30 min, followed by quenching by the addition of saturated aqueous sodium bicarbonate (70 mL). The organic layer was collected the aqueous layer was extracted with dichloromethane (3 X, 70 mL). The combined organic layers were dried over anhydrous sodium sulfate and solvent was removed under reduced pressure to afford a yellow oil that was purified by SiO$_2$ flash

chromatography (15 % – 20 % EtOAc in hexanes) to provide pure **54** as a colorless oil (93%).

$[\alpha]^{25}_D$ = -46.4° (c = 0.132, DCM). ^{1}H NMR (500 MHz, CDCl$_3$) δ 6.40 (d, J = 2.3 Hz, 1H), 6.25 (d, J = 2.3 Hz, 1H), 5.52 – 5.29 (m, 2H), 4.49 (d, J = 6.8 Hz, 1H), 4.40 (d, J = 6.8 Hz, 1H), 3.82 (s, 3H), 3.76 (s, 3H), 3.68 – 3.61 (m, 1H), 3.24 (s, 2H), 2.80 (dd, J = 13.7, 8.0 Hz, 1H), 2.71 (dd, J = 13.7, 5.7 Hz, 1H), 2.23 – 2.13 (m, 1H), 1.81 (dt, J = 15.1, 7.3 Hz, 1H), 1.64 (dd, J = 6.0, 1.0 Hz, 3H), 0.96 (s, 9H), 0.90 (d, J = 6.9 Hz, 3H), 0.20 (s, 6H). ^{13}C NMR (126 MHz, CDCl$_3$) δ 168.88, 160.73, 154.18, 139.85, 130.18, 126.34, 119.84, 108.86, 103.80, 96.46, 81.71, 55.63, 55.44, 52.04, 36.64, 36.08, 36.01, 29.85, 25.69, 18.14, 14.33, -4.23, -4.24. HRMS (ESI, *m/z*): calcd for $[C_{25}H_{42}O_5Si]^+$, ($[M + Na]^+$): 473.2699, found 473.2704.
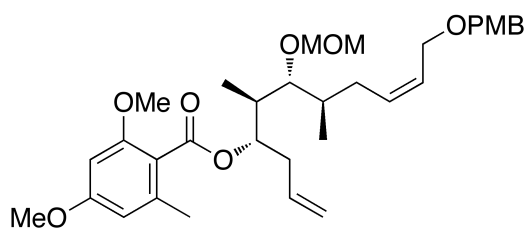
(4S,5R,6R,7R,Z)-11-((4-methoxybenzyl)oxy)-6-(methoxymethoxy)-5,7-dimethylundeca-1,9-dien-4-yl 2,4-dimethoxy-6-methylbenzoate, 59

A 25 mL flask was flame dried and flushed with argon before DCM (10 mL) and 2,4-dimethoxy-6-methylbenzoic acid (590 mg, 3.06 mmol, 3 eq.) were added. The suspension was cooled to 0 °C and oxalyl bromide (300 μL, 3.20 mmol, 3.1 eq.) was added dropwise. The suspension was allowed to warm to rt and stirred until all solid was dissolved at which point 4 drops of anhydrous DMF was added. Stirring was continued at rt for 1 h and the solution was cooled 0 °C before DIPEA (1.12 mL, 6.40 mmol, 6.2 eq.) was added. Stirring was continued at 0 °C for 30 min before a solution of alcohol **37** (400 mg, 1.02 mmol, 1 eq.) in DCM (1.00 mL) and DMAP (250 mg, 2.04 mmol, 2 eq.) were added. The reaction mixture was allowed to warm to rt and stirring was continued for 30 min at which point the reaction was quenched by the addition of

deionized water (10 mL). The organic layer was collected and the aqueous layer was extracted with DCM (4 X, 15 mL). The combined organic layers were dried over anhydrous sodium sulfate and solvent was removed to afford a brown oil that was purified by SiO_2 flash chromatography (15 % – 20 % EtOAc in hexanes) to provide ester **59** as a faint yellow oil (530 mg, 91%). $[\alpha]^{25}_D = 2.8°$ (c = 0.074, DCM). ^{1}H NMR (500 MHz, CDCl$_3$) δ 7.31 – 7.24 (m, 2H), 6.90 – 6.84 (m, 2H), 6.32 – 6.27 (m, 2H), 5.84 (ddt, J = 17.1, 10.1, 7.1 Hz, 1H), 5.70 – 5.62 (m, 1H), 5.62 – 5.54 (m, 1H), 5.26 (m, 1H), 5.13 (ddt, J = 17.2, 1.8, 1.4 Hz, 1H), 5.09 (ddt, J = 10.2, 1.8, 0.98 Hz, 1H), 4.65 (d, J = 6.8 Hz, 1H), 4.63 (d, J = 6.8 Hz, 1H) 4.44 (s, 2H), 4.05 (d, J = 6.3 Hz, 2H), 3.80 (s, 3H), 3.80 (s, 3H), 3.77 (s, 3H), 3.43 (s, 3H), 3.33 (t, J = 5.1 Hz, 1H), 2.59 – 2.47 (m, 2H), 2.29 (s, 3H), 2.25 – 2.20 (m, 1H), 2.04 – 1.95 (m, 1H), 1.95 – 1.82 (m, 2H), 1.03 (d, J = 6.8 Hz, 3H), 0.87 (d, J = 6.5 Hz, 3H). ^{13}C NMR (126 MHz, CDCl$_3$) δ 168.15, 161.24, 159.25, 158.02, 138.03, 133.96, 132.26, 130.56, 129.56, 127.59, 118.09, 117.07, 113.86, 106.55, 98.75, 96.16, 84.64, 75.25, 72.00, 65.76, 56.33, 55.64, 55.50, 55.40, 37.88, 36.61, 36.14, 29.91, 20.14, 16.83, 10.13. HRMS (ESI, *m/z*): calcd for $[C_{33}H_{46}O_8]^+$, ($[M + K]^+$): 609.2830, found 609.2824.
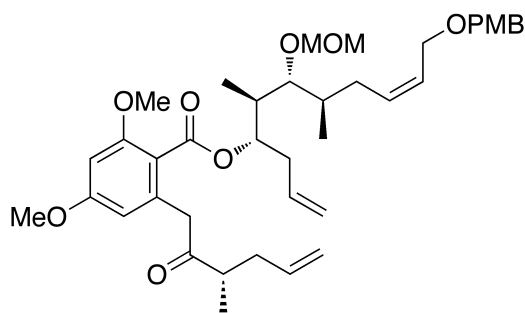
(4*S*,5*R*,6*R*,7*R*,*Z*)-11-((4-methoxybenzyl)oxy)-6-(methoxymethoxy)-5,7-dimethylundeca-1,9-dien-4-yl 2,4-dimethoxy-6-((*S*)-3-methyl-2-oxohex-5-en-1-yl)benzoate, 68

A 10 mL flask was flame dried and flushed with argon before THF (0.2 mL) and ester **59** (100 mg, 0.18 mmol, 1 eq.) were added. The solution was cooled to -78 °C before a 1 M solution of

lithium diisopropylamide (370 μL, 0.37 mmol, 2.1 eq.) in THF was added dropwise. Stirring was continued at -78 °C for 5 min at which point weinreb amide **47** (70 mg, 0.44 mmol, 2.5 eq.) in THF (100 μL) was quickly added. The solution was stirred for 5 min at -78 °C and the reaction was quenched by the addition of half saturated aqueous ammonium chloride (1 mL). The biphasic mixture was allowed to warm to rt while stirring continued. The organic layer was collected, and the aqueous layer was extracted with EtOAc (4 X, 1 mL). The combined organic layers were dried over anhydrous sodium sulfate and solvent was removed under reduced pressure to afford a colorless oil that was purified by SiO_2 flash chromatography (15 % – 25 % EtOAc in hexanes) to provide compound **68** as a colorless oil (100 mg, 83 %). $[\alpha]^{25}_D = 8.6°$ (c = 0.002, DCM). ^{1}H NMR (500 MHz, CDCl$_3$) δ 7.30 – 7.24 (m, 2H), 6.89 – 6.85 (m, 2H), 6.38 (d, J = 2.2 Hz, 1H), 6.26 (d, J = 2.2 Hz, 1H), 5.90 – 5.79 (m, 1H), 5.77 – 5.68 (m, 1H), 5.68 – 5.62 (m, 1H), 5.62 – 5.54 (m, 1H), 5.26 – 5.19 (m, 1H), 5.15 – 4.98 (m, 4H), 4.68 – 4.60 (m, 2H), 4.44 (s, 2H), 4.05 (d, J = 6.3 Hz, 2H), 3.80 (s, 3H), 3.79 (s, 3H), 3.79 (s, 3H), 3.83 – 3.72 (m, 2H), 3.42 (s, 3H), 3.34 (t, J = 5.2 Hz, 1H), 2.72 (m, 1H), 2.58 – 2.44 (m, 2H), 2.45 – 2.37 (m, 1H), 2.26 – 2.18 (m, 1H), 2.14 – 2.04 (m, 1H), 1.99 (m, 1H), 1.95 – 1.78 (m, 2H), 1.08 (d, J = 7.0 Hz, 3H), 1.02 (d, J = 6.8 Hz, 3H), 0.87 (d, J = 6.7 Hz, 3H). ^{13}C NMR (126 MHz, CDCl$_3$) δ 210.14, 167.72, 161.60, 159.30, 158.89, 135.89, 135.65, 134.15, 132.23, 130.62, 129.54, 127.62, 117.98, 116.97, 113.90, 107.25, 98.78, 97.74, 84.63, 75.37, 72.01, 65.80, 56.29, 55.69, 55.56, 55.41, 46.64, 45.24, 37.86, 37.21, 36.67, 36.14, 29.89, 16.89, 16.19, 10.10. HRMS (ESI, *m/z*): calcd for $[C_{39}H_{54}O_9]^+$, $([M + Na]^+)$: 689.3666, found 689.3662.
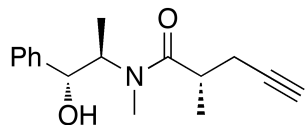
(*S*)-*N*-((1*R*,2*R*)-1-hydroxy-1-phenylpropan-2-yl)-*N*,2-dimethylpent-4-ynamide, 71

A 250 mL flask was flame dried and flushed with argon before anhydrous THF (17 mL), anhydrous lithium chloride (3 g, 68 mmol, 5 eq.), and DIPA (4.4 mL, 31 mmol, 2.25 eq.) were added. The suspension was cooled to -78 °C, butyllithium (2.5 M in hexanes, 11.3 mL, 28 mmol, 2.08 eq.) was added, and stirring was continued as the solution was briefly warmed to 0 °C and then cooled back to -78 °C. An ice cooled solution of *R,R*-pseudoephedrinepropionamide (3 g, 13.6 mmol, 1 eq.) in anhydrous THF (43 mL) was added *via* cannula followed by a wash with THF (5 mL). Stirring was continued at -78 °C for 2 h, 0 °C for 30 min, and rt for 5 min, before the reaction mixture was finally cooled to 0 °C. Propargyl bromide (80% in toluene, 3.03 g, 20.4 mmol, 1.5 eq.) was then added in one portion, and the reaction mixture was stirred for 2 h at 0 °C. Reaction was quenched at 0 °C by the addition of saturated aqueous ammonium chloride (2 mL) and the mixture was partitioned between saturated aqueous ammonium chloride (130 mL) and EtOAc (50 mL). The organic layer was collected and the aqueous layer was extracted with EtOAc (3 X, 50 mL). The combined organic layers were dried over anhydrous sodium sulfate and solvent was removed under reduced pressure to afford a yellow oil that was purified by SiO_2 flash chromatography (30 % EtOAc in hexanes) to provide pure **71** as a colorless oil (94 %). Diastereoselectivity (>20:1) was assessed using Myers oxazolium technique (*vide infra*). $[\alpha]^{25}_D$ = -69.5° (c = 0.029, DCM). (*Denotes minor rotamer peak) ^{1}H NMR (500 MHz, CDCl$_3$) δ 7.41 – 7.31 (m, 5H), *7.29 – 7.24 (m, 5H), 4.66 – 4.61 (m, 1H), 4.59 (d, *J* = 8.5 Hz, 1H), 4.48 (bs, 1H), *4.39 (bs, 1H), *4.20 – 3.95 (m, 1H), *4.09 – 4.04 (m, 1H), *3.15 – 3.06 (m, 1H), 2.92 (s, 3H), *2.90 (s, 3H), 2.97 – 2.80 (m, 1H), *2.51 (ddd, *J* = 16.8, 6.8, 2.7 Hz, 1H), 2.45 (ddd, *J* = 16.8,

6.8, 2.7 Hz, 1H), *2.37 (ddd, J = 16.8, 8.0, 2.6 Hz, 1H), 2.29 (ddd, J = 16.8, 7.6, 2.6 Hz, 1H),

*1.99 (t, J = 2.6 Hz, 1H), 1.96 (t, J = 2.6 Hz, 1H), 1.19 (d, J = 6.8 Hz, 1H), *1.16 (d, J = 7.0 Hz,

1H), 1.11 (d, J = 6.6 Hz, 3H), *1.04 (d, J = 6.8 Hz, 3H). ^{13}C NMR (126 MHz, CDCl$_3$) δ 177.22,

*177.14, 142.43, *140.99, 128.55, *128.47, 127.86, *127.79, 126.52, *126.49, *83.42, 82.61,

76.62, *76.32, *75.62, 69.57, 69.50, *58.29, 36.62, *35.91, 23.21, *23.19, 23.11, *17.11, 17.06,

14.55, *14.50. HRMS (ESI, m/z): calcd for [C$_{16}$H$_{21}$NO$_2$]$^+$, ([M + Na]$^+$): 282.1470, found

282.1469.
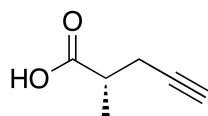
(S)-2-methylpent-4-ynoic acid, 72

A 500 mL flask was charged with *tert*-butanol (42 mL) and deionized water (136 mL) before

amide **71** (3.53 g, 13.6 mmol, 1 eq.) and tetrabutylammonium hydroxide (1.5 M in deionized

water, 50 mL, 68 mmol, 5 eq.) were added. The solution was heated at reflux for 23 h. Once the

reaction was complete, the solution was allowed to cool to rt and suspended between 0.5 M

aqueous sodium hydroxide (1.76 L) and diethyl ether (250 mL). The organic layer was removed,

and the aqueous layer was extracted with diethyl ether (3 X, 250 mL). The aqueous layer was

cooled to 0 °C, saturated with sodium chloride, and acidified to pH 2 with 4 N aqueous

hydrochloric acid. The acid solution was extracted with diethyl ether (4 X, 300 mL) and the

combined organic extracts were dried over anhydrous sodium sulfate. Solvent was removed

under reduced pressure to afford pure acid **72** as a colorless liquid (1.43 g, 94%). [α]$^{25}_D$ = -1.23°

(c = 0.269, DCM). ^{1}H NMR (500 MHz, CDCl$_3$) δ 9.09 (s, 1H), 2.76 – 2.64 (m, 1H), 2.56 (ddd, J

= 16.8, 6.0, 2.7 Hz, 1H), 2.39 (ddd, J = 16.8, 7.6, 2.7 Hz, 1H), 2.02 (t, J = 2.7 Hz, 1H), 1.31 (d, J

= 7.1 Hz, 3H). ^{13}C NMR (126 MHz, CDCl$_3$) δ 180.87, 81.32, 70.24, 38.67, 22.45, 16.27. HRMS (ESI, *m/z*): calcd for [C$_6$H$_8$O$_2$]$^-$, ([2M + Na – 2H]$^-$): 245.0790, found 245.0790.
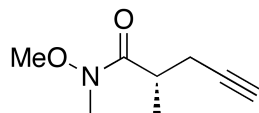
**(*S*)-*N*-methoxy-*N*,2-dimethylpent-4-ynamide, 73**

A 100 mL flask was flame dried and flushed with argon before DMF (20 mL), acid **72** (mg, 10.5 mmol, 1 eq.), and DIPEA (2.4 mL, 22.1 mmol, 2.1 eq.) were added. COMU (3.13 g, 11.6 mmol, 1.1 eq.) was then added in one portion and the reaction mixture was stirred at rt for 45 min at which point *N,O*-Dimethylhydroxylamine hydrochloride (1.3 g, 21 mmol, 2 eq.) was added. Stirring was continued for 1 hr and the reaction was quenched by the careful addition of saturated aqueous sodium bicarbonate (15 mL). The resulting slurry was then extracted with EtOAc (5 X, 30 mL) and the combined organic portions were dried over anhydrous sodium sulfate. Solvent was removed under reduced pressure to afford a red oil that was purified by SiO$_2$ flash chromatography (5 % – 15% EtOAc in hexanes) to provide pure amide **73** as a colorless oil. [α]^{25}$_D$ = 11.2° (c = 0.038, DCM). ^{1}H NMR (500 MHz, CDCl$_3$) δ 3.71 (s, 3H), 3.19 (s, 3H), 3.15 – 3.01 (m, 1H), 2.52 (ddd, *J* = 16.7, 7.1, 2.6 Hz, 1H), 2.28 (ddd, *J* = 16.7, 7.5, 2.7 Hz, 1H), 1.97 (t, *J* = 2.7 Hz, 1H), 1.20 (d, *J* = 6.9 Hz, 3H). ^{13}C NMR (126 MHz, CDCl$_3$) δ 176.03, 82.65, 69.47, 61.72, 35.32, 32.28, 22.68, 17.10. HRMS (ESI, *m/z*): calcd for [C$_8$H$_{13}$NO$_2$]$^+$, ([M + Na]$^+$): 178.0844, found 178.0843.
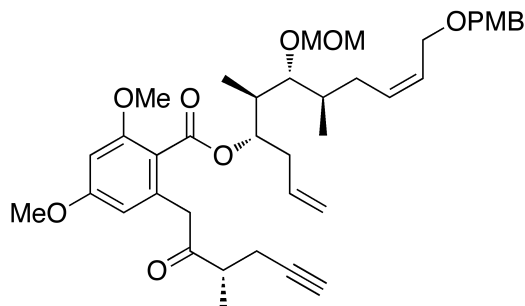
(4*S*,5*R*,6*R*,7*R*,*Z*)-11-((4-methoxybenzyl)oxy)-6-(methoxymethoxy)-5,7-dimethylundeca-1,9-dien-4-yl 2,4-dimethoxy-6-((*S*)-3-methyl-2-oxohex-5-yn-1-yl)benzoate, 74

A 10 mL flask was flame dried and flushed with argon before THF (0.2 mL) and ester **59** (100 mg, 0.18 mmol, 1 eq.) were added. The solution was cooled to -78 °C before a 1 M solution of freshly prepared lithium diisopropylamide (370 μL, 0.37 mmol, 2.1 eq.) in THF was added dropwise. Stirring was continued at -78 °C for 5 min at which point weinreb amide **73** (70 mg, 0.44 mmol, 2.5 eq.) in THF (100 μL) was quickly added. The solution was stirred for 5 min at -78 °C and the reaction was quenched by the addition of half saturated aqueous ammonium chloride (1 mL). The biphasic mixture was allowed to warm to rt while stirring continued. The organic layer was collected, and the aqueous layer was extracted with EtOAc (4 X, 1 mL). The combined organic layers were dried over anhydrous sodium sulfate and solvent was removed under reduced pressure to afford a colorless oil that was purified by SiO_2 flash chromatography (15 % – 25 % EtOAc in hexanes) to provide compound **74** as a colorless oil (74 %). $[\alpha]^{25}_D = 4.2°$ (c = 0.002, DCM). ^{1}H NMR (500 MHz, CDCl$_3$) δ 7.32 – 7.22 (m, 2H), 6.91 – 6.85 (m, 2H), 6.39 (d, *J* = 2.2 Hz, 1H), 6.29 (d, *J* = 2.1 Hz, 1H), 5.90 – 5.77 (m, 1H), 5.70 – 5.62 (m, 1H), 5.58 (m, 1H), 5.22 (m, 1H), 5.11 (m, 2H), 4.68 – 4.59 (m, 2H), 4.44 (s, 2H), 4.05 (d, *J* = 6.3 Hz, 2H), 3.88 – 3.71 (m, 2H), 3.80 (s, 6H), 3.79 (s, 3H), 3.42 (s, 3H), 3.36 – 3.32 (m, 1H), 2.91 – 2.81 (m, 1H), 2.58 – 2.43 (m, 3H), 2.34 – 2.19 (m, 2H), 1.98 (m, 1H), 1.97 (t, *J* = 2.7 Hz, 1H), 1.95 – 1.87 (m, 1H), 1.84 (m, 1H), 1.22 (d, *J* = 7.1 Hz, 3H), 1.02 (d, *J* = 6.8 Hz, 3H), 0.87 (d, *J* = 6.8 Hz, 3H).

^{13}C NMR (126 MHz, CDCl$_3$) δ 208.81, 167.69, 161.71, 159.30, 159.03, 135.63, 134.16, 132.21, 130.62, 129.54, 127.63, 117.99, 113.90, 107.48, 100.13, 98.77, 97.83, 84.60, 77.37, 75.41, 72.02, 69.94, 65.80, 56.31, 55.71, 55.57, 55.42, 46.65, 44.58, 37.88, 36.69, 32.08, 31.10, 21.86, 16.88, 16.30, 10.11. HRMS (ESI, *m/z*): calcd for [C$_{39}$H$_{52}$O$_9$]$^+$, ([M + Na]$^+$): 687.3509, found 687.3511.
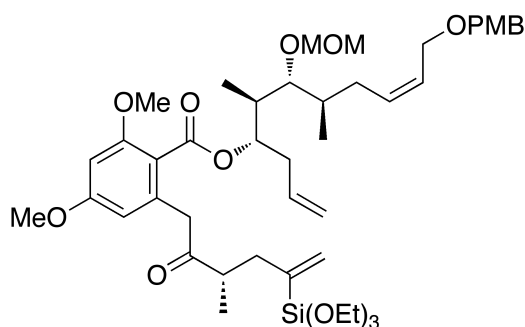
(4S,5R,6R,7R,Z)-11-((4-methoxybenzyl)oxy)-6-(methoxymethoxy)-5,7-dimethylundeca-1,9-dien-4-yl 2,4-dimethoxy-6-((S)-3-methyl-2-oxo-5-(triethoxysilyl)hex-5-en-1-yl)benzoate, 75

A 5 mL flask was flame dried and flushed with argon before DCM (200 μL), compound **74** (10 mg, 0.015 mmol, 1 eq.), and triethoxysilane (4 μL, 0.018 mmol, 1.2 eq.) were added. The solution was cooled to 0 °C, Pentamethylcyclopentadienyltris (acetonitrile)ruthenium(II) hexafluorophosphate (0.1 mg, 0.00015 mmol, 0.01 eq.) was added and stirring was continued for 3 h. Solvent was removed under reduced pressure to afford a brown oil that was purified by SiO$_2$ flash chromatography (10 % EtOAc in hexanes) to provide pure vinyl silane **75** as a colorless oil (97 %). [α]$^{25}_D$ = 6.3° (c = 0.001, DCM). ^{1}H NMR (500 MHz, CDCl$_3$) δ 7.27 (m, 2H), 6.91 – 6.84 (m, 2H), 6.37 (d, *J* = 2.2 Hz, 1H), 6.25 (d, *J* = 2.2 Hz, 1H), 5.84 (m, 1H), 5.73 – 5.53 (m, 4H), 5.19 (m, 1H), 5.10 (m, 2H), 4.65 (d, *J* = 6.9 Hz, 1H), 4.63 (d, *J* = 6.8 Hz, 1H), 4.44 (s, 2H), 4.05 (d, *J* = 6.2 Hz, 2H), 3.92 – 3.76 (m, 2H), 3.82 (q, *J* = 7.0 Hz, 6H), 3.80 (s, 3H), 3.79 (s, 3H), 3.78 (s, 3H), 3.41 (s, 3H), 3.35 (m, 1H), 2.99 – 2.91 (m, 1H), 2.61 (dd, *J* = 13.9, 5.8 Hz, 1H), 2.57 – 2.43 (m, 2H), 2.24 – 2.18 (m, 1H), 2.10 – 2.03 (m, 1H), 1.99 (m, 1H), 1.95 – 1.87 (m, 1H), 1.87

– 1.79 (m, 1H), 1.23 (t, J = 7.0 Hz, 9H), 1.05 (d, J = 6.9 Hz, 3H), 1.02 (d, J = 6.8 Hz, 3H), 0.87 (d, J = 6.8 Hz, 3H). ^{13}C NMR (126 MHz, CDCl$_3$) δ 210.29, 167.64, 161.56, 158.93, 155.59, 141.29, 136.09, 134.21, 132.28, 131.51, 130.63, 129.54, 127.58, 117.90, 116.83, 113.90, 107.51, 98.80, 97.62, 84.66, 77.37, 75.20, 72.01, 65.82, 58.72, 56.28, 55.67, 55.50, 55.41, 46.64, 44.54, 39.55, 37.78, 36.07, 31.10, 29.85, 18.39, 16.90, 16.18, 10.08. HRMS (ESI, m/z): calcd for [C$_{45}$H$_{68}$O$_{12}$Si]$^+$, ([M + Na]$^+$): 851.4378, found 851.4377.
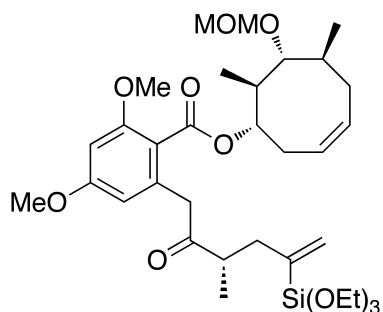
(1S,6S,7R,8R,Z)-7-(methoxymethoxy)-6,8-dimethylcyclooct-3-en-1-yl 2,4-dimethoxy-6-((S)-3-methyl-2-oxo-5-(triethoxysilyl)hex-5-en-1-yl)benzoate, 76

A 10 mL flask was flame dried and flushed with argon before anhydrous toluene (6 mL) and vinyl siloxane **75** (10 mg, 0.012 mmol, 1 eq.) were added. After addition of dichloro[1,3-Bis(2-methylphenyl)-2-imidazolidinylidene](benzylidene)(tricyclohexylphosphine)ruthenium(II)   (2 mg, 0.0024 mmol, 0.2 eq.), high vacuum was applied to the reaction flask for 5 min and subsequently recharged with argon. After repeating this operation cycle 5 times, the reaction mixture was warmed to 35 °C and vigorously stirred. Progress of the reaction was monitored by TLC (20 % EtOAc in hexanes) at 20 min intervals until complete consumption of starting material was observed (2.5 h), at which point the solution was filtered through a plug of SiO$_2$ that was thoroughly washed with EtOAc (100 mL). Solvent was removed under reduced pressure to afford a yellow oil that was purified by SiO$_2$ flash chromatography (10 % EtOAc in hexanes) to provide major cyclic product **76** (69 %). No desired product was identified after spectral

analysis (ESI MS and ^{1}H NMR) of minor components. ^{1}H NMR (500 MHz, CDCl$_3$) δ 6.37 (d, J = 2.2 Hz, 1H), 6.26 (d, J = 2.2 Hz, 1H), 5.83 – 5.65 (m, 4H), 4.87 (ddd, J = 7.5, 6.0, 3.7 Hz, 1H), 4.62 (d, J = 6.8 Hz, 1H), 4.57 (d, J = 6.8 Hz, 1H), 4.00 – 3.74 (m, 2H), 3.82 (q, J = 7.0 Hz, 6H), 3.79 (s, 3H), 3.78 (s, 3H), 3.63 (dd, J = 6.0, 2.8 Hz, 1H), 3.37 (s, 3H), 2.99 – 2.91 (m, 1H), 2.62 (dd, J = 13.9, 5.9 Hz, 1H), 2.54 – 2.42 (m, 2H), 2.38 – 2.16 (m, 3H), 2.15 – 2.01 (m, 2H), 1.23 (t, J = 7.0 Hz, 9H), 1.05 (d, J = 6.9 Hz, 3H), 0.98 (d, J = 7.2 Hz, 3H), 0.96 (d, J = 6.4 Hz, 3H). ^{13}C NMR (126 MHz, CDCl$_3$) δ 210.19, 167.75, 161.53, 158.81, 141.27, 135.71, 131.53, 127.31, 117.16, 107.48, 97.63, 96.45, 78.82, 78.26, 58.73, 55.79, 55.51, 46.46, 44.50, 39.63, 36.32, 30.96, 30.10, 29.85, 18.39, 16.16, 16.14, 13.76. HRMS (ESI, m/z): calcd for $[C_{34}H_{54}O_{10}Si]^+$, ([M + Na]$^+$): 673.3384, found 673.3383.
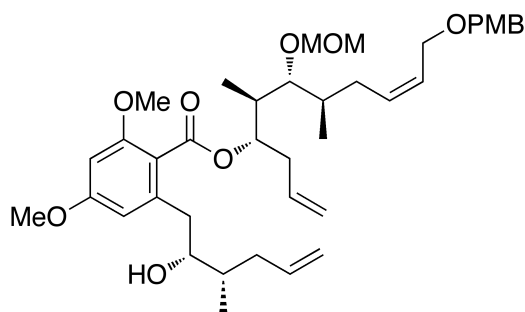
(4S,5R,6R,7R,Z)-11-((4-methoxybenzyl)oxy)-6-(methoxymethoxy)-5,7-dimethylundeca-1,9-dien-4-yl 2-((2R,3S)-2-hydroxy-3-methylhex-5-en-1-yl)-4,6-dimethoxybenzoate, 77

A 1 dram vial was flushed with argon before DCM (100 μL), deionized water (100 μL), compound **68** (10 mg, 0.015 mmol, 1 eq.), tetrabutylammonium chloride (2 mg, 0.0075 mmol, 0.5 eq.), and sodium formate (10.2 mg, 0.15 mmol, 10 eq.) were added. The resultant suspension was cooled to 5 °C and RuCl[(S,S)-Tsdpen](p-cymene) (0.5 mg, 0.00075 mmol, 0.05 eq.) was added. Stirring was continued at 5 °C for 48 h at which point the reaction mixture was diluted with deionized water (0.5 mL) and EtOAc (0.5 mL). The organic layer was collected and the aqueous layer was extracted with EtOAc (7 X, 0.75 mL). The combined organic layers were

dried over anhydrous sodium sulfate and solvent was removed under reduced pressure to afford an orange oil that was purified by SiO$_2$ flash chromatography (15 % – 25 % EtOAc in hexanes) to provide alcohol **77**, 5:1 mixture of alcohol epimers, as a colorless oil (9.5 mg, 91 %). Stereochemistry of the major alcohol epimer was confirmed using Mosher ester analysis. $[\alpha]^{25}_{D}$ = 10.7° (c = 0.001, DCM). ^{1}H NMR (500 MHz, CDCl$_3$) (Major product peaks are reported) δ 7.31 – 7.21 (m, 2H), 6.91 – 6.84 (m, 2H), 6.36 (d, *J* = 2.3 Hz, 1H), 6.34 (d, *J* = 2.1 Hz, 1H), 5.94 – 5.74 (m, 2H), 5.70 – 5.52 (m, 2H), 5.31 – 5.23 (m, 1H), 5.18 – 4.96 (m, 4H), 4.67 – 4.58 (m, 2H), 4.44 (s, 2H), 4.05 (d, *J* = 6.3 Hz, 2H), 3.81 (s, 3H), 3.80 (s, 3H), 3.78 (s, 3H), 3.67 – 3.60 (m, 1H), 3.42 (s, 3H), 3.32 – 3.28 (m, 1H), 2.80 (dd, *J* = 13.6, 2.9 Hz, 1H), 2.59 – 2.43 (m, 2H), 2.39 – 2.28 (m, 1H), 2.28 – 2.17 (m, 1H), 2.06 – 1.93 (m, 3H), 1.92 – 1.87 (m, 1H), 1.86 – 1.79 (m, 1H), 1.76 – 1.68 (m, 1H), 0.99 (d, *J* = 6.9 Hz, 3H), 0.95 (d, *J* = 6.8 Hz, 3H), 0.86 (d, *J* = 6.7 Hz, 3H). ^{13}C NMR (126 MHz, CDCl$_3$) δ 169.22, 161.85, 159.30, 158.61, 140.70, 137.74, 133.92, 132.09, 130.59, 129.54, 127.70, 118.04, 117.12, 115.96, 113.90, 106.36, 98.62, 97.10, 84.32, 77.37, 76.26, 72.02, 65.76, 56.30, 55.68, 55.54, 55.41, 39.35, 37.69, 37.65, 37.19, 36.46, 36.45, 30.10, 16.73, 15.17, 10.14. HRMS (ESI, *m/z*): calcd for $[C_{39}H_{56}O_9]^{+}$, $([M + K]^{+})$: 707.3561, found 707.3562.
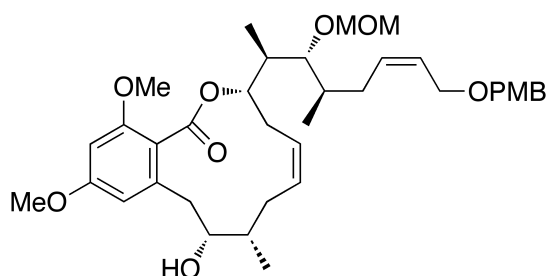
(3*S*,8*S*,9*R*,*Z*)-9-hydroxy-12,14-dimethoxy-3-((2*R*,3*R*,4*R*,*Z*)-8-((4-methoxybenzyl)oxy)-3-(methoxymethyl)-4-methyloct-6-en-2-yl)-8-methyl-3,4,7,8,9,10-hexahydro-1*H*-benzo[*c*][1]oxacyclododecin-1-one, 78

A 250 mL flask was flame dried and flushed with argon before DCM (150 mL) and alcohol **77** (50 mg, 0.0075 mmol, 1 eq.) were added. The solution was cooled to 0 °C and Grubbs second generation catalyst (3.4 mg, 0.004 mmol, 0.05 eq.) was added. The reaction mixture was allowed to warm to rt and stirring continued for 4 h at which point the reaction was quenched by the addition of saturated aqueous potassium carbonate (10 mL). Solvent was removed under reduced pressure and the resultant slurry was diluted with DCM (10 mL). The organic layer was collected and the aqueous layer was extracted with DCM (5 X, 10 mL). The combined organic layers were dried over anhydrous sodium sulfate and solvent was removed under reduced pressure to afford a brown oil that was purified by SiO_2 flash chromatography (30 % EtOAc in hexanes) to provide macrocycle **78**, 3:1 mixture of *cis*:*trans* isomers at allylic ether olefin, as a colorless oil (63%). $[\alpha]^{25}_D$ = 9.9° (c = 0.001, DCM). (*Denotes minor *trans* allylic ether product) ^{1}H NMR (500 MHz, CDCl$_3$) δ 7.29 – 7.25 (m, 2H), 6.87 (m, 2H), 6.36 (d, J = 2.1 Hz, 1H), 6.34 (d, J = 2.0 Hz, 1H), 5.71 – 5.56 (m, 2H), 5.56 – 5.44 (m, 2H), 5.40 – 5.31 (m, 1H), 4.67 – 4.57 (m, 2H), 4.44 (s, 2H), *4.43 (s, 2H), 4.05 (d, J = 6.1 Hz, 2H), *3.94 (d, J = 5.8 Hz, 2H), 3.81 (s, 3H), 3.80 (s, 3H), 3.77 (s, 3H), 3.75 (bs, 1H), *3.43 (s, 3H), 3.42 (s, 3H), *3.31 – 3.28 (m, 1H), 3.27 (t, J = 5.0 Hz, 1H), 3.00 (m, 1H), 2.78 – 2.56 (m, 3H), *2.55 – 2.45 (m, 1H), 2.44 – 2.18 (m, 3H), 2.06 – 1.75 (m, 4H), 1.06 (d, J = 6.8 Hz, 3H), *1.01 (d, J = 6.8 Hz, 3H), 1.00 (d, J = 6.8 Hz, 3H), *0.90 (d, J = 6.6 Hz, 3H), 0.89 (d, J = 6.5 Hz, 3H). ^{13}C NMR (126 MHz, CDCl$_3$) δ 166.58, 161.45, 159.23, 158.77, 139.41, 133.31, 132.23, 130.57, 129.57, *128.98, 128.25, 127.59, 113.86, 104.02, 98.81, 98.73, 97.19, 84.94, 84.69, 77.37, *72.00, 71.68, 70.68, 65.71, *60.57, 56.39, *55.99, 55.54, 55.41, *55.40, 53.60, 38.15, 36.27, 35.96, 35.01, *34.44, *33.27, 32.07, 30.07, 29.85, 16.68, 14.34, *14.30, 10.45, *10.39. HRMS (ESI, *m/z*): calcd for [C$_{37}$H$_{52}$O$_9$]$^+$, ([M + Na]$^+$): 663.3509, found 663.3514.
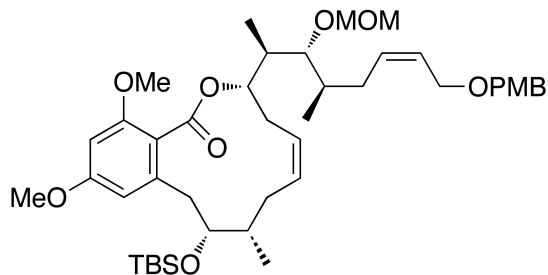
(3*S*,8*S*,9*R*,*Z*)-9-((*tert*-butyldimethylsilyl)oxy)-12,14-dimethoxy-3-((2*R*,3*R*,4*R*,*Z*)-8-((4-methoxybenzyl)oxy)-3-(methoxymethoxy)-4-methyloct-6-en-2-yl)-8-methyl-3,4,7,8,9,10-hexahydro-1*H*-benzo[*c*][1]oxacyclododecin-1-one, 79

A 5 mL flas was flame dried and flush with argon before DCM (500 μL), compound **78** (27 mg, 0.042 mmol, 1 eq.), and 2,6-lutidine (17 μL, 0.14 mmol, 3.2 eq.) were added. The solution was cooled to 0 °C and *tert*-butyldimethylsilyl trifluoromethanesulfonate (TBSOTf) (30 μL, 0.13 mmol, 3 eq.) was added dropwise over 5 min. Stirring was continued for 30 min as the reaction mixture was allowed to reach rt at which point saturated aqueous ammonium chloride (500 μL) was added to quench. The organic layer was collected and the aqueous layer was extracted with DCM (5 X, 500 μL). The combined organic layers were dried over anhydrous sodium sulfate and solvent was removed under reduced pressure to afford a yellow oil that was purified by SiO_2 flash chromatography (10 % – 15 % EtOAc in hexanes) to provide pure **79** as a colorless oil (30 mg, 94%). $[\alpha]^{25}_D = 5.3°$ (c = 0.003, DCM). (*Denotes minor *trans* allylic ether product) ^{1}H NMR (500 MHz, CDCl$_3$) δ 7.27 (m, 2H), 6.88 (m, 2H), 6.32 (d, *J* = 2.1 Hz, 1H), 6.30 (d, *J* = 2.1 Hz, 1H), 5.73 – 5.52 (m, 3H), 5.33 (m, 2H), 4.65 – 4.55 (m, 2H), 4.44 (s, 2H), *4.43 (s, 2H), 4.05 (d, *J* = 5.1 Hz, 2H), *3.95 (d, *J* = 6.0 Hz, 2H), *3.80 (s, 3H), 3.80 (s, 3H), 3.79 (s, 3H), 3.77 (bs, 1H), 3.74 (s, 3H), *3.42 (s, 3H), 3.40 (s, 3H), *3.26 – 3.23 (m, 1H), 3.23 – 3.20 (m, 1H), 3.13 (m, 1H), 2.65 (m, 1H), 2.35 – 2.08 (m, 4H), 2.00 – 1.81 (m, 5H), 1.01 (d, *J* = 6.4 Hz, 3H), 0.99 (d, *J* = 6.4 Hz, 3H), *0.91 (d, *J* = 6.6 Hz, 3H), 0.89 (d, *J* = 6.6 Hz, 3H), 0.76 (s, 9H), -0.19 (s,

3H), -0.60 (s, 3H). ^{13}C NMR (126 MHz, CDCl$_3$) δ 166.47, 160.65, 159.32, 158.78, 140.70, 132.36, *130.73, 130.69, 129.59, 129.53, *128.20, 127.94, *127.72, 127.55, 113.92, 109.33, 98.97, *98.92, 97.30, 85.40, *85.23, 72.74, 71.99, 71.68, 70.74, 65.78, 56.35, 56.23, *55.42, 55.41, 55.39, 40.44, 40.25, *36.15, 36.09, 35.77, 34.16, 32.34, 32.19, *29.84, 29.79, 29.62, 25.97, 17.97, 17.04, *10.56, 10.52, -5.01, -5.67. HRMS (ESI, *m/z*): calcd for [C$_{43}$H$_{66}$O$_9$Si]$^+$, ([M + Na]$^+$): 777.4374, found 777.4367.
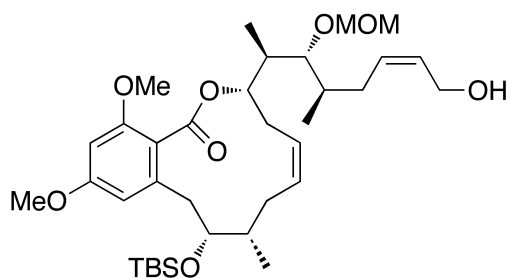
(3*S*,8*S*,9*R*,*Z*)-9-((*tert*-butyldimethylsilyl)oxy)-3-((2*R*,3*R*,4*R*,*Z*)-8-hydroxy-3-(methoxymethyl)-4-methyloct-6-en-2-yl)-12,14-dimethoxy-8-methyl-3,4,7,8,9,10-hexahydro-1*H*-benzo[*c*][1]oxacyclododecin-1-one, 81

A 1 dram vial was charged with DCM (400 μL), deionized water (25 μL), and compound **79** (25 mg, 0.033 mmol, 1 eq.). The solution was stirred at rt and 2,3-dichloro-5,6-dicyano-1,4-benzoquinone (DDQ) (12 mg, 0.05 mmol, 1.5 eq.) was added at once. The reaction mixture was stirred at rt for 45 min and quenched by the addition of saturated aqueous sodium bicarbonate (700 μL). The organic layer was collected and the aqueous layer was extracted with DCM (5 X, 1 mL). The combined organic layers were dried over anhydrous sodium sulfate and solvent was removed under reduced pressure to afford a red oil that was purified by SiO$_2$ flash chromatography (10 % – 35 % EtOAc in hexanes) to provide pure **81** as a colorless oil (18 mg, 86 %). [α]$^{25}_D$ = 8.7° (c = 0.001, DCM). (*Denotes minor *trans* allylic ether product) ^{1}H NMR (500 MHz, CDCl$_3$) δ 6.32 (d, *J* = 2.2 Hz, 1H), 6.30 (d, *J* = 2.2 Hz, 1H), 5.73 – 5.53 (m, 3H), 5.34

(m, 2H), 4.60 (m, 2H), 4.19 (ddd, J = 30.1, 12.7, 6.9 Hz, 2H), *4.09 (d, J = 3.1 Hz, 2H), 3.79 (s, 3H), 3.76 (bs, 1H), *3.75 (s, 3H), 3.74 (s, 3H), 3.40 (s, 3H), *3.39 (s, 3H), *3.27 (t, J = 4.5 Hz, 1H), 3.25 – 3.21 (m, 1H), 3.12 (dd, J = 12.6, 5.3 Hz, 1H), 2.76 – 2.61 (m, 1H), 2.34 – 2.07 (m, 4H), 2.03 – 1.82 (m, 5H), 1.01 (d, J = 6.4 Hz, 3H), 1.01 (d, J = 6.7 Hz, 3H), 0.93 (d, J = 6.5 Hz, 3H), *0.91 (d, J = 6.4 Hz, 3H), 0.76 (s, 9H), -0.19 (s, 3H), -0.60 (s, 3H). ^{13}C NMR (126 MHz, CDCl$_3$) δ 166.60, 160.72, 158.80, 140.77, 131.93, *131.87, 130.85, 129.74, 109.42, 99.00, 98.74, 97.33, 85.55, 84.60, 72.78, 63.93, 58.67, *56.33, 56.26, 55.40, *40.58, 40.23, *36.09, 36.06, *34.65, *34.19, 34.15, 32.20, *29.85, 29.33, 25.98, 22.09, 17.97, 17.31, 16.75, 13.76, 10.60, *10.57, -5.00, -5.66. HRMS (ESI, *m/z*): calcd for [C$_{35}$H$_{58}$O$_8$Si]$^+$, ([M + Na]$^+$): 657.3799, found 657.3805.
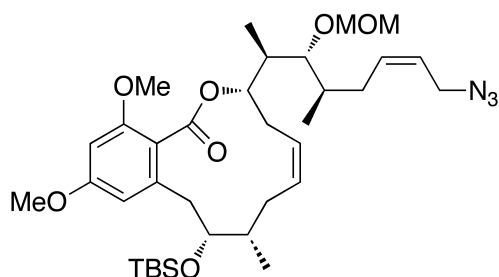
(3*S*,8*S*,9*R*,*Z*)-3-((2*R*,3*R*,4*R*,*Z*)-8-azido-3-(methoxymethoxy)-4-methyloct-6-en-2-yl)-9-((*tert*-butyldimethylsilyl)oxy)-12,14-dimethoxy-8-methyl-3,4,7,8,9,10-hexahydro-1*H*-benzo[*c*][1]oxacyclododecin-1-one, 82

A 5 mL flask was flame dried and flushed with argon before anhydrous toluene (300 μL), compound **82** (10 mg, 0.016 mmol, 1 eq.), PPh$_3$ (16 mg, 0.064 mmol, 4 eq.), and Zn(N$_3$)$_2$(C$_5$H$_5$N)$_2$ (25 mg, 0.08 mmol, 5 eq.) were added. The suspension was cooled to 0 °C and DIAD (13.2 μL, 0.067 mmol, 4.2 eq.) was added dropwise over 15 min and the reaction mixture was stirred at this temperature for an additional 10 min before warming to rt, followed by an additional 30 min of stirring. Precipitate was removed by filtering through SiO$_2$ with Et$_2$O (50

mL) and solvent was removed under reduced pressure to afford an amorphous white solid that was purified by SiO$_2$ flash chromatography (5 % – 10 % EtOAc in hexanes) to provide pure **82** as a colorless oil (9 mg, 89%). [α]^{25}$_D$ = 2.1° (c = 0.001, DCM). (*Denotes minor *trans* allylic ether product) ^{1}H NMR (500 MHz, CDCl$_3$) δ 6.33 (d, *J* = 2.2 Hz, 1H), 6.30 (d, *J* = 2.1 Hz, 1H), 5.82 – 5.48 (m, 3H), 5.42 – 5.23 (m, 2H), 4.69 – 4.52 (m, 2H), 3.80 (s, 3H), 3.78 – 3.71 (bs, 1H), 3.75 (s, 3H), 3.69 (t, *J* = 6.6 Hz, 1H), 3.42 (s, 3H), 3.25 (dt, *J* = 11.0, 5.6 Hz, 1H), 3.12 (d, *J* = 12.9 Hz, 1H), 2.75 – 2.59 (m, 1H), 2.38 – 2.08 (m, 4H), 2.03 – 1.81 (m, 5H), 1.31 – 1.27 (m, 1H), 1.01 (d, *J* = 6.8 Hz, 3H), 1.01 (d, *J* = 6.7 Hz, 3H), 0.92 (d, *J* = 6.5 Hz, 3H), 0.76 (s, 9H), -0.19 (s, 3H), -0.60 (s, 3H). ^{13}C NMR (126 MHz, CDCl$_3$) δ 166.49, 160.64, 158.77, 140.73, 135.94, 135.08, 129.72, 129.67, 127.66, 124.52, 123.36, 109.26, 98.94, 97.26, 85.38, 85.12, 72.72, 56.37, 56.22, 55.40, 53.01, 47.39, 40.22, 35.79, 35.49, 34.47, 34.13, 32.17, 29.85, 25.96, 17.96, 17.11, 16.92, 13.78, 10.68, 10.60, -5.02, -5.69. HRMS (ESI, *m/z*): calcd for [C$_{35}$H$_{57}$N$_3$O$_7$Si]$^+$, ([M + Na]$^+$): 682.3864, found 682.3863.
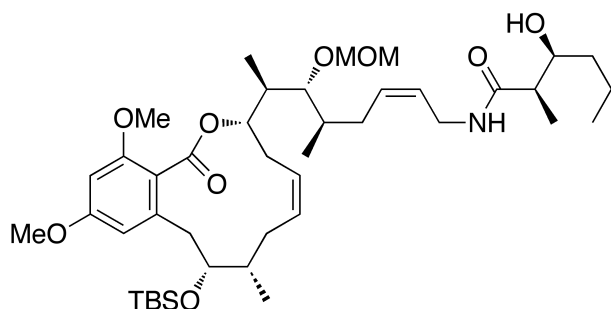
(2R,3S)-N-((5R,6R,7R,Z)-7-((3S,8S,9R,Z)-9-((*tert*-butyldimethylsilyl)oxy)-12,14-dimethoxy-8-methyl-1-oxo-3,4,7,8,9,10-hexahydro-1*H*-benzo[*c*][1]oxacyclododecin-3-yl)-6-(methoxymethoxy)-5-methyloct-2-en-1-yl)-3-hydroxy-2-methylhexanamide, 83

Flask A: A 5 mL flask was flame dried and flushed with argon before THF (400 µL), compound **82** (8 mg, 0012 mmol, 1 eq.), and PPh$_3$ (8 mg, 0.03 mmol, 2.5 eq.) were added. The reaction mixture was heated at 50 °C for 2 h and then allowed to cool to rt.

Flask B: A separate 5 mL flask was flame dried and flushed with argon before DMF (200 μL), acid **5** (3.4 mg, 0.024 mmol, 2 eq.), DIPEA (21 μL, 0.12 mmol, 10 eq.), and COMU (11 mg, 0.025 mmol, 2.1 eq.) were sequentially added. The reaction mixture was stirred for 30 min at rt. After stirring the reaction mixtures for the designated time, the contents of flask B were added to flask A (rinse 1X with 100 μL DMF), and the combined reaction mixtures were stirred for 1 h at rt. Reaction was quenched by the addition of saturated aqueous sodium bicarbonate (1 mL). The resultant slurry was partitioned between Et_2O (3 mL) and deinionized water (1 mL). The organic layer was collected and the aqueous layer was extracted with Et_2O (10 X, 3 mL) and the combined organic extracts were dried over anhydrous sodium sulfate followed by the removal of solvent under reduced pressure to afford a red oil that was purified by SiO_2 flash chromatography (15 % – 35 % EtOAc in hexanes) to provide pure **83** as a colorless oil (7 mg, 72%). $[\alpha]^{25}_D = 1.2°$ (c = 0.001, DCM). (*Denotes minor *trans* allylic ether product) ^1H NMR (500 MHz, $CDCl_3$) δ 6.31 (m, 2H), 6.27 (s, 1H), 5.70 – 5.45 (m, 3H), 5.39 – 5.20 (m, 2H), 4.61 (d, J = 6.6 Hz, 1H), 4.58 (d, J = 6.6 Hz, 1H), *4.53 – 4.49 (m, 1H), 4.03 – 3.94 (m, 1H), 3.92 – 3.81 (m, 2H), 3.80 (s, 3H), 3.73 (s, 3H), 3.76 – 3.67 (m, 1H), *3.39 (s, 3H), 3.32 (s, 3H), 3.29 – 3.25 (m, 1H), *3.22 – 3.18 (m, 1H), 3.11 (m, 1H), 2.69 (m, 1H), 2.38 – 2.05 (m, 4H), 2.00 – 1.82 (m, 3H), 1.55 – 1.43 (m, 3H), 1.37 – 1.21 (m, 4H), 1.14 (t, J = 7.1 Hz, 3H), *1.03 (d, J = 6.9 Hz, 3H), 1.01 (d, J = 6.8 Hz, 3H), 1.00 (d, J = 6.9 Hz, 3H), *0.93 (d, J = 6.6 Hz, 3H), 0.93 (d, J = 7.0 Hz, 3H), 0.90 (d, J = 6.3 Hz, 3H), 0.76 (s, 9H), -0.20 (s, 3H), -0.62 (s, 3H). ^{13}C NMR (126 MHz, $CDCl_3$) δ *176.97, 176.85, 166.97, 160.72, 158.67, 140.84, *140.77, 132.68, *132.55, *129.84, 129.78, *127.51, 127.30, 126.38, 116.31, 109.26, *99.04, 98.38, *97.18, 97.15, 85.69, 83.60, 72.90, *72.80, 71.79, *71.73, *56.33, *56.14, 56.11, 56.08, 55.41, *44.55, 44.50, 41.53, 40.20, 36.53, 36.44, 36.30, 35.98, 35.95, 34.82, 34.11, *34.06, 32.16, 25.95, 19.40, *17.95, 16.33,

14.23, *14.22, 13.76, *11.18, 11.13, *10.70, 10.45, -5.00, -5.71. HRMS (ESI, *m/z*): calcd for [$C_{43}H_{73}NO_8Si$]$^+$, ([M + Na]$^+$): 782.5003, found 782.5011.
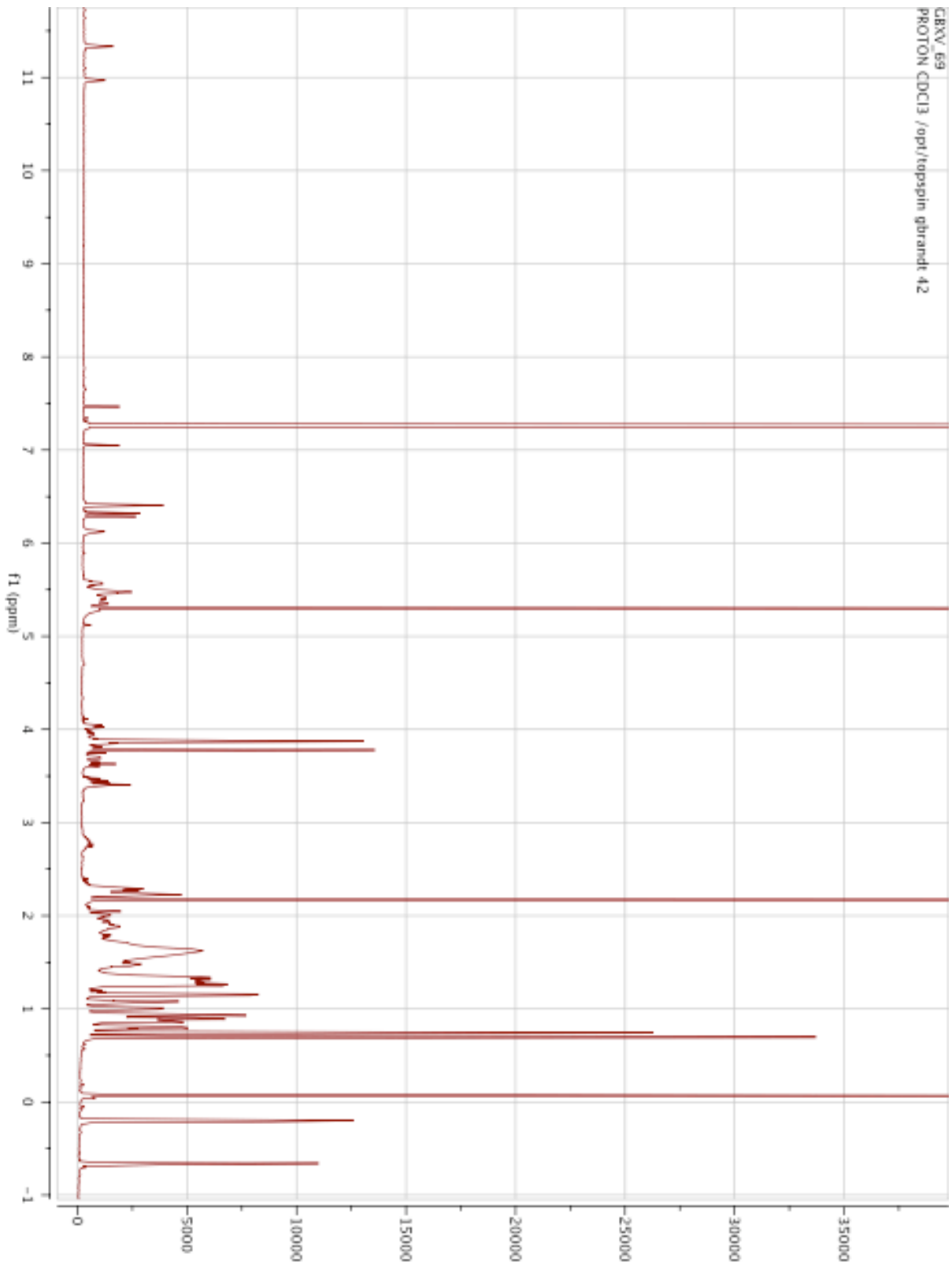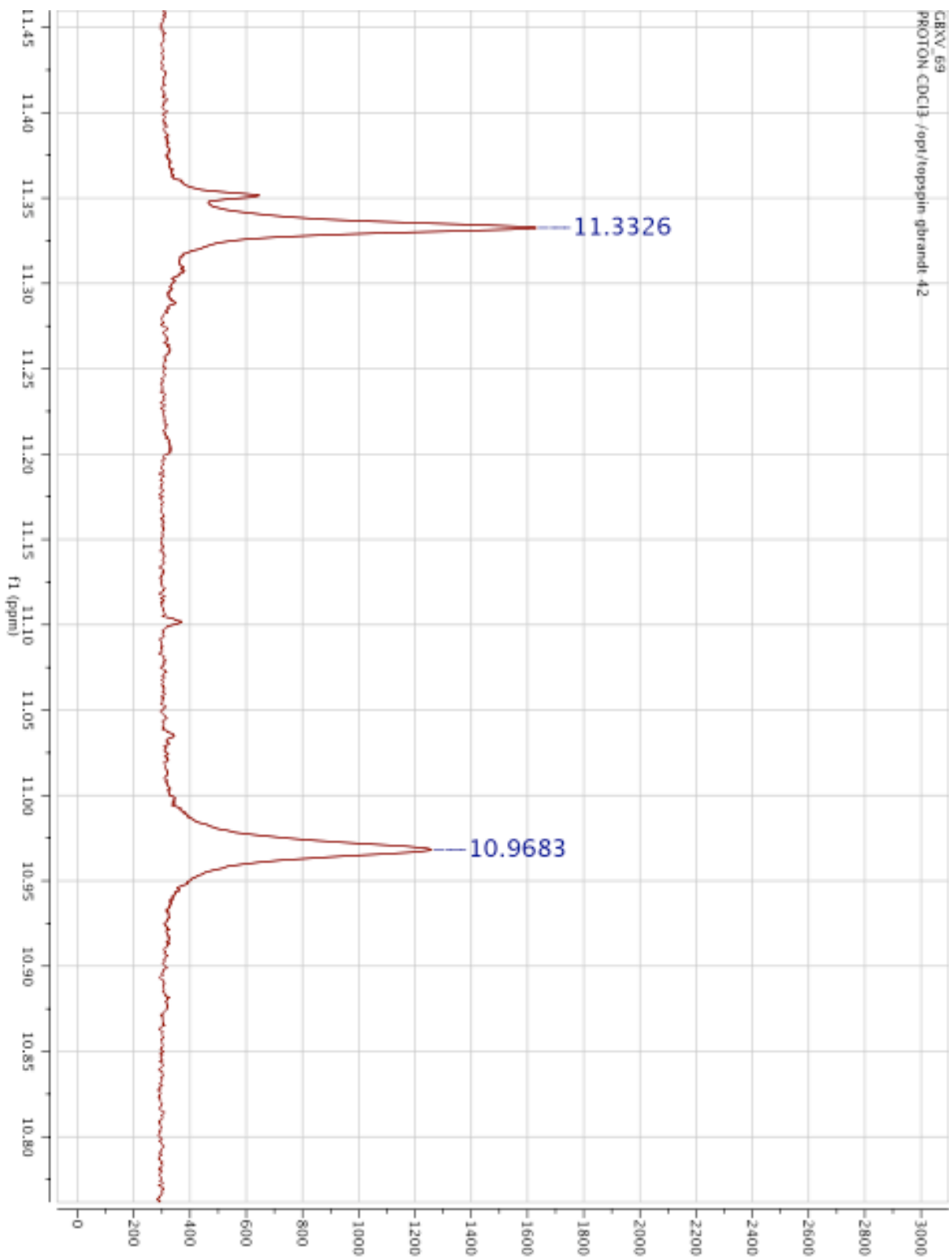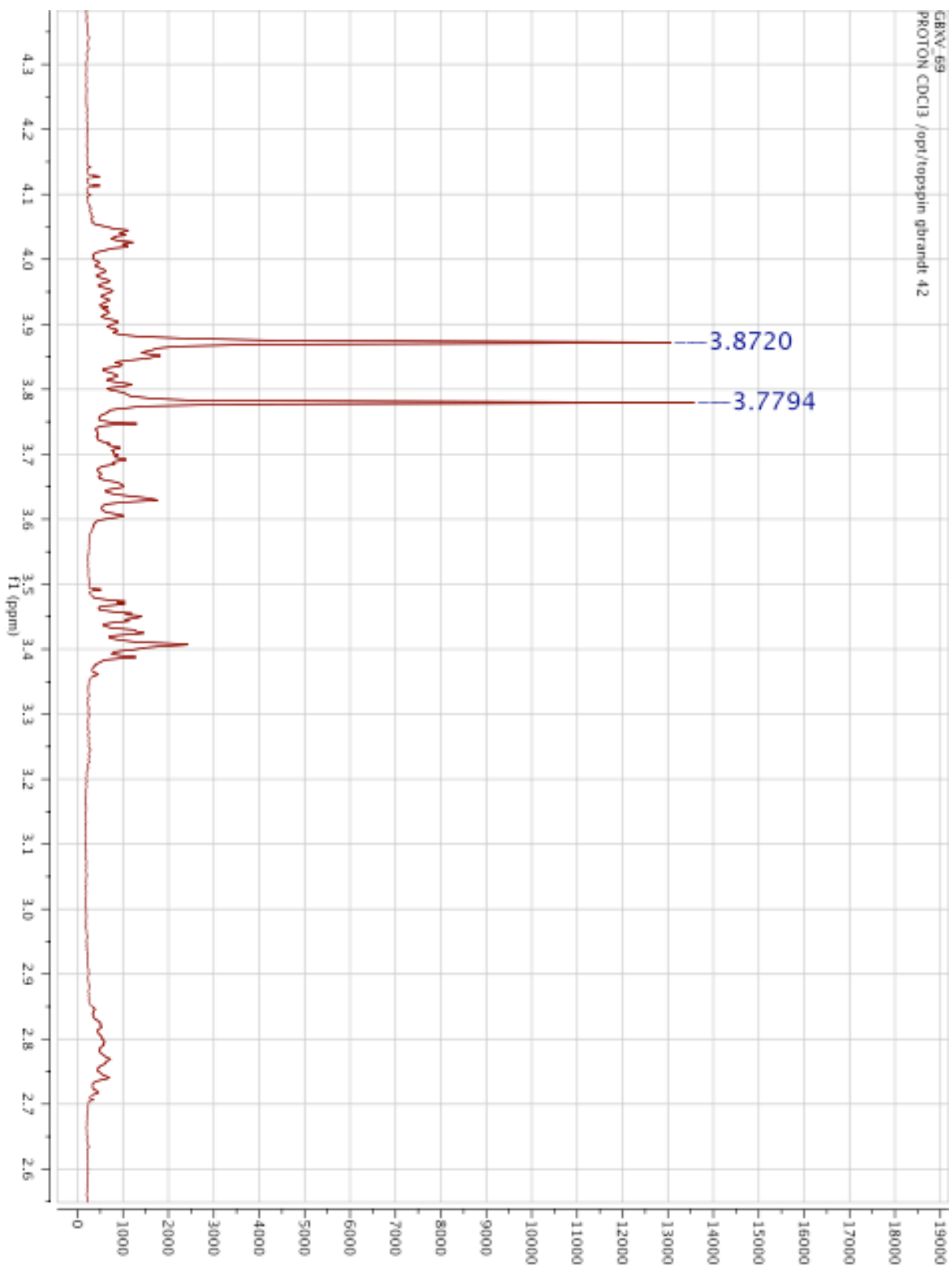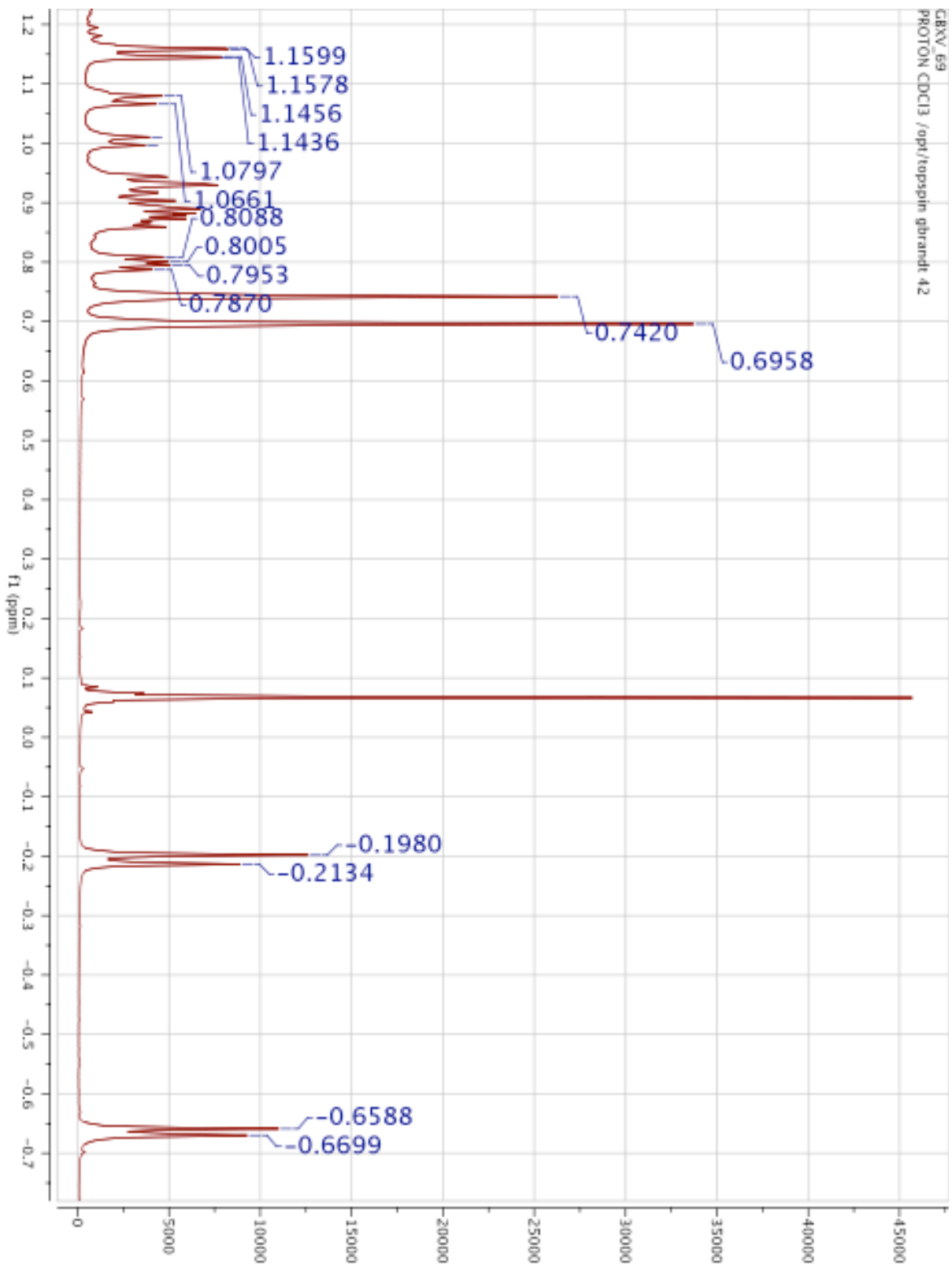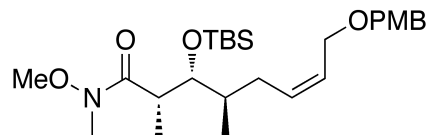

84   **87**

(2*R*,3*S*)-*N*-((5*R*,6*R*,7*S*,*Z*)-7-((3*S*,8*S*,9*R*,*Z*)-9-((*tert*-butyldimethylsilyl)oxy)-14-hydroxy-12-methoxy-8-methyl-1-oxo-3,4,7,8,9,10-hexahydro-1*H*-benzo[*c*][1]oxacyclododecin-3-yl)-6-hydroxy-5-methyloct-2-en-1-yl)-3-hydroxy-2-methylhexanamide, 84 and ring expanded product (2*R*,3*S*)-*N*-((*S*,*Z*)-5-((3*R*,4*R*,5*S*,10*S*,11*R*,*Z*)-11-((*tert*-butyldimethylsilyl)oxy)-5,16-dihydroxy-14-methoxy-4,10-dimethyl-1-oxo-3,4,5,6,9,10,11,12-octahydro-1*H*-benzo[*c*][1]oxacyclotetradecin-3-yl)hex-2-en-1-yl)-3-hydroxy-2-methylhexanamide, 87

A 1 mL reaction vessel was flame dried and flushed with argon before DCM (200 μL) and compound **83** (3 mg, 0.004 mmol, 1 eq.) were added. The solution was cooled to -78 °C and boron trichloride (1M in DCM, 16 μL, 0.016 mmol, 4 eq.) was added dropwise over 10 min. Stirring was continued at -78 °C for 3.5 h at which point the reaction was quenched by the addition of saturated aqueous sodium acetate (2 mL) and subsequently diluted with DCM (1 mL). The organic layer was collected and the aqueous layer was extracted with DCM (5 X, 1 mL). The combined organic layers were dried over anhydrous sodium sulfate and solvent was removed under reduced pressure to afford a light yellow oil that was purified by SiO₂ flash

chromatography (35 % – 50 % EtOAc in hexanes) to provide isomerically pure **84** as an amorphous solid (2.5 mg, 75 %). HRMS (ESI, *m/z*): calcd for $[C_{39}H_{65}NO_8Si]^+$, $([M + Na]^+)$: 726.4377, found 726.4383. ^1H NMR (500 MHz, CDCl$_3$) and ^{13}C NMR (126 MHz, CDCl$_3$) spectra suggest a ~1:1 mixture of **84** and **87**. In lieu of chemical shift data, full ^1H NMR and ^{13}C NMR are included. Specific regions of the ^1H NMR spectrum in support of the proposed ring-expansion byproduct are provided.

11.3326

10.9683

f1 (ppm)

———3.8720

———3.7794

f1 (ppm)

1.1599
1.1578
1.1456
1.1436
1.0797
1.0661
0.8088
0.8005
0.7953
0.7870
0.7420
0.6958
-0.1980
-0.2134
-0.6588
-0.6699

f1 (ppm)

(2S,3R,4R,Z)-3-((tert-butyldimethylsilyl)oxy)-N-methoxy-8-((4-methoxybenzyl)oxy)-N,2,4-trimethyloct-6-enamide, 90

A flame dried 50 mL flask was flame dried and flushed with argon before DCM (13 mL), amide **34** (1.0 g, 2.7 mmol, 1 eq.), and 2-6-lutidine (0.70 mL, 5.94 mmol, 2.2 eq.) were added. The solution was cooled to 0 °C, *tert*-butyldimethylsilyl trifluoromethanesulfonate (1.24 mL, 5.4 mmol, 2 eq.) was added dropwise, and stirring was continued for 30 min as the reaction mixture was allowed to warm to rt at which point the reaction was quenched by the addition of saturated aqueous sodium bicarbonate (10 mL). The organic layer was collected, and the aqueous layer was extracted with DCM (3 X, 10 mL). The combined organic layers were dried over anhydrous sodium sulfate and solvent was removed under reduced pressure to afford a yellow oil that was purified by SiO_2 flash chromatography (20 % EtOAc in hexanes) to provide pure amide **90** as a colorless oil (1.23 g, 94 %). $[\alpha]^{25}_D = 4.7°$ (c = 0.031, DCM). ^1H NMR (500 MHz, $CDCl_3$) δ 7.26 (m, 2H), 6.90 – 6.85 (m, 2H), 5.68 – 5.57 (m, 1H), 5.57 – 5.50 (m, 1H), 4.42 (s, 2H), 4.03 (d, J = 6.3 Hz, 2H), 3.86 (dd, J = 8.3, 2.7 Hz, 1H), 3.80 (s, 3H), 3.66 (s, 3H), 3.14 (s, 3H), 3.21 – 3.01 (m, 1H), 2.19 – 2.08 (m, 1H), 1.85 (dt, J = 14.2, 9.7 Hz, 1H), 1.64 – 1.48 (m, 1H), 1.14 (d, J = 6.9 Hz, 3H), 0.91 (s, 9H), 0.90 (d, J = 7.0 Hz, 3H), 0.08 (s, 3H), 0.06 (s, 3H). ^{13}C NMR (126 MHz, $CDCl_3$) δ 177.11, 159.28, 132.79, 130.65, 129.50, 127.26, 113.90, 77.64, 72.01, 65.90, 61.57, 55.41, 39.02, 38.73, 32.35, 29.48, 26.31, 18.55, 16.72, 15.73, -3.62. HRMS (ESI, *m/z*): calcd for $[C_{26}H_{45}NO_5Si]^+$, $([M + Na]^+)$: 502.2965, found 502.2964.
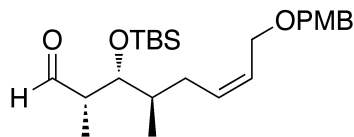
(2*S*,3*R*,4*R*,*Z*)-3-((*tert*-butyldimethylsilyl)oxy)-8-((4-methoxybenzyl)oxy)-2,4-dimethyloct-6-enal, 89

A 25 mL flask was flame dried and flushed with argon before DCM (7 mL) and Weinreb amide **90** (400 mg, 0.834 mmol, 1 eq.) were added. The solution was cooled to -78 °C and DIBAL-H (180 µL, 1.0 mmol, 1.2 eq.) in DCM (2 mL) was added dropwise over several minutes. The reaction mixture was stirred for 30 min at -78 °C and quenched by the careful addition of half saturated aqueous sodium potassium tartrate (10 mL) and stirred for an additional 4 hours while warming to rt. The organic layer was collecged and the aqueous layer was extracted with EtOAc (5 X, 10 mL). The combined organic layers were dried over anhydrous sodium sulfate and solvent was removed under reduced pressure to afford a colorless oil that was purified by SiO$_2$ flash chromatography (5 % EtOAc in hexanes) to provide pure aldehyde **89** as a colorless oil 323 mg, 92%). $[\alpha]^{25}_D$ = -3.6° (c = 0.014, DCM). ^{1}H NMR (500 MHz, CDCl$_3$) δ 9.72 (d, *J* = 0.8 Hz, 1H), 7.30 – 7.24 (m, 10H), 6.88 (m, 2H), 5.70 – 5.51 (m, 2H), 4.44 (s, 2H), 4.02 (d, *J* = 6.9 Hz, 2H), 4.00 (dd, *J* = 5.7, 3.5 Hz, 1H), 3.81 (s, 3H), 2.48 (qd, *J* = 6.9, 0.8 Hz, 1H), 2.24 – 2.14 (m, 1H), 1.89 – 1.76 (m, 1H), 1.76 – 1.65 (m, 1H), 1.10 (d, *J* = 7.0 Hz, 3H), 0.88 (d, *J* = 6.7 Hz, 3H), 0.87 (s, 9H), 0.06 (s, 3H), 0.00 (s, 3H). ^{13}C NMR (126 MHz, CDCl$_3$) δ 205.26, 159.32, 132.84, 131.84, 129.57, 127.79, 113.91, 77.37, 75.00, 72.10, 65.69, 55.42, 50.28, 38.36, 30.67, 26.07, 16.25, 8.63, -3.90, -4.02. HRMS (ESI, *m/z*): calcd for [C$_{24}$H$_{40}$O$_4$Si]$^+$, ([M + Na]$^+$): 443.2594, found 443.2591.
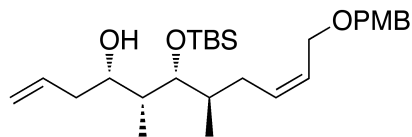
(4*S*,5*R*,6*R*,7*R*,*Z*)-6-((*tert*-butyldimethylsilyl)oxy)-11-((4-methoxybenzyl)oxy)-5,7-

dimethylundeca-1,9-dien-4-ol, 88

A 25 mL flask was flame dried and flushed with argon before Et$_2$O (13 mL) and (–)-9-(1*R*,2*R*-

Pseudoephedrinyl)-(10*S*)-(trimethylsilyl)-9-borabicyclo[3.3.2]decane (500 mg, 1.34 mmol, 2 eq.)

were added. The suspension was cooled to -78 °C and allylmagnesium bromide (1M solution in

Et$_2$O, 1.3 mL, 1.3 mmol, 1.9 eq.) was added dropwise. The solution was continually stirred for 1

h, allowed to warm, and then cooled back to -78 °C and a solution of aldehyde **89** (280 mg, 0.67

mmol, 1 eq.) in Et$_2$O (500 mL) was added dropwise. The reaction mixture was stirred for 4 h at -

78 °C and then allowed to warm to rt. Solvent was removed under reduced pressure and the

resulting white solid was suspended in hexanes and solids removed by filtering through celite

with hexanes (100 mL). Solvent was removed under reduced pressure, (*R*,*R*)-pseudoephedrine

(222 mg, 1.34 mmol, 2 eq.) and ACN (2.7 mL) were added and the solution was heated at reflux

for 4 h. After cooling to rt, precipitate was removed by decantation and washed thoroughly with

hexanes. Decanted solution was combined with the hexane washes, and solvent was removed

under reduced pressure to afford a yellow oil that was purified by SiO$_2$ flash chromatography (5

% – 10 % EtOAc in hexanes) to provide diastereomerically pure **88** as a colorless oil (290 mg,

93%). $[\alpha]^{25}_D$ = -14.1° (c = 0.011, DCM). ^{1}H NMR (500 MHz, CDCl$_3$) δ 7.29 – 7.24 (m, 2H),

6.91 – 6.83 (m, 2H), 5.84 – 5.74 (m, 1H), 5.65 (ddd, *J* = 12.8, 11.7, 6.5 Hz, 1H), 5.61 – 5.53 (m,

1H), 5.18 – 5.05 (m, 2H), 4.44 (s, 2H), 4.03 (d, *J* = 6.4 Hz, 2H), 3.80 (s, 3H), 3.67 (dd, *J* = 4.4,

3.5 Hz, 1H), 3.69 – 3.62 (m, 1H), 2.28 – 2.09 (m, 3H), 1.91 – 1.80 (m, 1H), 1.81 – 1.71 (m, 1H),

1.71 – 1.62 (m, 1H), 0.93 (d, *J* = 7.0 Hz, 3H), 0.90 (s, 9H), 0.89 (d, *J* = 7.1 Hz, 3H), 0.08 (s, 3H),

0.07 (s, 3H). ^{13}C NMR (126 MHz, CDCl$_3$) δ 159.32, 135.44, 132.60, 130.53, 129.56, 127.27, 117.88, 113.91, 78.25, 77.36, 73.75, 72.07, 65.71, 55.42, 39.88, 39.70, 38.95, 31.02, 26.23, 18.50, 16.28, 9.16, -3.31, -4.00. HRMS (ESI, *m/z*): calcd for [C$_{27}$H$_{46}$O$_4$Si]$^+$, ([M + Na]$^+$): 485.3063, found 485.3070.
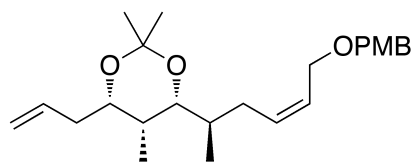
(4*S*,5*R*,6*R*)-4-allyl-6-((*R*,*Z*)-6-((4-methoxybenzyl)oxy)hex-4-en-2-yl)-2,2,5-trimethyl-1,3-dioxane, 39

A 1 dram vial was charged with THF (200 mL) and compound **88** (6 mg, 0.013 mmol, 1 eq.) and tetrabutylammonium fluoride (1M in THF, 40 mL, 0.04 mmol, 3 eq.) was added dropwise. The reaction mixture was stirred at rt for 1 h and quenched by the addition of saturated aqueous ammonium chloride (500 mL) and then diluted with EtOAc (300 mL). The organic layer was collected and the aqueous layer was extracted with EtOAc (5 X, 500 mL). The combined organic layers were dried over anhydrous sodium sulfate and solvent as removed under reduced pressure to afford a yellow oil that was purified by SiO$_2$ flash chromatography (15 % – 30 % EtOAc in hexanes) to provide pure 1,3-diol as colorless oil. The oil was dissolved in DMP (300 mL) and *p*-Toluenesulfonic acid (0.3 mg, 0.001 mmol, 0.1 eq.) was added followed by stirring for 2 h at rt. After 2 h, the reaction was quenched by the addition of sodium bicarbonate (5 mg). Solvent was removed under reduced pressure to afford a white slurry that was purified by SiO$_2$ flash chromatography (5 % – 10 % EtOAc in hexanes) to provide pure **39** as a colorless oil (4 mg, 87%). All spectroscopic data matched what was previously observed for **39** from **37**. ^{1}H NMR (500 MHz, C$_6$D$_6$) δ 7.31 – 7.26 (m, 2H), 6.85 – 6.78 (m, 2H), 5.91 – 5.85 (m, 1H), 5.81 (dddd, *J* = 17.1, 10.2, 7.9, 6.1 Hz, 1H), 5.60 – 5.53 (m, 1H), 5.08 (m, 2H), 4.43 (d, *J* = 1.7 Hz, 2H), 4.16

(dd, J = 12.2, 6.4 Hz, 1H), 4.11 (dd, J = 12.0, 6.3 Hz, 1H), 3.71 (ddd, J = 8.0, 6.0, 2.2 Hz, 1H), 3.29 (s, 3H), 3.24 (dd, J = 9.9, 2.1 Hz, 1H), 2.48 – 2.35 (m, 2H), 2.10 – 1.96 (m, 2H), 1.75 – 1.63 (m, 1H), 1.49 (s, 3H), 1.29 (s, 3H), 1.27 – 1.18 (m, 1H), 0.88 (d, J = 6.8 Hz, 3H), 0.64 (d, J = 6.9 Hz, 3H). ^{13}C NMR (126 MHz, C$_6$D$_6$) δ 159.72, 135.37, 131.33, 130.99, 129.50, 128.69, 116.75, 114.09, 99.01, 76.94, 73.42, 72.10, 66.09, 54.75, 37.93, 34.82, 32.71, 31.18, 30.36, 19.71, 13.94, 4.80. HRMS (ESI, m/z): calcd for [C$_{24}$H$_{36}$O$_4$]$^+$, ([M + Na]$^+$): 411.2511, found 411.2512.
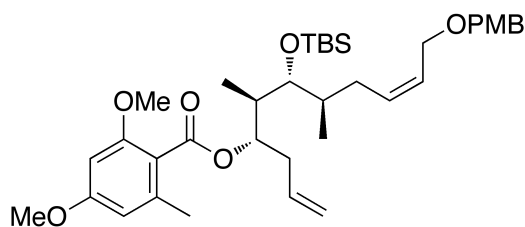
(4S,5R,6R,7R,Z)-6-(($tert$-butyldimethylsilyl)oxy)-11-((4-methoxybenzyl)oxy)-5,7-dimethylundeca-1,9-dien-4-yl 2,4-dimethoxy-6-methylbenzoate, 96

A 25 mL flask was flame dried and flushed with argon before DCM (4.3 mL) and 2,4-dimethoxy-6-methylbenzoic acid (165 mg, 0.86 mmol, 2 eq.) were added. The suspension was cooled to 0 °C and oxalyl bromide (85 mL, 0.9 mmol, 2.1 eq.) was added dropwise. The suspension was allowed to warm to rt and stirred until all solid was dissolved at which point 4 drops of anhydrous DMF were added. Stirring was continued at rt for 1 h and the solution was cooled 0 °C before DIPEA (390 mL, 2.2 mmol, 5 eq.) was added. Stirring was continued at 0 °C for 30 min before a solution of alcohol **88** (200 mg, 0.43 mmol, 1 eq.) in DCM (0.5 mL) and DMAP (105 mg, 0.86 mmol, 2 eq.) were added. The reaction mixture was allowed to warm to rt and stirring was continued for 30 min at which point the reaction was quenched by the addition of deionized water (5 mL). The organic layer was collected and the aqueous layer was extracted with DCM (4 X, 10 mL). The combined organic layers were dried over anhydrous sodium sulfate and solvent was removed to afford a brown oil that was purified by SiO$_2$ flash

chromatography (5 % – 10 % EtOAc in hexanes) to provide ester **96** as a colorless oil (256 mg, 93%). $[\alpha]^{25}_D = 3.9°$, c = 0.009, DCM). ^{1}H NMR (400 MHz, CDCl$_3$) δ 7.26 (m, 2H), 6.92 – 6.80 (m, 2H), 6.31 (d, *J* = 9.9 Hz, 2H), 5.91 – 5.75 (m, 1H), 5.69 – 5.50 (m, 2H), 5.20 (m, 1H), 5.10 (m, 2H), 4.43 (s, 2H), 4.04 (d, *J* = 5.8 Hz, 2H), 3.79 (s, 6H), 3.76 (s, 3H), 3.55 (t, *J* = 4.2 Hz, 1H), 2.58 – 2.38 (m, 2H), 2.29 (s, 3H), 2.23 – 2.14 (m, 1H), 1.99 – 1.81 (m, 2H), 1.81 – 1.68 (m, 1H), 0.99 (d, *J* = 6.8 Hz, 3H), 0.91 (s, 9H), 0.86 (d, *J* = 6.7 Hz, 3H), 0.08 (s, 3H), 0.05 (s, 3H). ^{13}C NMR (126 MHz, CDCl$_3$) δ 168.07, 161.24, 159.28, 158.12, 138.05, 135.44, 134.11, 132.67, 130.64, 129.53, 127.36, 117.95, 113.90, 106.61, 96.22, 76.67, 75.52, 72.02, 65.87, 55.72, 55.48, 55.40, 39.88, 38.89, 37.92, 36.84, 30.04, 26.35, 20.22, 17.06, 10.90, -3.42. HRMS (ESI, *m/z*): calcd for $[C_{37}H_{56}O_7Si]^+$, $([M + Na]^+)$: 663.3693, found 663.3698.
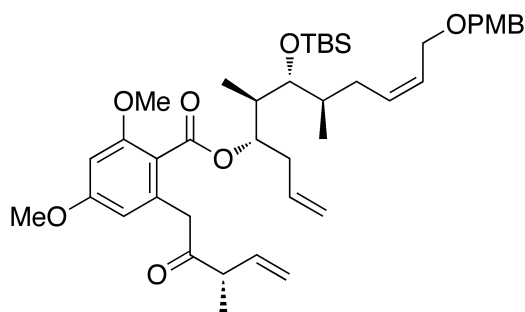
(4*S*,5*R*,6*R*,7*R*,*Z*)-6-((*tert*-butyldimethylsilyl)oxy)-11-((4-methoxybenzyl)oxy)-5,7-dimethylundeca-1,9-dien-4-yl 2,4-dimethoxy-6-((*S*)-3-methyl-2-oxopent-4-en-1-yl)benzoate, 97
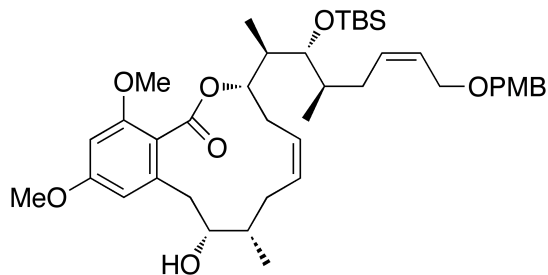
A 5 mL flask was flame dried and flushed with argon before THF (600 μL) and compound **96** (150 mg, 0.234 mmol, 1 eq.) were added. The solution was cooled to -78 °C and a freshly prepared 1M solution of LDA (468 μL, 0.468 mmol, 2 eq.) in THF was added dropwise. After stirring for 5 min at -78 °C, Weinreb amide **47** (92 mg, 0.585 mmol, 2.5 eq.) in THF (200 μL) was added at once and the solution was stirred for an additional 10 min at -78 °C at which point saturated aqueous ammonium chloride (1 mL) was added to quench. Stirring was continued as

the heterogenous mixture was allowed to warm to rt. The organic layer was collected and the aqueous layer was extracted with EtOAc (5 X, 2 mL). The combined organic layers were dried with anhydrous sodium sulfate and solvent was evaporated to afford a yellow oil that was purified by SiO$_2$ flash chromatography (5 % – 10 % EtOAc in hexanes) to provide pure **97** as a colorless oil (140 mg, 81%). $[\alpha]^{25}_D$ = 10.2° , c = 0.005, DCM). ^{1}H NMR (500 MHz, CDCl$_3$) δ 7.26 (m, 2H), 6.87 (m, 2H), 6.38 (d, J = 2.0 Hz, 1H), 6.27 (d, J = 2.0 Hz, 1H), 5.85 (ddt, J = 17.1, 10.1, 7.0 Hz, 1H), 5.71 (ddt, J = 17.1, 10.1, 7.1 Hz, 1H), 5.66 – 5.52 (m, 1H), 5.17 (q, J = 6.1 Hz, 1H), 5.14 – 4.98 (m, 2H), 4.43 (s, 2H), 4.04 (d, J = 6.2 Hz, 2H), 3.79 (s, 3H), 3.79 (s, 3H), 3.78 (s, 3H), 3.81 – 3.70 (m, 1H), 3.56 (t, J = 4.5 Hz, 1H), 2.73 (h, J = 6.9 Hz, 1H), 2.51 (dt, J = 12.3, 6.1 Hz, 1H), 2.47 – 2.37 (m, 2H), 2.23 – 2.15 (m, 1H), 2.13 – 2.03 (m, 1H), 1.97 – 1.81 (m, 2H), 1.80 – 1.68 (m, 1H), 1.08 (d, J = 7.0 Hz, 3H), 0.98 (d, J = 6.8 Hz, 3H), 0.92 (s, 9H), 0.86 (d, J = 6.8 Hz, 3H), 0.09 (s, 3H), 0.06 (s, 3H). ^{13}C NMR (126 MHz, CDCl$_3$) δ 210.06, 167.64, 161.59, 159.34, 158.98, 135.95, 135.68, 134.28, 132.57, 130.72, 129.50, 127.46, 117.85, 116.91, 113.95, 107.29, 100.15, 97.85, 76.58, 75.73, 72.04, 65.91, 55.80, 55.54, 55.41, 46.64, 45.20, 38.91, 38.07, 38.00, 37.20, 36.90, 30.21, 26.35, 17.00, 16.22, 10.85, -3.33, -3.43. HRMS (ESI, m/z): calcd for [C$_{43}$H$_{64}$O$_8$Si]$^+$, ([M + Na]$^+$): 759.4268, found 759.4271.
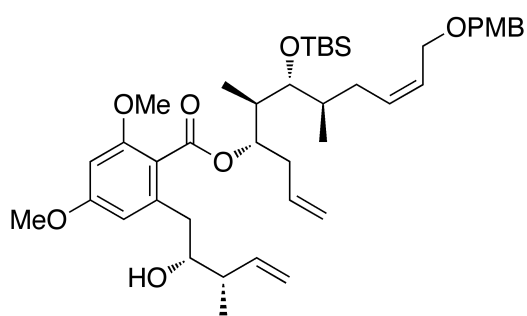
(4S,5R,6R,7R,Z)-6-((tert-butyldimethylsilyl)oxy)-11-((4-methoxybenzyl)oxy)-5,7-dimethylundeca-1,9-dien-4-yl **2-((2R,3S)-2-hydroxy-3-methylpent-4-en-1-yl)-4,6-dimethoxybenzoate, 98**

A 5 mL flask was flused with argon and charged with ketone **97** (110 mg, 0.15 mmol, 1 eq.), DMF (250 mL), deionized water (250 mL), sodium formate (156 mg, 2.3 mmol, 15 eq.), and RuCl[(S,S)-Tsdpen](p-cymene) (10 mg, 0.015 mmol, 0.1 eq.). The reaction mixture was stirred at 40 °C for 35 h and subsequently quenched by the addition of saturated aqueous ammonium chloride (2 mL) and then diluted with Et_2O (1 mL). The organic layer was collected and the aqueous layer was extracted with Et_2O (10 X, 1 mL). The combined organic layers were dried over anhydrous sodium sulfate and solvent was removed under reduced pressure to afford a brown oil that was purified by SiO_2 flash chromatography (5 % – 15 % EtOAc in hexanes) to provide **98** in a 9:1 diastereomeric mixture as a colorless oil (82 mg, 74%). $[\alpha]^{25}_D = 15.3°$, c = 0.003, DCM). (*Denotes minor epimeric alcohol product) ^{1}H NMR (500 MHz, $CDCl_3$) δ 7.30 – 7.22 (m, 2H), 6.91 – 6.82 (m, 2H), *6.37 (d, J = 2.1 Hz, 1H), 6.35 (d, J = 2.1 Hz, 1H), 6.33 (d, J = 2.1 Hz, 1H), 5.95 – 5.71 (m, 2H), 5.68 – 5.50 (m, 2H), 5.21 (dd, J = 12.1, 6.3 Hz, 1H), 5.17 – 4.96 (m, 4H), *4.43 (s, 2H), 4.43 (s, 2H), *4.04 (d, J = 6.0 Hz, 2H), 4.03 (d, J = 6.3 Hz, 2H), 3.81 (s, 3H), 3.79 (s, 3H), 3.77 (s, 3H), *3.76 – 3.70 (m, 1H), 3.66 – 3.58 (m, 1H), *3.56 (t, J = 4.6 Hz, 1H), 3.51 (t, J = 4.5 Hz, 1H), 2.77 (dd, J = 13.6, 2.9 Hz, 1H), 2.58 – 2.39 (m, 3H), 2.37 – 2.26 (m, 1H), 2.24 – 2.15 (m, 1H), 2.03 – 1.89 (m, 2H), 1.89 – 1.79 (m, 1H), 1.79 – 1.65 (m, 2H), *1.02 (d, J = 6.8 Hz, 3H), *0.96 (d, J = 6.2 Hz, 3H), 0.94 (d, J = 6.5 Hz, 6H), *0.92 (s, 9H), 0.91 (s, 9H), 0.84 (d, J = 6.8 Hz, 3H), *0.10 (s, 3H), 0.07 (s, 3H), *0.06 (s, 3H), 0.04 (s, 3H). ^{13}C NMR (126 MHz, $CDCl_3$) δ 169.33, 161.90, 159.29, 158.68, 140.91, 137.76, 134.01, 132.49, 130.60, 129.53, 127.47, 117.93, 116.62, 115.93, 113.90, 106.22, 97.12, 77.36, 76.43, 76.37, 72.03, 65.84, 55.72, 55.52, 55.40, 39.48, 38.23, 37.97, 37.56, 37.25, 36.74, 30.34, 26.31, 16.87, 15.12, 10.78, -3.40, -3.49. HRMS (ESI, *m/z*): calcd for $[C_{43}H_{66}O_8Si]^+$, $([M + Na]^+)$: 761.4425, found 761.4420.
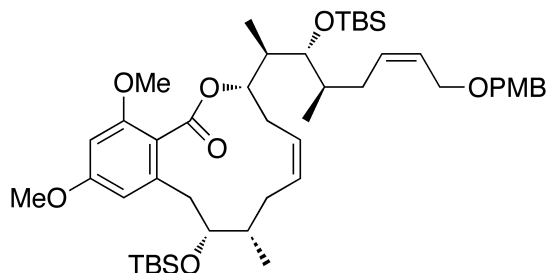
(3S,8S,9R,Z)-3-((2R,3R,4R,Z)-3-((*tert*-butyldimethylsilyl)oxy)-8-((4-methoxybenzyl)oxy)-4-methyloct-6-en-2-yl)-9-hydroxy-12,14-dimethoxy-8-methyl-3,4,7,8,9,10-hexahydro-1*H*-benzo[*c*][1]oxacyclododecin-1-one, 99

A 100 mL flask was flame dried and flushed with argon before DCM (54 mL) and alcohol **98** (20 mg, 0.0271 mmol, 1 eq.) were added. The solution was cooled to 0 °C, Grubbs' second generation catalyst (1.2 mg, 0.0014 mmol, 0.05 eq.) was added, and the solution was continually stirred while warming to rt. After 4.5 h of stirring at rt, a catalyst was refreshed (1.2 mg, 0.0014 mmol, 0.05 eq.) and the reaction mixture was stirred for an additional 4.5 h at which point solvent was removed under reduced pressure at 10 °C to afford a brown oil that was purified by SiO$_2$ flash chromatography (15 % – 40 % EtOAc in hexanes) to provide **99** in a 4:1 mixture of side chain olefin isomers (*cis*:*trans*) as a colorless oil (13 mg, 79% based on desired epimeric alcohol). [α]$^{25}_{D}$ = 9.7° , c = 0.002, DCM). (*Denotes minor *trans* side chain olefin isomer) ^{1}H NMR (500 MHz, CDCl$_3$) δ 7.30 – 7.22 (m, 2H), 6.91 – 6.82 (m, 2H), 6.35 (d, *J* = 2.2 Hz, 1H), 6.33 (d, *J* = 1.7 Hz, 1H), 5.68 – 5.54 (m, 2H), 5.54 – 5.44 (m, 2H), 5.32 – 5.26 (m, 1H), 4.42 (s, 2H), *4.42 (s, 2H), 4.02 (d, *J* = 5.6 Hz, 2H), *3.91 (d, *J* = 6.0 Hz, 2H), 3.81 (s, 3H), 3.80 (s, 3H), 3.76 (s, 3H), 3.76 – 3.72 (m, 1H), *3.57 – 3.54 (m, 1H), 3.54 – 3.51 (m, 1H), 3.07 – 2.91 (m, 1H), 2.81 – 2.54 (m, 2H), 2.44 – 2.33 (m, 1H), 2.16 – 2.09 (m, 1H), 2.00 – 1.92 (m, 1H), 1.92 – 1.82 (m, 2H), 1.82 – 1.71 (m, 2H), 1.05 (d, *J* = 6.8 Hz, 3H), *0.97 (d, *J* = 6.9 Hz, 3H), 0.97 (d, *J*

= 6.9 Hz, 3H), 0.90 (s, 9H), 0.88 (d, J = 6.9 Hz, 3H), 0.07 (s, 3H), *0.03 (s, 3H), 0.02 (s, 3H).
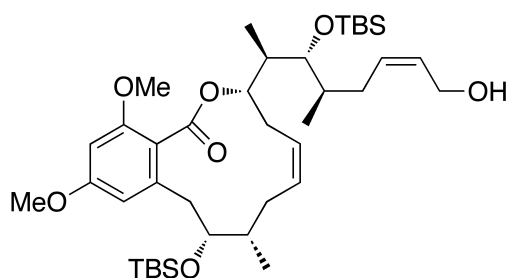
HRMS (ESI, m/z): calcd for $[C_{41}H_{62}O_8Si]^+$, ($[M + Na]^+$): 733.4112, found 733.4105.

(3S,8S,9R,Z)-9-(($tert$-butyldimethylsilyl)oxy)-3-((2R,3R,4R,Z)-3-(($tert$-butyldimethylsilyl)oxy)-8-((4-methoxybenzyl)oxy)-4-methyloct-6-en-2-yl)-12,14-dimethoxy-8-methyl-3,4,7,8,9,10-hexahydro-1H-benzo[c][1]oxacyclododecin-1-one, 100

A 1 dram vial was flame dried and flushed with argon before DCM (100 mL), **99** (6 mg, 0.008 mmol, 1 eq.), and DIPEA (6 mL, 0.032 mmol, 4 eq.) were added. The solution was cooled to 0 °C and $tert$-butyldimethylsilyl triflluromethanesulfonate (6.4 mL, 0.028 mmol, 3.5 eq.) was added dropwise. Stirring was continued for 30 min as the reaction mixture was allowed to warm to rt at which point the reaction was quenched by the addition of saturated aqueous ammonium chloride (1 mL). The biphasic mixture was diluted with DCM (1 mL), the organic layer was collected and the aqueous layer was extracted with DCM (10 X, 1 mL). The combined organic layers were dried over anhydrous sodium sulfate and solvent was removed under reduced pressure to afford a colorless oil that was purified by SiO$_2$ flash chromatography (5 % − 10 % EtOAc in hexanes) to provide **100** in a 4:1 mixture of side chain olefin isomers (cis:$trans$) as a colorless oil (6 mg, 91%). $[\alpha]^{25}_D$ = 4.7° , c = 0.002, DCM). (*Denotes minor $trans$ side chain olefin isomer) ^{1}H NMR (500 MHz, CDCl$_3$) δ 7.29 − 7.24 (m, 2H), 6.90 − 6.84 (m, 2H), 6.31 (d, J = 2.2 Hz, 1H), 6.29 (d, J = 1.7 Hz, 1H), 5.71 − 5.52 (m, 3H), 5.39 − 5.30 (m, 1H), 5.29 − 5.22 (m, 1H), 4.43 (s, 2H), *4.42 (s, 2H), 4.03 (d, J = 5.0 Hz, 2H), *3.93 (m, 2H), 3.80 (s, 3H), 3.79 (s, 3H), 3.77 − 3.74 (m,

1H), 3.74 (s, 3H), 3.52 – 3.41 (m, 1H), 3.13 (d, J = 12.9 Hz, 1H), 2.74 – 2.60 (m, 1H), 2.28 – 2.09 (m, 3H), 2.09 – 2.01 (m, 1H), 1.98 – 1.70 (m, 5H), 1.01 (d, J = 6.8 Hz, 3H), *0.96 (d, J = 6.9 Hz, 3H), 0.94 (d, J = 6.9 Hz, 3H), 0.89 (s, 9H), 0.88 (d, J = 7.2 Hz, 3H), 0.76 (s, 9H), *0.01 (s, 3H), -0.00 (s, 3H), -0.01 (s, 3H), -0.19 (s, 3H), -0.61 (s, 3H). ^{13}C NMR (126 MHz, CDCl$_3$) δ 166.39, 160.55, 159.27, 158.78, 140.76, 134.04, 132.85, *130.72, 130.66, *129.63, 129.54, *127.78, 127.68, 127.20, 116.58, 113.89, 109.21, 97.22, 77.37, 72.76, 71.98, 71.64, 65.82, 56.20, *55.42, 55.40, 55.37, *53.58, 41.58, 40.23, 37.84, 34.16, 32.55, 32.16, 31.74, 29.85, 29.52, 26.34, 25.97, 18.62, 17.96, *17.43, 11.31, -3.50, -3.68, *-3.70, -5.03, -5.68. HRMS (ESI, m/z): calcd for [C$_{47}$H$_{76}$O$_8$Si$_2$]$^+$, ([M + Na]$^+$): 847.4976, found 847.4983.

(3S,8S,9R,Z)-9-((*tert*-butyldimethylsilyl)oxy)-3-((2R,3R,4R,Z)-3-((*tert*-butyldimethylsilyl)oxy)-8-hydroxy-4-methyloct-6-en-2-yl)-12,14-dimethoxy-8-methyl-3,4,7,8,9,10-hexahydro-1*H*-benzo[*c*][1]oxacyclododecin-1-one, 101

A 1 dram vial was charged with DCM (200 mL), deionized water (13 mL), and **100** (5.2 mg, 0.0063 mmol, 1 eq.). DDQ (2.3 mg, 0.01 mmol, 1.5 eq.) was added in one portion and the reaction mixture was stirred at rt for 30 min and subsequently quenched by the addition of saturated aqueous sodium bicarbonate (2 mL). The biphasic mixture was diluted with DCM (2 mL), the organic layer was collected, and the aqueous layer was extracted with DCM (10 X, 2 mL). The combined organic layers were dried over anhydrous sodium sulfate and solvent was removed under reduced pressure to afford an orange oil that was purified by SiO$_2$ flash

chromatography (15 % – 30 % EtOAc in hexanes) to provide **101** in a 4:1 mixture of side chain olefin isomers (*cis*:*trans*) as a colorless oil (4.4 mg, 99%). $[\alpha]^{25}_D = 7.7°$, c = 0.001, DCM). (*Denotes minor *trans* side chain olefin isomer) ^{1}H NMR (500 MHz, CDCl$_3$) δ 6.32 (d, $J = 2.3$ Hz, 1H), 6.30 (d, $J = 1.9$ Hz, 1H), 5.69 – 5.51 (m, 3H), 5.40 – 5.22 (m, 2H), 4.22 (dd, $J = 12.2$, 5.6 Hz, 1H), 4.13 (dd, $J = 12.2$, 6.6 Hz, 1H), 4.10 – 4.01 (m, 1H), 3.79 (s, 3H), *3.75 (s, 3H), 3.74 (s, 3H), 3.76 – 3.71 (m, 1H), *3.51 (dd, $J = 5.3$, 3.5 Hz, 1H), 3.46 (dd, $J = 5.9$, 3.1 Hz, 1H), 3.12 (d, $J = 12.7$ Hz, 1H), 2.79 – 2.61 (m, 1H), *2.55 – 2.44 (m, 1H), 2.28 – 2.11 (m, 3H), 2.11 – 2.02 (m, 1H), 1.98 – 1.74 (m, 4H), 1.00 (d, $J = 6.8$ Hz, 3H), 0.96 (d, $J = 7.1$ Hz, 3H), *0.95 (d, $J = 7.7$ Hz, 3H), 0.90 (d, $J = 6.7$ Hz, 3H), 0.89 (s, 9H), *0.87 (s, 9H), 0.76 (s, 9H), 0.01 (s, 3H), *-0.00 (s, 3H), -0.03 (s, 3H), *-0.07 (s, 3H), -0.20 (s, 3H), -0.62 (s, 3H). ^{13}C NMR (126 MHz, CDCl$_3$) δ 166.56, 160.59, 158.77, 140.86, *132.35, 132.17, *130.58, *129.70, 129.50, 127.60, *126.49, 116.49, 109.24, 97.20, 75.80, 72.81, 64.03, 58.79, 56.20, *56.16, 55.38, 41.45, 40.19, 38.01, 34.11, 32.59, 32.15, 30.10, 29.85, 29.26, 26.30, *26.24, 25.97, 17.96, 13.78, 11.40, *11.24, -3.56, -3.76, *-3.99, -5.03, -5.69. HRMS (ESI, *m/z*): calcd for $[C_{39}H_{68}O_7Si_2]^+$, ([M + Na]$^+$): 727.4401, found 727.4410.
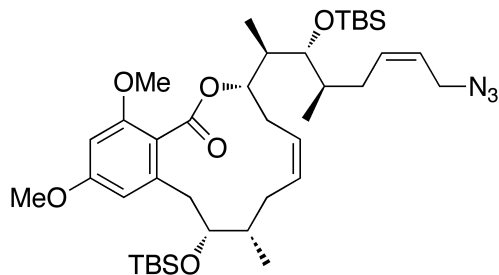
(3S,8S,9R,Z)-3-((2R,3R,4R,Z)-8-azido-3-((*tert*-butyldimethylsilyl)oxy)-4-methyloct-6-en-2-yl)-9-((*tert*-butyldimethylsilyl)oxy)-12,14-dimethoxy-8-methyl-3,4,7,8,9,10-hexahydro-1*H*-benzo[*c*][1]oxacyclododecin-1-one, 102

A 5 mL flask was flame dried and flushed with argon before anhydrous toluene (300 μL), compound (4.4 mg, 0.006 mmol, 1 eq.), PPh$_3$ (6 mg, 0.024 mmol, 4 eq.), and Zn(N$_3$)$_2$(C$_5$H$_5$N)$_2$ (9 mg, 0.030 mmol, 5 eq.) were added. The suspension was cooled to 0 °C and DIAD (5 mg, 0.025 mmol, 4.2 eq.) was added dropwise over 15 min and the reaction mixture was stirred at this temperature for an additional 10 min before warming to rt, followed by an additional 30 min of stirring. Precipitate was removed by filtering through SiO$_2$ with Et$_2$O (50 mL) and solvent was removed under reduced pressure to afford an amorphous white solid that was purified by SiO$_2$ flash chromatography (5 % – 10 % EtOAc in hexanes) to provide **102** in a 4:1 mixture of side chain olefin isomers (*cis*:*trans*) as a colorless oil (4 mg, 89 %). [α]$^{25}_D$ = 1.9° , c = 0.001, DCM). (*Denotes minor *trans* side chain olefin isomer) ^{1}H NMR (500 MHz, CDCl$_3$) δ 6.32 (d, *J* = 2.2 Hz, 1H), 6.30 (d, *J* = 2.2 Hz, 1H), 5.80 – 5.66 (m, 1H), 5.63 – 5.43 (m, 2H), 5.40 – 5.31 (m, 1H), 5.30 – 5.22 (m, 1H), 3.80 (s, 3H), 3.78 – 3.72 (m, 2H), 3.75 (s, 3H), 3.66 (dd, *J* = 7.6, 3.8 Hz, 1H), 3.49 (ddd, *J* = 11.4, 5.7, 3.2 Hz, 1H), 3.14 (d, *J* = 12.8 Hz, 1H), 2.69 (dd, *J* = 24.3, 11.2 Hz, 1H), 2.33 – 2.13 (m, 3H), 2.12 – 2.03 (m, 2H), 1.99 – 1.75 (m, 4H), 1.01 (d, *J* = 6.8 Hz, 3H), 0.96 (d, *J* = 6.8 Hz, 3H), 0.91 (d, *J* = 3.5 Hz, 3H), *0.90 (s, 9H), 0.90 (s, 9H), 0.75 (s, 9H), *0.08 – 0.05 (s, 3H), 0.02 (s, 3H), -0.01 (s, 3H), -0.19 (s, 3H), -0.61 (s, 3H). ^{13}C NMR (126 MHz,

CDCl$_3$) δ 166.38, 160.60, 158.79, 140.83, 135.50, 129.72, 128.99, 127.59, 116.46, 109.26, 97.22, 76.77, 76.40, 72.77, 56.20, 55.38, 53.58, 53.03, 47.37, 41.59, 40.21, 37.74, 34.16, 32.16, 30.10, 29.85, 26.32, 25.97, 18.62, 14.28, 11.38, -3.48, -3.71, -5.03, -5.68. HRMS (ESI, *m/z*): calcd for [C$_{39}$H$_{67}$N$_3$O$_6$Si$_2$]$^+$, ([M + Na]$^+$): 752.4466, found 752.4459.
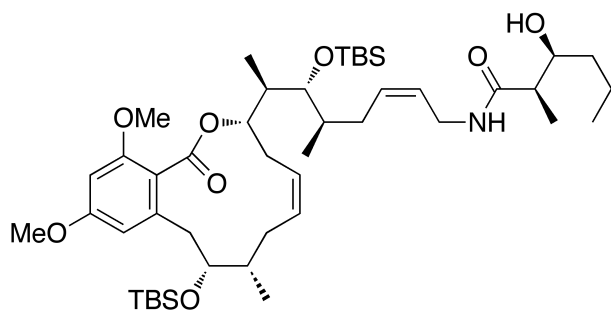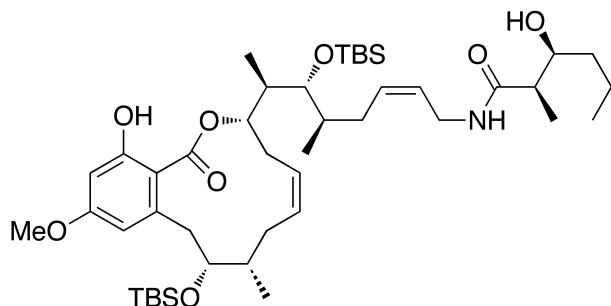

(2*R*,3*S*)-*N*-((5*R*,6*R*,7*R*,*Z*)-6-((*tert*-butyldimethylsilyl)oxy)-7-((3*S*,8*S*,9*R*,*Z*)-9-((*tert*-butyldimethylsilyl)oxy)-12,14-dimethoxy-8-methyl-1-oxo-3,4,7,8,9,10-hexahydro-1*H*-benzo[*c*][1]oxacyclododecin-3-yl)-5-methyloct-2-en-1-yl)-3-hydroxy-2-methylhexanamide, 103

Flask A: A 5 mL flask was flame dried and flushed with argon before THF (400 μL), compound **102** (8 mg, 0012 mmol, 1 eq.), and PPh$_3$ (8 mg, 0.03 mmol, 2.5 eq.) were added. The reaction mixture was heated at 50 °C for 2 h and then allowed to cool to rt.

Flask B: A separate 5 mL flask was flame dried and flushed with argon before DMF (200 μL), acid **5** (3.4 mg, 0.024 mmol, 2 eq.), DIPEA (21 μL, 0.12 mmol, 10 eq.), and COMU (11 mg, 0.025 mmol, 2.1 eq.) were sequentially added. The reaction mixture was stirred for 30 min at rt. After stirring the reaction mixtures for the designated time, the contents of flask B were added to flask A (rinse 1X with 100 μL DMF), and the combined reaction mixtures were stirred for 1 h at rt. Reaction was quenched by the addition of saturated aqueous sodium bicarbonate (1 mL). The resultant slurry was partitioned between Et$_2$O (3 mL) and deinionized water (1 mL). The organic layer was collected and the aqueous layer was extracted with Et$_2$O (10 X, 3 mL) and the

combined organic extracts were dried over anhydrous sodium sulfate followed by the removal of solvent under reduced pressure to afford a red oil that was purified by SiO_2 flash chromatography (5 % – 10 % EtOAc in hexanes) to provide **103** as a colorless oil (5 mg, 50%).

$[\alpha]^{25}_D = 2.2°$, c = 0.001, DCM). ^{1}H NMR (500 MHz, CDCl$_3$) δ 6.32 (d, J = 2.3 Hz, 1H), 6.30 (d, J = 2.2 Hz, 1H), 6.25 (s, 1H), 5.62 (m, 1H), 5.55 (ddd, J = 10.7, 3.0, 1.1 Hz, 1H), 5.48 (ddd, J = 10.8, 4.5, 2.0 Hz, 1H), 5.38 – 5.24 (m, 2H), 3.99 (dddd, J = 14.7, 7.1, 5.9, 1.6 Hz, 1H), 3.92 – 3.85 (m, 1H), 3.86 – 3.77 (m, 1H), 3.80 (s, 3H), 3.73 (s, 3H), 3.67 (d, J = 2.5 Hz, 1H), 3.43 (dd, J = 5.9, 3.0 Hz, 1H), 3.10 (d, J = 12.6 Hz, 1H), 2.74 (dt, J = 14.1, 11.3 Hz, 1H), 2.33 – 2.12 (m, 5H), 2.08 – 2.01 (m, 1H), 1.98 – 1.82 (m, 2H), 1.83 – 1.74 (m, 1H), 1.61 – 1.40 (m, 2H), 1.38 – 1.18 (m, 2H), 1.15 (d, J = 7.2 Hz, 3H), 1.01 (d, J = 6.8 Hz, 3H), 0.98 (d, J = 7.0 Hz, 3H), 0.92 (t, J = 7.0 Hz 3H), 0.89 (d, J = 7.2 Hz, 6H), 0.88 (s, 9H), 0.76 (s, 9H), 0.00 (s, 3H), -0.04 (s, 3H), -0.20 (s, 3H), -0.62 (s, 3H). ^{13}C NMR (126 MHz, CDCl$_3$) δ 177.03, 172.20, 169.99, 166.89, 158.69, 132.86, 127.57, 126.22, 109.24, 106.49, 97.14, 77.74, 72.88, 72.84, 71.70, 56.11, 55.39, 44.49, 40.18, 40.09, 38.28, 36.43, 36.39, 35.95, 34.05, 32.15, 32.08, 29.85, 28.96, 26.27, 25.95, 19.40, 17.95, 14.23, 13.75, 11.50, 11.16, -3.56, -3.81, -5.00, -5.73. HRMS (ESI, *m/z*): calcd for $[C_{46}H_{81}NO_8Si_2]^+$, ([M + Na]$^+$): 854.5398, found 854.5401.

(2*R*,3*S*)-*N*-((5*R*,6*R*,7*R*,*Z*)-6-((*tert*-butyldimethylsilyl)oxy)-7-((3*S*,8*S*,9*R*,*Z*)-9-((*tert*-butyldimethylsilyl)oxy)-14-hydroxy-12-methoxy-8-methyl-1-oxo-3,4,7,8,9,10-hexahydro-1*H*-benzo[*c*][1]oxacyclododecin-3-yl)-5-methyloct-2-en-1-yl)-3-hydroxy-2-methylhexanamide, 104

A 1 mL reaction vessel was flame dried and flushed with argon before DCM (200 μL) and compound **103** (2.2 mg, 0.003 mmol, 1 eq.) were added. The solution was cooled to -78 °C and boron trichloride (1M in DCM, 12 μL, 0.012 mmol, 4 eq.) was added dropwise over 10 min. Stirring was continued at -78 °C for 3.5 h at which point the reaction was quenched by the addition of saturated aqueous sodium acetate (2 mL) and subsequently diluted with DCM (1 mL). The organic layer was collected and the aqueous layer was extracted with DCM (5 X, 1 mL). The combined organic layers were dried over anhydrous sodium sulfate and solvent was removed under reduced pressure to afford a light yellow oil that was purified by SiO$_2$ flash chromatography (35 % – 50 % EtOAc in hexanes) to provide isomerically pure **104** as an amorphous solid (1.9 mg, 78 %). [α]^{25}$_D$ = 10.2° , c = 0.001, DCM). ^{1}H NMR (500 MHz, CDCl$_3$) δ 11.56 (s, 1H), 6.31 (d, *J* = 2.6 Hz, 1H), 6.29 (d, *J* = 2.6 Hz, 1H), 5.73 (bt, 1H), 5.47 (dd, *J* = 20.6, 10.4 Hz, 1H), 5.40 – 5.32 (m, 2H), 5.31 – 5.25 (m, 1H), 5.11 (dd, *J* = 11.3, 4.5 Hz, 1H), 3.90 – 3.81 (m, 2H), 3.78 (s, 3H), 3.78 – 3.72 (m, 2H), 3.67 (dd, *J* = 14.5, 6.7 Hz, 1H), 3.59 (d, *J* = 11.8 Hz, 1H), 3.49 (bs, 1H), 2.73 (dd, *J* = 25.1, 10.9 Hz, 1H), 2.27 (dt, *J* = 16.3, 12.6 Hz, 2H), 2.22 – 2.13 (m, 2H), 2.11 – 2.05 (m, 2H), 1.97 – 1.93 (m, 1H), 1.93 – 1.82 (m, 2H), 1.80 – 1.71

(m, 2H), 1.67 – 1.59 (m, 3H), 1.17 (d, J = 7.2 Hz, 3H), 1.01 (d, J = 6.8 Hz, 3H), 0.96 (d, J = 6.7 Hz, 3H), 0.93 (d, J = 7.2 Hz, 3H), 0.91 (s, 9H), 0.88 (t, J = 7.0 Hz, 3H), 0.74 (s, 9H), 0.10 (s, 3H), 0.06 (s, 3H), -0.21 (s, 3H), -0.67 (s, 3H). ^{13}C NMR (126 MHz, CDCl$_3$) δ 176.60, 171.70, 165.17, 163.39, 144.87, 132.20, 131.63, 126.40, 125.88, 114.22, 105.30, 99.62, 78.27, 76.59, 73.59, 71.77, 55.43, 44.62, 40.17, 39.90, 38.17, 36.31, 35.88, 33.25, 32.08, 29.59, 29.39, 29.21, 26.18, 25.88, 24.88, 22.85, 19.37, 14.28, 14.21, 11.18, -3.19, -4.27, -4.83, -5.84. HRMS (ESI, m/z): calcd for $[C_{45}H_{79}NO_8Si_2]^+$, ($[M + Na]^+$): 840.5242, found 840.5245.
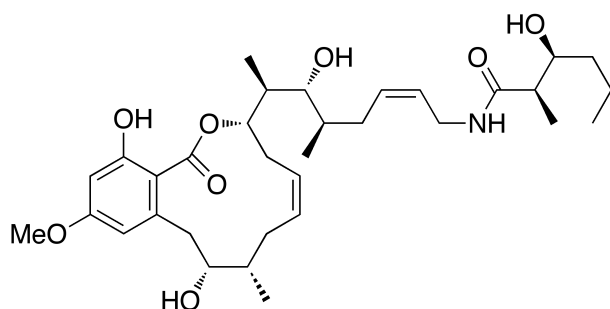
Cruentaren A, 1

A Teflon reaction vessel was equipped with a stir bar and charged with ACN (200 mL) and compound **104** (2.0 mg, 0.0021 mmol, 1 eq.). The solution was cooled to 0 °C and aqueous HF (48 % w/w, 200 mL) and stirring was continued for 1 h at 0 °C then continued for 1 h at rt. The reaction mixture was cooled back to 0 °C and was quenched by the addition of saturated aqueous sodium bicarbonate (5 mL) and diluted with EtOAc (5 mL). The organic layer was collected and the aqueous layer was extracted with EtOAc (5 X, 5 mL). The combined organic layers were dried over anhydrous sodium sulfate and solvent was removed under reduced pressure to afford an organge oil that was purified by thin-layer chromatography (20 % acetone in DCM) to afford cruentaren A (**1**) as a colorless amorphous solid (0.6 mg, 51 %). $[\alpha]^{25}_D$ = 3.2°, c =0.0006 , DCM). ^{1}H NMR (500 MHz, CDCl$_3$) δ 11.50 (br s, 1H), 6.37 (d, J = 2.7 Hz, 1H), 6.31 (d, J = 2.6 Hz, 1H), 6.09 (t, J = 5.4 Hz, 1H), 5.56 (dddt, J = 10.8, 8.6, 7.1, 1.4 Hz, 1H), 5.46–5.52 (m, 1H),

5.44 (ddd, J = 11.1, 4.5, 1.6 Hz, 1H), 5.40 (dddd, J = 11.0, 11.0, 4.5, 2.0 Hz, 1H), 5.30 (ddd, J = 11.6, 5.6, 1.9 Hz, 1H), 3.91 (dddd, J = 14.9, 7.5, 5.8, 1.3, 1H), 3.80–3.87 (m, 2H), 3.80 (s, 3H), 3.74 (dd, J = 12.8, 1.6 Hz, 1H), 3.64 (ddd, J = 10.8, 2.9, 1.7 Hz, 1H), 3.45 (ddd, J = 9.1, 6.7, 2.1 Hz, 1H), 3.10 (d, J = 3.3 Hz, 1H), 2.83 (dt, J = 14.1, 11.5 Hz, 1H), 2.75 (d, J = 6.7 Hz, 1H), 2.34 (dt, J = 14.3, 11.6 Hz, 1H), 2.27 (dq, J = 7.2, 2.9 Hz, 1H) 2.20–2.28 (m, 4H), 1.95–2.05 (m, 3H), 1.70 (dddq, J = 9.1, 6.8, 6.8, 4.7 Hz, 1H), 1.42–1.51 (m, 2H), 1.27–1.35 (m, 3H), 1.15 (d, J = 7.2 Hz, 3H), 1.01 (d, J = 6.9 Hz, 3H), 0.92 (t, J = 7.0 Hz, 3H), 0.89 (d, J = 7.0 Hz, 3H), 0.79 (d, J = 6.9 Hz, 3H); ^{13}C NMR (126 MHz, CDCl$_3$) δ 176.35, 171.48, 165.67, 163.48, 143.73, 132.22, 130.88, 126.74, 125.80, 112.27, 104.85, 99.64, 78.00, 74.68, 73.12, 71.74, 55.39, 44.80, 39.17, 38.32, 36.81, 36.72, 36.55, 35.85, 31.60, 30.69, 29.82, 19.20, 16.11, 14.22, 14.01, 11.29, 8.55. HRMS (ESI, m/z): calcd for [C$_{33}$H$_{51}$NO$_8$]$^+$, ([M + Na]$^+$): 612.3506, found 612.3508.
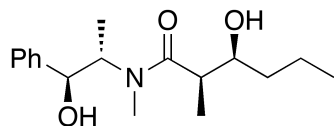
**(2R,3S)-3-hydroxy-N-((1S,2S)-1-hydroxy-1-phenylpropan-2-yl)-N,2-dimethylhexanamide, 50**

A 250 mL flask was flame dried and flushed with argon before anhydrous THF (25 mL) and DIPA (2.70 mL, 19.0 mmol, 2.1 eq.) were added. The solution was cooled to -78 °C and *n*-butyllithium (2.5 M in hexanes, 7.42 mL, 18.6 mmol, 2.05 eq.) was slowly added. Stirring was continued as the solution was allowed to warm to 0 °C and then cooled back to -78 °C at which point a solution of *S,S*-pseudoephedrine propionamide (2.0 g, 9.05 mmol, 1 eq.) in anhydrous THF (25 mL) was added slowly *via* cannula. Stirring was continued at -78 °C for 2 hr, 0 °C for 30 min, and rt for 10 min. The reaction mixture was cooled back to -78 °C followed by the addition of a solution of Bis(cyclopentadienyl)zirconium(IV) dichloride (5.80 g, 19.9 mmol, 2.2

eq.) in anhydrous THF (56 mL). The deep orange solution was stirred at -78 °C for 3 hr and then cooled to -116 °C when a solution butyraldehyde (2.30 g, 9.05 mmol, 1 eq.) in anhydrous THF (5.6 mL) was added dropwise. Stirring was continued at -116 °C for 3 hr at which point the reaction was quenched by the addition of saturated aqueous ammonium chloride (25 mL). The biphasic reaction mixture was warmed to rt and filtered through a pad of celite using EtOAc (150 mL) to rinse. The organic layer was collected, and the aqueous layer was extracted with EtOAc (3 X, 50 mL). The combined organic layers were dried over anhydrous sodium sulfate and solvent was removed under reduced pressure to afford an orange oil that was purified by SiO_2 flash chromatography (40 % – 70%) to provide pure **50** as a colorless oil (84 %). $[\alpha]^{25}_D = 69.7°$ (c = 0.006, DCM). ^{1}H NMR (500 MHz, CDCl$_3$) δ 7.41 – 7.27 (m, 5H), 4.66 – 4.62 (m, 1H), 4.61 (d, J = 8.0 Hz, 1H), 4.56 (bs, 1H), 4.23 (s, 1H), 4.06 (m, 1H), 3.85 – 3.80 (m, 1H), 3.75 (m, 1H), 2.94 (s, 3H), 2.87 (s, 3H), 2.73 (m, 1H), 2.53 (qd, J = 7.0, 2.1 Hz, 1H), 1.56 – 1.41 (m, 2H), 1.40 – 1.29 (m, 1H), 1.29 – 1.18 (m, 1H), 1.16 – 1.03 (m, 6H), 1.01 – 0.88 (m, 3H). ^{13}C NMR (126 MHz, CDCl$_3$) δ 179.86, 179.16, 142.25, 141.33, 129.02, 128.76, 128.61, 128.00, 126.82, 126.43, 77.37, 76.42, 76.02, 71.37, 71.06, 57.85, 40.04, 39.00, 36.13, 35.89, 27.45, 19.45, 19.38, 15.84, 14.34, 14.28, 14.22, 10.52, 9.68. HRMS (ESI, m/z): calcd for $[C_{17}H_{27}NO_3]^+$, $([M + Na]^+)$: 316.1889, found 316.1890.
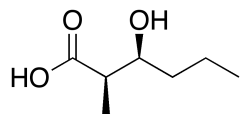
(2*R*,3*S*)-3-hydroxy-2-methylhexanoic acid, 5

A 50 mL flask was charged with *tert*-butanol (2 mL) and deionized water (6.3 mL) before amide # (200 mg, 0.68 mmol, 1 eq.) and tetrabutylammonium hydroxide (1.5 M in deionized water, 2.3 mL, 3.4 mmol, 5 eq.) were added. The solution was heated at reflux for 23 h. Once the reaction

was complete, the solution was allowed to cool to rt and suspended between 0.5 M aqueous sodium hydroxide (82 mL) and diethyl ether (12 mL). The organic layer was removed, and the aqueous layer was extracted with diethyl ether (3 X, 12 mL). The aqueous layer was cooled to 0 °C, saturated with sodium chloride, and acidified to pH 2 with 4 N aqueous hydrochloric acid. The acid solution was extracted with diethyl ether (4 X, 15 mL) and the combined organic extracts were dried over anhydrous sodium sulfate. Solvent was removed under reduced pressure to afford pure acid # as a colorless, amorphous solid (94%). $[\alpha]^{25}_D$ = -12.5° (c = 0.021, DCM). ^{1}H NMR (500 MHz, CDCl$_3$) δ 3.96 (dt, J = 8.7, 3.8 Hz, 1H), 3.32 (bs, 1H), 2.63 (qd, J = 7.2, 3.5 Hz, 1H), 1.58 – 1.31 (m, 4H), 1.21 (d, J = 7.2 Hz, 3H), 0.95 (t, J = 7.1 Hz, 3H). ^{13}C NMR (126 MHz, CDCl$_3$) δ 179.74, 71.63, 44.11, 35.71, 19.32, 14.09, 10.69. HRMS (ESI, *m/z*): calcd for [C$_7$H$_{14}$O$_3$]$^-$, ([2M + Na − 2H]$^+$): 313.1627, found 313.1627.

III.6   References

1.   Gruber, G.; Wieczorek, H.; Harvey, W. R.; Muller, V. F1Fo, V1Vo and A1Ao enzymes are essential cellular energy converters which transduce the chemical energy of ATP hydrolysis into transmembrane ionic electrochemical potential differences. *J. Exp. Biol.* **2001,** 204, 2597-2605.

2.   Pedersen, P. L. Transport ATPases: structure, motors, mechanism and medicine: a brief overview. *J. Bioenerg. Biomembr.* **2005,** 37, 349-257.

3.   Pedersen, P. L. Transport ATPases into the year 2008: a brief overview related to types, structures, functions and roles in health and disease. *J. Bioenerg. Biomembr.* **2007,** 39, 349-355.

4.   Gledhill, J. R.; Walker, J. E. Inhibition sites in F1-ATPase from bovine heart mitochondria. *Biochem. J.* **2005,** 386, 591-598.

5.   Seelert, H.; Dencher, N. A. ATP synthase superassemblies in animals and plants: two or more are better. *Biochim. Biophys. Acta* **2011,** 1807, 1185-1197.

6.   Velours, J.; Dautant, A.; Salin, B.; Sagot, I.; Brekhes, D. Mitochondrial F(1)F(0)-ATP synthase and organellar internal architecture. *Int. J. Biochem. Cell Biol.* **2009,** 41, 1783-1789.

7.   Groth, G.; Pohl, E. The structure of the chloroplast F1-ATPase at 3.2 A resolution. *J. Biol. Chem.* **2001,** 276, 1345-1352.

8.   Capuano, F.; Guerrieri, F.; Papa, S. Oxidative phosphorylation enzymes in normal and neoplatic cell growth. *J. Bioenerg. Biomembr.* **1997,** 29, 379-384.

9.   Panfoli, I.; Ravera, S.; Brushi, M.; Candiano, G.; Morelli, A. Proteomics unravels the exportability of mitochondrial respiratory chains. *Expert. Rev. Proteomics* **2011,** 8, 231-239.

10.   Kim, J. W.; Adachi, H.; Shin-Ya, K.; Hayakawa, Y.; Seto, H. Apoptolidin, a new apoptosis inducer in transformed cells from *Nocardiopsis* sp. *J. Antibiot.* **1997,** 50, 628-630.

11.   Hayakawa, Y.; Kim, J. W.; Adachi, H.; Shin-Ya, K.; Fujita, H. S. Structure of apoptolidin; a specific apoptosis inducer in transformed-cells. *J. Am. Chem. Soc.* **1998,** 120, 3524-3525.

12.   Salomon, A. R.; Voehringer, D. W.; Herzenberg, L. A.; Khosla, C. Understanding and exploiting the mechanistic basis for selectivity of polyketide inhibitors of F0F1-ATPase. *Proc. Natl. Acad. Sci. USA* **2000,** 97, 14766-14771.

13.   Salomon, A. R.; Voehringer, D. W.; Herzenberg, L. A.; Khosla, C. Apoptolidin, a selective cytotoxic agent, is an inhibitor of F0F1-ATPase. *Chem. Biol.* **2001,** 8, 71-80.

14.   Blatt, N. B.; Boitano, A. E.; Lyssiotis, C. A.; Opipari, A. W.; Glick, G. D. Bz-423 superoxide signals B cell apoptosis via Mcl-1, Bak, and Bax. *Biochem. Pharmacol.* **2009,** 78, 966-973.

15.   Sundberg, T. B.; Ney, G. M.; Subramanian, C.; Opipari, A. W.; Glick, G. D. The immunomodulatory benzodiazepine Bz-423 inhibits B-cell proliferation by targeting c-Myc protein for rapid and specific degradation. *Cancer Res.* **2006,** 66, 1775-1782.

16.   Johnson, K. M.; Chen, X. N.; Boitano, A. E.; Swenson, L.; Opipari, A. W.; Glick, G. D. Identification and validation of the mitochondrial F1F0-ATPase as the molecular target for the immunomodulatory benzodiazepine Bz-423. *Chem. Biol.* **2005,** 12, 485-496.

17.   Mowery, Y. M.; Pizzo, S. V. Targeting cell surface F1F0 ATP synthase in cancer therapy. *Cancer Biol. Ther.* **2008,** 7, 1836-1838.

18.   Wang, J.; Han, Y.; Liang, J.; Cheng, X.; Yan, L.; Wang, Y.; Liu, J.; Luo, G.; Chen, X.; Zhao, L.; Zhou, X.; Wu, K.; Fan, D. Effect of a novel inhibitor mAb against beta-subunit of F1F0 ATPase on HCC. *Cancer Biol. Ther.* **2008,** 7, 1829-1835.

19.   Dang, C. V.; Hamaker, M.; Sun, P.; Gao, A. L. P. Therapeutic targeting of cancer cell metabolism. *J. Mol. Med.* **2011,** 89, 205-212.

20.   Bayley, J.-P.; Devilee, P. Warburg tumours and the mechanisms of mitochondrial tumour suppressor genes. Barking up the right tree? *Curr. Opin. Genet. Dev.* **2010,** 20, 324-329.

21.   Das, A. M. Regulation of the mitochondrial ATP-synthase in health and disease. *Mol. Genet. Metab.* **2003,** 79, 71-82.

22.   Ferreira, L. M. R. Cancer metabolism: the warburg effect today. *Exp. Mol. Pathol.* **2010,** 89, 372-380.

23.   Scatena, R.; Bottoni, P.; Pontoglio, A.; Giardina, B. Revisiting the Warburg effect in cancer cells with proteomics. The emergence of new approaches to diagnosis, prognosis, and therapy. *Proteomics Clin. Appl.* **2010,** 4, 143-158.

24.   Willers, I. M.; Cuezva, J. M. Post-transcriptional regulation of the mitochondrial H+-ATP synthase: a key regulator of the metabolic phenotype of cancer. *Biochim. Biophys. Acta* **2011,** 1807, 543-551.

25.   Martinez-Outschoorn, U. E.; Lin, Z.; Ko, Y.-H.; Goldberg, A. F.; Flomenberg, N.; Wang, C.; Pavlides, S.; Pestell, R. G.; Howell, A.; Sotgia, F.; Lisanti, M. P. Understanding the metabolic basis of drug resistance: therapeutic induction of the Warburg effect kills cancer cells. *Cell Cycle* **2011,** 10, 2521-2528.

26.   Fosslien, E. Mitochondrial medicine - molecular pathology of defective oxidative phosphorylation. *Ann. Clin. Lab. Sci.* **2001,** 31, 25-67.

27.   Huttemann, M.; Lee, I.; Pecinova, A.; Pecina, P.; Przyklenk, K.; Doan, J. W. Regulation of oxidative phosphorylation, the mitochondrial membrane potential, and their role in human disease. *J. Bioenerg. Biomembr.* **2008,** 40, 445-456.

28.   Kucharczyk, R.; Zick, M.; Bietenhader, M.; Rak, M.; Couplan, E.; Blondel, M.; Caubet, S.-D.; Rago, J.-P. d. Mitochondrial ATP synthase disorders: molecular mechanisms and the quest for curative therapeutic approaches. *Biochim. Biophys. Acta* **2009,** 1793, 186-199.

29.   Kenan, D. J.; Wahl, M. L. Ectopic localization of mitochondrial ATP synthase: a target for anti-angiogenesis intervention? *J. Bioenerg. Biomembr.* **2005,** 37, 461-465.

30.   Pavlides, S.; Tsirigos, A.; Vera, I.; Flomenberg, N.; Frank, P. G.; Casimiro, M. C.; Wang, C.; Pestell, R. G.; Martinez-Outschoorn, U. E.; Howell, A.; Sotgia, F.; Lisanti, M. P. Transcriptional evidence for the "Reverse Warburg Effect" in human breast cancer tumor stroma

and metastasis: similarities with oxidative stress, inflammation, Alzheimer's disease, and "neuron-glia metabolic coupling". *Aging* **2010,** 2, 185-199.

31.   Pavlides, S.; Whitaker-Menezes, D.; Castello-Cros, R.; Flomenberg, N.; Witkiewicz, A. K.; Frank, P. G.; Casimiro, M. C.; Wang, C.; Fortina, P.; Addya, S.; Pestell, R. G.; Martinez-Outschoorn, U. E.; Sotgia, F.; Lisanti, M. P. The reverse Warburg effect: aerobic glycolysis in cancer associated fibroblasts and the tumor stroma. *Cell Cycle* **2009,** 8, 3984-4001.

32.   Bonuccelli, G.; Whitaker-Menezes, D.; Castello-Cros, R.; Pavlides, S.; Pestell, R. G.; Fatatis, A.; Witkiewicz, A. K.; Vander Heiden, M. G.; Migneco, G.; Chivarina, B.; Frank, P. G.; Capozza, F.; Flomenberg, N.; Martinez-Outschoorn, U. E.; Sotgia, F.; Lisanti, M. P. The reverse Warburg effect: glycolysis inhibitors prevent tumor promoting effects of caveolin-1 deficient cancer associated fibroblasts. *Cell Cycle* **2010,** 9, 1950-1971.

33.   Dang, C. V. p32 (C1QBP) and cancer cell metabolism: is the Warburg effect a lot of hot air? *Mol. Cell. Biol.* **2010,** 30, 1300-1302.

34.   Migneco, G.; Whitaker-Menezes, D.; Chiavarina, B.; Castello-Cros, R.; Pavlides, S.; Pestell, R. G.; Fatatis, A.; Flomenberg, N.; Tsirigos, A.; Howell, A.; Martinez-Outschoorn, U. E.; Sotgia, F.; Lisanti, M. P. Glycolytic cancer associated fibroblasts promote breast cancer tumor growth, without a measureable increase in angiogenesis: evidence for stromal-epithelial metabolic coupling. *Cell Cycle* **2010,** 9, 2412-2422.

35.   Martinez-Outschoorn, U. E.; Pavlides, S.; Howell, A.; Pestell, R. G.; Tanowits, H. B.; Sotgia, F.; Lisanti, M. P. Stromal-epithelial metabolic coupling in cancer: integrating autophagy and metabolism in the tumor microenvironment. *Int. J. Biochem. Cell Biol.* **2011,** 43, 1045-1051.

36.   Lisanti, M. P.; Martinez-Outschoorn, U. E.; Chivarina, B.; Pavlides, S.; Whitaker-Menezes, D.; Tsirigos, A.; Witkiewicz, A. K.; Lin, Z.; Balliet, R.; Howell, A.; Sotgia, F.

Understanding the "lethal" drivers of tumor-stroma co-evolution: emerging role(s) for hypoxia, oxidative stress and autophagy/mitophagy in the tumor micro-environment. *Cancer Biol. Ther.* **2010,** 10, 537-542.

37.   Bonuccelli, G.; Tsirigos, A.; Whitaker-Menezes, D.; Pavlides, S.; Pestell, R. G.; Chivarina, B.; Frank, P. G.; Flomenberg, N.; Howell, A.; Martinez-Outschoorn, U. E.; Sotgia, F.; Lisanti, M. P. Ketones and lactate "fuel" tumor growth and metastasis: evidence that epithelial cancer cells use oxidative mitochondrial metabolism. *Cell Cycle* **2010,** 9, 3506-3514.

38.   Martinez-Outschoorn, U. E.; Balliet, R.; Rivadeneira, D. B.; Chivarina, B.; Pavlides, S.; Wang, C.; Whitaker-Menezes, D.; Daumer, K. M.; Lin, Z.; Witkiewicz, A. K.; Flomenberg, N.; Howell, A.; Pestell, R. G.; Knudsen, E. S.; Sotgia, F.; Lisanti, M. P. Oxidative stress in cancer associated fibroblasts drives tumor-stroma co-evolution: a new paradigm for understanding tumor metabolism, the field effect and genomic instability in cancer cells. *Cell Cycle* **2010,** 9, 3256-3276.

39.   Martinez-Outschoorn, U. E.; Lin, Z.; Trimmer, C.; Flomenberg, N.; Wang, C.; Pavlides, S.; Pestell, R. G.; Howell, A.; Sotgia, F.; Lisanti, M. P. Cancer cells metabolically "fertilize" the tumor microenvironment with hydrogen peroxide, driving the Warburg effect. *Cell Cycle* **2011,** 10, 2504-2520.

40.   Moser, T. L.; Kenan, D. J.; Ashley, T. A.; Roy, J. A.; Goodman, M. D.; Misra, U. K.; Cheek, D. J.; Pizzo, S. V. Endothelial cell surface F1-Fo ATP synthase is active in ATP synthesis and is inhibited by angiostatin. *Proc. Natl. Acad. Sci. USA* **2001,** 98, 6656-6661.

41.   Francis, B. R.; Thorsness, P. E. Hsp90 and mitochondrial proteases Yme1 and Yta10/12 participate in ATP synthase assembly in *Sarccharomyces cerevisiae. Mitochondrion* **2011,** 11, 587-600.

42.   Papathanassiu, A. E.; MacDonald, N. J.; Bencsura, A.; Vu, H. A. F1F0-ATP synthase functions as a co-chaperone of Hsp90-substrate protein complexes. *Biochem. Biophys. Res. Commun.* **2006,** 345, 419-429.

43.   Giorgio, V.; Bisetto, E.; Franca, R.; Harris, D. A.; Passamonti, S.; Lippe, G. The ectopic F(O)F(1) ATP synthase of rat liver is modulated in acute cholestasis by the inhibitor protein IF(1). *J. Bioenerg. Biomembr.* **2010,** 42, 117-123.

44.   Chi, S. L.; Pizzo, S. V. Cell surface F1Fo ATP synthase: a new paradigm? *Ann. Med.* **2006,** 38, 429-438.

45.   Papathanassiu, A. E.; MacDonald, N. J.; Emlet, D. R.; Vu, H. A. Antitumor activity of efrapeptins, alone or in combination with 2-deoxyglucose, in breast cancer *in vitro* and *in vivo*. *Cell Stress Chaperones* **2011,** 16, 181-193.

46.   Jundt, L.; Steinmetz, H.; Luger, P.; Weber, M.; Kunze, B.; Reichenbach, H.; Hofle, G. Isolation and structure elucidation of cruentarens A and B - novel members of the benzolactone class of ATPase inhibitors from myxobacterium *Byssovorax cruenta*. *European J. Org. Chem.* **2006,** 2006, 5036-5044.

47.   Kunze, B.; Sasse, F.; Wieczorek, H.; Huss, M. Cruentaren A, a highly cytotoxic benzolactone from Myxobacteria is a novel selective inhibitor of F1-ATPases. *FEBS Lett.* **2007,** 581, 3523-3527.

48.   Kunze, B.; Steinmetz, H.; Hofle, G.; Huss, M.; Wieczorek, H.; Reichenbach, H. Cruentaren, a new antifungal salicylate-type macrolide from *Byssovorax cruenta* (myxobacteria) with inhibitory effect on mitochondrial ATPase activity. Fermentation and biological properties. *J. Antibiot.* **2006,** 59, 664-668.

49.   Bindl, M.; Jean, L.; Hermann, J.; Muller, R.; Furstner, A. Preparation, modification, and evaluation of cruentaren a and analogues. *Chem. Eur. J.* **2009,** 15, 12310-12319.

50.   Furstner, A.; Bindl, M.; Jean, L. Concise total synthesis of cruentaren a. *Angew. Chem. Int. Ed.* **2007,** 46, 9275-9278.

51.   Vintonyak, V. V.; Cala, M.; Lay, F.; Kunze, B.; Sasse, F.; Maier, M. E. Synthesis and biological evaluation of cruentaren a analogues. *Chem. Eur. J.* **2008,** 14, 3709-3720.

52.   Vintonyak, V. V.; Maier, M. E. Synthesis of the core structure of cruentaren a. *Org. Lett.* **2007,** 9, 655-658.

53.   Vintonyak, V. V.; Maier, M. E. Total synthesis of cruentaren a. *Angew. Chem. Int. Ed.* **2007,** 46, 5209-5211.

54.   Prasad, B. R. V.; Meshram, H. M. Synthetic studies on cytotoxic macrolides cruentarens A and B: stereoselective synthesis of the C(8)-C(19) segment of cruentarens A and B. *Tetrahedron Asymmetry* **2010,** 22, 713-716.

55.   Maier, M. E.; Ritschel, J. A second generation synthesis of cruentaren A core structure based on oxetane and oxirane opening reactions. *ARKIVOC* **2008,** xiv, 314-329.

56.   Myers, A. G.; Yang, B. H.; Chen, H.; McKinstry, L.; Kopecky, D. J.; Gleason, J. L. Pseudoephedrine as a practical chiral auxiliary for the synthesis of highly enantiomerically enriched carboxylic acids, alcohols, aldehydes, and ketones. *J. Am. Chem. Soc.* **1997,** 119, 6496-6511.

57.   Rodriguez, M.; Vicario, J. L.; Badia, D.; Carrillo, L. (*S,S*)-(+)-pseudoephedrine as a chiral auxiliary in asymmetric acetate aldol reactions. *Org. Biomol. Chem.* **2005,** 3, 2026-2030.

58.   Dohi, T.; Ito, M.; Yamaoka, N.; Morimoto, K.; Fujioka, H.; Kita, Y. Hypervalent iodine(III): selective and efficient single-electron-transfer (SET) oxidizing agent. *Tetrahedron* **2009,** 65, 10797-10815.

59.   Brown, H. C.; Bhat, K. B.; Randad, R. S. Chiral synthesis via organoboranes .21. allylboration and crotylboration of alpha-chiral aldehydes with diisopinocampheylboron as the chiral auxiliary. *J. Org. Chem.* **1989,** 54, 1570-1576.

60.   Nicholas, K. M. Chemistry and synthetic utility of cobalt-complexed propargyl cations. *Acc. Chem. Res.* **1987,** 20, 207-214.

61.   Kobl, H. C.; VanNieuwenhze, M. S.; Sharpless, B. Catalytic asymmetric dihydroxylation. *Chem. Rev.* **1994,** 94, 2483-2547.

62.   Ishihara, K.; Gao, Q.; Yamamoto, H. *J. Am. Chem. Soc.* **1994,** 115, 10412.

63.   Soto-Cairoli, B.; Soderquist, J. A. Strict reagent control in the asymmetric allylboration of N-TIPS-alpha-amino aldehydes with B-allyl-10-TMS-9-borabicyclo[3.3.2]decanes. *Org. Lett.* **2009,** 11, 401.

64.   Hoye, T. R.; Jeffrey, C. S.; Shao, F. Mosher ester analysis for the determination of absolute configuration of stereogenic (chiral) carbinol carbons. *Nat. Protoc.* **2007,** 2, 2451-2458.

65.   Rychnovsky, S. D.; Richardson, T. I.; Rogers, B. N. Two-dimensional NMR analysis of acetonide derivatives in the stereochemical assignment of polyol chains: the absolute configurations of dermostatins A and B. *J. Org. Chem.* **1997,** 62, 2925-2934.

66.   Corey, E. J.; Helal, C. J. Reduction of carbonyl compounds with chiral oxazaborolidine catalysts: a new paradigm for enantioselective catalysis and a powerful new synthetic method. *Angew. Chem. Int. Ed.* **1998,** 37, 1986-2012.

67.   Lee, C. W.; Grubbs, R. H. Stereoselectivity of macrocyclic ring-closing olefin metathesis. *Org. Lett.* **2000,** 2, 2145-2147.

68.   Gradillas, A.; Perez-Castellis, J. Macrocyclization by ring-closing metathesis in the total synthesis of natural products: reaction conditions and limitations. *Angew. Chem. Int. Ed.* **2006,** 45, 6086-6101.

69.   Wang, Y.; Jimenez, M.; Hansent, A. S.; Raibert, E. A.; Schreiber, S. L.; Young, D. W. Controll of olefin geometry in macrocyclic ring-closing metathesis using a removable silyl group. *J. Am. Chem. Soc.* **2011,** 133, 9196-9199.

70.   Trost, B. M.; Ball, Z. T. Alkyne hydrosilylation catalyzed by a cationic ruthenium complex: efficient and general trans addition. *J. Am. Chem. Soc.* **2005,** 127, 17644-17655.

71.   Chatterjee, A. K.; Choi, T. L.; Sanders, D. P.; Grubbs, R. H. A general model for selectivity in olefin cross metathesis. *J. Am. Chem. Soc.* **2003,** 125, 11360-11370.

72.   Gladiali, S.; Alberico, E. Asymmetric transfer hydrogenation: chiral ligands and applications. *Chem. Soc. Rev.* **2006,** 36, 226-236.

73.   Noyori, R.; Hashiguchi, S. Asymmetric transfer hydrogenation catalyzed by chiral ruthenium complexes. *Acc. Chem. Res.* **1997,** 30, 97-102.

74.   Hong, S. H.; Sanders, D. P.; Lee, C. W.; Grubbs, R. H. Prevention of undesirable isomerization during olefin metathesis. *J. Am. Chem. Soc.* **2005,** 127, 17160-17161.

75.   Viaud, M. C.; Rollin, P. Zinc azide mediated Mitsunobu substitution. An expedient method for the one-pot azidation of alcohols. *Synthesis* **1990,** 2, 130-132.

76.   Chandra, J. S.; Reddy, M. V. R. Stereoselective allylboration using (B)-gamma-alkoxyallyldiisopinocampheylboranes: highly selective reactions for organic synthesis. *ARKIVOC* **2007**, 121-144.

Chapter IV

A Conformation-Based Approach for the Design of Simplified

Natural Product Analogues of Trienomycin A

IV.1 Therapeutic Relevance of Macrocyclic Natural Products

Secondary metabolites have a historically dominant presence in the pharmacopeia. They have also remained a major contemporary contributor to human medicine, particularly in anticancer and antibiotic drug classes.[1-3] Of the more than 100,000 known secondary metabolites, only 3% are macrocycles, *i.e.* contain a 12+-membered ring system.[4] Despite this low natural abundance, a significant number of FDA approved natural product(-derived) drugs are macrocycles.[5] Even among synthetic medicines, a macrocyclization strategy often provides compounds with improved pharmacological profiles in comparison to their linear counterparts. Therefore, the macrocycle is an important structural motif in drug development.[6]

IV.1.1 *The origin of macrocycle pharmacological attributes*

The application of bioactive molecules discovered in living organisms to the treatment of human disease is a remarkable phenomenon. Their clinical success is attributed to the limited use of protein domains common to every species. Despite vast interspecies genomic differences, these protein domains display an inherent pre-organization to form common three-dimensional structures from non-homologous amino acid sequences.[5]

Large natural products (>500 Da) commonly incorporate macrocycles. Despite commonly being in violation of the "Rule of 5", these compounds oftentimes display favorable pharmacological profiles in conjunction with high target specificity. Similar to the selectivity observed for three-dimensional protein-ligand interactions, this target specificity is a consequence of inherent pre-organization imparted by the macrocyclic geometry. As a result,

macrocycles maintain a delicate balance between flexibility and rigidity that influences solubility and permeability, and conformationally constrains the present pharmacophore.[4, 5]

IV.1.2 *Macrocycles and drug development*

Despite their inherent drug-like properties, the complicated architecture exhibited by such macrocyclic natural products represents a significant challenge toward their utility in drug development. While the discovery of novel chemical methodologies has led to the *de novo* synthesis of numerous macrocyclic natural products, approaches toward simplified analogues remains underinvestigated. This chapter describes a conformation-based strategy for predicting simplified, macrocyclic natural product analogues from limited SAR data.

IV.2 Conformation-Based Approach to Predict Simplified Trienomycin A Analogues

Mycobacteria produce the ansamycin family of natural products, which manifest diverse biological activities. Structural characteristics of this family include a macrocyclic polyketide bridged by an aromatic core. Several ansamycins display significant clinical attributes, including rifampicin, which manifests antimicrobial activity for the treatment tuberculosis,[7] and geldanamycin, derivatives of which have entered phase III clinical trials for the treatment of cancer.[8] In general, the ansamycin family exhibits a high degree of broad inhibitory activities that include antiviral, antifungal, and immunosuppressant activity.[9, 10]

Trienomycin A (Figure 4.1, **1**) is a member of the ansamycin family first isolated from *Streptomyces* sp. No. 83-16 by Umezawa and coworkers.[11] In contrast to other members of the ansamycin family that possess a *p*-quinone or *p*-hydroquinone moiety within the aromatic bridge, trienomycin A contains a non-redox active phenol. In addition, trienomycin A displays a biological profile that contrasts the activity manifested by other ansamycins. For example, mycotrienin II, which is structurally identical to trienomycin A with the exception of a *p*-

hydroquinone moiety, is a potent antifungal agent as well as a promising anticancer agent.[9, 12] In contrast, trienomycin A manifests potent anticancer activity (IC_{50} of 128 nM against HeLa cervical cancer cells),[13] but displays no antifungal activity, nor does it display any significant antimicrobial, antiviral, or immunosuppressant activity.[9, 11, 13-15]

A previous report indicated that while trienomycin A exhibits potent anticancer and antitumor activity, it was found to be significantly less toxic to non-transformed cells.[8] Thus, the unique biological activity manifested by trienomycin A poses this natural product as an attractive lead compound for cancer chemotherapeutic development.
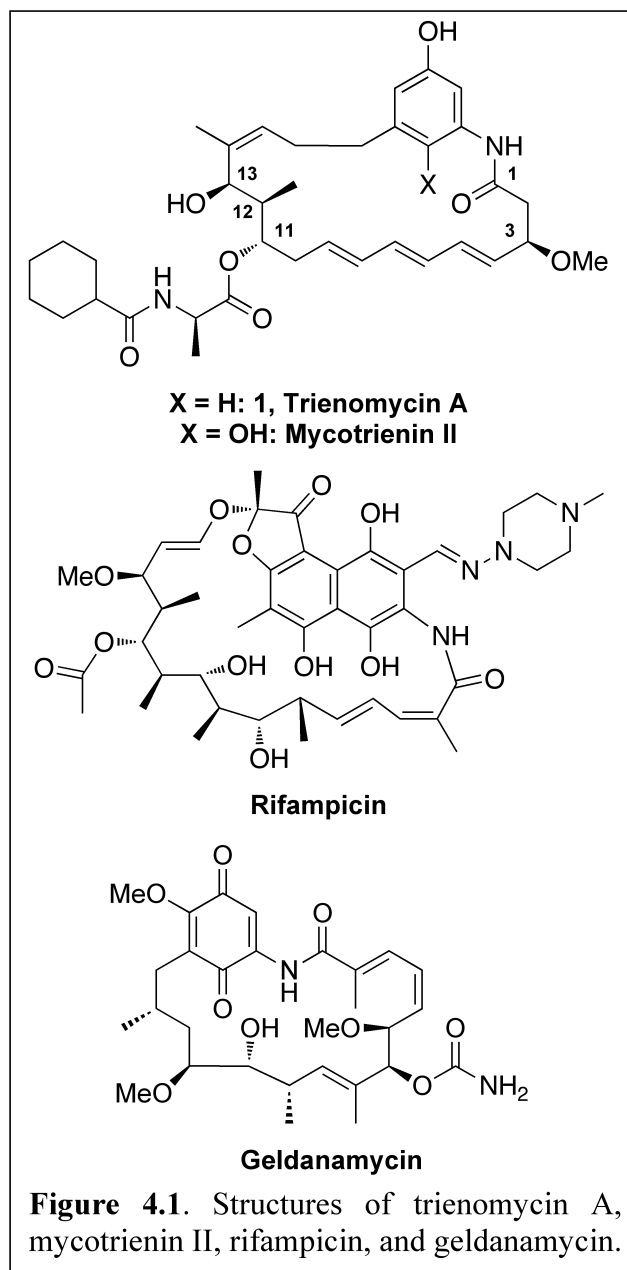
Figure 4.1. Structures of trienomycin A, mycotrienin II, rifampicin, and geldanamycin.

Unfortunately, limited structure-activity relationships (SAR) for trienomycin A have been reported and the mechanism of action remains unknown. Furthermore, significant quantities of the natural product are not available and only one total synthesis has been reported, which produces the natural product in 31 linear steps.[16] Although elegant in nature, this route does not afford a succinct method for evaluation of SAR. Therefore, a generalized method for the

production of synthetically useful trienomycin A analogues employing a conformation-based approach was pursued.

IV.2.1 *Trienomycin A SAR*

Previously reported semi-synthetic modifications to the natural product including acetylation of the 13-OH (**2**), saturation of the triene motif (**3**), and deletion of the *N*-cyclohexylcarbonyl D-Ala (NCxDA) side chain (**4**), resulted in almost complete ablation of anticancer activity (Figure 4.2, **2**–**4**).[9] However, methylation of the free phenol did produce an analogue equipotent to the natural product (Figure 4.2, **5**). Without apparent SAR trends, and the lack of activity for semi-synthetic derivatives, no obvious hypothesis for further exploration was available. Therefore, an alternate approach was pursued based on the overall conformation of the macrocyclic compounds, and the lowest energy conformations of such analogues.

IV.2.2 *Conformational analysis of trienomycin A analogues*

The natural product (**1**) and four semi-synthetic derivatives (**2-5**) were constructed in the lowest energy conformations using SYBYL. The three-dimensional geometries of these compounds were then analyzed using the Surflex Ligand Similarity tool (default parameter settings).[17] Rigid superposition maintained low energy conformations and provided informative differences in ligand similarity (Figure 4.2). Semi-synthetic derivatives **2**–**4** exhibited significant conformational perturbations in macrocycle geometry and placement of NCxDA side chain, but methyl-phenyl ether **5** retained the native geometry. Because these semi-synthetic derivatives maintain most of the hydrogen bonding capabilities of trienomycin A, we hypothesized that orientation of the NCxDA side chain and projection of the phenol are critical to the biological activity manifested by trienomycin A.

Figure 4.2. A) Overlay of energy minimized trienomycin A and select semi-synthetic derivatives using the Ligand Similarity tool (rigid superposition) from the Surflex software suite. B) Relative energies and similarity score from the Ligand Similarity tool.

238
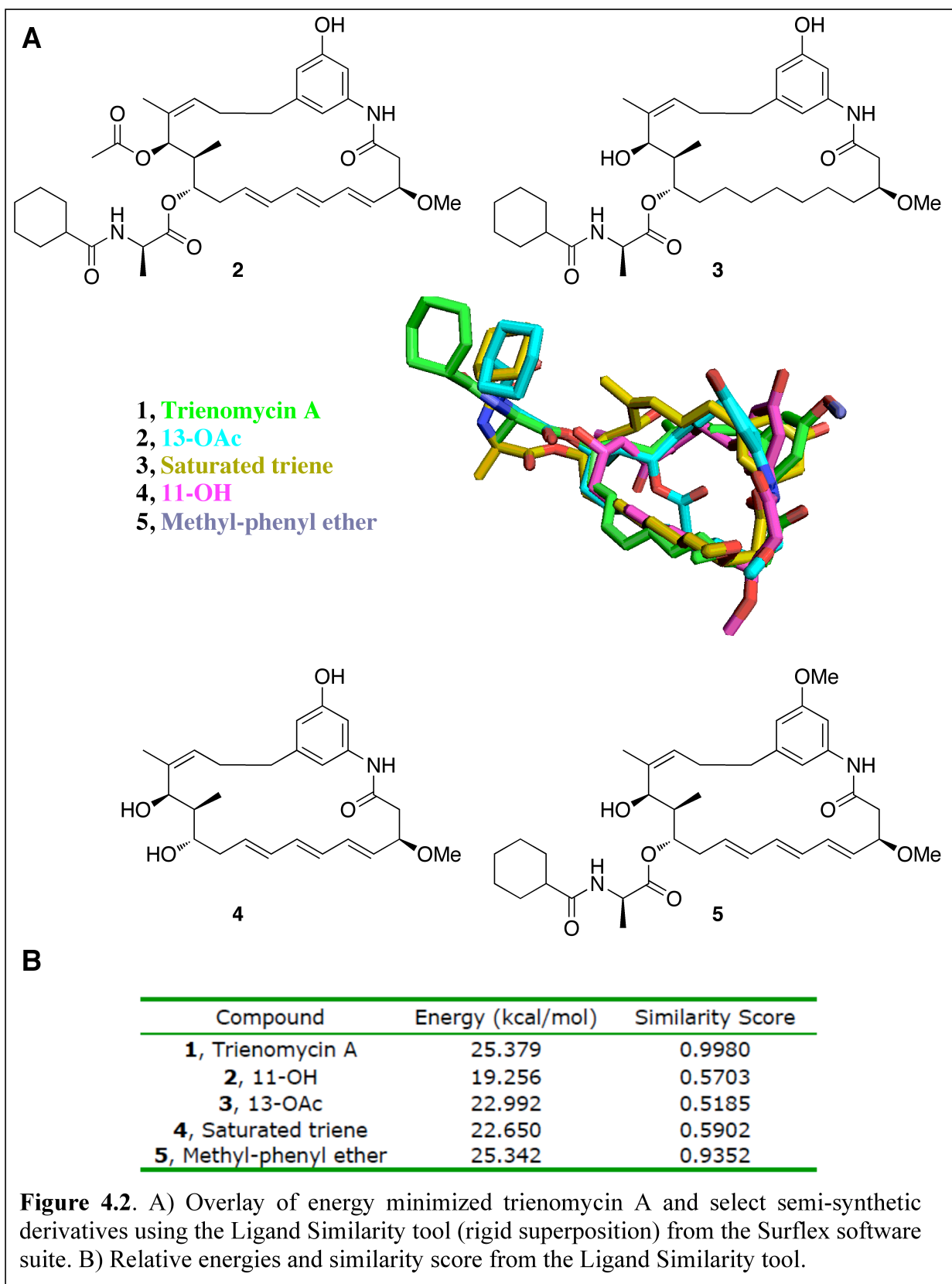
The efficiency by which simplified analogues of trienomycin A could overlay with the natural product was evaluated *in silico,* also *via* Surflex calculations. Sequential removal of functionality and subsequent comparison of the energy-minimized derivatives to the natural product were analyzed. The 13-OH, 12-CH_3, and 3-OCH_3 functionalities appeared to exhibit little effect on the overall conformation, which suggested they could be omitted without significantly affecting biological activity (Figure 4.3).

The triene motif was evaluated next, with the aim of generating the most synthetically accessible derivatives. Twelve energy minimized "monoene" derivatives, containing all possible olefin isomers and the methyl ether of the reported derivative, were evaluated based upon their ability to adopt a conformation that allowed both the phenol and NCxDA side chain to occupy the same conformational space as the natural product. Olefin geometry was critical in these structures and was responsible for orienting both the NCxDA side chain and the phenol into conformations that were similar to the natural product. Most of the monoene derivatives exhibited significant differences in macrocycle geometry compared to trienomycin A. However, derivatives **7–10** manifested macrocycle geometry similar to the natural product and produced

Figure 4.3. A) Structure of theoretical trienomycin A analogue **6** that lacks the 13-OH, 12-CH_3, and 3-OMe functional groups. B) Overlay of trienomycin A and **6** (calculated energy = 21.527 kcal/mol; similarity score with trienomycin A = 0.7935).
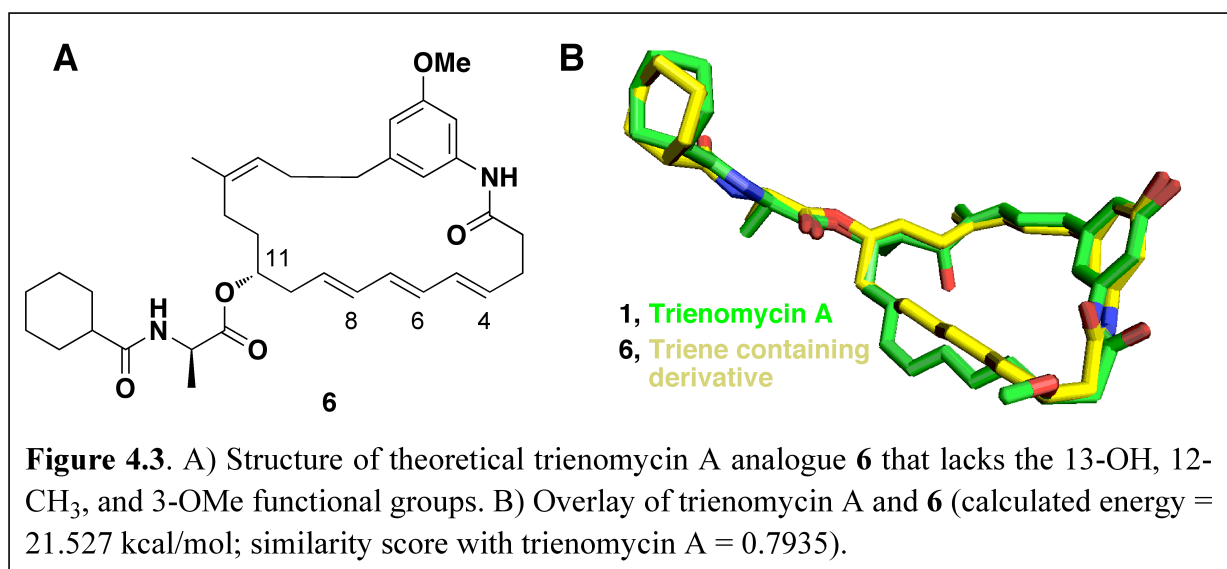
relatively high similarity scores (Figure 4.4). Monoene A, which contains *trans* olefins at both C8 and C14, occupied the closest three-dimensional orientation to trienomycin A and exhibited the highest similarity score (0.7815).

IV.3.3 *Synthesis and biological evaluation of a simplified trienomycin A analogue*

Since monoene A (**7**) exhibited the highest similarity score to trienomycin A, it was the target for chemical synthesis. Synthesis of **7** was envisioned


Figure 4.4. A) Key for monoene containing trienomycin A analogues. B) Overlay depiction of the energy minimized theoretical monoene analogues with trienomycin A. C) Theoretical relative energies of hypothesized monoene analogues and associated similarity scores with trienomycin A generated by the Ligand Similarity Tool of the Sybyl Software Suite.

Compound	Energy (kcal/mol)	Similarity Score	Olefin Isomer
1, Trienomycin A	25.379	0.9980	Native
7, Monoene A	16.788	0.7815	W *trans*, X *trans*
8, Monoene B	20.139	0.6841	W *cis*, Z *cis*
9, Monoene C	18.339	0.6267	W *trans*, Z *cis*
10, Monoene D	20.750	0.7275	W *cis*, Z *trans*
11, Monoene E	19.083	0.5761	W *cis*, Z *trans*

retrosynthetically to occur through a Wittig olefination between salt **12** and ketone **13**,[18] followed by Mitsunobu coupling of the D-Ala side chain **14**,[19] and subsequent ring-closing metathesis (Figure 4.5).[20] This synthetic route would also provide access to monoene E (**11**), which

Figure 4.5. Retrosynthetic analysis of and synthetic strategy for monoene A (**7**).
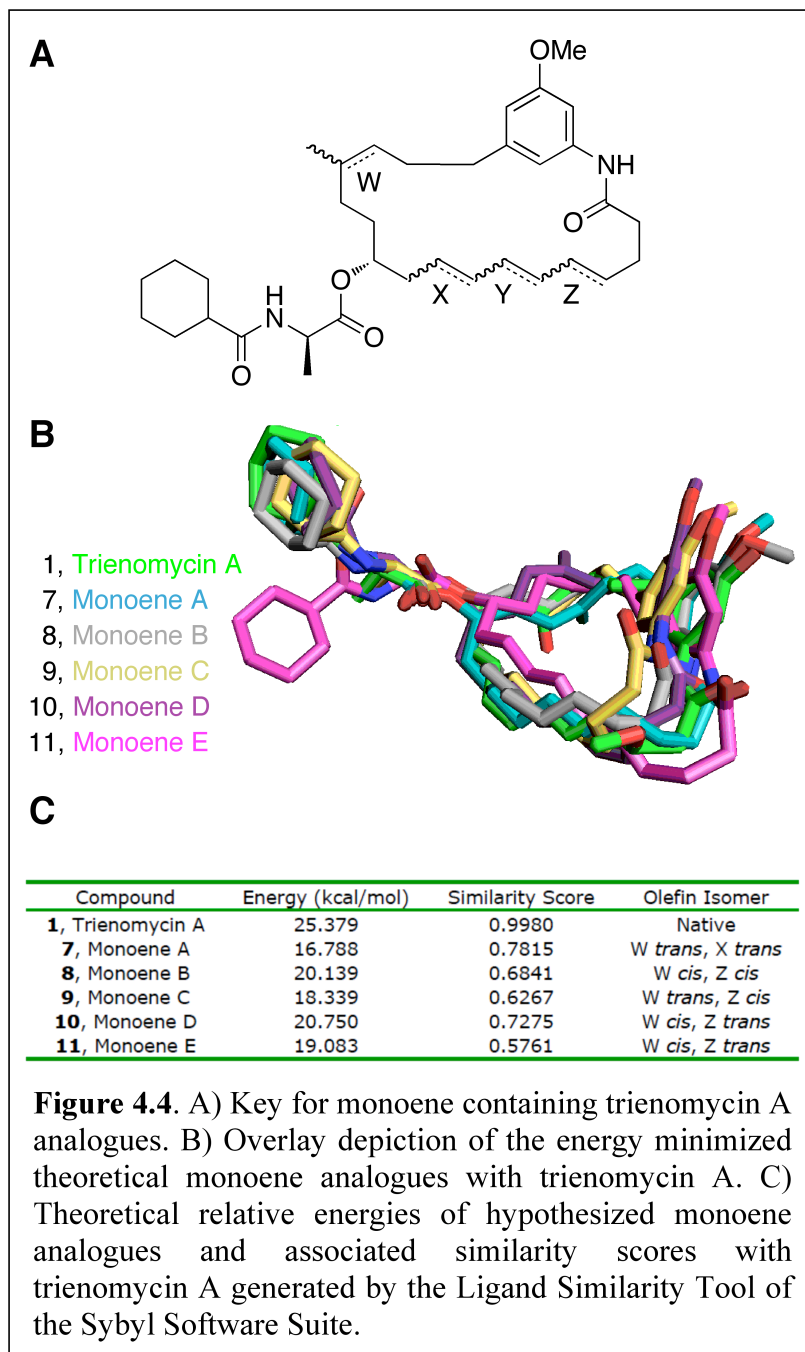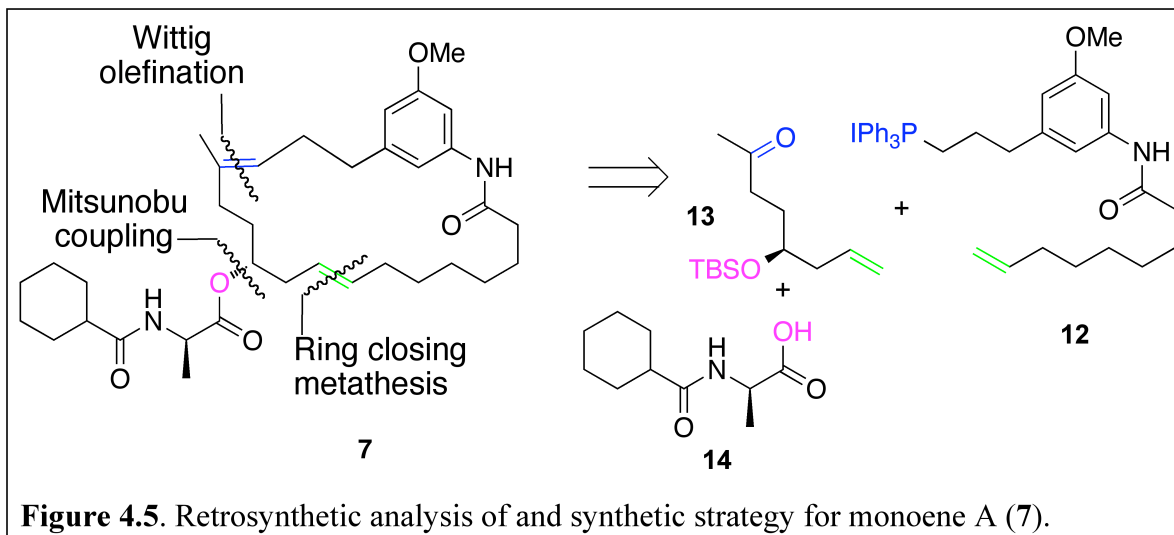
exhibited the lowest similarity score and could be used as a negative control to evaluate our conformation-based approach.

Synthesis of Wittig salt **12** commenced with nucleophillic aromatic substitution of methyl 3,5-dinitrobenzoate **15** by lithium methoxide to provide methyl-phenyl ether **16**,[21] which was then reduced to aldehyde **17** by diisobutylaluminum hydride.[22] Aldehyde **17** was subjected to Horner–Wadsworth–Emmons conditions to furnish **18**,[23] which was subjected to diimide mediated reduction to provide **19**.[24] The ethyl ester of **19** was reduced to the alcohol using diisobutylaluminum hydride to yield **20**, the nitro moiety of which was reduced to the aniline **21** by palladium on carbon under a hydrogen atmosphere. Selective amidation of compound **21** with non-8-enoic acid was accomplished using (1-Cyano-2-ethoxy-2-oxoethylidenaminooxy)dimethylamino-morpholino-carbenium hexafluorophosphate (COMU) to afford amido-alcohol **22**.[25] Until this point, no chromatographic separation was required, enabling the preparation of large quantities. Amido-alcohol **22** was then iodinated and converted to Wittig salt **12** (Scheme 4.1).
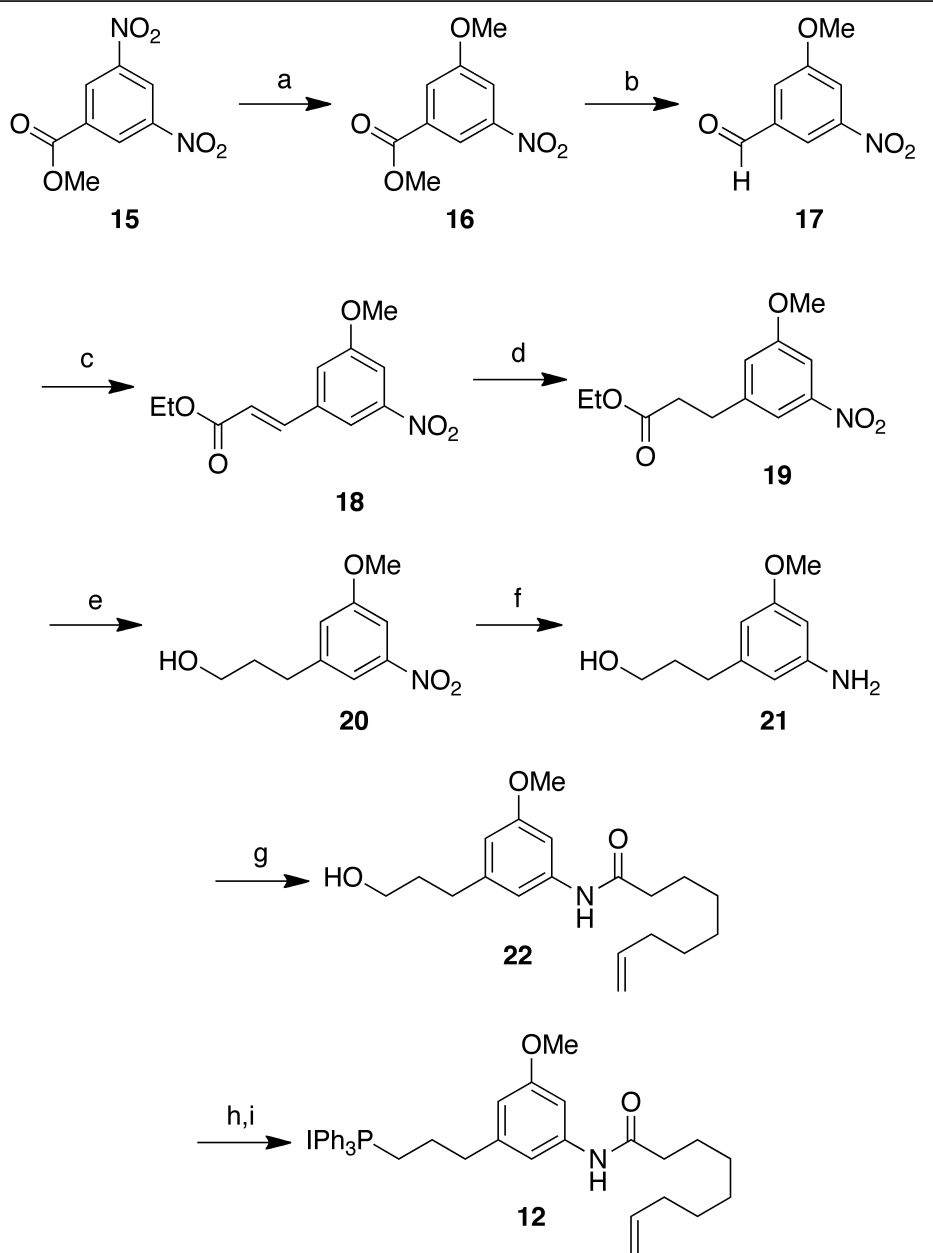
Scheme 4.1. Reaction conditions: a) LiOMe, MeOH, reflux, 97%; b) DIBAl-H, DCM, -78°C, 93%; c) triethylphosphonoacetate, NaH, THF, 0°C, 94%; d) potassium azodicarboxylate, AcOH, DME, 50°C, 97%; e) DIBAl-H, PhMe, 0°C, 97%; f) 10% Pd/C, H$_2$, EtOAc; g) Non-8-enoic acid, COMU, DIPEA, DMF, 93% over two steps; h) PPh$_3$, imidazole, I$_2$, DCM, 83%; i) PPh$_3$, CAN, 90%.

Scheme 4.2. Reaction conditions: a) PCC, DCM; b) allyl magnesium bromide, (+)-B-methoxydiisopinocampheylborane, Et$_2$O, *ee* > 95%, 82% (chiral borane as limiting reagent) over two steps; c) TBSCl, imidazole, DMF, 79%.
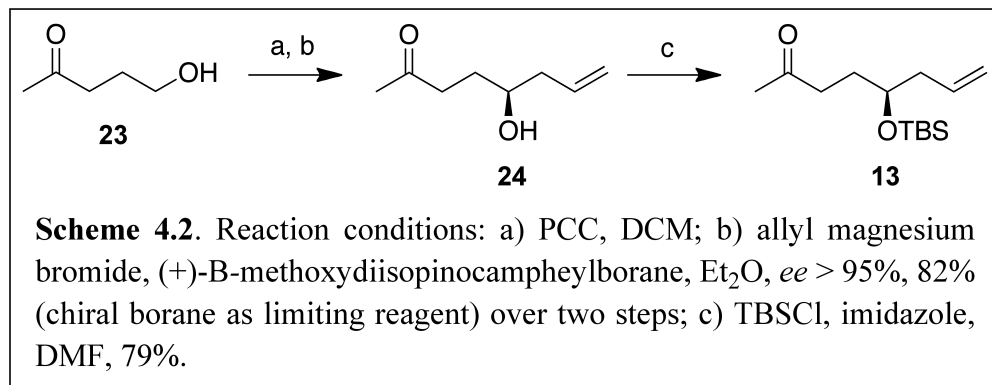
Synthesis of ketone **13** was similarly straightforward. Oxidation of ketol **23** to the ketoaldehyde and treatment of the dicarbonyl species with 0.5 eq. of Brown's allylborane furnished optically active ketol **24**.[26] Synthesis of ketone **13** was completed following silyl ether formation (Scheme 4.2).

N-Cyclohexylcarbonyl D-alanine acid **14** was constructed in one step by treating D-alanine with cyclohexylcarbonyl chloride in the presence of tribasic potassium phosphate in tetrahydrofuran (Scheme 4.3).

With the synthons in hand, Wittig olefination reaction between **12** and **13**, followed by silyl deprotection, and Mitsunobu coupling between **25** and **14** led to metathesis precursors **26** (*trans*) and **27** (*cis*) in a 1:1 mixture, which was separable by chromatography. Originally, it was desired to obtain the macrocyclic alcoholafter ring closing metathesis, which could subsequently undergo diversification at a later stage. However, the macrocyclic alcohol failed to efficiently undergo esterification *via* Mitsunobu conditions or direct acylation, due to steric constraints resulting from the macrocyclic

Scheme 4.3. Reaction conditions: a) K$_3$PO$_4$, THF, 76%.
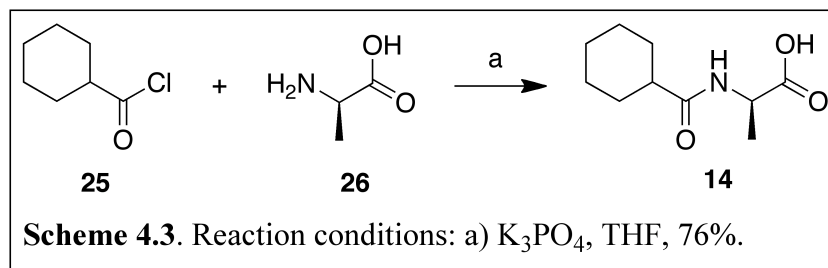
conformation. Therefore, the NCxDA side was appended prior to cyclization. Each isomer was subjected to ring-closing metathesis with Grubbs first generation catalyst to yield products **7** and **11** as a 2:1 and 5:1 (*trans:cis*) mixture of olefin isomers, respectively (Scheme 4.4). The isomeric mixtures were evaluated for anti-proliferative activity against MCF-7 and HeLa cancer cells. As predicted by our conformation based design, compound **7** retained anti-proliferative activity (IC_{50} = 0.47 μM) while compound **11** was inactive.

Scheme 4.4. Reaction conditions: a) KHMDS, toluene, 78%; b) TBAF, THF, 97%; c) Diethyl azodicarboxylate, PPh$_3$, **14**, 37% (**26**), 39% (**27**); d) Grubbs' first generation catalyst, DCM, 76 - 83%.

Figure 4.6. Chemical structures of monoenomycins **28-34**.
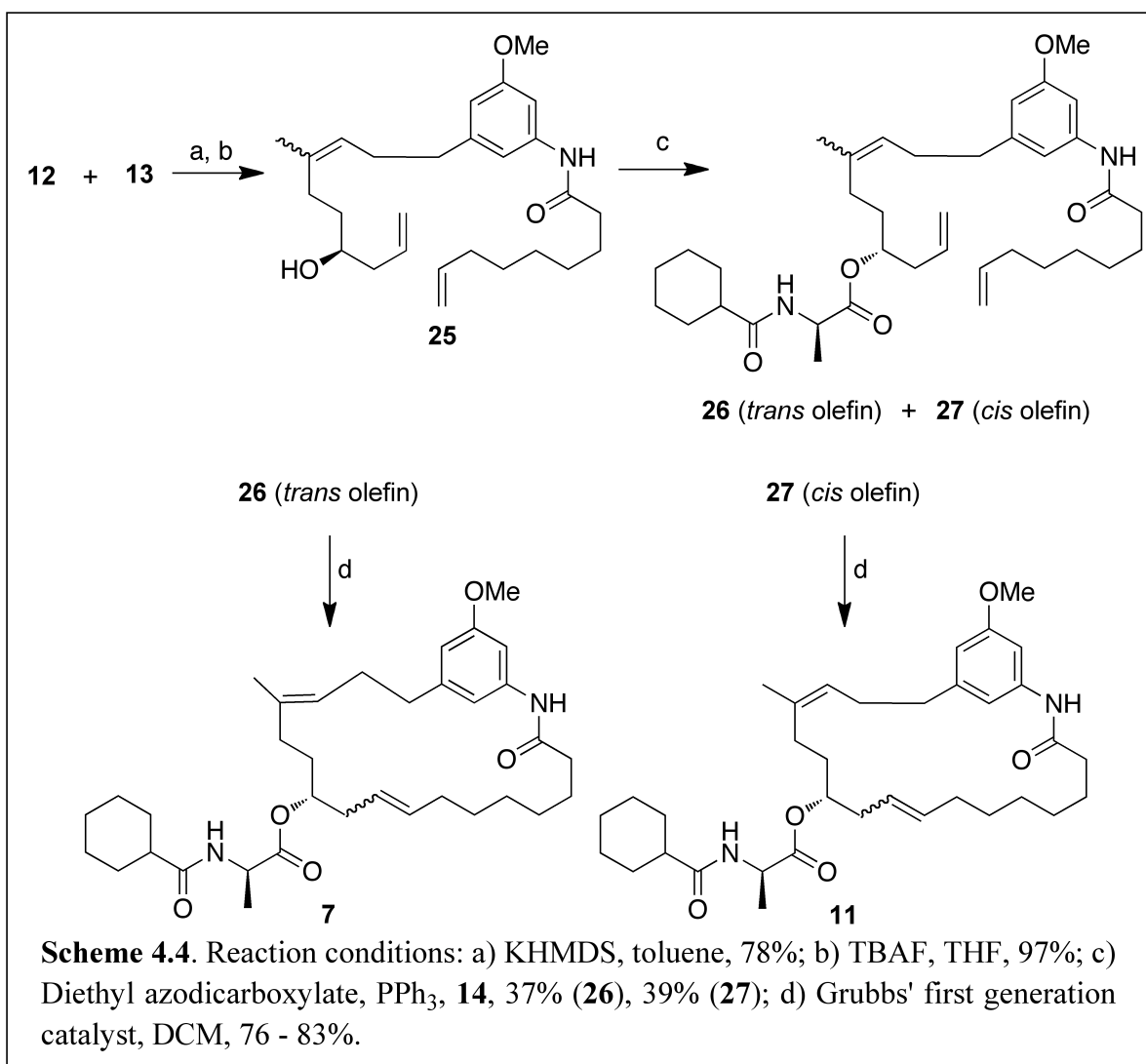
IV.3.4 *Synthesis and biological evaluation of analogues to probe NCxDA side chain*

The anticancer activity exhibited by compound **7** prompted investigations into the amino acid side chain. Specifically, the effects of increasing steric bulk in lieu of the methyl substituent and alterations of the amide to include small alkyl groups were pursued. The various side chains were synthesized from the corresponding amino acids and appropriate acyl chlorides similar to compound **14**. Once synthesized, the side chains were coupled with compound **25** using Mitsunobu conditions and subsequently cyclized with Grubbs first generation catalyst (Figure 4.6, **28-34**).
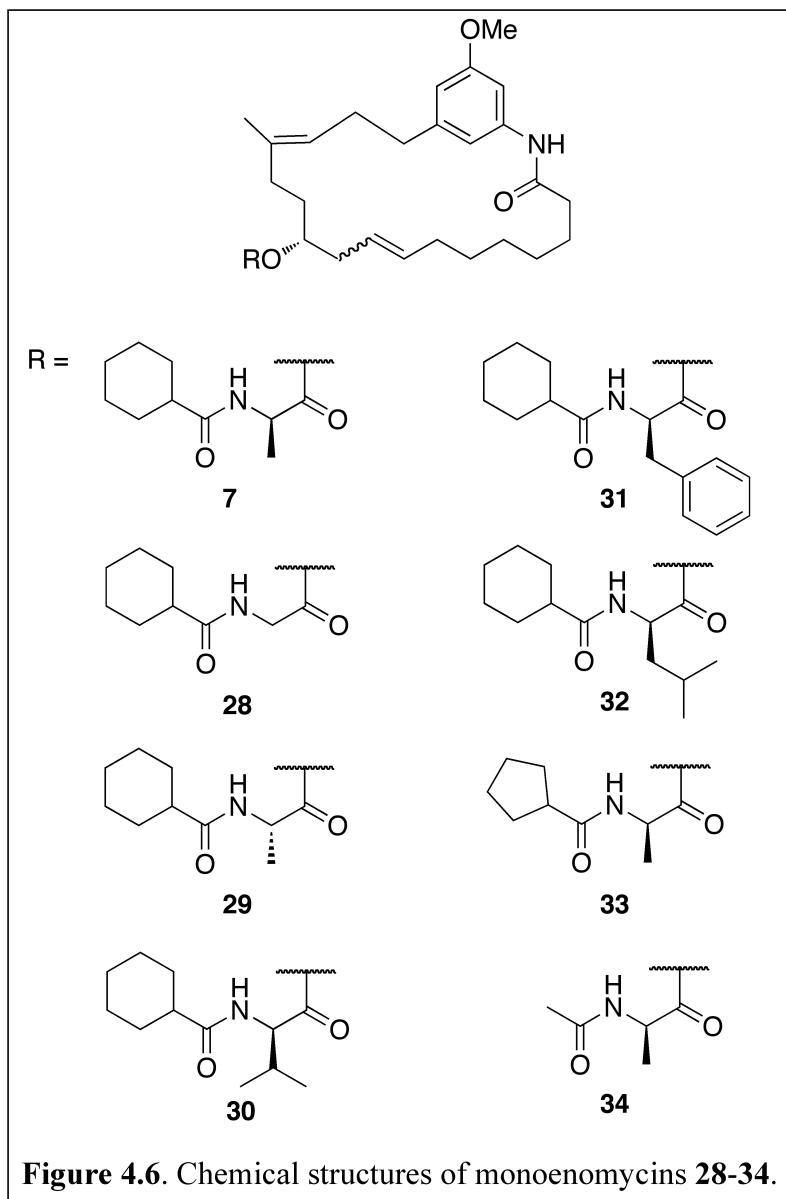
These compounds were evaluated for anti-proliferative activity against HeLa and MCF-7 cancer cells (Table 4.1). From the data presented, deviation in steric bulk, with functionalities

that exhibit smaller or larger groups than methyl, is not tolerated at the *alpha* position of the D-Ala side chain. Similarly, decreasing steric bulk of the alkyl amide decreases biological activity.

Table 4.1: Anti-proliferative effects of Trienomycin A compound library against HeLA and MCF-7 cancer cell lines.[a]

Compound	HeLa IC$_{50}$ (μM)	MCF-7 IC$_{50}$ (μM)
7	0.47 ± 0.04	0.53 ± 0.02
11	>100	>100
28	13 ± 0.5	12 ± 0.5
29	1.7 ± 0.03	1.9 ± 0.05
30	9.1 ± 0.09	1.0 ± 0.04
31	4.6 ± 0.09	5.1 ± 0.07
32	>100	>100
33	1.6 ± 0.09	0.72 ± 0.5
34	2.5 ± 0.9	1.7 ± 0.4
Geldanamycin	>5	0.053 ± 0.001

[a]IC$_{50}$ value based on MTS assay run in triplicate.

IV.4   Concluding Remarks

In conclusion, molecular modeling was used to predict simplified derivatives of trienomycin A that were energetically predisposed to adopt a conformation similar to the natural product. The analogues manifested potent anti-proliferative activities against MCF-7 and HeLa cancer cell lines and provide the first SAR for these natural product analogues. As a validation of the conformation-based approach, these simplified derivatives provided a method for rapid elucidation of SAR.

IV.5 Methods and Experimentals

General Methods. All reactions were carried out in flame dried glassware under argon atmosphere unless otherwise stated. Dichloromethane (DCM), diethyl ether, tetrahydrofuran (THF), and toluene were purchased from Sigma Aldrich and were passed through a column of activated alumina prior to use. Anhydrous methanol, acetonitrile, dimethylformamide (DMF), and dimethoxyethane (DME) were purchased from Sigma Aldrich and used without further purification. All reagents and other solvents [ethyl acetate (EtOAc) and hexanes (Hex)] were purchased from Sigma Aldrich and were used without further purification unless otherwise stated. Flash column chromatography was performed using silica gel (40 – 63 m particle size) from Sorbent Technologies. The ^{1}H and ^{13}C-NMR (proton decoupled) spectra were recorded at 500 and 126 MHz, respectively, on a Bruker AM 500 using CDCl$_3$ or DMSO purchased from Cambridge Isotope Laboratories, Inc., using solvent as an internal standard (CDCl$_3$ at 7.260 ppm for ^{1}H and 77.160 ppm for ^{13}C) or tetramethylsilane (0.00 ppm) unless otherwise stated. Data are reported as p = pentet, q = quartet, t = triplet, d = doublet, s = singlet, bs = broad singlet, m = multiplet; coupling constant(s) in Hz. ^{19}F-NMR spectra were recorded at 376 MHz on a Bruker DRX 400 in C$_6$D$_6$ using (R)-3,3,3-trifluoro-2-methoxy-2-phenylpropanoic acid as an internal standard unless otherwise stated. Two-dimensional NMR experiments were run on a Bruker AM 500 at 500 MHz. High resolution mass spectral data were obtained on a Ribermag R10-10 quadrupole, VG Analytical ZA. Optical rotations were recorded with a Perkin Elmer polarimeter at 589 nm.
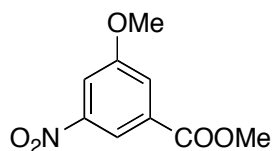
Methyl 3-Methoxy-5-nitrobenzoate (16):

A flame dried 500 mL round bottom flask was flushed with argon before anhydrous methanol (200 mL) and lithium wire (0.231 g, 33.2 mmol, 1.5 eq) were added slowly at 0 °C. Methyl dinitrobenzoate (5 g, 22.1 mmol, 1 eq.) was added in one portion to the homogenous solution, and stirred at reflux for 2 h. The solution was cooled to rt, and quenched with a 2M solution of methanolic HCL and acidified to pH = 2. The solvent was removed to afford a brown solid, which was redissolved in EtOAc (70 mL) and washed with saturated aqueous sodium bicarbonate (2 X 30 mL) and saturated aqueous sodium chloride (2X, 30 mL). The organic layer was removed, dried with anhydrous sodium sulfate, filtered and triturated with Hex to give methyl 3-methoxy-5-nitrobenzoate crystallized as a white solid (4.53 g, 97%). ^{1}H NMR (500 MHz, CDCl$_3$) δ 8.46 (dd, J = 2.0, 1.4 Hz, 1H), 7.92 (t, J = 2.3 Hz, 1H), 7.88 (dd, J = 2.6, 1.3 Hz, 1H), 3.98 (s, 3H), 3.94 (s, 3H).^{13}C NMR (126 MHz, CDCl$_3$) δ 165.11, 160.37, 149.33, 132.75, 121.26, 116.79, 113.06, 56.40, 53.01. HRMS (ESI, m/z): calcd for [C$_9$H$_{10}$NO$_5$]$^+$ ([M +H]$^+$): 212.0559, found 212.0554.
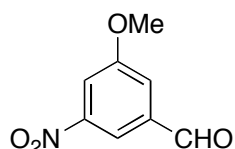
3-Methoxy-5-nitrobenzaldehyde (17):

A flame dried 500 mL round bottom flask was flushed with argon before anhydrous DCM (100 mL) and **16** (4.53 g, 21.5 mmol, 1 eq.) were added. The solution was cooled to -78°C, and a freshly made 0.258M solution of diisobutylaluminum hydride (100mL, 25.8mmol, 1.2 eq.) was added slowly *via* cannula . The solution was stirred for 10 min at -78 °C, and then quenched by the careful addition of saturated aqueous sodium potassium tartrate and stirred at RT for 5 hours. The organic layer was collected and the aqueous later was extracted with EtOAc (5X, 100 mL).

The combined organic layers were collected and dried with anhydrous sodium sulfate. Solvent was removed to afford a tan solid, which was dissolved in EtOAc (70 mL) and subsequently triturated with Hex to give 3-methoxy-5-nitrobenzaldehyde crystallized as a beige solid (3.62 g, 93%). ^{1}H NMR (500 MHz, CDCl$_3$) δ 10.05 (s, 1H), 8.30 (dd, J = 1.9, 1.3 Hz, 1H), 7.99 (t, J = 2.3 Hz, 1H), 7.72 (dd, J = 2.5, 1.2 Hz, 1H), 3.97 (s, 3H). ^{13}C NMR (126 MHz, CDCl$_3$) δ 189.80, 161.00, 149.83, 138.35, 119.31, 117.26, 114.72, 56.53. HRMS (ESI, m/z): calcd for [C$_8$H$_8$NO$_4$]$^+$ ([M +H]$^+$): 182.0453, found 182.0448.
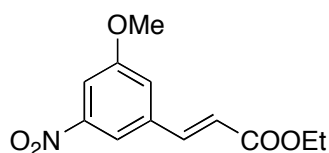
(E)-Ethyl 3-(3-Methoxy-5-nitrophenyl)acrylate (18):

A flame dried 500 mL round bottom flask was flushed with argon before anhydrous THF (100 mL) and sodium hydride (60%, 796 mg, 19.9 mmol, 1.2 eq.) were added. The suspension was cooled to 0°C and triethylphosphono acetate (3.6 mL, 18.3 mmol, 1.1 eq.) was added. The solution was warmed to rt and stirred for 30 min. After cooling the solution to 0 °C, aldehyde **17** (3 g, 16.6 mmol, 1 eq.) was added in one portion. The solution changed from colorless to dark green, at which point the reaction was quenched by the addition of saturated aqueous ammonium chloride. The organic layer was collected and the aqueous layer extracted with EtOAc (3X, 70 mL). The combined organic layers were collected and dried with anhydrous sodium sulfate. The volume was condensed to ~30%, and the solution was filtered through a silica plug with 40% EtOAc in Hex. Solvent was removed to afford a yellow solid (3.91 g, 94%). ^{1}H NMR (500 MHz, CDCl$_3$) δ 7.99 (t, J = 1.6 Hz, 1H), 7.73 (t, J = 2.2 Hz, 1H), 7.65 (d, J = 16.0 Hz, 1H), 7.37 – 7.27 (m, 1H), 6.53 (d, J = 16.0 Hz, 1H), 4.29 (q, J = 7.1 Hz, 1H), 3.92 (s, 3H), 1.35 (t, J = 7.1 Hz,

1H). ^{13}C NMR (126 MHz, CDCl$_3$) δ 166.28, 160.60, 149.77, 141.97, 137.03, 121.69, 120.26, 114.93, 109.42, 61.08, 56.20, 14.42. HRMS (ESI, *m/z*): calcd for [C$_{12}$H$_{14}$NO$_5$]$^+$ ([M +H]$^+$): 252.0872, found 252.0876.
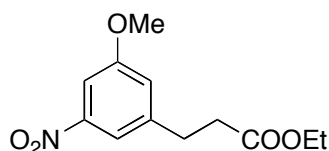
Ethyl 3-(3-Methoxy-5-nitrophenyl)propanoate (19):

A 500 mL round bottom flask was flushed with argon before 1,2-dimethoxy ethane (80 mL), a,b-unsaturated ester **18** (3.2 g, 12.7 mmol, 1 eq.), and potassium azodicarboxylate (14.8 g, 76.2 mmol, 6 eq.) were added. AcOH (1.85 mL, 45.72 mmol, 3.6 eq.) in 1,2-dimethoxy ethane (30 mL) was added slowly, and the suspension was stirred at 50°C for 24 h. The solids were filtered off with celite and washed with EtOAc (300 mL). The combined organic layers were dried over anyhydrous sodium sulfate, and the solvent removed to afford a yellow solid (3.12 g, 97%). ^{1}H NMR (500 MHz, CDCl$_3$) δ 7.69 (q, *J* = 1.5 Hz, 1H), 7.58 (t, *J* = 2.2 Hz, 1H), 7.08 (dd, *J* = 2.2, 1.6 Hz, 1H), 4.14 (q, *J* = 7.1 Hz, 1H), 3.87 (s, 1H), 3.01 (t, *J* = 7.6 Hz, 1H), 2.66 (t, *J* = 7.6 Hz, 1H), 1.24 (t, *J* = 7.1 Hz, 2H). ^{13}C NMR (126 MHz, CDCl$_3$) δ 172.31, 160.28, 149.44, 143.56, 121.57, 115.89, 106.20, 77.41, 77.16, 76.91, 60.86, 55.97, 35.32, 30.75, 14.34. HRMS (ESI, *m/z*): calcd for [C$_{12}$H$_{16}$NO$_5$]$^+$ ([M +H]$^+$): 254.1028, found 254.1025.
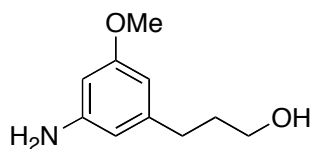
3-(3-Amino-5-methoxyphenyl)propan-1-ol (21):

A flame dried 500 mL round bottom flask was flushed with argon before toluene (50 mL) and ester **19** (3.1 g, 12.24 mmol, 1 eq.) were added. A fresh solution of diisobutylaluminun hydride (7.64 mL, 42.8 mmol, 3.5 eq.) in toluene (50 mL) was prepared. The solutions were cooled to -78°C, and the diisobutylaluminum hydride solution was cannulated into the solution of ester **19** slowly. The reaction mixture was stirred and allowed to warm to rt at which point the reaction was quenched by the careful addition of saturated aqueous sodium potassium tartrate (150 mL). The emulsion was stirred at rt until the layers separated. The organic layer was collected and the aqueous layer was extracted with EtOAc (3X, 70 mL). The combined organic layers were collected and dried over anhydrous sodium sulfate. Solvent was removed to afford a yellow oil that was resuspended in EtOAc (90 mL). 10% Palladium on carbon (200 mg) was added and the reaction mixture was stirred at rt under a hydrogen atmosphere for 10 h. The reaction vessel was flushed with argon to remove hydrogen, and the solution was then filtered through a celite pad using EtOAc. Solvent was removed to afford amino-alcohol **5** as a colorless oil (2.1 g, 93% over two steps). ^{1}H NMR (500 MHz, CDCl$_3$) δ 6.20 – 6.17 (m, 1H), 6.16 (dd, J = 1.9, 1.4 Hz, 1H), 6.09 (t, J = 2.1 Hz, 1H), 3.75 (s, 3H), 3.67 (t, J = 6.4 Hz, 2H), 3.63 (bs, 2H), 2.60 – 2.56 (m, 2H), 1.90 – 1.83 (m, 2H). ^{13}C NMR (126 MHz, CDCl$_3$) δ 160.95, 147.77, 144.46, 108.20, 104.62, 98.73, 77.41, 77.16, 76.91, 62.52, 55.22, 34.08, 32.41. HRMS (ESI, m/z): calcd for [C$_{10}$H$_{16}$NO$_2$]$^+$ ([M +H]$^+$): 182.1181, found 182.1185.
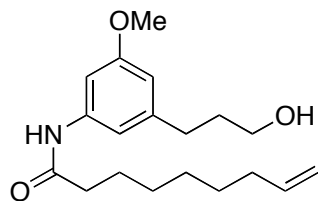
N-(3-(3-Hydroxypropyl)-5-methoxyphenyl)non-8-enamide (22):

A 50 mL round bottom flask was flushed with argon before DMF (10 mL), diisopropylethylamine (1.62 mL, 9.3 mmol, 2.1 eq.), non-8-enoic acid (690.5 mg, 4.42 mmol, 1 eq.), and COMU (2.1 g, 4.9 mmol, 1.1 eq.) were added. The reaction mixture was stirred at RT for 30 min, at which point amino-alcohol **21** (800 mg, 4.42 mmol, 1 eq.) was added. Stirring was continued for 1 h at rt and the reaction was quenched by the addition of saturated aqueous ammonium chloride (15 mL). EtOAc (20 mL) was added and the organic layer was collected. The aqueous layer was extracted with EtOAc (5X, 20 mL) and the combined organic layers were collected and dried over anhydrous sodium sulfate. Solvent was removed to afford a red oil that was purified by SiO$_2$ flash chromatography (5% – 20% EtOAc in Hex). Amide-alcohol **22** was isolated as a colorless oil (1.28 g, 91%). ^{1}H NMR (500 MHz, CDCl$_3$) δ 7.13 (s, 1H), 7.11 (s, 1H), 6.86 (s, 1H), 6.51 (s, 1H), 5.80 (ddt, J = 16.9, 10.2, 6.7 Hz, 1H), 4.99 (ddd, J = 17.1, 3.6, 1.6 Hz, 1H), 4.93 (ddt, J = 10.2, 2.2, 1.2 Hz, 1H), 3.79 (s, 3H), 3.66 (t, J = 6.4 Hz, 2H), 2.68 – 2.61 (m, 2H), 2.33 (t, J = 7.5 Hz, 2H), 2.04 (dd, J = 14.0, 6.9 Hz, 2H), 1.87 (dq, J = 12.9, 6.4 Hz, 2H), 1.72 (dt, J = 14.8, 7.5 Hz, 2H), 1.45 – 1.30 (m, 8H). ^{13}C NMR (126 MHz, CDCl$_3$) δ 171.49, 160.33, 144.03, 139.19, 139.13, 114.46, 112.07, 110.55, 102.91, 62.28, 55.44, 38.00, 34.06, 33.84, 32.29, 29.22, 28.97, 28.83, 25.62. HRMS (ESI, m/z): calcd for [C$_{19}$H$_{30}$NO$_3$]$^+$ ([M +H]$^+$): 320.2226, found 320.2225.
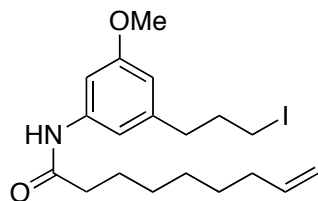
_N_-(3-(3-Iodopropyl)-5-methoxyphenyl)non-8-enamide (35):

A 100 mL round bottom flask was flushed with argon before DCM (30 mL), amide-alcohol **22** (1g, 3.2 mmol, 1 eq.), triphenylphosphine (725 mg, 3.2 mmol, 1 eq.), and imidazole (265 mg,

3.84 mmol, 1,2 eq.) were added. The reaction mixture was cooled to 0 °C and iodine (813 mg, 3.2 mmol, 1 eq.) was added slowly. The reaction mixture was allowed to warm to RT at which point the reaction was quenched by the addition of saturate aqueous ammonium chloride. The organic layer was collected and the aqueous layer was extracted with DCM (3X, 30 mL). The combined organic layers were washed sequentially with saturated aqueous sodium thiosulfate (1X, 30 mL) and saturate aqueous sodium chloride (2X, 30 mL). The organic layers were collected and dried over anhydrous sodium sulfate. Solvent was removed to afford alkyl iodide **35** as a colorless oil (1.14 g, 83%). ^{1}H NMR (500 MHz, CDCl$_3$) δ 7.23 – 7.07 (m, 2H), 6.85 (s, 1H), 6.50 (s, 1H), 5.80 (ddt, J = 16.9, 10.2, 6.7 Hz, 1H), 4.99 (ddd, J = 17.1, 3.6, 1.6 Hz, 1H), 4.93 (ddt, J = 10.2, 2.2, 1.2 Hz, 1H), 3.78 (s, 3H), 3.15 (t, J = 6.8 Hz, 2H), 2.66 (t, J = 7.3 Hz, 2H), 2.34 (t, J = 7.5 Hz, 2H), 2.16 – 2.06 (m, 2H), 2.06 – 2.00 (m, 2H), 1.76 – 1.68 (m, 6H).
^{13}C NMR (126 MHz, CDCl$_3$) δ 171.51, 160.37, 142.56, 139.31, 139.11, 114.46, 112.07, 110.65, 103.15, 77.41, 77.16, 76.91, 55.45, 37.99, 36.37, 34.68, 33.83, 29.21, 28.96, 28.83, 25.60, 6.50.
HRMS (ESI, m/z): calcd for [C$_{19}$H$_{29}$INO$_2$]$^+$ ([M +H]$^+$): 430.1243, found 430.1246.
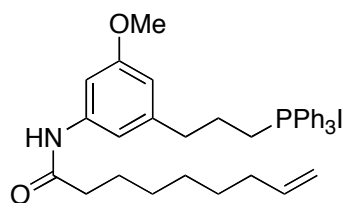
_N_-(3-(3-(Iodotriphenylphosphoranyl)propyl)-5-methoxyphenyl)non-8-enamide (12):

A flame dried 100 mL round bottom flask was flushed with argon before anhydrous acetonitrile (15 mL), alkyl iodide **35** (1.0 g, 2.53 mmol, 1 eq.), and triphenylphosphine (1.15 g, 5.06 mmol, 2 eq.) were added. The reaction mixture was refluxed under argon for 12 hours. The reaction mixture was allowed to cool to rt and then extracted with Hex (13X, 20 mL). The Hex extract was back extracted with acetonitrile (2X, 20 mL) and the combined acetonitrile layers were dried

over anhydrous sodium sulfate. Solvent was removed to afford Wittig salt **8** as a pale yellow foamy solid (1.58 g, 90%). ^{1}H NMR (500 MHz, CDCl$_3$) δ 8.91 (s, 1H), 7.79 (m, 4H), 7.71 – 7.60 (m, 12H), 7.39 (s, 1H), 6.33 (s, 1H), 5.80 (ddt, J = 16.9, 10.2, 6.7 Hz, 1H), 4.98 (ddd, J = 17.1, 3.7, 1.6 Hz, 1H), 4.91 (ddt, J = 10.2, 2.3, 1.2 Hz, 1H), 3.79 (s, 3H), 3.43 – 3.35 (m, 2H), 2.82 (t, J = 6.2 Hz, 2H), 2.54 (t, J = 7.5 Hz, 2H), 2.07 – 2.00 (m, 2H), 1.97 – 1.86 (m, 2H), 1.73 (dt, J = 15.1, 7.6 Hz, 2H), 1.45 – 1.29 (m, 6H). ^{13}C NMR (126 MHz, CDCl$_3$) δ 173.07, 160.47, 140.83, 140.07, 139.43, 135.35, 135.32, 133.75, 133.67, 130.84, 130.74, 118.37, 117.69, 114.23, 113.43, 110.24, 103.28, 77.41, 77.16, 76.91, 55.63, 37.78, 35.40, 35.27, 33.94, 29.24, 29.18, 28.95, 25.70, 24.14. HRMS (ESI, *m/z*): calcd for [C$_{37}$H$_{43}$NO$_2$P]$^+$ ([M +H]$^+$): 564.3031, found 564.3032.
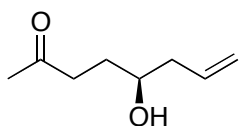
(*S*)-5-Hydroxyoct-7-en-2-one (24):

A 250 mL round bottom flask was flushed with argon before DCM (125 mL) and 5-hydroxypentan-2-one (2.5 g, 24.5 mmol, 1 eq.) were added. Pyridinium chlorochromate (11 g, 51.0 mmol, 2.1 eq.) was added slowly in 0.5 g portions over 1 hour at rt. The reaction mixture was stirred for 3 h at rt at which point diethyl ether (100 mL) was added. The heterogenous solution was then filtered through SiO$_2$ and subsequently washed with diethyl ether. The organic filtrate was then dried over anhydrous sodium sulfate. Solvent was removed to afford a light green oil (2.45 g, quant.) (aldehyde was carried forward without purification). A flame dried 500 mL round bottom flask was flushed with argon before diethyl ether (240 mL) and (+)-*B*-methoxydiisopinocampheylborane (7.6 g, 24 mmol, 2.4 eq.) were added. Solid was allowed to dissolve and the solution was cooled to -78 °C. Allylmagnesium bromide (1 M in diethyl ether, 5.55 mL, 5.5 mmol, 0.5 eq.) was added slowly and the solution was allowed to warm to 0 °C

over 2 h. The reaction mixture became cloudy at which point it was cooled back to -78 °C.
Aldehyde (1g, 10 mmol, 1 eq.) was dissolved in 2 mL diethyl ether and was added dropwise to
the reaction mixture at -78 °C. The solution was stirred for 1 h at -78 °C and subsequently
allowed to warm to RT. Ethanolamine (4 mL) was added and the solution was stirred for 10 h. A
yellow precipitate was formed, and the heterogenous solution was filtered through SiO2 (40%
diethyl ether in Hex). The organic layer was dried over anhydrous sodium sulfate. Solvent was
removed to afford a colorless oil that was purified by flash SiO_2 chromatography (2% – 10%
EtOAc in Hex) to afford **9** as a colorless oil (*ee* > 95% (see ^{19}F NMR experiments of **53** and **54**),
1.16 g, 82% [BRSM], isolated as a mixture of ketone and hemiketal). $[\alpha]^{23}_D$ = -9.5° (c = 0.015,
DCM). ^{1}H NMR (500 MHz, CDCl$_3$) δ 5.85 – 5.76 (m, 1H), 5.17 – 5.00 (m, 2H), 3.66 – 3.60 (m,
1H), 2.67 – 2.54 (m, 2H), 2.36 – 2.21 (m, 1H), 2.16 (s, 3H), 2.21 – 2.09 (m, 1H), 1.81 (dtd, *J* =
14.4, 7.2, 3.5 Hz, 1H), 1.72 – 1.59 (m, 1H). ^{13}C NMR (126 MHz, CDCl$_3$) δ 209.62, 134.59,
118.47, 70.19, 42.34, 40.16, 30.40, 30.18. HRMS (ESI, *m/z*): calcd for $[C_8H_{15}O_2]^+$ ($[M +H]^+$):
143.1072, found 143.1069.
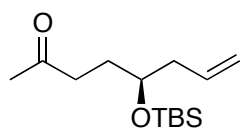
(*S*)-5-(((*tert*-Butyldimethylsilyl)oxy)oct-7-en-2-one (13):

A 50 mL round bottom flask was flushed with argon before DMF (5 mL), imidazole (980 mg,
14.4 mmol, 2 eq.), and *tert*-butyldimethylsilyl chloride (2.17 g, 14.4 mmol, 2 eq.) were added.
The solution was stirred for 30 min at rt followed by the addition of alcohol **24** (1 g, 7.04 mmol,
1 eq.). The reaction mixture was stirred for 5 h at rt at which point the reaction was quenched by
the addition of saturate aqueous ammoniun chloride (20 mL) and EtOAc (10 mL). The organic
layer was collected and the aqueous layer was extracted with EtOAc (5X, 20 mL). The combined

organic layers were collected and dried over anhydrous sodium sulfate. Solvent was removed to afford a colorless oil that was purified by flash SiO$_2$ chromatography (1% – 5% EtOAc in Hex). to afford **10** as a colorless oil (1.43 g, 79%). $[\alpha]^{23}_D$ = -12.1° (c = 0.01, DCM). ^{1}H NMR (500 MHz, CDCl$_3$) δ 5.78 (ddt, *J* = 17.7, 10.5, 7.2 Hz, 1H), 5.06 (dtd, *J* = 4.1, 2.1, 1.2 Hz, 1H), 5.03 (t, *J* = 1.2 Hz, 1H), 3.77 – 3.69 (m, 1H), 2.56 – 2.41 (m, 2H), 2.24 – 2.17 (m, 2H), 2.14 (s, 3H), 1.77 (dddd, *J* = 13.3, 8.9, 6.5, 4.4 Hz, 1H), 1.63 (dddd, *J* = 14.0, 8.8, 6.9, 6.3 Hz, 1H), 0.88 (s, 9H), 0.05 (s, 3H), 0.04 (s, 3H). ^{13}C NMR (126 MHz, CDCl$_3$) δ 209.15, 134.88, 117.25, 70.95, 42.00, 39.46, 30.38, 30.10, 26.00, 18.23, -4.23, -4.49. HRMS (ESI, *m/z*): calcd for $[C_{14}H_{29}O_2Si]^+$ ($[M+H]^+$): 257.1937, found 257.1939.
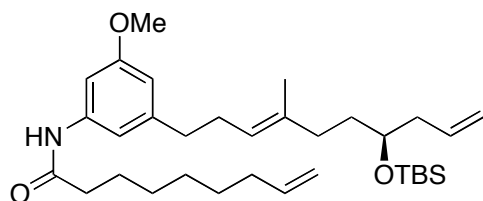

(*S,E/Z*)-*N*-(3-(7-((*tert*-Butyldimethylsilyl)oxy)-4-methyldeca-3,9-dien-1-yl)-5-methoxyphenyl)non-8-enamide (36): A flame dried 50 mL round bottom flask was flushed with argon before anhydrous DMF (10 mL), Wittig salt **12** (1.4 g, 2.01 mmol, 1 eq.), and 2.5 Å molecular sieves were added. The solution was stirred 12 h at rt and subsequently cooled to 0°C. Potassium bis(trimethylsilyl)amide (0.5 M in toluene, 8.44 mL, 4.22 mmol, 2.1 eq.) was added dropwise. The reaction mixture was allowed to warm to RT and stirred for 1 h, followed by addition of ketone **13** (564 mg, 2.2 mmol, 1.1 eq.). After 30 min of stirring at rt, the reaction was quenched by the careful addition of saturated aqueous ammonium chloride (15 mL) and EtOAc (15 mL). The organic layer was collected and the aqueous layer was extracted with EtOAc (5X, 20 mL). The combined organic layers were collected and dried over anhydrous sodium sulfate. Solvent was removed to afford a yellow oil that was purified by SiO$_2$ flash chromatography (5%

– 10% EtOAc in Hex) to afford compound **36** as a colorless oil (850 mg, 78%, isolated as a 1:1 mixture of olefin isomers). $[\alpha]^{23}_D$ = -6.5° (c = 0.009, DCM). ^{1}H NMR (500 MHz, CDCl$_3$) δ 7.20/7.16 (s, 1H), 7.05 (s, 1H), 6.80/6.75 (s, 1H), 6.50/6.50 (s, 1H), 5.86 – 5.75 (m, 2H), 5.17 – 5.11 (m, 1H), 5.07 – 4.90 (m, 4H), 3.79 (s, 3H), 3.72 – 3.62 (m, 1H), 2.60 – 2.50 (m, 2H), 2.33 (t, *J* = 7.5 Hz, 2H), 2.27 (dd, *J* = 15.2, 7.4 Hz, 2H), 2.24 – 2.16 (m, 2H), 2.13 – 1.85 (m, 3H), 1.77 – 1.69 (m, 2H), 1.66/1.57 (s, 3H), 1.55 – 1.44 (m, 2H), 1.44 – 1.31 (m, 7H), 0.89/0.89 (s, 9H), 0.05/0.04 (s, 6H). ^{13}C NMR (126 MHz, CDCl$_3$) δ 171.36, 160.24, 160.23, 144.62, 144.45, 139.13, 139.05, 136.38, 136.17, 135.48, 135.41, 124.04, 123.40, 116.92, 116.83, 114.46, 111.95, 110.64, 110.61, 102.81, 102.74, 77.41, 77.16, 76.91, 72.20, 71.90, 55.43, 41.98, 41.92, 38.04, 36.51, 36.34, 35.61, 35.39, 35.29, 33.85, 30.10, 29.90, 29.56, 29.23, 28.97, 28.84, 27.93, 26.06, 25.63, 23.63, 18.29, 18.27, 16.24, -4.18, -4.19, -4.35. HRMS (ESI, *m/z*): calcd for $[C_{33}H_{56}NO_3Si]^+$ ($[M +H]^+$): 542.4029, found 542.4030.
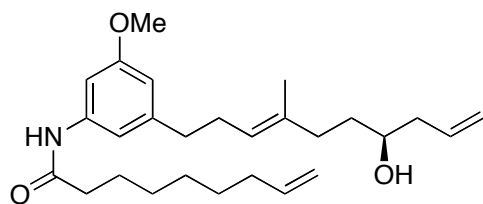
(*S*,*E*)-*N*-(3-(7-Hydroxy-4-methyldeca-3,9-dien-1-yl)-5-methoxyphenyl)non-8-enamide (25):

A 50 mL round bottom flask was flushed with argon before THF (10 mL) and compound **36** (630 mg, 1.16 mmol, 1 eq.) were added. The solution was cooled to 0 °C and tetrabutylammonium fluoride (1M in THF, 2.9 mL, 2.9 mmol, 2.5 eq.) was added dropwise over 10 min. The reaction mixture was allowed to warm to rt and stirred for 12 h. Saturated aqueous ammoniun chloride (15 mL) and EtOAc (15 mL) were added and the organic layer was collected. The aqueous layer was extracted with EtOAc (3X, 20 mL). The combined organic layers were collected and dried over anhydrous sodium sulfate. Solvent was removed to afford a

colorless oil that was purified by flash SiO$_2$ chromatography (10% – 30% EtOAc in Hex) to afford compound **25** as a colorless oil (610 mg, 97%, isolated as a 1:1 mixture of olefin isomers). $[\alpha]^{23}_D$ = -4.2° (c = 0.012, DCM). ^{1}H NMR (500 MHz, CDCl$_3$) δ 7.25 (s, 1H), 7.14 (s, 1H), 6.82/6.81 (s, 1H), 6.48 (s, 1H), 5.88 – 5.73 (m, 2H), 5.23 – 5.08 (m, 4H), 4.99 (ddd, J = 17.1, 3.5, 1.6 Hz, 1H), 4.95 – 4.90 (m, 1H), 3.78/3.78 (s, 3H), 3.66 – 3.47 (m, 1H), 2.57 (t, J = 7.6 Hz, 2H), 2.35 – 2.23 (m, 4H), 2.20 – 2.00 (m, 4H), 1.82 (dd, J = 15.9, 3.2 Hz, 1H), 1.76 – 1.68 (m, 1H), 1.67 (d, J = 1.1 Hz, 1.5H)/1.55 (s, 1.5H), 1.54 – 1.29 (m, 10H). ^{13}C NMR (126 MHz, CDCl$_3$) δ 171.53, 160.18/160.14, 144.39, 139.12, 135.85/135.79, 135.01, 134.96, 124.78/124.14, 118.15/118.09, 114.44, 112.26/112.10, 110.75/110.62, 102.85/102.83, 70.70/70.46, 55.41, 42.15/42.08, 37.96, 36.39/36.21, 35.93, 34.94/34.78, 33.83, 29.69/29.52, 28.96/28.83, 28.11, 25.62, 23.46, 16.03. HRMS (ESI, *m/z*): calcd for [C$_{27}$H$_{42}$NO$_3$]$^+$ ([M +H]$^+$): 428.3165, found 428.3167.

General Procedure A (synthesis of acylated amino acids):

A flame dried 25 mL round bottom flask was flushed with argon before THF (4 mL), tribasic potassium phosphate (1.06 g, 5 mmol, 2.5 eq.), and appropriate acyl chloride (2.2 mmol, 1.1 eq.) were added. Appropriate amino acid (2 mmol, 1eq.) was added and the heterogenous solution was stirred vigorously for 24 h. Deionized water (10 mL) and EtOAc (10 mL) were added to the reaction mixture. The aqueous layer was collected and the organic layer was washed with deionized water (10 mL). The combined aqueous layers were collected and acidified (pH = 2) by the addition of 2N aqueous hydrochloric acid. The heterogenous solution was extracted with EtOAc (3X, 10 mL) and the combined organic layers were collected and dried over anhydrous sodium sulfate. Solvent was removed to afford pure acylated amino acid.
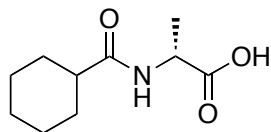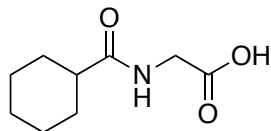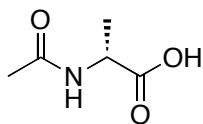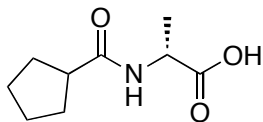
(*R*)-2-(Cyclohexanecarboxamido)propanoic acid (14):

General procedure A was followed using cyclohexanecarbonyl chloride (323 mg, 2.2 mmol, 1.1 eq.) and D-alanine (178 mg, 2 mmol, 1 eq.). Obtained as a fine white powder (300 mg, 76%). $[\alpha]^{23}_D = 24.3°$ (c = 0.01, DCM). ^{1}H NMR (500 MHz, DMSO) δ 12.29 (s, 1H), 7.95 (d, *J* = 7.4 Hz, 1H), 4.16 (p, *J* = 7.4 Hz, 1H), 2.16 (tt, *J* = 11.4, 3.4 Hz, 1H), 1.80 (dd, *J* = 12.9, 2.7 Hz, 1H), 1.73 – 1.50 (m, 3H), 1.37 – 1.25 (m, 2H), 1.24 (d, *J* = 7.3 Hz, 2H), 1.22 – 1.08 (m, 2H). ^{13}C NMR (126 MHz, DMSO) δ 174.97, 174.35, 47.12, 43.48, 29.08, 29.01, 28.62, 25.43, 25.19, 24.88, 17.11. HRMS (ESI, *m/z*): calcd for [C$_{10}$H$_{16}$NO$_3$]$^-$ ([M - H]$^-$): 198.1130, found 198.1131.
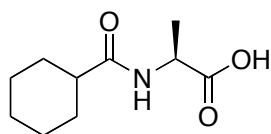
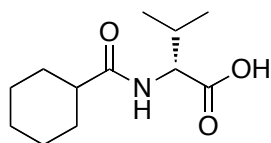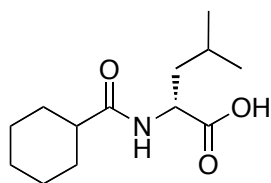**(*S*)-2-(Cyclohexanecarboxamido)propanoic acid (37):**

General procedure A was followed using cyclohexanecarbonyl chloride (323 mg, 2.2 mmol, 1.1 eq.) and L-alanine (178 mg, 2 mmol, 1 eq.). Obtained as a fine white powder (300 mg, 76%). $[\alpha]^{23}_D = -24.5°$ (c = 0.01, DCM). ^{1}H NMR (500 MHz, DMSO) δ 12.29 (s, 1H), 7.95 (s, 1H), 4.16 (p, *J* = 7.4 Hz, 1H), 2.16 (tt, *J* = 11.4, 3.4 Hz, 1H), 1.80 (dd, *J* = 12.9, 2.7 Hz, 1H), 1.73 – 1.50 (m, 3H), 1.37 – 1.25 (m, 2H), 1.24 (d, *J* = 7.3 Hz, 2H), 1.22 – 1.08 (m, 2H). ^{13}C NMR (126 MHz, DMSO) δ 174.97, 174.35, 47.12, 43.48, 29.08, 28.62, 25.43, 25.19, 24.88, 17.11. HRMS (ESI, *m/z*): calcd for [C$_{10}$H$_{16}$NO$_3$]$^-$ ([M - H]$^-$): 198.1130, found 198.1129.

2-(Cyclohexanecarboxamido)acetic acid (38):

General procedure A was followed using cyclohexane carbonyl chloride (323 mg, 2.2 mmol, 1.1 eq.) and glycine (150 mg, 2 mmol, 1 eq.). Obtained as a fine white powder (308 mg, 83%). ^{1}H NMR (500 MHz, DMSO) δ 12.26 (s, 1H), 7.99 (d, J = 4.5 Hz, 1H), 3.70 (d, J = 5.3 Hz, 2H), 2.16 (m, 1H), 1.80 (m, 1H), 1.75 – 1.53 (m, 3H), 1.41 – 1.06 (m, 6H). ^{13}C NMR (126 MHz, DMSO) δ 175.47, 171.45, 43.60, 29.08, 28.62, 25.44, 25.39, 25.19, 24.89. HRMS (ESI, *m/z*): calcd for $[C_9H_{14}NO_3]^-$ ([M - H]⁻): 184.0974, found 184.0973.

(*R*)-2-Acetamidopropanoic acid (39):

General procedure A was followed using acetyl chloride (172 mg, 2.2 mmol, 1.1 eq.) and D-alanine (178 mg, 2 mmol, 1 eq.). Obtained as a colorless oil (92 mg, 35%). ^{1}H NMR (500 MHz, DMSO) δ 12.38 (s, 1H), 8.22 (d, J = 7.2 Hz, 1H), 4.23 (p, J = 7.3 Hz, 1H), 1.89 (s, 3H), 1.30 (d, J = 7.3 Hz, 3H). ^{13}C NMR (126 MHz, DMSO) δ 174.28, 168.95, 47.37, 22.28, 17.15. HRMS (ESI, *m/z*): calcd for $[C_5H_8NO_3]^-$ ([M - H]⁻): 130.0504, found 130.0508.

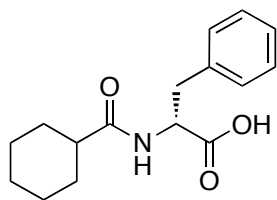**(*R*)-2-(Cyclopentanecarboxamido)propanoic acid (40):**

General procedure A was followed using cyclohexanecarbonyl chloride (323 mg, 2.2 mmol, 1.1 eq.) and D-alanine (178 mg, 2 mmol, 1 eq.). Obtained as a fine white powder (300 mg, 76%, isolated as a mixture of amide rotamers). $[\alpha]^{23}_D$ = 35.8° (c = 0.01, DCM). ^{1}H NMR (500 MHz,

DMSO) δ 12.42 (s, 1H), 8.15/8.03 (d, J = 7.3 Hz, 1H), 4.23/4.17 (p, J = 7.3 Hz, 1H), 2.64 – 2.57

(m, 1H), 1.76 – 1.69 (m, 2H), 1.65 – 1.54 (m, 4H), 1.53 – 1.48 (m, 2H), 1.26/1.25 (d, J = 7.3 Hz,

3H). ^{13}C NMR (126 MHz, DMSO) δ 175.31/175.14, 174.34/173.35, 47.45/47.34, 43.65/43.58,

29.84/29.80, 25.70/25.69, 25.64/25.62, 17.13, 16.89. HRMS (ESI, m/z): calcd for $[C_9H_{14}NO_3]^-$

$([M - H]^-)$: 184.0974, found 184.0973.

(*R*)-2-(Cyclohexanecarboxamido)-3-methylbutanoic acid (41):

General procedure A was followed using cyclohexanecarbonyl chloride (323 mg, 2.2 mmol, 1.1

eq.) and D-valine (235 mg, 2 mmol, 1 eq.). Obtained as an amorphous colorless solid (410 mg,

90%). $[\alpha]^{23}_D$ = 3.31° (c = 0.01, DCM). ^{1}H NMR (500 MHz, DMSO) δ 12.33 (s, 1H), 7.79 (d, J =

8.7 Hz, 1H), 4.12 (dd, J = 8.7, 6.0 Hz, 1H), 2.28 (tt, J = 11.4, 3.3 Hz, 1H), 2.07 – 1.98 (m, 1H),

1.84 – 1.76 (m, 1H), 1.64 (m, 3H), 1.38 – 1.08 (m, 6H), 0.87 (d, J = 6.8 Hz, 3H), 0.85 (d, J = 6.8

Hz, 3H). ^{13}C NMR (126 MHz, DMSO) δ 175.48, 173.27, 56.72, 43.36, 29.74, 29.53, 28.93,

28.62, 25.28, 24.88, 19.14, 18.00. HRMS (ESI, m/z): calcd for $[C_{12}H_{20}NO_3]^-$ $([M - H]^-)$:

226.1443, found 226.1439.

(*R*)-2-(Cyclohexanecarboxamido)-4-methylpentanoic acid (42):

General procedure A was followed using cyclohexanecarbonyl chloride (323 mg, 2.2 mmol, 1.1

eq.) and D-valine (273 mg, 2 mmol, 1 eq.). Obtained as a colorless oil (454 mg, 94%). $[\alpha]^{23}_D$ =

80.39° (c = 0.01, DCM). ^{1}H NMR (500 MHz, DMSO) δ 12.22 (s, 1H), 7.89 (d, J = 8.1 Hz, 1H), 4.19 (ddd, J = 10.2, 8.2, 4.9 Hz, 1H), 2.17 (qt, J = 11.7, 3.3 Hz, 1H), 1.84 – 1.76 (m, 1H), 1.74 – 1.38 (m, 6H), 1.37 – 1.08 (m, 6H), 0.88 (d, J = 6.6 Hz, 3H), 0.83 (d, J = 6.5 Hz, 3H). ^{13}C NMR (126 MHz, DMSO) δ 175.21, 174.36, 49.78, 43.56, 29.31, 28.92, 28.62, 25.38, 25.15, 24.88, 24.34, 22.87, 21.17. HRMS (ESI, m/z): calcd for $[C_{13}H_{22}NO_3]^-$ ([M - H]$^-$): 240.1600, found 240.1599.

(R)-2-(Cyclohexanecarboxamido)-3-phenylpropanoic acid (43):

General procedure A was followed using cyclohexanecarbonyl chloride (323 mg, 2.2 mmol, 1.1 eq.) and D-phenylalanine (331 mg, 2 mmol, 1 eq.). Obtained as a colorless amorphous solid (534 mg, 97%). $[\alpha]^{23}_D$ = -29.1° (c = 0.01, DCM). ^{1}H NMR (500 MHz, DMSO) δ 12.37 (s, 1H), 7.97 (d, J = 8.2 Hz, 1H), 7.29 – 7.14 (m, 5H), 4.39 (ddd, J = 10.0, 8.3, 4.7 Hz, 1H), 3.05 (dd, J = 13.8, 4.7 Hz, 1H), 2.84 (dd, J = 13.8, 10.0 Hz, 1H), 2.22 – 2.06 (m, 1H), 1.84 – 1.76 (m, 1H), 1.70 – 1.53 (m, 3H), 1.52 – 1.44 (m, 1H), 1.37 – 1.03 (m, 5H). ^{13}C NMR (126 MHz, DMSO) δ 175.04, 173.27, 137.79, 129.07, 128.03, 126.28, 53.00, 43.49, 36.63, 29.04, 28.87, 28.62, 25.38, 25.16, 25.10, 24.88. HRMS (ESI, m/z): calcd for $[C_{16}H_{21}NO_3]^-$ ([M - H]$^-$): 275.1521, found 275.1517.

General Procedure B (synthesis of pre-metathesis intermediates):

A flame dried 5 mL flask was flushed with argon before THF (1 mL), appropriate acid (0.047 mmol, 1eq.), triphenylphosphine (63 mg, 0.24 mmol, 5 eq.), and compound **12** (20 mg, 0.047 mmol, 1 eq.) were added. Diethyl azodicarboxylate (40% in toluene, 128 mg, 0.24 mmol, 5 eq.)

was added dropwise at rt. After stirring for 4 h, the reaction mixture was quenched by the addition of saturated aqueous sodium bicarbonate (1 mL). The organic layer was collected and the aqueous layer was extract with EtOAc (4X, 2 mL). The combined organic layers were collected and dried over anhydrous sodium sulfate. Solvent was removed to afford a colorless oil that was purified by flash SiO$_2$ chromatography (1% − 40% EtOAc in Hex). Pre-metathesis intermediates were isolated as colorless oils.
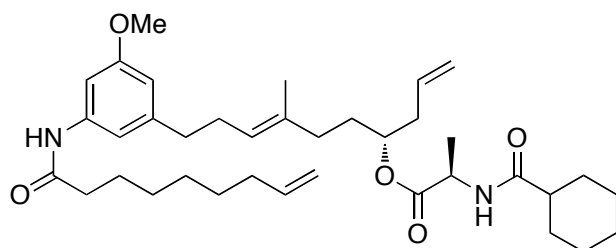
(*R*)-(*R*,*E*)-10-(3-Methoxy-5-(non-8-enamido)phenyl)-7-methyldeca-1,7-dien-4-yl 2-(cyclohexanecarboxamido)propanoate (26):

General procedure B was followed using acid **14** (9.4 mg, 0.047 mmol, 1 eq.) Compound **26** was separated from compound **27** using SiO$_2$ (10% − 30% EtOAc in Hex), isolated as a colorless oil (10.6 mg, 37%, isolated as a mixture of amide rotamers). $[\alpha]^{23}_D = 2.43°$ (c = 0.005, DCM). ^{1}H NMR (500 MHz, CDCl$_3$) δ 7.66/7.59 (s, 1H), 7.33/7.29 (s, 1H), 6.73/6.66 (s, 1H), 6.47/6.46 (s, 1H), 6.09/6.05 (d, *J* = 7.2 Hz, 1H), 5.80 (ddt, *J* = 16.9, 10.2, 6.7 Hz, 1H), 5.70 (ddt, *J* = 14.0, 9.5, 6.9 Hz, 1H), 5.20 − 5.10 (m, 1H), 5.10 − 5.03 (m, 2H), 4.99 (ddd, *J* = 17.1, 3.5, 1.6 Hz, 1H), 4.95 − 4.91 (m, 1H), 4.90 − 4.82 (m, 1H), 4.63 − 4.51 (m, 1H), 3.79 (s, 3H), 2.61 − 2.48 (m, 2H), 2.40 − 2.18 (m, 5H), 2.11 (tt, *J* = 11.7, 3.5 Hz, 2H), 2.04 (dd, *J* = 13.9, 6.8 Hz, 2H), 1.98 (t, *J* = 7.3 Hz, 2H), 1.91 − 1.83 (m, 2H), 1.81 − 1.75 (m, 2H), 1.74 − 1.70 (m, 2H), 1.70 − 1.61 (m, 4H), 1.51 (s, 3H), 1.48 − 1.15 (m, 10H), 1.37 (d, *J* = 7.1 Hz, 3H). ^{13}C NMR (126 MHz, CDCl$_3$) δ 175.76, 173.21, 171.62, 160.26, 144.22, 139.30, 139.15, 134.55, 133.35, 124.53, 118.21, 114.43, 112.07, 110.49, 102.69, 74.27, 55.42, 48.05, 45.43, 38.72, 37.94, 36.04, 35.27, 33.86, 31.56,

29.72, 29.68, 29.65, 29.28, 29.02, 28.86, 25.84, 25.80, 25.79, 25.66, 18.92, 15.94. HRMS (ESI,

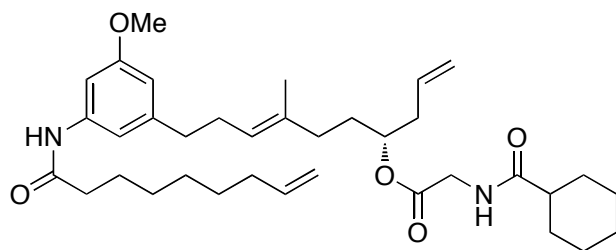*m/z*): calcd for $[C_{37}H_{56}KN_2O_5]^+$ ($[M + K]^+$): 647.3826, found 647.3830.
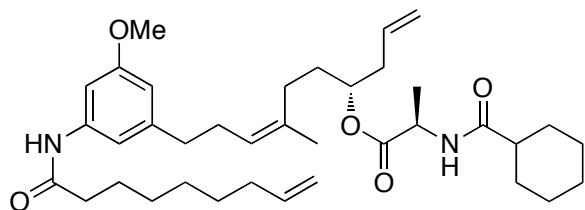
(*R*)-(*R,Z*)-10-(3-Methoxy-5-(non-8-enamido)phenyl)-7-methyldeca-1,7-dien-4-yl   2-(cyclohexanecarboxamido)propanoate (27):

General procedure B was followed using acid **14** (9.4 mg, 0.047 mmol, 1 eq.) Compound **26** was separated from compound **27** using SiO$_2$ (10% – 30% EtOAc in Hex), isolated as a colorless oil (11.2 mg, 39%). $[\alpha]^{23}_D$ = 1.97° (c = 0.005, DCM). ^{1}H NMR (500 MHz, CDCl$_3$) δ 8.62 (s, 1H), 7.64 – 7.57 (m, 1H), 6.51 (s, 1H), 6.43 (s, 1H), 6.23 (d, *J* = 7.6 Hz, 1H), 5.80 (ddt, *J* = 16.9, 10.1, 6.7 Hz, 1H), 5.77 – 5.65 (m, 1H), 5.21 (t, *J* = 7.2 Hz, 1H), 5.10 – 5.04 (m, 1H), 4.98 (ddd, *J* = 17.1, 3.6, 1.6 Hz, 1H), 4.95 – 4.87 (m, 1H), 4.69 – 4.61 (m, 1H), 4.33 – 4.23 (m, 1H), 3.79 (s, 3H), 2.52 – 2.45 (m, 2H), 2.42 – 2.37 (m, 2H), 2.37 – 2.25 (m, 3H), 2.23 – 2.08 (m, 3H), 2.08 – 1.98 (m, 2H), 1.98 – 1.91 (m, 2H), 1.85 (dd, *J* = 14.2, 12.9 Hz, 2H), 1.83 – 1.70 (m, 6H), 1.66 (d, *J* = 1.0 Hz, 3H), 1.62 – 1.58 (m, 1H), 1.36 (d, *J* = 7.1 Hz, 3H), 1.46 – 1.11 (m, 10H). ^{13}C NMR (126 MHz, CDCl$_3$) δ 175.97, 173.10, 172.27, 160.18, 143.92, 140.20, 139.20, 134.76, 133.24, 125.19, 118.35, 114.38, 111.01, 110.61, 102.74, 74.56, 55.43, 47.97, 45.50, 38.96, 37.73, 36.44, 33.89, 31.93, 29.85, 29.77, 29.65, 29.09, 28.92, 27.40, 25.78, 25.76, 25.74, 23.24, 19.21, 14.28. HRMS (ESI, *m/z*): calcd for $[C_{37}H_{56}KN_2O_5]^+$ ($[M + K]^+$): 647.3826, found 647.3823.
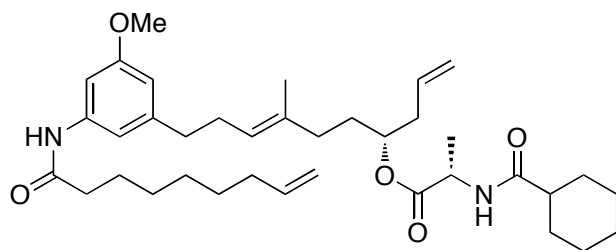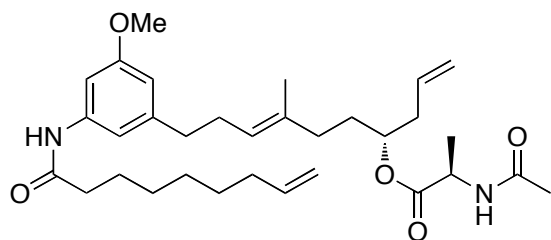
(*S*)-(*R,E*)-10-(3-Methoxy-5-(non-8-enamido)phenyl)-7-methyldeca-1,7-dien-4-yl   2-(cyclohexanecarboxamido)propanoate (44):

General procedure B was followed using acid **37** (9.4 mg, 0.047 mmol, 1 eq.) Compound **44** was purified by SiO$_2$ chromatography (10% − 30% EtOAc in Hex), isolated as a colorless oil (10.6 mg, 37%). [α]$^{23}_D$ = 0.97° (c = 0.005, DCM). ^{1}H NMR (500 MHz, CDCl$_3$) δ 7.67 (s, 1H), 7.29 (s, 1H), 6.73 (s, 1H), 6.46 (s, 1H), 6.10 (d, *J* = 7.6 Hz, 1H), 5.80 (ddt, *J* = 16.9, 10.2, 6.7 Hz, 1H), 5.75 − 5.65 (m, 1H), 5.18 (t, *J* = 6.9 Hz, 1H), 5.10 − 5.03 (m, 2H), 4.99 (ddd, *J* = 17.1, 3.6, 1.6 Hz, 1H), 4.93 (ddt, *J* = 10.2, 2.2, 1.2 Hz, 1H), 4.90 − 4.81 (m, 1H), 4.64 − 4.51 (m, 1H), 3.79 (s, 3H), 2.53 (t, *J* = 7.9 Hz, 2H), 2.39 − 2.30 (m, 3H), 2.30 − 2.16 (m, 3H), 2.12 (tt, *J* = 11.7, 3.4 Hz, 1H), 2.04 (dt, *J* = 13.0, 3.9 Hz, 2H), 1.98 (t, *J* = 8.0 Hz, 2H), 1.91 − 1.82 (m, 2H), 1.81 − 1.75 (m, 2H), 1.74 − 1.70 (m, 2H), 1.69 − 1.63 (m, 2H), 1.65 (s, 3H), 1.62 − 1.50 (m, 2H), 1.49 − 1.32 (m, 7H), 1.35 (d, *J* = 7.1 Hz, 3H), 1.31 − 1.13 (m, 3H). ^{13}C NMR (126 MHz, CDCl$_3$) δ 175.74, 172.80, 171.74, 160.17, 144.12, 139.47, 139.14, 134.83, 133.30, 125.20, 118.31, 114.43, 111.79, 110.71, 102.85, 74.66, 55.43, 48.12, 45.42, 38.61, 37.91, 36.40, 33.86, 31.67, 29.75, 29.70, 29.68, 29.28, 29.02, 28.87, 27.47, 25.84, 25.80, 25.79, 25.69, 23.36, 18.90. HRMS (ESI, *m/z*): calcd for [C$_{37}$H$_{56}$KN$_2$O$_5$]$^+$ ([M + K]$^+$): 647.3826, found 647.3829.

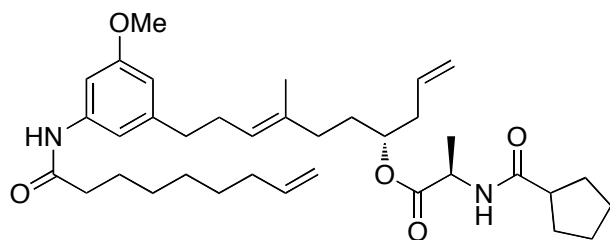**(*R*,*E*)-10-(3-Methoxy-5-(non-8-enamido)phenyl)-7-methyldeca-1,7-dien-4-yl 2-(cyclohexanecarboxamido)acetate (45):**

General procedure B was followed using acid **38** (8.7 mg, 0.047 mmol, 1 eq.) Compound **45** was purified by SiO$_2$ chromatography (20% – 40% EtOAc in Hex), isolated as a colorless oil (8.5 mg, 31%). $[\alpha]^{23}_{D}$ = 4.72° (c = 0.005, DCM). ^{1}H NMR (500 MHz, CDCl$_3$) δ 7.48 (s, 1H), 7.28 (s, 1H), 6.70 (s, 1H), 6.48 (s, 1H), 5.99 (s, 1H), 5.80 (ddt, *J* = 16.9, 10.2, 6.7 Hz, 1H), 5.70 (ddt, *J* = 11.3, 9.4, 7.1 Hz, 1H), 5.11 (t, *J* = 6.7 Hz, 1H), 5.09 – 5.03 (m, 2H), 5.02 – 4.86 (m, 4H), 4.00 (qd, *J* = 18.5, 5.1 Hz, 2H), 3.79 (s, 3H), 2.55 (t, *J* = 7.5 Hz, 2H), 2.39 – 2.22 (m, 5H), 2.16 (tt, *J* = 11.5, 3.4 Hz, 1H), 2.04 (dd, *J* = 12.7, 7.0 Hz, 2H), 1.98 (t, *J* = 7.4 Hz, 2H), 1.89 (dd, *J* = 12.6, 1.5 Hz, 2H), 1.83 – 1.76 (m, 2H), 1.76 – 1.62 (m, 5H), 1.60 (s, 3H), 1.39 – 1.21 (m, 11H). ^{13}C NMR (126 MHz, CDCl$_3$) δ 176.38, 171.59, 170.08, 160.25, 144.25, 139.26, 139.15, 134.56, 133.29, 124.51, 118.29, 114.44, 112.08, 110.54, 102.72, 74.62, 55.43, 45.36, 41.51, 38.65, 37.95, 36.06, 35.31, 33.86, 31.40, 29.85, 29.71, 29.70, 29.66, 29.27, 29.01, 28.86, 25.84, 25.80, 25.65, 15.95. HRMS (ESI, *m/z*): calcd for [C$_{36}$H$_{54}$KN$_2$O$_5$]$^+$ ([M + K]$^+$): 633.3670, found 633.3671.
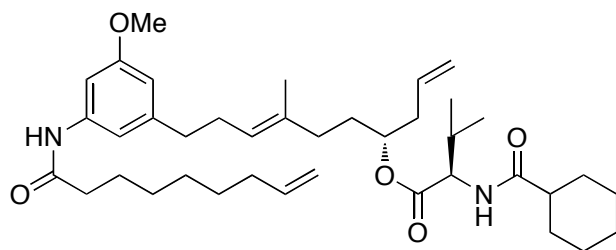
(*R*)-(*R,E*)-10-(3-Methoxy-5-(non-8-enamido)phenyl)-7-methyldeca-1,7-dien-4-yl **2-acetamidopropanoate (46):**

General procedure B was followed using acid **39** (6.2 mg, 0.047 mmol, 1 eq.) Compound **46** was purified by SiO$_2$ chromatography (30% − 50% EtOAc in Hex), isolated as a colorless oil (8.5 mg, 31%, mixture of amide rotamers). $[\alpha]^{23}_D$ = 3.52° (c = 0.005, DCM). ^{1}H NMR (500 MHz, CDCl$_3$) δ 7.50/7.47 (s, 1H), 7.29/7.22 (s, 1H), 6.75/6.70 (s, 1H), 6.48/6.47 (s, 1H), 6.19/6.08 (d, *J* = 7.2 Hz, 1H), 5.80 (ddt, *J* = 16.9, 10.2, 6.7 Hz, 1H), 5.75 − 5.64 (m, 1H), 5.18/5.13 (t, *J* = 7.0 Hz, 1H), 5.11 − 5.03 (m, 2H), 4.99 (ddd, *J* = 17.1, 3.5, 1.6 Hz, 1H), 4.95 − 4.84 (m, 2H), 4.63 − 4.51 (m, 1H), 3.79 (s, 1H), 2.58 − 2.51 (m, 2H), 2.40 − 2.16 (m, 6H), 2.02/2.01 (s, 3H), 2.08 − 1.91 (m, 4H), 1.77 − 1.61 (m, 4H), 1.59/1.52 (s, 3H), 1.44 − 1.3 (m, 6H), 1.38/1.36 (d, *J* = 7.3 Hz, 3H). ^{13}C NMR (126 MHz, CDCl$_3$) δ 173.04/172.72, 171.67/171.57, 169.71, 160.25/160.17, 144.29/144.23, 139.36/139.24, 139.15/139.14, 134.89/134.60, 133.34/133.27, 125.13/124.51, 118.33/118.24, 114.45, 112.03/111.89, 110.75/110.55, 102.83/102.74, 74.74/74.39, 55.44, 48.44/48.40, 38.73/38.64, 36.42/36.09, 36.06, 35.32/35.24, 33.85, 31.71/31.65, 29.85/29.79, 29.68/29.26, 28.99/28.85, 27.54, 25.66/25.64, 23.39/23.31, 18.86/18.78, 15.97/15.94. HRMS (ESI, *m/z*): calcd for [C$_{32}$H$_{48}$KN$_2$O$_5$]$^+$ ([M + K]$^+$): 579.3200, found 579.3199.
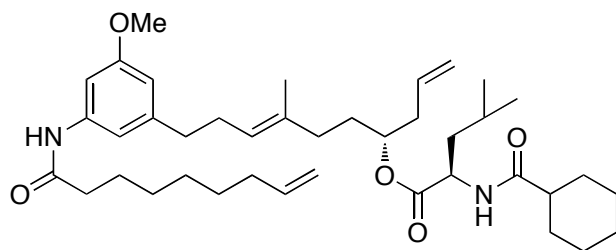
(*R*)-(*R,E*)-10-(3-Methoxy-5-(non-8-enamido)phenyl)-7-methyldeca-1,7-dien-4-yl   2-(cyclopentanecarboxamido)propanoate (47):

General procedure B was followed using acid **40** (8.7 mg, 0.047 mmol, 1 eq.) Compound **47** was purified by SiO$_2$ chromatography (10% – 30% EtOAc in Hex), isolated as a colorless oil (13.1 mg, 47%, mixture of amide rotamers). $[\alpha]^{23}_D$ = 3.25° (c = 0.005, DCM). ^{1}H NMR (500 MHz, CDCl$_3$) δ 8.55 (s, 1H), 7.58 (s, 1H), 6.53 (s, 1H), 6.43 (s, 1H), 6.22 (d, *J* = 7.5 Hz, 1H), 5.80 (ddt, *J* = 16.9, 10.2, 6.7 Hz, 1H), 5.75 – 5.65 (m, 1H), 5.20 (t, *J* = 7.2 Hz, 1H), 5.10 – 5.03 (m, 2H), 4.98 (ddd, *J* = 17.1, 3.6, 1.6 Hz, 1H), 4.95 – 4.87 (m, 2H), 4.72 – 4.60 (m, 1H), 3.79 (s, 3H), 2.62 – 2.52 (m, 1H), 2.49 (t, *J* = 8.1 Hz, 2H), 2.41 – 2.24 (m, 4H), 2.22 – 2.13 (m, 2H), 2.02 (dt, *J* = 17.1, 5.2 Hz, 3H), 1.97 – 1.83 (m, 4H), 1.66 (d, *J* = 0.9 Hz, 3H), 1.81 – 1.44 (m, 5H), 1.37 (d, *J* = 7.1 Hz, 3H), 1.43 – 1.30 (m, 10H). ^{13}C NMR (126 MHz, CDCl$_3$) δ 176.12, 173.10, 172.22, 160.19, 143.95, 140.16, 139.21, 134.81, 133.24, 125.16, 118.35, 114.38, 111.04, 110.63, 102.74, 74.58, 55.42, 48.16, 45.86, 38.94, 37.69, 36.44, 33.89, 31.96, 30.59, 30.42, 29.95, 29.33, 29.08, 28.91, 27.43, 26.14, 26.06, 25.72, 23.27, 19.20. HRMS (ESI, *m/z*): calcd for [C$_{36}$H$_{54}$KN$_2$O$_5$]$^+$ ([M + K]$^+$): 633.3670, found 633.3667.
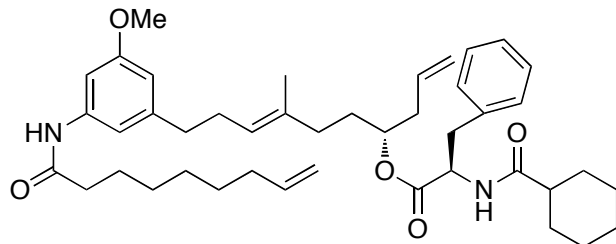
(*R*)-(*R*,*E*)-10-(3-Methoxy-5-(non-8-enamido)phenyl)-7-methyldeca-1,7-dien-4-yl   2-(cyclohexanecarboxamido)-3-methylbutanoate (48):

General procedure B was followed using acid **42** (10.6 mg, 0.047 mmol, 1 eq.) Compound **48** was purified by SiO$_2$ chromatography (10% − 30% EtOAc in Hex), isolated as a colorless oil (10.5 mg, 35%, mixture of amide rotamers). $[\alpha]^{23}_D$ = 1.86° (c = 0.005, DCM). ^{1}H NMR (500 MHz, CDCl$_3$) δ 7.64 (s, 1H), 7.39/7.35 (s, 1H), 6.68/6.65 (s, 1H), 6.47/6.45 (s, 1H), 5.94/5.92 (d, *J* = 7.2 Hz, 1H), 5.80 (ddt, *J* = 16.9, 10.2, 6.7 Hz, 1H), 5.70 (tdd, *J* = 17.5, 8.8, 5.1 Hz, 1H), 5.22 − 5.03 (m, 3H), 5.03 − 4.95 (m, 1H), 4.95 − 4.83 (m, 2H), 4.59/4.57 (dd, *J* = 8.8, 4.5 Hz, 1H), 3.79 (s, 3H), 2.61 − 2.49 (m, 2H), 2.37 − 2.30 (m, 3H), 2.29 − 2.23 (m, 1H), 2.22 − 2.10 (m, 2H), 2.04 (dd, *J* = 13.4, 6.4 Hz, 2H), 1.98 (t, *J* = 7.4 Hz, 2H), 1.91 − 1.85 (m, 4H), 1.78 (ddd, *J* = 18.0, 11.1, 7.2 Hz, 2H), 1.74 − 1.70 (m, 4H), 1.70 − 1.62 (m, 2H), 1.50 (s, 3H), 1.49 − 1.17 (m, 10H), 0.95 (d, *J* = 6.9 Hz, 3H), 0.88 (d, *J* = 6.9 Hz, 3H). ^{13}C NMR (126 MHz, CDCl$_3$) δ 176.20, 172.26, 171.64, 160.27, 144.19, 139.32, 139.15, 134.57, 133.35, 124.53, 118.30, 114.43, 112.09, 110.51, 102.70, 74.43, 56.74, 55.43, 45.69, 38.56, 37.94, 36.04, 35.19, 33.86, 31.47, 31.40, 30.12, 30.07, 29.61, 29.29, 29.02, 28.87, 25.85, 25.75, 25.67, 19.35, 17.62, 15.92. HRMS (ESI, *m/z*): calcd for [C$_{39}$H$_{60}$KN$_2$O$_5$]$^+$ ([M + K]$^+$): 675.4139, found 675.4138.

(*R*)-(*R*,*E*)-10-(3-Methoxy-5-(non-8-enamido)phenyl)-7-methyldeca-1,7-dien-4-yl 2-(cyclohexanecarboxamido)-4-methylpentanoate (49):

General procedure B was followed using acid **42** (11.3 mg, 0.047 mmol, 1 eq.) Compound **49** was purified by SiO$_2$ chromatography (10% – 30% EtOAc in Hex), isolated as a colorless oil (11.6 mg, 38%, mixture of amide rotamers). $[\alpha]^{23}_D$ = 1.93° (c = 0.005, DCM). ^{1}H NMR (500 MHz, CDCl$_3$) δ 7.83/7.69 (s, 1H), 7.54/7.50 (s, 1H), 7.36/7.33 (s, 1H), 6.69/6.66 (d, *J* = 7.1 Hz, 1H), 6.48/6.46 (s, 1H), 5.79 (ddt, *J* = 17.0, 10.2, 6.7 Hz, 1H), 5.75 – 5.59 (m, 1H), 5.14 (t, *J* = 7.1 Hz, 1H), 5.09 – 5.02 (m, 2H), 4.98 (ddd, *J* = 17.1, 3.6, 1.6 Hz, 1H), 4.92 (ddt, *J* = 10.2, 2.2, 1.1 Hz, 1H), 4.89 – 4.75 (m, 1H), 4.32 (q, *J* = 7.1 Hz, 1H), 3.79 (s, 3H), 2.64 – 2.46 (m, 2H), 2.37 – 2.18 (m, 5H), 2.15 – 2.07 (m, 3H), 2.07 – 2.00 (m, 2H), 1.96 – 1.90 (m, 3H), 1.90 – 1.53 (m, 8H), 1.49 (d, *J* = 3.6 Hz, 3H), 1.44 – 1.16 (m, 13H), 0.95 (d, *J* = 6.6 Hz, 3H), 0.88 (d, *J* = 6.7 Hz, 3H). ^{13}C NMR (126 MHz, CDCl$_3$) δ 175.97/173.25, 171.65/171.58, 168.38/168.33, 162.96/160.25, 150.76, 139.21/139.16, 134.68/134.61, 133.43/133.37, 133.11/133.01, 124.51/124.42, 118.35/118.23, 114.41, 112.25/112.15, 110.72/110.50, 102.78/102.69, 75.44/74.22, 64.41/63.70, 55.42, 42.96/42.91, 42.07/42.04, 38.62/38.58, 38.17/38.14, 37.91/37.59, 36.41/36.14, 34.79/34.70, 33.86, 31.70/31.57, 29.86/29.77, 29.29/29.26, 29.05/29.04, 28.87, 26.11/26.09, 26.05/25.99, 25.71/25.63, 24.51/24.48, 24.17/24.15, 23.47/23.46, 23.05/23.04, 16.08/16.03, 14.31/14.28. HRMS (ESI, *m/z*): calcd for [C$_{40}$H$_{62}$KN$_2$O$_5$]$^+$ ([M + K]$^+$): 675.4139, found 675.4138.

(*R*)-(*R*,*E*)-10-(3-Methoxy-5-(non-8-enamido)phenyl)-7-methyldeca-1,7-dien-4-yl   2-(cyclohexanecarboxamido)-3-phenylpropanoate (50):

General procedure B was followed using acid **43** (12.9 mg, 0.047 mmol, 1 eq.) Compound **50** was purified by SiO$_2$ chromatography (10% − 30% EtOAc in Hex), isolated as a colorless oil (12.2 mg, 38%). $[\alpha]^{23}_D$ = -1.03° (c = 0.005, DCM). ^{1}H NMR (500 MHz, CDCl$_3$) δ 8.67 (s, 1H), 7.67 (s, 1H), 7.23 (ddd, *J* = 5.1, 3.2, 1.1 Hz, 3H), 7.09 (dd, *J* = 7.6, 1.6 Hz, 2H), 6.53 (s, 1H), 6.44 (s, 1H), 6.03 (d, *J* = 8.2 Hz, 1H), 5.80 (ddt, *J* = 16.9, 10.2, 6.7 Hz, 1H), 5.69 (ddt, *J* = 17.3, 10.2, 7.1 Hz, 1H), 5.21 (t, *J* = 7.2 Hz, 1H), 5.14 − 5.07 (m, 2H), 4.98 (ddd, *J* = 17.1, 3.6, 1.5 Hz, 2H), 4.95 − 4.87 (m, 2H), 3.80 (s, 3H), 3.16 (dd, *J* = 13.9, 5.9 Hz, 1H), 2.95 (dd, *J* = 13.9, 6.6 Hz, 1H), 2.56 − 2.42 (m, 2H), 2.39 − 2.23 (m, 3H), 2.18 (dd, *J* = 15.7, 8.0 Hz, 2H), 2.12 − 1.99 (m, 4H), 1.89 (ddd, *J* = 13.1, 10.8, 5.9 Hz, 1H), 1.83 − 1.67 (m, 7H), 1.66 (d, *J* = 0.9 Hz, 3H), 1.54 − 1.44 (m, 1H), 1.42 − 1.09 (m, 13H). ^{13}C NMR (126 MHz, CDCl$_3$) δ 175.88, 172.24, 171.80, 160.21, 143.88, 140.33, 139.19, 135.90, 134.85, 133.30, 129.58, 128.56, 127.20, 125.12, 118.50, 114.39, 110.95, 110.56, 102.64, 75.23, 55.43, 52.77, 45.49, 38.76, 38.54, 37.70, 36.52, 33.89, 31.93, 29.95, 29.87, 29.47, 29.39, 29.13, 28.95, 27.44, 25.78, 25.70, 25.65, 23.28. HRMS (ESI, *m/z*): calcd for $[C_{43}H_{60}KN_2O_5]^+$ ($[M + K]^+$): 723.4139, found 723.4141.

General Procedure C (ring-closing metathesis with Grubbs first generation catalyst):

A 25 mL round bottom flask was flushed with argon before DCM (13 mL) and appropriate pre-metathesis intermediate (0.013 mmol, 1 eq.) was added. Grubbs first generation catalyst (2.15 mg, 20 mol %) was added in one portion and the reaction was stirred at rt. After 30 min, solvent was removed to afford a black oil that was purified using SiO_2 flash chromatography (2X, 1: 20% − 40% EtOAc in Hex; 2: 1% − 20% acetone in DCM). Compounds were isolated as a mixture of *cis* and *trans* olefin macrocycles as colorless oils.
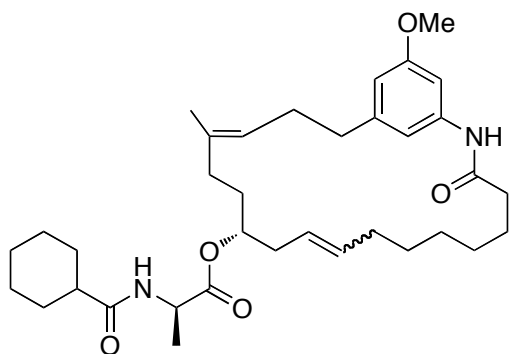
Macrocycle 7:

General procedure C was followed. Macrocycle **7** was isolated as a 2:1 mixture of olefin isomers. (6 mg, 83%). $[\alpha]^{23}_D = 9.54°$ (c = 0.005, DCM). ^{1}H NMR (500 MHz, CDCl$_3$) δ 8.00/7.96 (s, 1H), 7.50/6.96 (s, 1H), 6.70/6.60 (s, 1H), 6.43/6.39 (s, 1H), 6.01/5.94 (d, J = 7.3 Hz, 1H), 5.50 − 5.38 (m, 1H), 5.33 − 5.22 (m, 1H), 5.19/5.10 (t, J = 7.2 Hz, 1H), 4.91 − 4.71 (m, 1H), 4.59 (dq, J = 14.3, 7.1 Hz, 1H), 3.79/3.78 (s, 3H), 2.63 − 2.46 (m, 2H), 2.44 − 2.31 (m, 3H), 2.30 − 2.13 (m, 3H), 2.07 (m, 2H), 1.99 − 1.89 (m, 2H), 1.87 − 1.80 (m, 3H), 1.79 − 1.70 (m, 2H), 1.69 − 1.54 (m, 2H), 1.66/1.62 (d, J = 0.8 Hz, 3H), 1.54 − 1.30 (m, 6H), 1.38 (d, J = 7.1 Hz, 3H), 1.30 − 1.13 (m, 8H). ^{13}C NMR (126 MHz, CDCl$_3$) δ 175.77/175.70, 173.82/173.76, 171.86/171.78, 160.25/160.21, 143.84, 139.40/139.04, 134.46/133.61, 127.94, 125.11/124.99, 124.36/123.88,

114.04/113.14, 110.75/110.30, 103.19/102.90, 75.16/74.50, 55.48/55.42, 48.30/48.21, 45.32/45.21, 38.42/37.92, 36.96/36.69, 35.63, 35.14/34.76, 31.80/31.53, 31.36/31.19, 29.85/29.71, 29.60/29.46, 28.83/28.28, 27.93/27.65, 27.47/27.26, 26.84/26.30, 25.83/25.79, 25.78/25.72, 25.45/25.31, 23.37, 18.95/18.76, 16.20/15.93. HRMS (ESI, *m/z*): calcd for $[C_{35}H_{52}KN_2O_5]^+$ ([M + K]$^+$): 619.3513, found 619.3513.
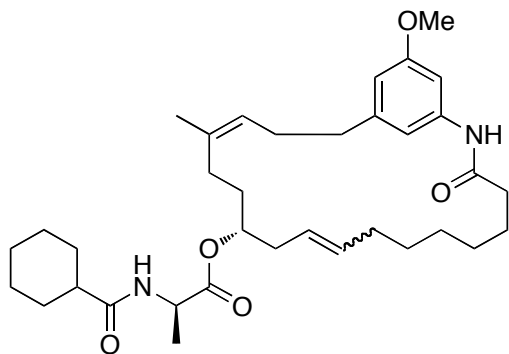
Macrocycle 11:

General procedure C was followed. Macrocycle **11** was isolated as a 5:1 mixture of olefin isomers. (6 mg, 83%). $[\alpha]^{23}_D$ = 8.63° (c = 0.005, DCM). ^{1}H NMR (500 MHz, CDCl$_3$) δ 7.99/7.96 (s, 1H), 7.50/7.29 (s, 1H), 6.70/6.60 (s, 1H), 6.43/6.39 (s, 1H), 6.00/5.93 (d, *J* = 7.1 Hz, 1H), 5.50 – 5.39 (m, 1H), 5.33 – 5.23 (m, 1H), 5.19/5.10 (t, *J* = 7.1 Hz, 1H), 4.91 – 4.82 (m, 1H), 4.78 – 4.70 (m, 1H), 4.64 – 4.55 (dq, *J* = 14.3, 7.1 Hz, 1H), 3.79/3.78 (s, 3H), 2.65 – 2.47 (m, 2H), 2.44 – 2.31 (m, 2H), 2.30 – 2.15 (m, 3H), 2.14 – 2.01 (m, 2H), 1.94 (t, *J* = 7.8 Hz, 2H), 1.87 – 1.79 (m, 3H), 1.78 – 1.69 (m, 3H), 1.68 – 1.59 (m, 2H), 1.66/1.62 (d, *J* = 0.6 Hz, 3H), 1.54 – 1.45 (m, 2H), 1.38 (d, *J* = 7.2 Hz, 3H), 1.45 – 1.30 (m, 5H), 1.29 – 1.14 (m, 6H). ^{13}C NMR (126 MHz, CDCl$_3$) δ 175.88/175.75, 173.55/173.43, 172.01/171.71, 160.20/159.89, 144.21/143.89, 139.81/139.52, 135.65/135.28, 134.07/133.46, 125.17/125.06, 124.81/124.16, 111.87/111.60, 111.27/110.87, 103.15/102.82, 76.13/76.03, 55.50/55.46, 48.18/48.09, 45.44/45.31, 38.24/37.89, 37.36/36.95, 36.27/36.05, 32.26/32.06, 31.91/31.78, 30.00/29.87, 29.70, 29.59/29.55,

28.67/28.15, 27.77/27.38, 26.29/25.85, 25.81/25.79, 25.77/25.73, 25.42/25.31, 23.45/23.28, 19.07, 18.89. HRMS (ESI, m/z): calcd for $[C_{35}H_{52}KN_2O_5]^+$ ($[M + K]^+$): 619.3513, found 619.3515.
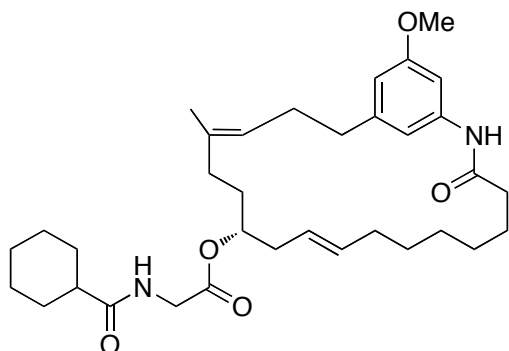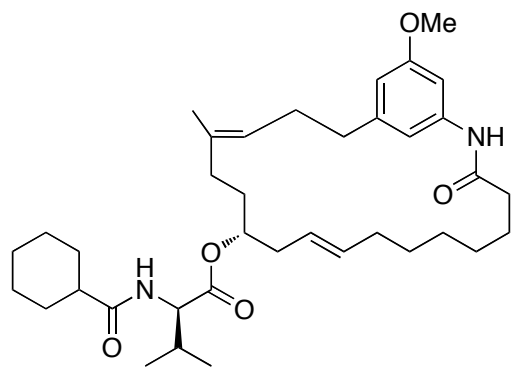

Macrocycle 28:

General procedure C was followed. Macrocycle **28** was isolated as a 1:1 mixture of olefin isomers. (6 mg, 83%). $[\alpha]^{23}_D = 13.33°$ (c = 0.005, DCM). ^{1}H NMR (500 MHz, CDCl$_3$) δ 8.23/7.91 (s, 1H), 7.62/7.32 (s, 1H), 6.61/6.49 (s, 1H), 6.49 (s, 1H), 5.94/5.86(t, J = 4.5 Hz, 1H), 5.54 − 5.36 (m, 1H), 5.33 − 5.16 (m, 1H), 5.15 − 5.02 (m, 1H), 5.01 − 4.72 (m, 1H), 4.04/3.98 (dd, J = 14.2, 5.1 Hz, 2H), 3.81/3.80 (s, 3H), 2.77 − 2.53 (m, 2H), 2.43 − 2.21 (m, 5H), 2.20 − 1.92 (m, 5H), 1.92 − 1.73 (m, 5H), 1.73 − 1.53 (m, 3H), 1.47 − 1.32 (m, 6H), 1.32 − 1.15 (m, 10H). ^{13}C NMR (126 MHz, CDCl$_3$) δ 180.93/179.41, 176.52/176.36, 170.30/170.12, 160.24/159.98, 144.26/144.19, 139.63/139.34, 135.69/135.38, 134.30/133.59, 125.05/125.01, 124.81/124.09, 112.57/111.96, 111.27/110.96, 103.77/103.28, 76.15/76.10, 55.47/55.44, 45.28, 41.74/41.70, 37.83/37.33, 37.15/36.36, 36.21/36.16, 32.34/32.29, 32.05/31.86, 30.16/30.09, 29.85/29.71, 29.68, 29.03/28.41, 28.21/28.13, 27.86/27.62, 27.38/26.46, 25.81/25.77, 25.53/25.35, 23.41/23.31. HRMS (ESI, m/z): calcd for $[C_{34}H_{50}KN_2O_5]^+$ ($[M + K]^+$): 605.3357, found 605.3355.
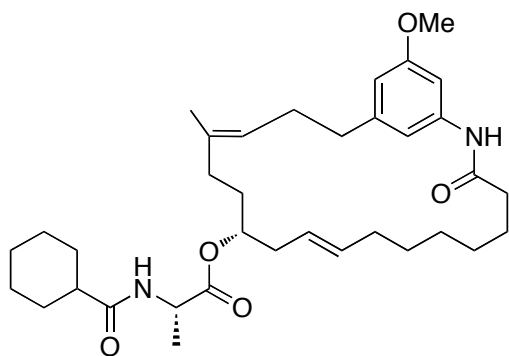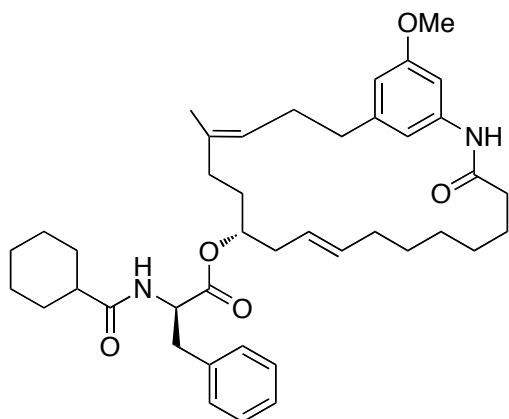
Macrocycle 29:

General procedure C was followed. Macrocycle **29** was isolated as a 2:1 mixture of olefin isomers. (6 mg, 83%). $[\alpha]^{23}_D = 2.66°$ (c = 0.005, DCM). ^{1}H NMR (500 MHz, CDCl$_3$) δ 7.85/7.63 (s, 1H), 7.42/7.04 (s, 1H), 6.86/6.66 (s, 1H), 6.50/6.46 (s, 1H), 6.12/6.03 (d, J = 7.3 Hz, 1H), 5.51 – 5.37 (m, 1H), 5.30 (m, 1H), 5.23/5.16 (t, J = 7.2 Hz, 1H), 4.92 – 4.78 (m, 1H), 4.62 – 4.51 (m, 1H), 3.80/3.78 (s, 3H), 2.65 – 2.47 (m, 2H), 2.41 – 2.33 (m, 2H), 2.30 – 2.16 (m, 3H), 2.14 – 2.04 (m, 2H), 2.03 – 1.89 (m, 3H), 1.88 – 1.81 (m, 2H), 1.81 – 1.69 (m, 4H), 1.67/1.65 (d, J = 0.9 Hz, 3H), 1.70 – 1.62 (m, 3H), 1.55 – 1.48 (m, 1H), 1.49 – 1.31 (m, 6H), 1.39 (d, J = 7.1 Hz, 3H), 1.31 – 1.17 (m, 5H). ^{13}C NMR (126 MHz, CDCl$_3$) δ 175.65/175.59, 173.50/173.36, 171.96/171.85, 160.30/160.06, 144.32/144.25, 139.65/139.18, 135.81/135.35, 134.16/133.17, 124.99, 124.21/124.14, 112.73/112.02, 111.20/110.94, 103.75/103.24, 76.23/75.75, 55.48, 48.24/48.21, 45.39, 37.17/36.96, 36.60/36.26, 32.41/32.24, 31.97/31.80, 30.40/29.99, 29.85/29.61, 29.77, 29.66, 28.58/28.28, 27.91/27.65, 27.55/27.26, 26.38/25.76, 25.85, 25.81, 25.78, 25.30/25.12, 23.44/23.37, 19.00/18.95. HRMS (ESI, m/z): calcd for $[C_{35}H_{52}KN_2O_5]^+$ ([M + K]$^+$): 619.3513, found 619.3510.
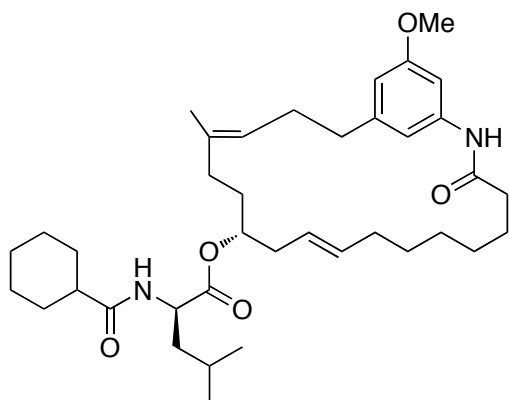
Macrocycle 30:

General procedure C was followed. Macrocycle **30** was isolated as a 2:1 mixture of olefin isomers. (7 mg, 83%). $[\alpha]^{23}_D = 6.00°$ (c = 0.005, DCM). ^{1}H NMR (500 MHz, CDCl$_3$) δ 7.95/7.86 (s, 1H), 7.44/7.24 (s, 1H), 6.71/6.62 (s, 1H), 6.43/6.39 (s, 1H), 5.90/5.87 (d, J = 9.1 Hz, 1H), 5.50 – 5.39 (m, 1H), 5.34 – 5.22 (m, 1H), 5.20/5.10 (t, J = 6.9 Hz, 1H), 4.91 – 4.72 (m, 1H), 4.57 (dd, J = 8.9, 4.9 Hz, 1H), 3.79/3.77 (s, 3H), 2.65 – 2.45 (m, 2H), 2.45 – 2.30 (m, 2H), 2.38 (t, J = 6.2 Hz, 2H), 2.30 – 2.01 (m, 6H), 2.01 – 1.89 (m, 3H), 1.89 – 1.74 (m, 4H), 1.74 – 1.55 (m,5H), 1.66/1.61 (s, 3H), 1.55 – 1.11 (m, 10H), 0.96/0.95 (d, J = 6.9 Hz, 3H), 0.91/0.90 (d, J = 6.9 Hz, 3H). ^{13}C NMR (126 MHz, CDCl$_3$) δ 176.16/176.02, 172.79/172.50, 171.98/171.83, 160.31/160.25, 143.82, 139.33/139.05, 134.87/134.28, 133.79/133.09, 125.03/124.71, 124.41/124.01, 113.07/112.31, 110.70/110.35, 103.15/102.96, 75.30/75.04, 55.48/55.42, 45.68/45.49, 37.93/37.75, 36.88/36.78, 35.59/35.20, 35.15/34.97, 31.85/31.76, 31.64/31.55, 31.33, 30.11, 29.85, 29.51, 29.46/28.77, 28.31/27.71, 27.53/27.28, 26.92/25.83, 25.74, 25.72/25.44, 25.33/23.44, 22.10, 19.37, 18.07/17.69, 16.15/15.88. HRMS (ESI, *m/z*): calcd for $[C_{37}H_{56}KN_2O_5]^+$ ([M + K]$^+$): 647.3826, found 647.3828.
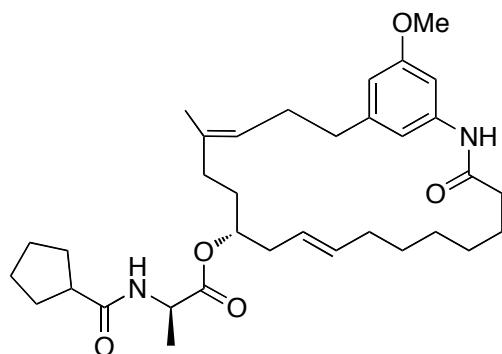
Macrocycle 31:

General procedure C was followed. Macrocycle **31** was isolated as a 2:1 mixture of olefin isomers. (8 mg, 85%). $[\alpha]^{23}_D$ = -1.81° (c = 0.005, DCM). ^{1}H NMR (500 MHz, CDCl$_3$) δ 7.94/7.79 (s, 1H), 7.40/7.30 (s, 1H), 7.29 – 7.11 (m, 3H), 7.17 – 7.10 (m, 2H), 6.68/6.63 (s, 1H), 6.44/6.39 (s, 1H), 5.84/5.81 (d, J = 8.1 Hz, 1H), 5.50 – 5.38 (m, 1H), 5.32 – 5.22 (m, 1H), 5.19/5.09 (t, J = 6.7 Hz, 1H), 4.92 – 4.85 (m, 1H), 4.85 – 4.69 (m, 1H), 3.79/3.77 (s, 3H), 3.21 – 3.12 (m, 1H), 3.07 – 2.99 (m, 1H), 2.63 – 2.47 (m, 2H), 2.42 – 2.31 (m, 3H), 2.31 – 2.15 (m, 4H), 2.14 – 1.78 (m, 8H), 1.78 – 1.58 (m, 6H), 1.65/1.60 (d, J = 0.9 Hz, 3H), 1.53 – 1.06 (m, 10H). ^{13}C NMR (126 MHz, CDCl$_3$) δ 175.75, 172.13/172.11, 171.66, 160.10/160.08, 143.79/143.75, 139.06, 135.77, 134.76/134.71, 133.16, 129.45, 128.42, 127.07, 125.04, 124.99, 118.41/118.37, 110.86/110.82, 110.46/110.43, 102.57/102.51, 75.10, 55.30, 52.63/52.59, 45.36, 38.62, 38.57, 38.41/38.36, 37.60/37.57, 36.43/36.38, 33.76/33.73, 31.92, 31.80, 29.97, 29.82, 29.73, 29.34/29.25, 28.99/28.82, 27.31, 25.64, 25.57/25.51, 23.15. HRMS (ESI, *m/z*): calcd for $[C_{41}H_{56}KN_2O_5]^+$ ([M + K]$^+$): 695.3826, found 695.3826.
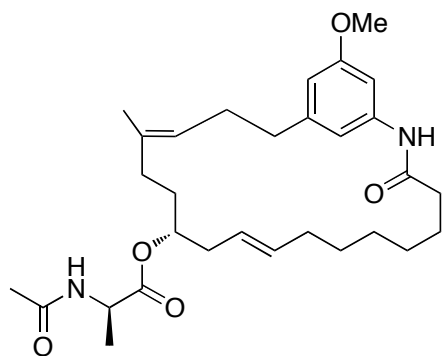
Macrocycle 32:

General procedure C was followed. Macrocycle **32** was isolated as a 2:1 mixture of olefin isomers. (8 mg, 85%). $[\alpha]^{23}_D$ = 12.22° (c = 0.005, DCM). ^{1}H NMR (500 MHz, CDCl$_3$) δ 8.00/7.97 (s, 1H), 7.50/7.28 (s, 1H), 6.70/6.61 (s, 1H), 6.43/6.40 (s, 1H), 5.79/5.74 (d, J = 8.6 Hz, 1H), 5.50 – 5.39 (m, 1H), 5.35 – 5.22 (m, 1H), 5.19/5.09 (t, J = 7.0 Hz, 1H), 4.91 – 4.70 (m, 1H), 4.66 – 4.56 (m, 1H), 3.79/3.78 (s, 3H), 2.70 – 2.46 (m, 2H), 2.38 (t, J = 6.4 Hz, 2H), 2.32 – 2.15 (m, 3H), 2.15 – 2.00 (m, 3H), 1.99 – 1.93 (m, 3H), 1.97 (t, J = 8.0 Hz, 2H), 1.93 – 1.70 (m, 5H), 1.70 – 1.55 (m, 5H), 1.66/1.61 (s, 3H), 1.55 – 1.45 (m, 3H), 1.47 – 1.29 (m, 5H), 1.36 – 1.11 (m, 5H), 0.95 (d, J = 3.7 Hz, 3H), 0.94 (d, J = 3.5 Hz, 3H). ^{13}C NMR (126 MHz, CDCl$_3$) δ 176.01/175.88, 173.61/173.36, 171.83/171.76, 160.23/160.11, 150.11, 144.21, 139.77/139.75, 135.72/134.00, 125.31/124.92, 125.06/124.11, 111.87/111.60, 111.26/110.84, 103.09/102.78, 76.24/75.99, 55.47/55.45, 50.86/50.80, 45.42/45.37, 42.03/41.82, 37.21/36.87, 36.35/35.90, 32.36/32.31, 31.88/31.82, 29.96, 29.89/29.84, 29.81, 29.52/29.49, 28.19/27.94, 27.69/27.65, 27.46/27.34, 25.81, 25.74, 25.36/25.09, 25.10, 23.36/23.31, 23.27, 23.16/23.17, 23.06, 22.18/22.15. HRMS (ESI, *m/z*): calcd for $[C_{38}H_{58}KN_2O_5]^+$ ([M + K]$^+$): 661.3983, found 661.3981.

Macrocycle 33:

General procedure C was followed. Macrocycle **33** was isolated as a 2:1 mixture of olefin isomers. (7 mg, 83%). $[\alpha]^{23}_D$ = 11.01° (c = 0.005, DCM). ^{1}H NMR (500 MHz, CDCl$_3$) δ 8.00/7.96 (s, 1H), 7.50/7.29 (s, 1H), 6.70/6.60 (s, 1H), 6.43/6.39 (s, 1H), 6.01/5.94 (d, J = 7.1 Hz, 1H), 5.52 – 5.39 (m, 1H), 5.34 – 5.22 (m, 1H), 5.19/5.11 (t, J = 6.8 Hz, 1H), 4.93 – 4.69 (m, 1H), 4.66 – 4.53 (m, 1H), 3.79/3.78 (s, 3H), 2.65 – 2.44 (m, 2H), 2.44 – 2.31 (m, 2H), 2.31 – 2.15 (m, 3H), 2.15 – 2.00 (m, 2H), 2.00 – 1.89 (m, 2H), 1.89 – 1.69 (m, 3H), 1.66/1.62 (d, J = 0.9 Hz, 3H), 1.69 – 1.54 (m, 3H), 1.53 – 1.29 (m, 2H), 1.38/1.37 (d, J = 7.2 Hz, 3H), 1.45 – 1.30 (m, 3H), 1.30 – 1.11 (m, 9H). ^{13}C NMR (126 MHz, CDCl$_3$) δ 176.12/175.87, 173.55/173.10, 172.31/172.22, 160.32/160.19, 144.00/143.95, 140.20/140.16, 139.21, 134.81, 133.24/133.19, 125.30/125.16, 118.41/118.35, 111.04/110.63, 102.74, 74.58, 55.42, 48.16/48.11, 45.86/45.76, 38.94, 37.69, 36.44, 33.89, 31.96, 30.59, 30.42, 29.95/29.85, 29.33/29.21, 29.08, 28.91, 27.43, 26.14/26.06, 25.72, 23.27, 19.20/18.83, 14.42/14.28. HRMS (ESI, *m/z*): calcd for $[C_{34}H_{50}KN_2O_5]^+$ ([M + K]$^+$): 605.3357, found 605.3356.

Macrocycle 34:

General procedure C was followed. Macrocycle **34** was isolated as a 2:1 mixture of olefin isomers. (5 mg, 75%). $[\alpha]^{23}_D$ = 7.45° (c = 0.005, DCM). ^{1}H NMR (500 MHz, CDCl$_3$) δ 7.84/7.81 (s, 1H), 7.44/7.37 (s, 1H), 6.78/6.64 (s, 1H), 6.44/6.41 (s, 1H), 6.07/6.01 (d, J = 7.3 Hz, 1H), 5.53 – 5.39 (m, 1H), 5.33 – 5.22 (m, 1H), 5.19/5.12 (t, J = 7.2 Hz, 1H), 4.90 – 4.72 (m, 1H), 4.66 – 4.55 (m, 1H), 3.79/3.78 (s, 3H), 2.63 – 2.49 (m, 2H), 2.42 – 2.33 (m, 2H), 2.30 – 2.17 (m, 2H), 2.00/1.97 (s, 3H), 2.16 – 1.97 (m, 4H), 1.97 – 1.67 (m, 4H), 1.66/1.63 (s, 3H), 1.39/1.38 (d, J = 7.2 Hz, 3H), 1.55 – 1.11 (m, 8H). ^{13}C NMR (126 MHz, CDCl$_3$) δ 172.95/172.92, 172.16/172.11, 169.93, 160.24/160.18, 143.99, 140.10/140.04, 139.20, 134.86/134.76, 133.25, 125.19/125.00, 118.35, 111.11/110.69, 102.76, 74.70/74.62, 55.43, 48.24, 38.95, 37.73, 36.45, 33.88/32.08, 31.97, 29.85/29.82, 29.33, 29.05, 28.89, 27.46, 25.72, 23.43, 23.27, 19.12. HRMS (ESI, *m/z*): calcd for $[C_{30}H_{44}KN_2O_5]^+$ ($[M + K]^+$): 579.3200, found 579.3199.
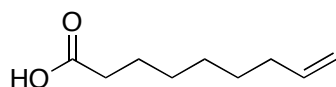
Non-8-enoic Acid:

A 100 mL round bottom flask was equipped with a magnetic stir bar and deionized water (5.2 mL), methanol (26 mL), 8-bromooct-1-ene (5g, 26.2 mmol, 1 eq.), and sodium cyanide (2.57 g, 52.4 mmol, 2 eq.) were added. The reaction mixture was refluxed for 10 h. Solvent was removed

and the remaining slurry was taken up in EtOAc (30 mL), washed with deionized water (2X, 20 mL) and saturated aqueous sodium chloride (2X, 20 mL), and dried over anhydrous sodium sulfate. Solvent was removed to afford a colorless oil that was dissolved in a mixture of deionized water and ethanol (17.5mL and 59 mL respectively) in a 250 mL round bottom flask. Potassium hydroxide (17.23 g, 307 mmol, 11 eq.) was added to the solution and the reaction mixture was refluxed for 10 h. Solvent was removed and the remaining slurry was taken up in EtOAc (30 mL) and deionized water (50 mL). The organic layer was removed and the aqueous later was extracted with EtOAc (2X, 30 mL). The aqueous layer was adjusted to pH = 2 using 3N HCl, and extracted with EtOAc (4X, 20 mL). The combined organic layers were collected and dried over anhydrous sodium sulfate. Solvent was removed to afford compound **35** as a colorless oil (3.8 g, 92% over two steps). ^{1}H NMR (500 MHz, CDCl$_3$) δ 10.95 (s, 1H), 5.80 (ddt, J = 16.9, 10.2, 6.7 Hz, 1H), 4.99 (ddd, J = 17.1, 3.6, 1.6 Hz, 1H), 4.93 (ddt, J = 10.2, 2.2, 1.2 Hz, 1H), 2.35 (t, J = 7.5 Hz, 2H), 2.07 – 2.01 (m, 2H), 1.68 – 1.59 (m, 2H), 1.43 – 1.27 (m, 6H). ^{13}C NMR (126 MHz, CDCl$_3$) δ 179.43, 139.12, 114.46, 34.01, 33.83, 29.01, 28.83, 28.80, 24.75. HRMS (ESI, m/z): calcd for [C$_9$H$_{15}$O$_2$]$^-$ ([M - H]$^-$): 155.1072, found 155.1076.
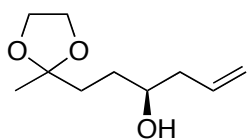
(**S**)-1-(2-Methyl-1,3-dioxolan-2-yl)hex-5-en-3-ol (51):

A 25 mL round bottom flask was charged with deionized water (5 mL), acetone (5 mL), compound **13** (200 mg, 0.78 mmol, 1 eq.), and pyridinium p-toluenesulfonate (608 mg, 2.4 mmol, 3.1 eq.) and the reaction mixture was refluxed for 10 h. Solvent was removed and the remaining slurry was dissolved in EtOAc (20 mL) and washed with saturated aqueous sodium bicarbonate. The organic layer was dried over anhydrous sodium sulfate and solvent was

removed to afford a colorless oil that was purified by SiO$_2$ flash chromatography (10% EtOAc in Hex) to afford compound **51** as a colorless oil (137 mg, 94%). $[\alpha]^{23}_D$ = -1.89° (c = 0.005, DCM).

^{1}H NMR (500 MHz, CDCl$_3$) δ 5.84 (dddd, J = 23.4, 10.6, 7.6, 6.8 Hz, 1H), 5.13 (dtd, J = 4.0, 2.0, 1.3 Hz, 1H), 5.11 (t, J = 1.2 Hz, 1H), 3.99 – 3.92 (m, 4H), 3.69 – 3.62 (m, 1H), 2.31 – 2.24 (m, 1H), 2.24 (d, J = 3.9 Hz, 1H), 2.22 – 2.13 (m, 1H), 1.84 (ddd, J = 14.2, 9.5, 5.9 Hz, 1H), 1.79 – 1.72 (m, 1H), 1.67 – 1.58 (m, 1H), 1.54 (dddd, J = 14.1, 9.4, 8.3, 5.9 Hz, 1H), 1.33 (s, 3H).

^{13}C NMR (126 MHz, CDCl$_3$) δ 135.05, 118.03, 110.15, 70.93, 64.79, 64.75, 42.16, 35.44, 31.17, 23.87. HRMS (ESI, m/z): calcd for [C$_{10}$H$_{19}$O$_3$]$^+$ ([M + H]$^-$): 187.1334, found 187.1338.
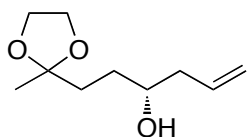
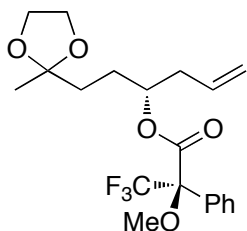**(*R*)-1-(2-Methyl-1,3-dioxolan-2-yl)hex-5-en-3-ol (52):**

Compound **41** was synthesized using the same procedures as compound **51** from 5-hydroxypentan-2-one using (-)-*B*-methoxydiisopinocampheylborane. $[\alpha]^{23}_D$ = 1.96° (c = 0.005, DCM). ^{1}H NMR (400 MHz, CDCl$_3$) δ 5.83 (dddd, J = 16.6, 10.7, 7.6, 6.8 Hz, 1H), 5.16 – 5.11 (m, 1H), 5.10 (t, J = 1.1 Hz, 1H), 4.00 – 3.91 (m, 4H), 3.70 – 3.59 (m, 1H), 2.35 – 2.09 (m, 3H), 1.90 – 1.69 (m, 2H), 1.69 – 1.45 (m, 2H), 1.33 (s, 3H). (EtOAc is present as an impurity). All spectral data matched the enantiomer, compound **51**.
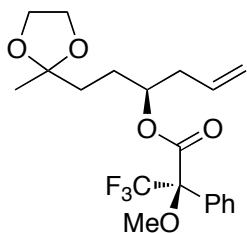
(*R*)-(*S*)-1-(2-Methyl-1,3-dioxolan-2-yl)hex-5-en-3-yl   **3,3,3-trifluoro-2-methoxy-2-phenylpropanoate (53):**

A flame dried 5 mL round bottom flask was flushed with argon before DCM (1 mL), triphenylphosphine (18 mg, 0.081 mmol, 1.5 eq.), (*R*)-3,3,3-trifluoro-2-methoxy-2-phenylpropanoic acid (19 mg, 0.081 mmol, 1.5 eq.), and compound **51** (10 mg, 0.054 mmol, 1 eq.) were added. 1-ethyl-3-(3-dimethylaminopropyl) carbodiimide (16 mg, 0.081 mmol, 1.5 eq.) was added to the solution and the reaction mixture was stirred for 10 h. Solvent was removed and the remaining slurry was dissolved in d^6-benzene. ^{19}F NMR (376 MHz, C$_6$D$_6$) δ 70.19, 71.15.

(*R*)-(*R*)-1-(2-Methyl-1,3-dioxolan-2-yl)hex-5-en-3-yl   3,3,3-trifluoro-2-methoxy-2-phenylpropanoate (54):

Compound **54** was synthesized following the procedure for compound **53**. ^{19}F NMR (376 MHz, C$_6$D$_6$) δ 70.19, 71.19.

Compounds **52** and **53** were combined and analyzed by NMR. ^{19}F NMR (376 MHz, C$_6$D$_6$) δ 70.19, 71.15, 71.18.

Molecular Modeling: Trienomycin A (**1**) and the four semi-synthetic derivatives (**2-5**) were constructed in the Sybyl software suite and their energy was minimized through dynamic simulations using default parameters. The structures were compared for overlay using the Similarity tool of Surflex software suite (default parameters). Functionality was sequentially removed, and each new structure was minimized. The structural overlays were compared using Surflex Sim after each minimization until a score of less than 0.7 was observed. The simplest

trienomycin A analogue, compound **6**, maintained a similarity score of 0.7935. 12 olefin isomers representing all possible monoene derivatives were then constructed in the same manner and compared using the Surflex Similarity tool.

Antiproliferation Assay. MCF-7 and HeLa cells were maintained in a 1:1 mixture of Advanced DMEM/F12 (Gibco) or F-12 Kaighn's médium (Gibco), respectively, supplemented with non-essential amino acids, L-glutamine (2 mM), streptomycin (500 g/mL), penicillin (100 units/mL), and 10% FBS. Cells were grown to confluence in a humidified atmosphere (37 °C, 5% CO2), seeded (2000 cells/well, 100 μL) in 96-well plates, and allowed to adhere overnight. Compound or GDA at varying concentrations in DMSO (1% DMSO final concentration) was added, and cells were returned to the incubator for 72 h. At 72 h, the number of viable cells was determined using an MTS/PMS cell proliferation kit (Promega) per the manufacturer's instructions. Cells incubated in 1% DMSO were used as 100% proliferation, and values were adjusted accordingly. IC_{50} values were calculated from three separate experiments performed in triplicate using GraphPad Prism.

IV.6   References

1.   Li, J. W.-H.; Vederas, J. C. Drug discovery and natural products: end of an era or an endless frontier? *Science* **2009,** 325, 161-165.

2.   Cragg, G. M.; Grothaus, P. G.; Newman, D. J. Impact of natural products on developing new anti-cancer agents. *Chem. Rev.* **2009,** 109, 3012-3043.

3.   Newman, D. J.; Cragg, G. M. Natural product scaffolds as leads to drugs. *Future Med. Chem.* **2009,** 1, 1415-1427.

4.   Driggers, E. M.; Hale, S. P.; Lee, J.; Terrett, N. K. The exploration of macrocycles for drug discovery - an underexploited structural class. *Nat. Rev. Drug Discov.* **2008,** 7, 608-624.

5.   Marsault, E.; Peterson, M. L. Macrocycles are great cycles - applications, opportunities, and challenges of synthetic macrocycles in drug discovery. *J. Med. Chem.* **2011,** 54, 1961-2004.

6.   Wessjohann, L. A.; Ruijter, E.; Garcia-Rivera, D.; Brandt, W. What can a chemist learn from nature's macrocycles - A, brief, conceptual view. *Molec. Div.* **2004,** 9, 171 - 186.

7.   Lalloo, U. G.; Ambarram, A. New antituberculous drugs in development. *Curr. HIV/AIDS Rep.* **2010,** 7, 143-151.

8.   Brandt, G. E. L.; Blagg, B. S. J. Alternate strategies of Hsp90 modulation for the treatment of cancer and other diseases. *Curr. Top. Med. Chem.* **2009,** 9, 1447-1461.

9.   Funayama, S.; Anraku, Y.; Mita, A.; Yang, Z.-B.; Shibata, K.; Komiyama, K.; Umezawa, I.; Omura, S. Structure-activity relationship of a novel antitumor ansamycin antibiotic trienomycin A and related compounds. *J. Antibiot.* **1988,** 41, 1223-1230.

10.   Grunicke, H.; Pushendorf, B.; Werchau, H. Mechanism of action of distamycin A and other antibiotics with antiviral activity. *Rev. Physiol. Biochem. Pharmacol.* **1976,** 75, 69-96.

11.   Funayama, S.; Okada, K.; Komiyama, K.; Umezawa, I. Structure of trienomycin A, a novel cytocidal ansamycin antibiotic. *J. Antibiot.* **1985,** 38, 1107-1109.

12.   Masse, C. E.; Yang, M.; Solomon, J.; Panek, J. S. Total Synthesis of (+)-mycotrienol and (+)-mycotrienin I: application of asymmetric crotylsilane bond constructions. *J. Am. Chem. Soc.* **1998,** 120, 4123-4134.

13.   Funayama, S.; Okada, K.; Iwasaki, K.; Komiyama, K.; Umezawa, I. Structures of trienomycins A, B and C, novel cytocidal ansamycin antibiotics. *J. Antibiot.* **1985,** 38, 1677-1683.

14.   Komiyama, K.; Hirokawa, Y.; Yamaguchi, K.; Funayama, S.; Masuda, K.; Anraku, Y.; Umezawa, I.; Omura, S. Antitumor activity of trienomycin A on murine tumors. *J. Antibiot.* **1987,** 40, 1768-1772.

15.   Umezawa, I.; Funayama, S.; Okada, K.; Iwasaki, K.; Satoh, J.; Masuda, K.; Komiyama, K. Studies on a novel cytocidal antibiotic, trienomycin A taxonomy, fermentation, isolation, and physico-chemical and biological characteristics. *J. Antibiot.* **1985,** 38, 699-705.

16.   Smith III, A. B.; Barbosa, J.; Wong, W.; Wood, J. L. Total syntheses of (+)-trienomycins A and F via a unified strategy. *J. Am. Chem. Soc.* **1996,** 118, 8316-8328.

17.   Jain, A. N. Ligand-based structural hypotheses for virtual screening. *J. Med. Chem.* **2004,** 47, 947-961.

18.   Maryanoff, B. E.; Reitz, A. B. The Wittig olefination reaction and modifications involving phosphoryl-stabilized carbanions. Stereochemistry, mechanism, and selected synthetic aspects. *Chem. Rev.* **1989,** 89, 863-927.

19.   Mitsunobu, O.; Yamada, M. Preparation of esters of carboxylic and phosphoric acid via quaternary phosphonium salts. *Bull. Chem. Soc. Jpn.* **1967,** 40, 2380-2382.

20.   Vougioukalakis, G. C.; Grubbs, R. H. Ruthenium-based heterocyclic carbene-coordinated olefin metathesis catalysts. *Chem. Rev.* **2010,** 110, 1746-1787.

21.   Herlt, A. J.; Kibby, J. J.; Rickards, R. W. Synthesis of unlabelled and carboxyl-labelled 3-Amino-5-hydroxybenzoic acid. *Aust. J. Chem.* **1981,** 34, 1319-1324.

22.   Ziegler, K.; Martin, H.; Krupp, F. Metallorganische verbindungen, XXVII aluminiumtrialkyle und dialkyl-aluminiumhydride aus aluminiumisobutyl-verbindungen. *Justus Liebigs Ann. Chem.* **1960,** 629, 14-19.

23.   Wadsworth Jr., W. S.; Emmons, W. D. The utility of phosphonate carbanions in olefin synthesis. *J. Am. Chem. Soc.* **1961,** 83, 1733-1738.

24.   Adam, W.; Eggelte, J. Cyclic peroxides. 57. Prostanoid endoperoxide model compounds: 2,3-dioxabicyclo[2.2.1]heptane via selective diimide reduction. *J. Org. Chem.* **1977,** 42, 3987-3988.

25.   El-Faham, A.; Funosas, R. S.; Prohens, R.; Albericio, F. COMU: a safer andmore effective replacement for benzotriazole-based uronium coupling reagents. *Chem. Eur. J.* **2009,** 15, 9404-9416.

26.   Jadhav, P. K.; Bhat, K. S.; Perumal, P. T.; Brown, H. C. Chiral synthesis via organoboranes. 6. Asymmetric allylboration via chiral allyldialkylboranes. Synthesis of homoallylic alcohols with exceptionally high enantiomeric excess. *J. Org. Chem.* **1986,** 51, 432-439.